UNIVERSITY OF CALIFORNIA
RIVERSIDE

Measuring the Succession, Functions and Resilience of Soil Microbes After a Chaparral Wildfire

A Dissertation submitted in partial satisfaction
of the requirements for the degree of

Doctor of Philosophy

in

Plant Pathology

by

Martha Fabiola Pulido-Chavez

December 2023

Dissertation Committee:
Dr. Sydney I. Glassman, Chairperson
Dr. Jason E. Stajich
Dr. Peter M. Homyak

The Dissertation of Martha Fabiola Pulido-Chavez is approved:

_____

_____

_____

Committee Chairperson

University of California, Riverside

Acknowledgements

To Dr. Sydney I. Glassman, whose guidance has nurtured my passion for fungi, thank you! Thank you for everything you have done for me. You have been more than a mentor to me; you have been a constant source of support, providing invaluable advice not only for my research but also for shaping my future career plans and life choices. I am thankful for your encouragement to actively participate in scientific committees, which has significantly contributed to my professional development and expanded my network. More importantly, thank you for giving me the confidence to speak freely about my personal and professional life, allowing us to build more than a mentor-mentee relationship. I thank you for all the wisdom, inspiration, and genuine conversations we have shared!

To my committee, Dr. Jason Stajich and Dr. Pete Homyak, thank you for being invaluable mentors, for your support and wisdom throughout the years. Dr. Stajich, I am thankful for the numerous insightful discussions we have shared over the years. Your guidance both on campus and at MSA, and for always giving insightful questions that allow me to think about my work in a way I had not conceived. Dr. Pete Homyak, thank you for being part of my research journey from year one and being a constant source of comfort. Thank you for your invaluable writing advice and for giving me honest and generous career advice that has never failed me.

To my Holy Fire collaborators, Dr. Loralee Larios and Dr. Cassandra Zalman, thank you for all your help with my research and for providing invaluable advice, feedback, suggestions, and support throughout the past five years.

To my amazing cohort, Dr. Biagio DiSalvo, Dr. Irene Lavagi, and Chris Drodz, thank you for being supportive and being a source of comfort during this journey. Thank you for all the study sessions, coffee walks, chocolate chip cookies, and weeknight dinners. To Linton Freund, thank you for always being there for me, for your wisdom about metagenomes, and for being my venting buddy and inspiration.

To my amazing lab mates, Dylan Enright, Arik Joukhajian, Marcos Vinicius Caiafa Sepulveda, Basubi Binti Zhilik, and Esbeiry Cordova-Ortiz, thank you for all the support, advice, laughs, and conversations we've had throughout the years. You all have become instrumental parts of my life, keeping me sane throughout my Ph.D. Dylan where would I be without you? We made a pact early on to always have each other's back, and I thank you for that. I am so grateful that we began our academic career together, and I cannot wait to collaborate with you. Thank you for always being there when I needed you. Remember, fungi are better than bacteria (on the love scale).

To our previous lab manager, Judy Chung and James Randolph, thank you for all your help with my research and the great talks; my project would not be complete without you. To Maria Ordonez, you are such a wonderful and caring person. You have an amazing power to make everyone around you feel like they are the most incredible and smartest person in the room, preventing us from having self-doubt and feeling confident in our lab skills/research. You are one of a kind. Thank you for the great

conversation, the wisdom you have passed down to me, and the care in which you treat the entire lab.

To Dr. Ernesto Alvarado, thank you for giving me the opportunity of a lifetime, for your advice, and for always believing in me. Your words of encouragement and our meaningful conversations have meant the world to me. Although I cannot fully express my gratitude, I want to let you know that your mentorship has not only shaped me professionally, but it has inspired me on a personal level. Gracias por todo!

Para ti, no tengo suficientes palabras para expresar mi gratitud. No sé cómo habría sobrevivido este año sin ti a mi lado, dándome la fuerza para seguir adelante, incluso en los momentos más difíciles. Gracias por enseñarme que tengo un valor inmenso y que puedo lograr cualquier cosa que me proponga. Gracias por regalarme tu confianza, por escucharme y por todo el amor que me has dado.

To my best friend and long lost sister Lesly, I am so grateful that you have been part of my journey. Thank you for your words of encouragement, for listening to me, offering advice and for all the thoughtful things you do for me. My academic journey would not been the same without you because no matter what this crazy life has thrown at me, you are always there, making me laugh, inspiring me and just being you! I love you tons!

To my little family, Kiko and Bootsy, thank you for your unwavering support over the past 17 years. Thank you for traveling across the west coast with me, for feeding me and for keeping me grounded. Most importantly thank you for your presence, which

has allowed me to grow into a confident version of myself—one who is unafraid to seize new opportunities and take more chances. I could not have done this without you.

Para mi madrecita hermosa, en esta vida no tengo las palabras suficientes para darte las gracias por todo lo que as hecho por mí y por mis hermanos. Lo único que tengo, es la fortaleza de seguir adelante para cumplir los sueños que tú y mi papá querían para nosotros y así poder darte todo lo que una madre como tú se merece. ¡Ama, tú siempre serás la persona más importante en mi vida, y quiero que sepas que siempre has sido tú la fuerza impulsora de mis éxitos y por eso y más te doy las gracias! ¡Te amo con mi alma!

To my brothers and sisters, everything I do is for you guys and mom. Thank you for always supporting and believing in me. It has been a long journey, but WE did it!

ABSTRACT OF THE DISSERTATION

Measuring the Succession, Functions and Resilience of Soil Microbes
After a
Chaparral Wildfire

by

Martha Fabiola Pulido-Chavez

Doctor of Philosophy, Graduate Program in Plant Pathology
University of California, Riverside, December 2023
Dr. Sydney I. Glassman, Chairperson

The increasing frequency and severity of wildfires worldwide have raised significant interest in understanding secondary successional and functional dynamics of post-fire microbes, bacteria, and fungi. It is well-known that wildfires alter microbial communities and the soil environments, resulting in a system dominated by pyrophilous "fire-loving" Ascomycetes and an environment rich in bioavailable nitrogen and chemically complex carbon (C), primarily in the form of highly aromatic pyrogenic organic matter (PyOM). Despite this knowledge, there is a gap in our understanding of microbial succession, their recovery rate, and whether post-fire microbes are equipped to degrade post-fire resources. To fill this knowledge gap, we performed the first fine-scale temporal study of post-fire soils, spanning 4.5 years from 17 days to 44 months, in a Southern California Chaparral ecosystem. We assessed biomass of bacteria with qPCR of 16S and fungi with 18S and richness and composition with Illumina MiSeq sequencing of

16S and ITS2 amplicons. We found that 1) wildfire decreased bacterial and fungal biomass and richness. Moreover, we found that post-fire microbes experienced rapid secondary succession, mirroring plant successional dynamics. Whereby succession was driven by putative tradeoffs in thermotolerance, colonization, and competition among dominant pyrophilous bacteria, *Massilia* and *Noviherbaspirillum,* and fungal *Aspergills, Pyronema,* and *Penicillium.* 2) Genes for PyOM degradation and N cycling increased over time, mirroring the rise in bacterial and fungal taxa within the first post-fire. Moreover, *Massilia* and *Noviherbaspirillium* exhibit distinct PyOM and N processing pathways, suggesting that specific traits related to post-fire resource acquisition and wildfire adaptation drive microbial secondary succession. 3) Bacteria demonstrated higher resistance and resilience, returning to pre-fire levels within 4.5 years due to the influence of multiple abiotic factors and vegetation recovery. In contrast, fungi had still not recovered from the effects of wildfire. Lastly, our study revealed that bacterial and fungal richness is linked to recovering vegetation and soil biogeochemistry. Together, our findings highlight the adaptability of ecological theories to soil microbes and indicate that dominant microbes likely facilitate microbial recovery during secondary succession. Our research has essential implications, such as providing long term monitoring of post-fire bacterial and fungal species, vegetation, and soil geochemical variables, while providing a list of pyrophilous bacterial and fungal taxa that could help inform ecological restoration and post-fire management strategies in global fire-affected regions.

Table of Contents

List of Figures

List of Tables

Chapter I

General Introduction

1.1 Wildfires

High-severity wildfires are an essential and natural component of chaparral ecosystems (Bond *et al.*, 2005; Burkle *et al.*, 2015) driving secondary succession (Hanes, 1971; Vogl, 1981; Keeley *et al.*, 2005) and maintaining ecosystem health. Historically, chaparral burns every 30-60 years (Hanes, 1971; Safford & Van de Water, 2014). However, changes in land-use patterns, previous management decisions, and climate change have altered the natural fire regime of this system, resulting in more frequent wildfires (10-20 years) (Hanes, 1971; Safford & Van de Water, 2014). Consequently, increased fire frequency alters the resilience (rate of recovery) of chaparral (Hanes, 1971; Safford & Van de Water, 2014) and threatens type conversion from fire-resistant shrubs to flammable invasive grasses (Keeley & Brennan, 2012). Due to the coevolution of

chaparral with wildfires, the impact of fire on plants and their secondary succession (changes in abundance and composition over time) is relatively well understood (Hanes, 1971; Vogl, 1981; Keeley *et al.*, 2005). However, the effect of wildfires on soil microbes and their functions remains highly understudied especially in dryland ecosystems which cover 41% of the terrestrial Earth surface (Feng & Fu, 2013). In California, these drylands are exemplified by the iconic chaparral ecosystem, covering 70% of federal lands in Southern California (Underwood *et al.*, 2018). However, despite extensive research on wildfire effects and ecosystem resilience in vegetation (Allen *et al.*, 2018; Syphard *et al.*, 2019), the dominant plant species in chaparral, such as manzanita (*Arctostaphylos glandulosa*) and chamise (*Adenostoma fasciculatum*), form mycorrhizal associations (Van der Heijden *et al.*, 1998; Baldrian, 2016), yet we lack understanding of the microbial pos-fire resilience dynamics. Understanding microbial response to wildfire and microbial functions will be vital to predicting the impact of changing fire regimes on chaparral, its resilience, its impact on chaparral carbon (C) and nitrogen (N) storage , and greenhouse gas emissions (Goodridge *et al.*, 2018).

1.2 Importance of soil microbes

Soil bacteria and fungi are among the most critical components of terrestrial environments, essential for ecosystem functions such as decomposition, nutrient cycling, and post-disturbance ecosystem recovery via symbiotic associations with the dominant vegetation (Van der Heijden *et al.*, 1998; Baldrian, 2016; Crowther *et al.*, 2019).

However, wildfires can affect the subsequent structure of the microbial communities directly via heat-induced mortality (Hart *et al.*, 2005) and indirectly via changes to the soil biogeochemical characteristics, such as increased soil temperature and soil pH, and decreased soil moisture and decomposition rates (Neary *et al.*, 1999). Since both manzanita and chamise, form mycorrhizal associations (Allen *et al.*, 2005), to properly understand vegetation succession, we must understand the response of the soil microbial community. Post-fire soil microbial research is historically biased toward pine forests, largely ignoring shrubland ecosystems (Dove & Hart, 2017). Moreover, microbial communities change rapidly, and determining microbial resilience (Allison & Martiny, 2008) requires immediate post-fire sampling over multiple time points. Existing research on post-fire fungi is mainly based on single time point measurements that occur on average two years post-fire (Dove & Hart, 2017; Pressler *et al.*, 2019), thereby missing fine-scale microbial succession, which may be critical for predicting post-fire plant and biogeochemical trajectories. Furthermore, bacteria are important members of the soil community, actively driving the soil N cycle. Yet, less than 3% of studies looking at wildfire effects on soil microbial communities have historically accounted for bacteria (Pressler *et al.*, 2019), thus underestimating wildfire impacts.

1.3 Effects of wildfire on soil microbes

Wildfires have been shown to reduce microbial biomass and richness (Pressler *et al.*, 2019), and chronosequence studies indicate that ectomycorrhizal resilience requires

15-18 years to return to unburned levels (Treseder *et al.*, 2004; Kipfer *et al.*, 2011). Although this information gives us a theoretical background to make predictions on the potential recovery rate of fungi in burned systems, the predictability is limited to ectomycorrhizal fungi in pine forests, thus missing a large portion of the fungal community and the entirety of the bacterial community. Furthermore, the absence of temporal soil sampling in post-fire systems has restricted our comprehension of microbial turnover rates. Additionally, we lack understanding about what environmental variables drive microbial community recovery. Given that chaparral is adapted to low frequency, high-severity wildfires, it is likely that their soil microbial communities evolved under similar selective pressures. Therefore, the loss of ecosystem resilience and type conversion may reflect post-fire changes to soil microbes. Thus, it is crucial to understand what environmental variables drive the post-fire changes in the microbial community and its resilience, allowing for a more holistic understanding of the drivers of vegetation regeneration and soil nutrient cycling.

1.4 Wildfire effects on vegetation and soil nutrients

Soil C and N pools are recognized as fundamental to post-fire vegetation recovery (DeBano *et al.*, 1979; Johnson & Curtis, 2001; Wan *et al.*, 2001; Caon *et al.*, 2014). Fires can have both negative and positive impacts on soil C storage. Fires cause immediate C losses through combustion (Certini, 2005), but the incomplete combustion of vegetation can lead to the formation of pyrogenic organic matter (PyOM), which is difficult for

microbes to decompose and may be a missing sink in the global C cycle (Santin *et al.*, 2015). Fires often lead to reduced decomposition rates by reducing microbial biomass and altering fungal composition (Semenova-Nelsen *et al.*, 2019). Finally, fires can cause a short-term enrichment of bioavailable N (Johnson & Curtis, 2001), which may amplify nitrous oxide emissions (N_2O; a greenhouse gas with 200x the warming potential of CO_2) (Niboyet *et al.*, 2011). Given that both C and N cycles are closely coupled with microbial metabolism (Gougoulias *et al.*, 2014), uncovering how fires and their interactions with shifting microbial communities influence C and N cycling is a significant knowledge gap critical for predicting climate change feedbacks and post-fire ecosystem regeneration.

1.5 Overview of dissertation and objectives

While it is clear that fires reduce microbial biomass (Dooley & Treseder, 2012) and richness (Pressler *et al.*, 2019), fire also selects for pyrophilous (fire loving) microbes that significantly increase in frequency post-fire (Whitman *et al.*, 2019; Bruns *et al.*, 2020; Fox *et al.*, 2022). These microbes can survive wildfires and thrive in a post-fire environment by various mechanisms, including thermotolerant spores, rapid colonization, and capitalizing on post-fire resources (Whitman *et al.*, 2019; Enright *et al.*, 2022). For example, researchers in Mediterranean oak woodlands in Spain found that genes necessary for N incorporation increased post-fire, showing that microbes can upregulate genes to process increased post-fire bioavailable N (Cobo-Díaz *et al.*, 2015). Hence, it is possible that microbial secondary succession is driven by the taxa that survive and can

rapidly inhabit the sites (pyrophilous microbes) and can capitalize on the flush of bioavailable nutrients. This dissertation aims to comprehensively explore the temporal dynamics of pyrophilous microbes in high resolution after fires, examining their abundance shifts, their utilization of post-fire bioavailable N, and the intricate processing of chemically complex PyOM. Additionally, it aims to determine the factors driving microbial resilience and recovery. This research will increase our understanding of the biogeochemical impacts of fire, enable predictions of post-fire ecosystem recovery, and potentially enable us to select microbes to apply for desired ecosystem outcomes.

1.6 Overarching goals

The aim of this dissertation is to address the following overarching objectives:

Objective 1: Examine bacterial and fungal biomass, richness, and succession at high temporal resolution in the first year after a chaparral wildfire.

Objective 2: Use metagenomics to determine the functions of pyrophilous microbes in C and N cycling and how they change over time in the first year post-fire.

Objective 3: Determine the factors predicting bacterial and fungal resilience to chaparral wildfires and link them to changes in vegetation and soil nitrogen concentrations.

1.7 References

Allen EB, Williams K, Beyers JL, Phillips M, Ma S, D'Antonio CM 2018. Chaparral Restoration. In: Underwood EC, Safford HD, Molinari NA, Keeley JE eds. *Valuing Chaparral: Ecological, Socio-Economic, and Management Perspectives*. Cham: Springer International Publishing, 347-384.

Allen MF, Egerton-Warburton L, Treseder K, Cario CH, Lindahl A, Lansing J, Querejeta J, Kårén O, Harney S, Zink T. 2005. Biodiversity of Mycorrhizal Fungi in Southern California. Planning for Biodiversity: Bringing Research and Management Together Proceedings of a Symposium for the South Coast Ecoregion: U.S. Department of Agriculture, Forest Service, Pacific Southwest Research Station.

Allison SD, Martiny JBH. 2008. Resistance, resilience, and redundancy in microbial communities. *Proceedings of the National Academy of Sciences* **105**(Supplement 1): 11512-11519.

Baldrian P. 2016. Forest microbiome: diversity, complexity and dynamics. *FEMS Microbiology Reviews*: fuw040.

Bond WJ, Woodward FI, Midgley GF. 2005. The global distribution of ecosystems in a world without fire. *New Phytologist* **165**(2): 525-538.

Bruns TD, Chung JA, Carver AA, Glassman SI. 2020. A simple pyrocosm for studying soil microbial response to fire reveals a rapid, massive response by Pyronema species. *PLoS One* **15**(3): e0222691.

Burkle LA, Myers JA, Belote RT. 2015. Wildfire disturbance and productivity as drivers of plant species diversity across spatial scales. *Ecosphere* **6**(10): art202.

Caon L, Vallejo VR, Ritsema CJ, Geissen V. 2014. Effects of wildfire on soil nutrients in Mediterranean ecosystems. *Earth-Science Reviews* **139**: 47-58.

Certini G. 2005. Effects of fire on properties of forest soils: a review. *Oecologia* **143**(1): 1-10.

Cobo-Díaz JF, Fernández-González AJ, Villadas PJ, Robles AB, Toro N, Fernández-López M. 2015. Metagenomic Assessment of the Potential Microbial Nitrogen Pathways in the Rhizosphere of a Mediterranean Forest After a Wildfire. *Microbial Ecology* **69**(4): 895-904.

Crowther TW, van den Hoogen J, Wan J, Mayes MA, Keiser AD, Mo L, Averill C, Maynard DS. 2019. The global soil community and its influence on biogeochemistry. *Science* **365**(6455): eaav0550.

DeBano LF, Rice RM, Eugene CC. 1979. Soil heating in chaparral fires: Effects on soil properties, plant nutrients, erosion, and runoff. . *PSW-RP-145 U.S. Department of Agriculture Forest Service, Pacific Southwest Forest and Range Experiment Station.* **145**: 21.

Dooley SR, Treseder KK. 2012. The effect of fire on microbial biomass: a meta-analysis of field studies. *Biogeochemistry* **109**(1/3): 49-61.

Dove NC, Hart SC. 2017. Fire Reduces Fungal Species Richness and In Situ Mycorrhizal Colonization: A Meta-Analysis. *Fire Ecology* **13**(2): 37-65.

Enright DJ, Frangioso KM, Isobe K, Rizzo DM, Glassman SI. 2022. Mega-fire in Redwood Tanoak Forest Reduces Bacterial and Fungal Richness and Selects for Pyrophilous Taxa that are Phylogenetically Conserved. *Molecular Ecology*.

Feng S, Fu Q. 2013. Expansion of global drylands under a warming climate. *Atmospheric Chemistry and Physics* **13**(19): 10081-10094.

Fox S, Sikes BA, Brown SP, Cripps CL, Glassman SI, Hughes K, Semenova-Nelsen T, Jumpponen A. 2022. Fire as a driver of fungal diversity — A synthesis of current knowledge. *Mycologia* **114**(2): 1-27.

Goodridge BM, Hanan EJ, Aguilera R, Wetherley EB, Chen Y-J, D'Antonio CM, Melack JM. 2018. Retention of Nitrogen Following Wildfire in a Chaparral Ecosystem. *Ecosystems* **21**(8): 1608-1622.

Gougoulias C, Clark JM, Shaw LJ. 2014. The role of soil microbes in the global carbon cycle: tracking the below-ground microbial processing of plant-derived carbon for manipulating carbon dynamics in agricultural systems. *J Sci Food Agric* **94**(12): 2362-2371.

Hanes TL. 1971. Succession after Fire in the Chaparral of Southern California. *Ecological Monographs* **41**(1): 27-52.

Hart SC, DeLuca TH, Newman GS, MacKenzie MD, Boyle SI. 2005. Post-fire vegetative dynamics as drivers of microbial community structure and function in forest soils. *Forest Ecology and Management* **220**(1): 166-184.

Johnson DW, Curtis PS. 2001. Effects of forest management on soil C and N storage: meta analysis. *Forest Ecology and Management* **140**(2-3): 227-238.

Keeley JE, Brennan TJ. 2012. Fire-driven alien invasion in a fire-adapted ecosystem. *Oecologia* **169**(4): 1043-1052.

Keeley JE, Fotheringham CJ, Baer-Keeley M. 2005. Determinants of Postfire Recovery and Succession in Mediterranean-Climate Shrublands of California. *Ecological Applications* **15**(5): 1515-1534.

Kipfer T, Moser B, Egli S, Wohlgemuth T, Ghazoul J. 2011. Ectomycorrhiza succession patterns in Pinus sylvestris forests after stand-replacing fire in the Central Alps. *Oecologia* **167**(1): 219-228.

Neary DG, Klopatek CC, DeBano LF, Ffolliott PF. 1999. Fire effects on belowground sustainability: a review and synthesis. *Forest Ecology and Management* **122**(1-2): 51-71.

Niboyet A, Brown JR, Dijkstra P, Blankinship JC, Leadley PW, Le Roux X, Barthes L, Barnard RL, Field CB, Hungate BA. 2011. Global Change Could Amplify Fire Effects on Soil Greenhouse Gas Emissions. *PLoS One* **6**(6): e20105.

Pressler Y, Moore JC, Cotrufo MF. 2019. Belowground community responses to fire: meta-analysis reveals contrasting responses of soil microorganisms and mesofauna. *Oikos* **128**(3): 309-327.

Safford HD, Van de Water KM. 2014. Using fire return interval departure (FRID) analysis to map spatial and temporal changes in fire frequency on national forest lands in California. Albany, CA: U.S. Department of Agriculture, Forest Service, Pacific Southwest Research Station.

Santin C, Doerr SH, Preston CM, Gonzalez-Rodriguez G. 2015. Pyrogenic organic matter production from wildfires: a missing sink in the global carbon cycle. *Glob Chang Biol* **21**(4): 1621-1633.

Semenova-Nelsen TA, Platt WJ, Patterson TR, Huffman J, Sikes BA. 2019. Frequent fire reorganizes fungal communities and slows decomposition across a heterogeneous pine savanna landscape. *New Phytologist* **224**(2): 916-927.

Syphard AD, Brennan TJ, Keeley JE. 2019. Extent and drivers of vegetation type conversion in Southern California chaparral. *Ecosphere* **10**(7): e02796.

Treseder KK, Mack MC, Cross A. 2004. Relationships Among Fires, Fungi, and Soil Dynamics in Alaskan Boreal Forests. *Ecological Applications* **14**(6): 1826-1838.

Underwood EC, Franklin J, Molinari NA, Safford HD. 2018. Global Change and the Vulnerability of Chaparral Ecosystems. *The Bulletin of the Ecological Society of America* **99**(4).

Van der Heijden MGA, Klironomos JN, Ursic M, Moutoglis P, Streitwolf-Engel R, Boller T, Wiemken A, Sanders IR. 1998. Mycorrhizal fungal diversity determines plant biodiversity, ecosystem variability and productivity. *Nature* **396**(6706): 69-72.

Vogl RJ 1981. Chaparral Succession.

Wan S, Hui D, Luo Y. 2001. Fire Effects on Nitrogen Pools and Dynamics in Terrestrial Ecosystems: A Meta-Analysis. *Ecological Applications* **11**(5): 1349-1365.

Whitman T, Whitman E, Woolet J, Flannigan MD, Thompson DK, Parisien M-A. 2019. Soil bacterial and fungal response to wildfires in the Canadian boreal forest across a burn severity gradient. *Soil Biology and Biochemistry* **138**: 107571.

Chapter II

Rapid bacterial and fungal successional dynamics in first year after chaparral wildfire

2.1 Abstract

The rise in wildfire frequency and severity across the globe has increased interest in secondary succession. However, despite the role of soil microbial communities in controlling biogeochemical cycling and their role in the regeneration of post-fire vegetation, the lack of measurements immediately post-fire and at high temporal resolution has limited understanding of microbial secondary succession. To fill this knowledge gap, we sampled soils at 17, 25, 34, 67, 95, 131, 187, 286, and 376 days after a southern California wildfire in fire-adapted chaparral shrublands. We assessed bacterial and fungal biomass with qPCR of 16S and 18S and richness and composition with Illumina MiSeq sequencing of 16S and ITS2 amplicons. Fire severely reduced bacterial biomass by 47%, bacterial richness by 46%, fungal biomass by 86%, and fungal richness by 68%. The burned bacterial and fungal communities experienced rapid succession, with

5-6 compositional turnover periods. Analogous to plants, turnover was driven by "fire-loving" pyrophilous microbes, many of which have been previously found in forests worldwide and changed markedly in abundance over time. Fungal secondary succession was initiated by the Basidiomycete yeast *Geminibasidium*, which traded off against the filamentous Ascomycetes *Pyronema*, *Aspergillus*, and *Penicillium*. For bacteria, the Proteobacteria *Massilia* dominated all year, but the Firmicute *Bacillus* and Proteobacteria *Noviherbaspirillum* increased in abundance over time. Our high-resolution temporal sampling allowed us to capture post-fire microbial secondary successional dynamics and suggest that putative tradeoffs in thermotolerance, colonization, and competition among dominant pyrophilous microbes control microbial succession with possible implications for ecosystem function.

2.2 Introduction

The rapid increase in wildfire frequency, severity, and extent in the western United States (Riley & Loehman, 2016) and around the globe (Abatzoglou et al., 2019) has renewed interest in secondary succession. Secondary succession, or the trajectory along which an ecosystem develops following a disturbance, such as a wildfire, has been extensively studied for plants (Derroire et al., 2016; Donato et al., 2012), but belowground microbial communities have been comparatively overlooked. Understanding how wildfires alter soil microbial succession may be necessary to predict post-fire effects on ecosystem recovery and function since soil microbes drive post-fire

organic matter decomposition (Semenova-Nelsen et al., 2019), nutrient cycling (Pérez-Valera et al., 2020), and plant regeneration (Dove & Hart, 2017).

Plant succession is a major process affecting the health and function of ecosystems. During succession, the dominant species may change in an orderly and predictable manner (Shugart, 2013). For example, early colonizers (fast-growing, short-lived species) are often replaced by late colonizers (slow-growing, long-lived species). However, wildfire can reset the successional clock, shifting the course away from stability (Reilly & Spies, 2016) and initiating secondary succession. Plant secondary succession is often contingent on the surviving vegetation and seedbanks present in the heterogeneous post-fire landscape (Jain et al., 2008). While early plant establishment often happens in low competition and nutrient-rich environments (Dalling, 2008), succession is often mediated by the quantity and identity of early colonizers (i.e., dispersal limitations and priority effects) (Kennedy et al., 2009), and their tradeoffs for space and resources (Tilman, 1990). Indeed, the trajectory of species replacement suggests that early colonizers with similar resource use (i.e., overlapping niches) will dominate open space but will inevitably be replaced by late-stage species with differentiation in resource use (i.e., complementarity), allowing for species coexistence (Pacala et al., 1996; Turnbull et al., 2013). This later-stage community is often considered stable, characterized by small fluctuations in community composition. However, whether the patterns recognized in plant successional theory translate to belowground soil microbes remains unclear.

Research on post-fire soil microbiomes suggests that fires can reset microbial successional trajectories via fire-induced mortality (Hart et al., 2005), changes in microbial richness and biomass (Dooley & Treseder, 2012; Pressler et al., 2019), and the replacement of fungal basidiomycetes and symbiotic mycorrhizal fungi with ascomycetes and saprobic fungi (Cairney & Bastias, 2007; Fox et al., 2022). For over a century, pyrophilous or "fire-loving" fungi have been consistently found in post-fire mushroom surveys (McMullan-Fisher et al., 2011; Seaver, 1909). More recently, next-generation sequencing indicates that the pyrophilous Ascomycete *Pyronema* can increase 100-fold after prescribed fires (Reazin et al., 2016) and dominate over 60% of the sequences in experimental pyrocosms (Bruns et al., 2020). Furthermore, there is increasing evidence of pyrophilous bacteria, such as the Proteobacteria *Massilia* (Enright et al., 2022; Whitman et al., 2019). This evidence suggests that pyrophilous microbes in systems that have evolved with wildfire (Dove et al., 2021) might have fire adaptations analogous to plants (Rundel, 2018) and, thus, likely follow successional dynamics akin to plants. Pyrophilous microbes have traits that allow them to survive fires (e.g., heat resistant spores, sclerotia) (Day et al., 2020; Petersen, 1970) and the post-fire environment (e.g., xerotolerance, affinity for nitrogen mineralization, and affinity for aromatic hydrocarbon degradation) (Fischer et al., 2021; Nelson et al., 2022; Steindorff et al., 2021). Moreover, since heat from fire often penetrates only the top few cm of soil (Neary et al., 1999; Pingree & Kobziar, 2019), like plants, secondary succession may be initiated by surviving microbes that make up the spore bank (Baar et al., 1999; Glassman et al., 2016). Currently, most research evaluating post-fire microbiomes is based on single timepoint sampling (Dove &

Hart, 2017; Pressler et al., 2019); thus, the succession of pyrophilous microbes is nearly unknown. However, recent research consisting of 2-3 sampling time points suggests that bacteria and fungi experience rapid post-fire community changes (Ferrenberg et al., 2013; Qin & Liu, 2021; Whitman et al., 2022), indicating that higher temporal resolution sampling is needed to understand bacterial and fungal successional trajectories.

Predicting soil microbial succession can be complicated by direct and indirect wildfire effects (Neary et al., 1999). Whereas soil burn severity controls direct fire impacts (Reazin et al., 2016; Whitman et al., 2019), changes in soil moisture can indirectly impact post-fire microbes (Placella et al., 2012; Yang et al., 2021), potentially driving succession, especially in arid environments where precipitation is limited. Previous research has established that bacteria rapidly respond to soil wet-up (Barnard et al., 2013; Placella et al., 2012), whereas fungi are less responsive to soil moisture changes (Barnard et al., 2013; Evans & Wallenstein, 2012). Furthermore, microbial life strategies can determine microbial response to fire. Research shows that fire decreases the richness of ectomycorrhizal fungi (EMF) (Cowan et al., 2016; Glassman et al., 2016; Pulido-Chavez et al., 2021) and arbuscular fungi (AMF) (Xiang et al., 2015), but can temporarily increase saprobic richness (Enright et al., 2022; Semenova-Nelsen et al., 2019). Yet, the limited studies on how fires affect multiple microbial guilds (Certini et al 2021) lack the resolution to identify the direct effect of wildfire and the length of time that mycorrhizal fungi survive after a wildfire, a question essential for post-fire ecosystem recovery.

We propose that microbial ecological succession theory can be developed and tested in nature by focusing on California chaparral. Chaparral is a shrubland adapted to high-severity fire and a biodiversity hotspot distributed in Mediterranean climates worldwide (Barro & Conard, 1991; Rundel, 2018). Chaparral plant secondary succession is relatively well understood and typically initiated by fire (Keeley et al., 2005). Yet, although the dominant chaparral vegetation forms mycorrhizal associations required for their establishment and survival (Allen et al., 2005), little is known about chaparral microbial succession. Indeed, only 13% of post-fire microbiome research occurs in shrublands (Pressler et al., 2019). With drylands covering nearly 41% of Earth's land surface and expanding with climate change (Feng & Fu, 2013), understanding secondary successional dynamics in dryland systems such as chaparral is critical (Osborne et al., 2022). While our focus is on chaparral, which is likely to have fire-adapted microbes due to chaparrals' evolutionary history with fire (Hanes, 1971), we expect that successional patterns will be broadly generalizable to other biomes since pyrophilous bacteria and fungi appear to be phylogenetically conserved (Enright et al., 2022). Indeed, fungal taxa within the Ascomycota family Pyronemataceae and a few Basidiomycota genera appear to be globally distributed in fire-disturbed Spanish shrublands (Pérez-Valera et al., 2018) and Pinaceae (Reazin et al., 2016; Whitman et al., 2019; Xiang et al., 2014), Eucalyptus (Ammitzboll et al., 2022; McMullan-Fisher et al., 2011), and redwood-tanoak forests (Enright et al., 2022).

Here, we performed the highest-resolution temporal sampling of post-fire microbiomes to date. We sampled soils at nine timepoints over one year following a

chaparral wildfire, allowing us to identify immediate and temporal effects of wildfire on microbial successional dynamics and test the following hypotheses: (H1) wildfire will decrease bacterial and fungal biomass and richness, leading to a shift in the community composition one year post-fire; (H2) wildfire will have a distinct impact on fungal guilds with symbiotic mycorrhizal fungi experiencing the largest declines; (H3) higher soil burn severity will lead to larger reductions in both bacteria and fungi while precipitation will impose a larger impact on bacterial than fungal succession; (H4) succession will be initiated by pyrophilous microbes, which like plants, will change in abundance over time based on differences in ecophysiological traits such as growth and nutrient acquisition.

2.3 Methods

2.3.1 Study Area, plot design, and soil collection

The Holy Fire burned 94 km^2 in the Cleveland National Forest in Southern California from August 6 to September 13, 2018. On September 30, 2018, we selected nine plots (6 burned and 3 unburned) (Fig. 2.1a). Plots were selected for similarity in aspect, slope, elevation, and pre-fire vegetation dominance by manzanita (Arctostaphylos glandulosa), an ectomycorrhizal host, and chamise (Adenostoma fasciculatum), an arbuscular and ectomycorrhizal host (Allen et al., 2005). Plots were placed on average 25 m from forest access roads (10-40 m) to avoid edge effects, and each contained four 1 m^2 subplots located 5 m from the center in each cardinal direction (Fig. 2.1b). Our study site experiences a Mediterranean-type climate with hot, dry summers and cool, wet winters,

with an average yearly temperature of 17˚C and total precipitation of 668 mm (average 51.39 mm). Precipitation data, based on monthly summaries, was gathered from the El Cariso weather station (raws.dri.edu). Soils are mapped in the Cieneba and Friant series and are classified as Typic Xerorthents and Lithic Haploxerolls. They are sandy and gravelly loams with an average pH of 6.8 for the burned plots and 6.2 for the unburned plots (additional plot information in Table S1). Although soil types differ, soil type did not affect bacterial or fungal biomass or richness (glmer.nb; $p > 0.05$).

We used BAER soil burn severity maps created within seven days after fire containment (https://burnseverity.cr.usgs.gov) to locate plots within moderate burn severity (Fig. 2.1a). Notably, the BAER coarse-scale measurement (30 m) does not coincide well with the spatial distribution and turnover rate of soil microbial communities (Bahram et al., 2013). Since ash depth increases with soil heating (Parson et al., 2010) and fire severity (Bodí et al., 2014), we used ash depth as a proxy for soil burn severity by averaging three separate measurements of ash depth (cm) per each 1 m^2 subplot (Fig. 2.1c). Since ash can be rapidly redistributed via post-fire wind and rain (Bodí et al., 2014), we measured ash before any precipitation event (first rains occurred on Oct 3) or high wind events (average wind Sept 3 -Sept 17 was 2.7 m/s). Hence, our measure of soil burn severity refers to initial ash depth.

We sampled soils at 17, 25, 34, 67, 95, 131, 187, 286, and 376 days, corresponding to approximately 2 and 3 weeks, and 1, 2, 3, 4, 6, 9, and 12 months post-fire. At each of the nine time points, we collected the top 10 cm of mineral soil (A horizons) beneath the ash layer from each burned subplot. Since wildfire results in the

combustion of the organic layer, to ensure homogeneity in sampling and direct comparison between treatments in the unburned plots, we removed the litter layer before sampling A horizons (Pulido-Chavez et al., 2021). Soils were collected with a ~250 mL releasable bulb planter cleaned with ethanol after each use to prevent cross-contamination, resulting in 36 soil samples (9 plots x 4 subplots) per sampling time point. Soils were transported in individual Whirl-Paks in a cooler to the University of California-Riverside (UCR) within hours of sampling, stored overnight at 4˚C, and sieved (2mm) at room temperature in ethanol cleaned sieves within 24 hours of sampling to minimize microbial community turnover (Phillips, 2021). A subsample was frozen at -80°C for future DNA extraction. While soils were stored at -80°C from 1 month to 1 year before DNA extractions were performed, differences in storage time at -80°C do not affect DNA quantity and integrity (Lauber et al., 2010; Pavlovska et al., 2021).

2.3.2 DNA extraction, amplification, and sequencing

DNA extractions for all nine timepoints were performed in the summer of 2019. Soils were weighed (0.25 g) using ethanol-cleaned spatulas and processed using Qiagen DNeasy PowerSoil Kits following the manufacturer's protocol, with an increase in centrifugation time to 1.5 min after adding the C3 solution (a solution used to precipitate the organic and inorganic matter) due to large amounts of precipitate still in the solution, then stored at -20˚C. Extracted DNA was amplified using the primer pair ITS4-fun and 5.8s to amplify the ITS2 region for fungi (Taylor et al., 2016) and the primer pair 515F-806R to amplify the V4 region of the 16S rRNA gene for archaea and bacteria (Caporaso

et al., 2011) using the Dual-Index Sequencing Strategy (DIP) (Kozich et al., 2013). Although our 16S primers amplify archaea and bacteria, for simplicity, we refer to 16S methods and results simply as bacteria since archaea only contributed <1% of sequencing reads. We conducted polymerase chain reaction (PCR) in two steps. The first PCR amplified gene-specific primers, and the second PCR ligated the DIP barcodes and adaptors for Illumina sequencing. For bacteria, we combined 1 µL of 1:10 diluted DNA, 10.5 µL of Ultra-Pure Sterile Molecular Biology Grade water (Genesee Scientific, San Diego, CA, USA), 12.5 µL of AccuStart ToughMix (2x concentration; Quantabio, Beverly, MA, USA), and 0.5 µL each of the 10 µM 515F and 806R primers. Thermocycler conditions for PCR1 were: 94°C for 2 min followed by 29 cycles of 94°C for 30 s, 55°C for 30 s, 68°C for 1 min, followed by a 2 min extension at 68°C. For fungi, we combined 5 µL of undiluted DNA, 6.5 µL of ultra-pure water, 12.5 µL of AccuStart ToughMix, and 0.5 µL each of the 10 µM ITS4-fun and 5.8s primers. Thermocycler conditions for PCR1 were: 94 °C for 2 min, followed by 30 cycles of 94 °C for 30 s, 55 °C for 30 s, 68 °C for 2 min, followed by a 10 min extension at 68°C. PCR1 products were cleaned with AMPure XP magnetic beads (Beckman Coulter Inc., Brea, CA), following the manufacturer's protocols. The DIP PCR2 primers containing the barcodes and adaptors for Illumina sequencing were ligated to the amplicons during the second PCR step in a 25 µL reaction containing 2.5 µL of the 10 µM DIP PCR2 primers, 6.5 µL of ultra-pure water, 12.5 µL of Accustart ToughMix, and 1 µL of PCR1 product. Thermocycler conditions for PCR2 for bacteria and fungi were: 94°C for 2 min followed by 10 cycles of 94°C for 30 s, 60°C for 30 s, and 72°C for 1 min. Bacterial and fungal

PCR products for the 324 samples (9 plots x 4 subplots x 9 timepoints) were then separately pooled based on gel electrophoresis band strength and cleaned with AMPure following established methods (Glassman et al., 2018). Each pool contained 2-3 timepoints from burned and unburned plots and was checked for quality and quantity with the Agilent Bioanalyzer 2100 before combining bacteria and fungi at a 2:3 ratio (0.4 units for bacteria to 0.6 units for fungi). Since each library only fit 2-3 timepoints for both bacteria and fungi, we sequenced the nine timepoints across four libraries with Illumina MiSeq 2x300bp at the UCR Institute for Integrative Genome Biology. In addition to our 324 experimental samples, we added negative DNA extractions and PCR controls from each time point and mock communities (ZymoBIOMICS microbial community standard, Zymo, Irvine, CA) to each library for additional quality control and inference.

2.3.4 Bacterial and fungal biomass

We estimated bacterial and fungal gene copy numbers with quantitative (q) PCR as a proxy for biomass using the Eub338/Eub518 primers for bacteria (Fierer et al., 2005) and FungiQuant-F/FungiQuant-R primers for fungi (Liu et al., 2012). For fungi, we used the small subunit since it is more conserved and has less length variation making it better suited for qPCR than the ITS2 region (Mayer et al., 2021), which is better at species-level identification (Schoch et al., 2012). We generated standard curves using a 10-fold serial dilution of the standards by cloning the 18S region of the fungus *Saccharomyces cerevisiae* or the 16S region of the bacteria *Escherichia coli* into puc57 plasmid vectors constructed by GENEWIZ, Inc. (NJ, USA) as previously established (Averill & Hawkes,

2016). The 10 µL qPCR reactions were performed in triplicate. Reactions contained 1 µL undiluted DNA, 1 µL of 0.05M Tris-HCl ph8.3, 1 µL of 2.5mM $MgCl_2$ (New England BioLabs (NEB); Ipswich, MA), 0.5 µL of 0.5mg/ml BSA, 0.5 µL of 0.25mM dNTP (NEB), 0.4 µL of both primers at 0.4µM, 0.5 µL of 20X Evagreen Dye (VWR International; Radnor, PA), 0.1 µL of Taq DNA polymerase (NEB) and 4.6 µL ultra-pure water. We employed the CFX384 Touch Real-Time PCR Detection System with the following conditions: 94˚C for 5 min, followed by 40 cycles of 94˚C for 20 seconds, 52˚C (for bacteria) or 50˚C (for fungi) for 30 seconds, followed by an extension at 72˚C for 30 seconds. Gene copy numbers were generated using the equation $10^{\wedge}$ (Cq-b)/m), using the quantification cycle (Cq), calculated as the average Cq value per sample in relation to the known/calculated copies in the Cq/threshold cycles, the y-intercept (b) and the slope (m) generated with CFX Maestro software. Values with an $R^2 > 0.994$ were considered acceptable. Gene copy numbers were normalized per gram of dry soil (Tatti et al., 2016). Notably, all methods of estimating microbial biomass have limitations (Gao et al., 2022), including qPCR, due to variation in target copy number (Lofgren et al., 2019; Song et al., 2014). However, the high sensitivity (Tellenbach et al., 2010) of qPCR for quantifying the selected marker gene (Smith & Osborn, 2009) makes it ideal for estimating microbial biomass from environmental samples when interest is not in species specificity but in estimates of total microbial biomass. Moreover, common biomass quantification methods for fungi are correlated (Cheeke et al., 2017).

2.3.5 Bioinformatics

Illumina data was processed with Qiime2 version 2020.8 (Bolyen et al., 2019). The demultiplexed fastQ files from the four Illumina sequencing runs were processed individually using cutadapt (Martin, 2011) to remove the primers and ran through DADA2 version 2020.8 with the defaults parameters to filter out and remove chimeric sequences and low-quality regions and to produce Amplicon Sequence Variants (ASVs) (Callahan et al., 2017). Reads were trimmed to a global quality control threshold (Q30), the benchmark for next-generation Illumina sequencing (Illumina, 2011). Bacteria forward reads were trimmed to 170 bp and reverse to 163 bp, while fungal forward reads were trimmed to 209 bp and the reverse reads to 201 bp. On average, 72% of forward and reverse sequences merged for bacteria, and 61% merged for fungi. DADA2 outputs from each library were combined into one library for downstream processing, including the removal of singletons and taxonomic assignments. We used SILVA version 132 for bacterial (Yilmaz et al., 2014) and UNITE version 8.2 for fungal (Abarenkov et al., 2020) taxonomic assignment using Qiime2 Naïve Bayes Blast+ classifier. Bacterial sequences assigned to mitochondria and chloroplasts and fungal sequences not assigned to Kingdom Fungi were removed. Fungal ASV tables were exported and parsed through FUNGuild (Nguyen et al., 2016) to assign functional ecological guilds, including only highly probable confidence rankings for AMF, EMF, saprotrophs, and pathogens. Moreover, negative and mock controls were inspected to ensure that sequences and/or ASVs in negative controls were negligible and that mock taxonomy correlated with known

communities. Sequences were submitted to the National Center for Biotechnology Information Sequence Read Archive under BioProject accession number PRJNA761539.

2.3.6 Statistical analysis

Acknowledging minor sequencing reads and a low number of ASVs across negative controls (Table S2), we took the conservative step of rarefying bacteria to a sequences/sample depth of 7,115 for bacteria and 11,480 for fungi, thus retaining the largest number of samples and sequencing depth within the dataset. Rarefaction removed all negative samples/controls. The four Illumina MiSeq runs resulted in 9.8 M bacterial and 24.6 M fungal sequences for an average of 31,052 bacterial and 78,202 fungal sequences/sample for downstream analysis. Fungal and bacterial alpha diversity was estimated using BiodiversityR version 2.14-2 (Kindt & Coe, 2005) with the following metrics: observed species richness, Simpson, Shannon, Chao1, ACE, Simpson's evenness, and Inverse Shannon. Although estimating richness from diverse soil communities has limitations (Willis et al., 2017), wildfire-affected soil constitutes low diversity communities, and patterns of species richness were similar across metrics (Fig. A.1.1). Thus, we focused on richness estimated as the number of observed ASVs after rarefaction for all downstream analyses. To test if wildfire decreased biomass and richness and if biomass and richness increased with time since fire (H1), if wildfire will have a distinct impact on fungal guilds (H2), and to determine if changes in biomass and richness are associated with precipitation and soil burn severity (H3), for both bacteria and fungi, we performed backward model selection and fitted nine statistical models with treatment (burned vs.

unburned), time (measured as days since fire), ash depth (cm), total monthly precipitation (mm), and second order interactions as predictors. We used generalized mixed effect models (glmer) with a negative binomial distribution in the MASS package version 7.3-57 (Venables & Ripley, 2002) to account for the over-dispersion of the data and the fact that the conditional variance was higher than the conditional mean (Bliss, 1953; Ross & Preece, 1985). Time since fire and precipitation were scaled and centered. The level of nestedness for all models was tested by running a null model with different nested levels (plot, subplot, and time since fire) and no predictors. Model selection was made using Akaike Information Criterion (AICc) in the MuMIN package version 1.46.0 (Barton, 2020). All richness models contained plot, subplot, and time since fire as random effects, and all biomass models included plot and time since fire as random effects. The subplot was not included for biomass analysis as it was not determined to be the best model (AIC selection). Pseudo R^2, or the variance explained (marginal and conditional) for all models, was calculated using the r.squaredGLMM function in the MuMIn Package.

We compared beta diversity by generating distance matrices with the vegan Avgdist function, calculating the square-root transformed median Bray-Curtis dissimilarity per 100 iterations. We used permutational multivariate analysis of variance (PERMANOVA) (Anderson, 2017) as implemented with the adonis function in vegan version 2.6-2 (Oksanen et al., 2018) to test for the significant effects of wildfire, time since fire, precipitation, ash depth, and second order interactions, on bacterial and fungal community composition overall. Moreover, we tested the significance of wildfire at each

independent time point (H1). Results were visualized using Non-Metric Multidimensional Scaling (NMDS) ordinations.

We employed several methods to quantify succession (H4). First, we visualized succession by characterizing community composition patterns at the genus level using phyloseq version 1.38.0 (McMurdie & Holmes, 2013) and grouping the relative abundance of the dominant ASVs (> 3% sequence abundance used for plot legibility) for each time point in burned and unburned communities independently. Second, we used the vegan mantel function to determine the correlation between temporal distance and community composition to determine how turnover varies in the presence or absence of fire, similar to a study examining Sorghum microbial succession (Gao et al., 2020). Third, to visualize spatial species turnover (Baselga, 2010), we took advantage of the fact that early successional periods display large variability (Collins, 1990; Pandolfi, 2008). Thus, we tested the homogeneity of the bacterial and fungal communities during succession using the vegan betadisper function to calculate the multivariate dispersion of Bray-Curtis dissimilarities and visualized the results using principal coordinates analysis (PCoA). Finally, we employed the codyn package version 2.0.5 (Hallett et al., 2016) to identify the patterns of community dynamics over successional time, including the rate of directional change, stability, and synchrony (Collins et al., 2000). Succession involves directional change via the replacement of early to late successional species (Clements, 1916; Platt & Connell, 2003); thus, we calculated the rate of directional change using the Euclidian distance of each microbial community. Then we measured species turnover to determine if species appearances or disappearances drive succession. Since stability

increases as diversity increases (diversity-stability hypothesis), we independently measured community stability in the burned and unburned plots as the mean abundance divided by the standard deviation at each temporal time point (Lehman & Tilman, 2000). However, community stability depends on species covariance over time; thus, we measured synchrony (Loreau & de Mazancourt, 2008), where perfect species synchrony is a value of 1 and 0 equals asynchrony (Valencia et al., 2020). Asynchrony can result in covariance in species populations, where tradeoffs among species can contribute to overall community stability.

All statistical analyses were conducted in R 4.1.1 (R Core Team, 2021), and plots were created with ggplot2 version 3.3.6 (Wickham, 2016). All statistical codes are available on GitHub https://github.com/pulidofabs/SecondarySuccession-Chaparral.

2.4 Results

2.4.1 Sequencing data

The four Illumina MiSeq runs resulted in 33,078 bacterial and 11,480 fungal ASVs. Compared to the experimental samples, bacterial negative controls, on average, had 10 ASVs, while fungal negative controls had 8 ASVs (Table S2). Rarefaction resulted in a total of 24,874 bacterial and 7,445 fungal ASVs, and the removal of all control samples. Extracting the fungal guilds from the rarefied fungal ASV table resulted in 208 EMF, 70 saprobic, 65 AMF, and 26 pathogenic fungal ASVs.

2.4.2 Wildfire effects on bacterial and fungal biomass and richness

Fire significantly reduced bacterial and fungal biomass and richness during the first post-fire year (Table S3). Fire had a larger effect on biomass than richness for both bacteria and fungi and larger effects on fungi than bacteria overall (Fig. 2.2). On average, across the year, fire reduced bacterial richness by 46% (Fig. A.1.1) and biomass by 47% (Fig. A.1.2a) and fungal richness by 68% (Fig. S1A) and biomass by 86% (Fig. A.1.2b). The direct, immediate effect of wildfire at 17 days post-fire was stronger for biomass than richness, with bacterial biomass decreasing by 84% (Fig. 2.2a) and fungal biomass by 97% (Fig. 2.2b; Table A.2.2). In contrast, at 17 days post-fire, fungal richness declined by 45% (Fig. 2.2d), but bacterial richness temporarily increased by 31% but declined by 29% at 25 days post-fire (Fig. 2.2c; Table A.2.2). While the differences in biomass and richness between the burned and unburned plots lessened with time since fire, one year was insufficient for bacterial and fungal biomass or richness to recover to unburned levels (Fig. 2.2). The effects of fire across time remained larger for fungi than for bacteria, with fungal biomass remaining 80% and richness 61% lower and bacterial biomass remaining 43% and richness 23% lower in the burned plots at 1-year post-fire (Fig. 2.2; Table A.2.2).

2.4.3 Fire directly and indirectly affects biomass and richness

Fire had direct, negative effects on bacterial and fungal biomass and richness. These direct effects were modified over time by positive interactions with fire for fungal biomass and with soil burn severity for fungal richness and bacterial biomass (Fig. 2.2;

Table A.2.4). Time since fire also directly positively impacted fungal richness (Table A.2.4). Soil burn severity had significant adverse direct effects on bacterial and fungal richness but no significant direct effects on biomass, meaning that biomass was equally reduced by fire regardless of severity (Figs. 2.2c,d; Table A.2.3). While precipitation had no significant direct effects, precipitation interacted with fire to positively impact bacterial biomass and fungal richness (Fig. 2.2a, d) but negatively affect bacterial richness (Fig. 2.2c; Table A.2.3).

2.4.4 Wildfire effects on the richness of different fungal guilds

Wildfire led to large and significant reductions in species richness for all fungal guilds (Fig. A.1.3; Table A.2.4), with the largest initial declines for AMF. On average, across time points, EMF decreased by 68%, pathogens by 71%, saprobes by 86%, and AMF by 98% in burned compared to unburned plots (Fig. A.1.3), and one year was insufficient for any guild to return to unburned levels (Fig. A.1.4). In fact, at 376 days, EMF were on average 91%, AMF 89%, pathogens 69%, and saprobes 61% lower in the burned plots (Fig. A.1.4). Ectomycorrhizal richness declined with soil burn severity and due to a fire and time interaction, whereas time since fire had a direct, negative effect on saprobic richness, which declined over time (Table A.2.4). Finally, an interaction between fire and precipitation negatively affected both EMF and pathogen richness (Table A.2.4).

2.4.5 Wildfire changes microbial community composition

Fire significantly affected bacterial and fungal community structure, explaining 13% of the compositional variation for bacteria and 10% for fungi (Fig. A.1.5). Time since fire had smaller impacts on community composition, explaining 4% of the variation for bacteria and 1% for fungi. Ash depth equally affected bacterial and fungal composition explaining 2% of the variance for both, whereas precipitation had slightly larger impacts on bacteria than fungi, explaining 3% of bacterial and 1% of the fungal variation (Table A.1.5). There were also small but significant interaction effects for both bacteria and fungi (Table A.1.5). Furthermore, community composition between burned and unburned plots significantly varied at all 9-time points for both bacteria (Fig. A.1.5) and fungi (Fig. A.1.6), with differences in community composition increasing over time from 12% to 21% for bacteria (Fig. A.1.5) and 9% to 13% for fungi (Fig. A.1.6) from day 17 to 376 post-fire. The overall changes in burned bacterial (Fig. A.1.4) and fungal composition (Fig. A.1.4a) were driven by the previously rare taxa, which increased in abundance over time (Fig. A.1.4b,d). Unlike fungi, burned bacterial communities were consistently dominated over time (57% average sequence abundance) by a single genus, the Proteobacteria *Massilia* (Fig. 4.4b). However, three Firmicutes quickly rose in dominance, with *Bacillus* (13%), an uncultured Clostridiales (26%), and *Paenibacillus* (4%) dominating at 34- and 67-days post-fire. Yet these Firmicutes rapidly declined as the Proteobacteria *Noviherbaspirillum* increased in abundance over time, from 1% at 34 days to 24% by the end of the year (Fig. 2.4b). For burned fungi, two Basidiomycetes that dominated at 17 days post-fire, the yeast *Geminibasidium* (45%) and the EMF *Inocybe*

(16%), rapidly declined while filamentous Ascomycetes increased over time (Fig. 2.4d). The genera *Pyronema* increased as *Geminibasidium* decreased and dominated from 25 to 95 days post-fire, peaking at 67 days post-fire with 67% sequence abundance. In addition, the Ascomycetes *Aspergillus* increased from 2% to 22% and *Penicillium* from 36% to 49% from 17 to 376 days post-fire (Fig. 2.4d).

2.4.6 Bacterial successional dynamics

Burned bacterial communities experienced rapid and distinct successional trajectories (Fig. 2.5a) at roughly double the rate of fungi (Fig. 2.5c,d) and were driven by six major compositional turnover points at 25, 34, 95, 131, 187, and 286 days (Fig. 2.5e). In contrast, the unburned bacterial communities experienced low dominance and remained stable over time (Fig. 2.6a) with no succession (Figs. 2,6c) or compositional turnover (Figs. 2.6e). These patterns are also reflected in the measures of successional dynamics (Table A.1.7). For example, burned bacterial communities experienced temporal changes in species composition that were directional and higher (0.16) than in the unburned communities (0.12; Table A.1.7). Burned bacterial communities also exhibited lower synchrony (0.03) than unburned communities (0.22), resulting in higher stability in burned (8.35) compared to unburned bacterial communities (5.36; Table A.1.7).

2.4.7 Fungal successional dynamics

Burned fungal communities experienced rapid and distinct successional

trajectories (Fig. 5B; Fig. 5D) that were driven by five major compositional turnover points at 25, 34, 67, 95, and 131 days post-fire (Fig. 2.5f). In contrast, the unburned fungal communities experienced low dominance (Fig. 2.6b) and remained stable over time with no succession (Fig. 2.6d) or compositional turnover (Fig. 2.6f). Like bacteria, these patterns were similarly reflected in the measures of successional dynamics (Table A.1.7) such that burned fungal communities had higher directional change (0.49) than the unburned communities (0.08), reflecting stronger patterns of succession as more species were introduced into the burned system. Burned fungal communities exhibited slightly lower synchrony (0.04) than unburned communities (0.05) but much lower community stability (6.42) than unburned communities (8.58), indicating higher susceptibility to change in burned fungal communities (Table A.1.7).

2.4.8 Taxa driving microbial succession

Bacterial and fungal succession was driven by taxa that traded off in abundance based on physiological traits, such as thermotolerance and fast colonization (Table 2.1). Early turnover events for bacteria (Fig. 2.5a) and fungi (Fig. 2.5b) in burned plots were driven by the disappearance of taxa, more so for bacteria (days 17-95) than fungi (days 17-25; Table A.2.6). Indeed, increased dominance by a few taxa, including the Firmicutes *Bacillus* at 25 days post-fire, *Paenibacillus* and *Domibacillus* (34-67 days), and the Proteobacteria *Noviherbaspirillum* (95 days), and the constant dominance of *Massilia* (34-286 days post-fire) resulted in the disappearance of early bacterial species, including RB41, *Conexibacter*, *Candidatus Udaeobacter*, and *Bacillus* over time (Fig. 2.5a; Table

A.2.6). In contrast, fungal succession was initiated by the rapid dominance of *Geminibasidium* and EMF genera that dominated the unburned communities, including *Inocybe*, *Cortinarius*, and *Tomentella* in the Basidiomycota and *Balsamia* in the Ascomycota and one previously rare Basidiomycete EMF genus *Mallocybe*, a subgenus of *Inocybe* (Fig. 2.5b, 2.6b). Interestingly, most species of EMF rapidly disappeared from the community at 25 days post-fire and were replaced by the constant dominance of *Pyronema*, *Penicillium*, and *Aspergillus* (Fig. 2.5b). However, as succession ensued, species appearance drove late-year successional turnover for bacteria (187-376 days; Fig. 2.5a) and mid-year successional turnover for fungi (67-187 days; 2.5b; Table A.2.6). For bacteria, the appearance of two Bacteroidetes, *Pedobacter* and *Adhaeribacter*, and the Actinobacteria *Blastococcus* shaped late-year (days 187-376) bacterial succession (Fig. 2.5a). For fungi, mid-year succession (days 95-187) was driven by the appearance of filamentous fungal Ascomycetes in the Pyronemataceae and the Sordariaceae genus *Gelasinospora*, and Basidiomycota mushroom-forming taxa (Fig. 2.5b). For example, the previously dominant EMF genus *Inocybe* remained in the community, but at a much lower abundance, declining with time since fire from 16% at 17 days to 0.1% at 376 days (Fig. 2.4d). In contrast, the pyrophilous Basidiomycete saprobes *Coprinellus* and *Tephrocybe*, which were rare in the unburned communities (<0.01% sequence abundance), appeared in the community later in the year (Fig. 2.5b). Late-year fungal succession (days 286-376) was driven by the increased dominance of *Tephrocybe* and *Aspergillus* and the Ascomycota *Rasamsonia*, and the decreased abundance of *Pyronema* (Fig. 2.5b).

2.5 Discussion

Here, we present the highest resolution temporal sampling of post-fire microbiomes to date, enabling us to show for the first time that bacteria and fungi experience rapid succession driven by the dominance of pyrophilous taxa that traded off in abundance over time (H4). Although our study was in California chaparral, many of the dominant pyrophilous taxa identified here also dominate other burned environments, including Spanish shrublands (Pérez-Valera et al., 2018) and pine (Bruns et al., 2020; Reazin et al., 2016), spruce (Whitman et al., 2019), Eucalyptus (Ammitzboll et al., 2022; McMullan-Fisher et al., 2011), and redwood-tanoak forests (Enright et al., 2022), indicating the generality of our results to wildfire-affected ecosystems. We found that wildfire decreased bacterial and fungal biomass and richness, leading to community composition shifts that persisted the entire year (H1). Fungal guilds were differentially affected by fire and time, with AMF and saprobes experiencing the largest immediate fire impacts, but over time, EMF experienced the largest declines (H2). Moreover, microbial richness and biomass changes were driven by multiple abiotic interactions, including interactions between time since fire, precipitation, and soil burn severity (H3).

2.5.*1 Wildfire decreased bacterial and fungal biomass and richness*

Fire decreased soil bacterial and fungal biomass and richness, corroborating previous post-fire studies in Mediterranean shrublands (Pérez-Valera et al., 2018) and forests (Dooley & Treseder, 2012). We noted a larger fire effect on fungal biomass and richness relative to bacteria, consistent with previous research showing that bacteria are

more resistant to fire than fungi (Certini et al., 2021; Glassman et al., 2021; Pourreza et al., 2014; Pressler et al., 2019). Although richness and biomass increased over time for both microbial groups, one year was insufficient for either group to recover to unburned levels, consistent with previous studies indicating that in shrublands, microbial biomass and richness recovery could take over two decades (Pérez-Valera et al., 2018). Interestingly, we observed a transient increase in bacterial richness directly post-fire, which may result from taxa such as the Actinobacteria genera *Soliribrobacter* and *Conexibacter* (Albuquerque & da Costa, 2014) that may be favored by the increase in soil pH observed here (Table S1) and in other studies (Neary et al., 1999) or by post-fire increases in nitrogen and phosphorus availability (Certini et al., 2021).

2.5.*2 Wildfire impacts on fungal guilds*

Fire-induced mortality was rapid for AMF and saprobes. Yet, EMF were most affected by fire over time, corroborating studies across ecosystems that point to the negative impact of fire on mycorrhizal richness, primarily driven by host mortality (Dove & Hart, 2017; Pulido-Chavez et al., 2021). Indeed, post-fire, all subplots were devoid of vegetation (0% vegetation cover) compared to 97% vegetation cover in unburned plots. However, we note that the rapid decline in AMF could be due to primer bias, as the ITS2 primer does not properly detect all AMF taxa (Lekberg et al., 2018). Moreover, we show that surviving ectomycorrhizal Basidiomycetes *Cortinarius*, *Inocybe*, and *Tomentella*, previously found in burned temperate pine forests (Owen et al., 2019; Pulido-Chavez et al., 2021) and pine-dominated Mediterranean systems (Gassibe et al., 2011; Hernández-

Rodríguez et al., 2013) also dominated early chaparral fungal succession and remained in the community for 1-2 months. Since EMF largely disappeared after two months, this potentially answers the question of how long it takes mycorrhizal fungi to perish after their hosts' death. Although it is possible that the EMF signal detected could be relic DNA (Carini et al., 2016), high soil temperatures typical of post-fire systems (Amacher et al., 2001; Neary et al., 1999) are likely to have degraded relic DNA (Sirois & Buckley, 2019; Torti et al., 2015), suggesting that these EMF could have survived the fire and clung to a dying host for at least two months. The survival of some EMF genera over others may be attributable to exploration type and specificity for current versus stored photosynthates (Gray & Kernaghan, 2020; Pena et al., 2010). For example, *Cortinarius*, a long/medium exploration type, which requires more carbon (C) for maintenance, only survived for 17 days post-fire. In contrast, *Inocybe*, a short-contact type (Agerer, 2001; Koide et al., 2014), survived at very low abundance for the entire year, perhaps because it may be less C demanding or adapted to warming (Fernandez et al., 2017). Our results indicate that early EMF could have survived on their hosts' stored photosynthates or the lower resources provided by the surviving and resprouting manzanita and chamise shrubs, while the vast majority of EMF experienced fire-induced mortality.

2.5.*3 Pyrophilous fungi dominate the burned communities*

Previously detected pyrophilous fungi across several ecosystems also dominated California chaparral, indicating that pyrophilous microbes are not biome-specific. Instead, these fungi may be activated by temperature thresholds reached during high-

severity fires, which are common in chaparral and some Pinaceae forests (Agee, 1993; Keeley & Zedler, 2009; Neary et al., 1999). Specifically, our burned communities were dominated by Ascomycota in the genera *Pyronema*, *Penicillium*, and *Aspergillus*, similar to dominant post-fire fungal species in Mediterranean shrublands (Livne-Luzon et al., 2021), boreal spruce (Whitman et al., 2019), and montane pine forests (Bruns et al., 2020; Pulido-Chavez et al., 2021). Both *Pyronema* (*P. omphalodes*) and *Aspergillus* (*A. fumigatus*) are known pyrophilous fungi of California chaparral (Dunn et al., 1982), and we identified additional species, including *P. domesticum*, *A. udagawae*, and *A. elsenburgensis*. These fungi are adapted to wildfire and produce fire-resistant structures, including dormant spores, sclerotia, and conidia, which are heat-activated (Gottlieb, 1950; Moore, 1962; Rhodes, 2006; Warcup & Baker, 1963). The rapid and efficient germination of *Aspergillus* (in the subgenus *Fumigati*, including *A. udagawae*) induced by high temperatures (Rhodes, 2006) and its ability to use various C and nitrogen sources, including NH_4^+ and NO_3^- (Krappmann & Braus, 2005), may position *Aspergillus* to rapidly dominate post-fire. Furthermore, *Pyronema domesticum* can mineralize pyrogenic organic matter ((Fischer et al., 2021), an abundant substrate in post-fire environments. Moreover, *Geminibasidium*, a recently described thermotolerant Basidiomycete yeast (Nguyen et al., 2013), dominated at 17 days post-fire. While not typically described as pyrophilous, presumably because most pyrophilous fungi are described from mushrooms (McMullan-Fisher et al., 2011), two other studies have found *Geminibasidium* to increase post-fire in pine forests (Pulido-Chavez et al., 2021; Yang et al., 2020), suggesting that *Geminibasidium* is an underrepresented pyrophilous fungus.

Together, these results indicate that dominant pyrophilous fungi are more widespread than expected and that their response to fire is likely due to fire adaptive traits and temperature thresholds.

2.5.*4 Pyrophilous fungi drive fungal secondary succession*

Although pyrophilous fungi are widespread across ecosystems, we lacked an understanding of how soon these pyrophilous fungi appear, their turnover rates, and if they change in abundance over time (Fox et al., 2022). Successional theory states that early successional stages are dominated by fast-growing or ruderal (R) organisms (Kinzig & Pacala, 2013) that tradeoff between stress tolerance (S) and competitive (C) life-history strategies over time (Grime, 1977; Zhang et al., 2018). Recent adaptations of Grime's C-S-R to microbiomes suggest that pyrophilous microbes survive and thrive post-fire with traits analogous to plants, including post-fire resource acquisition (C), thermotolerant structures (S), and fast growth (R) (Enright et al., 2022; Whitman et al., 2019). Our data suggest that chaparral pyrophilous microbes fit into these trait categories (Table 2.1) and that tradeoffs among these traits might drive microbial succession.

Early post-fire succession was driven by surviving thermotolerant fungi (i.e., *Geminibasidium* and *Pyronema*), followed by fast-colonizers (i.e., *Penicillium* and *Aspergillus*), which were overtaken by competitive fungi capable of exploiting post-fire resources. (i.e., *Coprinellus* and *Tephrocybe*). Whereas *Geminibasidium* is thermo- and xero-tolerant (Nguyen et al., 2013), *Pyronema* produces thermotolerant sclerotia

(Moore, 1962), enabling wildfire survival. Although both species are thermotolerant, differences in the morphological growth characteristics between the yeast *Geminibasidium* and the filamentous *Pyronema* may explain the tradeoff in dominance. For example, unicellular proliferation allowed *Geminibasidium* to dominate instantly, but the ability to forage for nutrients and rapidly increase surface colonization may allow the filamentous *Pyronema* to better dominate the open space. Interestingly, *Gelasinospora heterospora*, a fungus closely related to heat-activated *Neurospora crassa* (Dettman et al., 2001; Emerson, 1948), produces pigmented mycelia, and is known to require heat or chemical treatment for germination (Alexopoulous & Mims, 1952), was highly abundant at 25, 34, and 95 days post-fire, suggesting it is also pyrophilous. The decline of thermotolerators coincided with the dominance of fast-growing Ascomycete fungi in the genera *Penicillium* and *Aspergillus* (Dix & Webster, 1995; McGee et al., 2006), which both produce copious asexual conidia (Crow, 1992), allowing for rapid colonization of the open niche, analogous to early dominant post-fire plants, which are also often asexual (James, 1984). Lastly, like plants, competition appears to drive later successional dynamics (Tilman, 1990; Zhang et al., 2018), as suggested by the emergence of pyrophilous fungal decomposers, such as *Coprinellus* and *Tephrocybe* at 9-12 months, corroborating findings from Eucalyptus forests (Ammitzboll et al., 2022; McMullan-Fisher et al., 2011). Evidence suggests that *Coprinellus* can degrade aromatic hydrocarbons (Steindorff et al., 2021), supporting the idea that it is outcompeting earlier fungal taxa for this abundant and complex C source. Moreover, *Tephrocybe anthracophila* has a high affinity for ammonium-nitrogen (Legg, 1992; Suzuki, 2017),

allowing access to this abundant post-fire resource. In conclusion, our results indicate that tradeoffs among fire-adapted traits analogous to those in plants might drive post-fire microbial succession.

2.5.*5 Pyrophilous bacteria dominate and initiate bacterial secondary succession*

Our high temporal sampling enabled us to demonstrate that bacteria experience rapid succession and community turnover initiated by possible aerobic, heterotrophic bacteria that form endospores and produce antibiotics, which may improve their competitive abilities in the post-fire environment. Moreover, we show that previously detected putative pyrophilous bacteria from Canadian (Whitman et al., 2019), Chinese boreal (Xiang et al., 2014), and California redwood-tanoak forests (Enright et al., 2022) and Spanish shrublands also dominated California chaparral, suggesting that these pyrophilous bacteria might be widely distributed. Specifically, our burned communities favored taxa in the phyla Actinobacteria, Acidobacteria, Firmicutes, and Proteobacteria, similar to previous studies (Ammitzboll et al., 2022; Enright et al., 2022; Sáenz de Miera et al., 2020; Whitman et al., 2019; Xiang et al., 2014).

Bacterial successional dynamics differed from fungi in that the first few weeks were characterized by high diversity and a lack of dominance, mimicking the distributions observed in the unburned communities. In complex resource environments, such as those created by wildfire, niche complementarity is more important than competition because diverse communities can better exploit resources (Eisenhauer et al., 2013), further contributing to community stability. Our results support this idea, as the

dominant taxa in our study are likely to use different resources. For example, members of the genus *Paenibacillus* can fix nitrogen (Monciardini et al., 2003; Slepecky & Hemphill, 2006), *Bacillus* and *Conexibacter* can reduce nitrogen, and *Bacillus* can further solubilize phosphate (Espinosa-de-los-Monteros et al., 2001; Kalayu, 2019). However, at 25 days, bacteria experienced a large compositional turnover, which allowed for the dominance of pyrophilous bacteria with fire-adapted traits. While tradeoffs in abundance were not as stark for bacteria as for fungi, as indicated by the constant dominance of the Proteobacteria *Massilia*, the following most abundant bacteria did experience tradeoffs in dominance against other bacterial genera, possibly driven by physiological traits, such as thermotolerance and fast colonization (Table 1).

Firmicutes contain some of the most resistant, thermotolerant endospore-producing bacteria (Grady et al., 2016; Kaur et al., 2018; Mandic-Mulec et al., 2015), including members of the genera *Bacillus*, *Paenibacillus*, and *Clostridiales* which decreased in abundance as fast-colonizing genera in the Phylum Proteobacteria that may be capable of exploiting post-fire substrates (e.g., *Noviherspirillium* and *Massilia*) increased in dominance. Moreover, members of the Firmicute order Clostridiales can trigger sporulation in response to stress (Paredes-Sabja et al., 2011), potentially allowing for increased proliferation post-fire. While thermotolerance is crucial for fire survival, rapidly dominating the open niche and using post-fire resources may ensure post-fire growth. *Massilia* is a fast-reproducing bacteria that associates with the rhizosphere (Li et al., 2014) and colonizes AMF hyphae (Iffis et al., 2014) and the roots of various plants (Ofek et al., 2012). Thus, the dominance of *Massilia* in our study and other post-fire

environments (Enright et al., 2022; Whitman et al., 2019) suggests that its diverse ecology and rapid reproduction rate promote its proliferation within the soil (Toljander et al., 2005). Moreover, our results, coupled with current knowledge in the field, show that the continued dominance of *Massilia* and *Noviherbaspirillium* might be due to their ability to exploit post-fire resources. For example, the genera *Massilia* contains species that can degrade long-chain hydrocarbons (Ren et al., 2018) and reduce NO_3^- (Bailey et al., 2014). In contrast, *Noviherbaspirillium*, a mid-to late-year dominant bacterial genus, may degrade polycyclic aromatic hydrocarbon (Baldani et al., 2014; Grady et al., 2016; Woolet & Whitman, 2020). We conclude that although tradeoffs are not as distinctive for bacteria as they are for fungi, potentially due to interaction among traits such as fast growth under high resources and resource acquisition under low resources, our results provide evidence that pyrophilous bacteria have mechanisms to survive the fire that may drive them to trade off in abundance from early to late dominant taxa over time.

2.5.6 Microbial successional dynamics differ for bacteria and fungi

Chaparral vegetation successional patterns result from the self-replacement of the dominant pre-fire species (i.e., auto-succession), meaning the pre-fire dominant species establish early post-fire due to resprouting individuals, and these species gradually dominate the system (Hanes, 1971). However, this was not the case for bacterial or fungal succession. Most post-fire dominant genera were rare or absent pre-fire, and these initial colonizers experienced directional change over time via species replacement. Our results are consistent with successional concepts of non-catastrophic disturbances, which

show that species that survive a disturbance or recover quickly will dominate early successional dynamics but will inevitably be replaced by late-stage species via directional replacement mechanisms (Platt & Connell, 2003). Similar directional replacement patterns have been revealed after primary succession of fungi in a glacier foreland (Dong et al., 2016). Although a few genera dominated burned microbial communities, bacteria and fungi displayed different successional patterns. Bacterial burned communities exhibited lower synchrony and higher stability compared to unburned communities. The low synchrony indicates that stability may be conferred due to compensatory dynamics driven by tradeoffs in the abundance of cooccurring competitors (Tilman, 1999). Conversely, the lower stability in the unburned communities could be due to the increase in species synchrony reducing compensatory dynamics. In systems with high environmental variability, compensatory dynamics mediated by species asynchrony often contribute to stability (Yachi & Loreau, 1999). In contrast, burned fungal communities displayed lower community stability than unburned communities, while synchrony was similarly low in both. This lower stability may indicate that there was an overall increase in the variation of fungal taxa potentially due to the large loss of species observed in the fungal community (Tilman et al., 2014), resulting in priority effects and alternate communities with different dominant genera (Connell & Slatyer, 1977; Fukami, 2015). However, further research is needed to explore these microbial successional dynamics, as microbial communities are a vital driver of post-fire ecosystem recovery.

2.5.7 Precipitation and burn severity differentially affected bacterial and fungal communities

Although fire was the most influential driver of microbial change, we found that interactions between time and precipitation also drove successional dynamics by differentially affecting microbial biomass and richness. Precipitation interacted with time since fire resulting in a negative correlation with bacterial richness and a positive correlation with fungal richness, with bacterial richness declining but fungal richness increasing after rain events. At least one study that performed a three-year precipitation manipulation experiment showed that increased precipitation decreased bacterial richness (Yang et al., 2021). In contrast to richness, precipitation interacted with fire to positively affect bacterial biomass, while fungal biomass remained unaffected by rainfall. The distinct responses to precipitation could be due to microbial physiological and morphological differences (Blazewicz et al., 2014; Placella et al., 2012; Selbmann et al., 2013). For example, fungi have high morphological plasticity, including the ability to alternate growth forms based on environmental conditions, such as hyphal growth in low nutrient conditions versus unicellular form in rich nutrient conditions (Selbmann et al., 2013), which may allow fungi to survive small changes in moisture content, allowing for continued growth over time. Moreover, fungi can also activate or enhance resistance to drought (Evans & Wallenstein, 2012; Guhr & Kircher, 2020), allowing them to maintain a constant reproduction rate regardless of the external environmental conditions, thus explaining the positive impact on fungal richness. In contrast, bacteria can experience cell death due to rapid wet-up, while other bacterial groups enter a dormant state, inhibiting

growth (Schimel, 2018). Thus, to be evolutionarily successful, some bacteria may respond rapidly to favorable conditions (e.g., rain) (Leizeaga et al., 2022) and rapidly replicate to outcompete other microbes for the pulse of nutrients released during the rain event (Homyak et al., 2014), thus potentially explaining the peaks in richness observed after significant rainfall at day 131.

Previous research shows that ash depth correlates with fire intensity (Rice, 1993) and severity (Bodí et al., 2014; Parson et al., 2010). Here, we measured ash depth before the first rains or significant wind events could remove ash from the site, and we found that ash depth can serve as a proxy of soil burn severity on a scale relevant to soil microbes. Unlike the BAER maps, which classified all plots as moderate burn severity, we identified large variations in soil burn severity across our subplots (Fig. S7). It is well known that wildfires result in a heterogeneous landscape (Jain et al., 2008); thus, the discrepancy in soil burn severity in the BAER maps could be due to the lack of ground verification. Since our severity effects were similar to those found in other studies, we feel confident that ash depth can serve as a proxy for soil burn severity. We found that severity negatively affected bacterial and fungal richness but not biomass. Similar to studies in boreal (Whitman et al., 2019), oak (Pourreza et al., 2014), and Mediterranean forests (Lucas-Borja et al., 2019), bacterial and fungal richness decreased with soil burn severity. However, contrary to a meta-analysis (Dooley & Treseder, 2012), neither bacterial nor fungal biomass was directly impacted by soil burn severity, probably due to microbial adaptations to the natural high-severity fire regime of chaparral. However, since we observed an interaction effect of time since fire and severity on microbial

richness, it is possible that previously observed severity effects, derived from chronosequence studies where space is substituted for time and which, on average, occur two years post-fire (Pressler et al., 2019), may represent an interaction effect of time and severity and not a direct effect of soil burn severity.

2.6 Conclusion

Our high-resolution temporal sampling allowed us to detect rapid secondary succession in bacterial and fungal communities and marked tradeoffs in abundance among pyrophilous microbes over time. We found that the same pyrophilous bacteria and fungi that respond to fires in temperate and boreal forests and Mediterranean shrublands also dominate in California chaparral, allowing us to generalize knowledge of post-fire microbiomes to dryland habitats that are rapidly increasing with climate change (Feng & Fu, 2013). While pyrophilous microbes have been described in other systems, their turnover rates were unknown due to limited post-fire sampling (Fox et al., 2022). We hypothesize that tradeoffs among fire-adapted traits, with thermotolerators dominating first, followed by fast colonizers, and finally by competitors capable of capitalizing on post-fire resource acquisition, drive post-fire microbial successional dynamics. It appears likely that pyrophilous microbes share many analogous traits to plants, enabling us to adapt successional theory developed for plants to microbes while acknowledging that bacteria and fungi differ in how they respond to fire according to their physiology. We conclude that post-fire bacteria and fungi experience rapid successional changes after fire, suggesting that these dynamics can help increase our ability to predict if and how

ecosystems recover after a wildfire, an increasingly widespread disturbance with climate change.

2.7 Acknowledgments

We thank the Cleveland National Forest and the Trabuco Ranger District, including District Ranger Darrel Vance and Emily Fudge, Jeffrey Heys, Lauren Quon, Jacob Rodriguez, and Victoria Stempniewicz, for their guidance and help with permitting and site selection. We thank Judy A. Chung for her help with fieldwork and molecular work and Aral C. Greene, Dylan Enright, and Sameer S. Saroa for fieldwork assistance. We thank Amelia Nelson, Elizah Stephens, Kaleigh A. Russell, and anonymous reviewers for their helpful comments on the manuscript. This work was supported by UC Riverside, the BLM JFSP Award #012641-002 and Shipley Skinner Award to MFPC and SIG, the USDA-NIFA Award 2022-67014-36675 to SIG and PMH, and the DOE BER Award DE-SC0023127 to SIG and PMH.

2.8 Conflict of interest

The authors declare no conflicts of interest.

2.9 Data Availability

Raw sequence reads have been submitted to the National Centre for

Biotechnology Information (NCBI) Sequence Read Archive under BioProject accession number PRJNA761539; https://www.ncbi.nlm.nih.gov/sra/PRJNA761539. All statistical codes have been made available on GitHub https://github.com/pulidofabs/SecondarySuccession-Chaparral.

2.10 References

Abarenkov, K., Zirk, A., Piirmann, T., Pöhönen, R., Ivanov, F., Nilsson, R. H., & Kõljalg, U. (2020). *UNITE QIIME release for Fungi 2* (Version 04.02.2020). UNITE Community. https://doi.org/10.15156/BIO/786387.

Abatzoglou, J. T., Williams, A. P., & Barbero, R. (2019). Global Emergence of Anthropogenic Climate Change in Fire Weather Indices. *Geophysical Research Letters*, *46*(1), 326–336. https://doi.org/10.1029/2018GL080959

Agee, J. K. (1993). *Fire Ecology of Pacific Northwest Forests*. Island Press.

Agerer, R. (2001). Exploration types of ectomycorrhizae. *Mycorrhiza*, *11*(2), 107–114. https://doi.org/10.1007/s005720100108

Albuquerque, L., & da Costa, M. S. (2014). The Families Conexibacteraceae, Patulibacteraceae and Solirubrobacteraceae. In E. Rosenberg, E. F. DeLong, S. Lory, E. Stackebrandt, & F. Thompson (Eds.), *The Prokaryotes: Actinobacteria* (pp. 185–200). Springer. https://doi.org/10.1007/978-3-642-30138-4_200

Alexopoulous, C. J., & Mims, C. W. (1952). *Introductory mycology* (3rd ed.). John Wilet & Sons.

Allen, M., Egerton-Warburton, L., Treseder, K., Cario, C. H., Lindahl, A., Lansing, J., Querejeta, J., Kårén, O., Harney, S., & Zink, T. (2005). *Biodiversity of Mycorrhizal Fungi in Southern California 1*. /paper/Biodiversity-of-Mycorrhizal-Fungi-in-Southern-1-Allen-Egerton-Warburton/445d4f6878927a5307669f5e73df3174703f4d2a

Amacher, M. C., Johnson, A. D., Kutterer, D. E., & Bartos, D. L. (2001). *First-year postfire and postharvest soil temperatures in aspen and conifer stands* (RMRS-RP-27; p. RMRS-RP-27). U.S. Department of Agriculture, Forest Service, Rocky Mountain Research Station. https://doi.org/10.2737/RMRS-RP-27

Ammitzboll, H., Jordan, G. J., Baker, S. C., Freeman, J., & Bissett, A. (2022). Contrasting successional responses of soil bacteria and fungi to post-logging burn severity. *Forest Ecology and Management*, *508*, 120059. https://doi.org/10.1016/j.foreco.2022.120059

Anderson, M. J. (2017). Permutational Multivariate Analysis of Variance (PERMANOVA). In *Wiley StatsRef: Statistics Reference Online* (pp. 1–15). American Cancer Society. https://doi.org/10.1002/9781118445112.stat07841

Averill, C., & Hawkes, C. V. (2016). Ectomycorrhizal fungi slow soil carbon cycling. *Ecology Letters*, *19*(8), 937–947. https://doi.org/10.1111/ele.12631

Baar, J., Horton, T. R., Kretzer, A. M., & Bruns, T. D. (1999). Mycorrhizal colonization of Pinus muricata from resistant propagules after a stand-replacing wildfire. *New Phytologist*, *143*(2), 409–418. https://doi.org/10.1046/j.1469-8137.1999.00452.x

Bahram, M., Kõljalg, U., Courty, P.-E., Diédhiou, A. G., Kjøller, R., Põlme, S., Ryberg, M., Veldre, V., & Tedersoo, L. (2013). The distance decay of similarity in communities of ectomycorrhizal fungi in different ecosystems and scales. *Journal of Ecology*, *101*(5), 1335–1344. https://doi.org/10.1111/1365-2745.12120

Bailey, A. C., Kellom, M., Poret-Peterson, A. T., Noonan, K., Hartnett, H. E., & Raymond, J. (2014). Draft Genome Sequence of Massilia sp. Strain BSC265, Isolated from Biological Soil Crust of Moab, Utah. *Genome Announcements*, *2*(6), e01199-14, 2/6/e01199-14. https://doi.org/10.1128/genomeA.01199-14

Baldani, J. I., Rouws, L., Cruz, L. M., Olivares, F. L., Schmid, M., & Hartmann, A. (2014). The Family Oxalobacteraceae. In E. Rosenberg, E. F. DeLong, S. Lory, E. Stackebrandt, & F. Thompson (Eds.), *The Prokaryotes* (pp. 919–974). Springer Berlin Heidelberg. https://doi.org/10.1007/978-3-642-30197-1_291

Barnard, R. L., Osborne, C. A., & Firestone, M. K. (2013). Responses of soil bacterial and fungal communities to extreme desiccation and rewetting. *The ISME Journal*, *7*(11), 2229–2241. https://doi.org/10.1038/ismej.2013.104

Barro, S. C., & Conard, S. G. (1991). Fire effects on California chaparral systems: An overview. *Environment International*, *17*(2–3), 135–149. https://doi.org/10.1016/0160-4120(91)90096-9

Barton, K. (2020). *MuMIn: Multi-Model Inference* (R package version 1.43.17.). https://CRAN.R-project.org/package=MuMIn

Baselga, A. (2010). Partitioning the turnover and nestedness components of beta diversity. *Global Ecology and Biogeography*, *19*(1), 134–143. https://doi.org/10.1111/j.1466-8238.2009.00490.x

Blazewicz, S. J., Schwartz, E., & Firestone, M. K. (2014). Growth and death of bacteria and fungi underlie rainfall-induced carbon dioxide pulses from seasonally dried soil. *Ecology*, *95*(5), 1162–1172. https://doi.org/10.1890/13-1031.1

Bliss, C. I. (1953). *Fitting the negative binomial distribution to biological data (with "Note on the efficient fitting of the negative binomial" by R. A. Fisher), Biometrics, 9,* (9th ed.). Biometrics.

Bodí, M. B., Martin, D. A., Balfour, V. N., Santín, C., Doerr, S. H., Pereira, P., Cerdà, A., & Mataix-Solera, J. (2014a). Wildland fire ash: Production, composition and eco-hydro-geomorphic effects. *Earth-Science Reviews*, *130*, 103–127. https://doi.org/10.1016/j.earscirev.2013.12.007

Bodí, M. B., Martin, D. A., Balfour, V. N., Santín, C., Doerr, S. H., Pereira, P., Cerdà, A., & Mataix-Solera, J. (2014b). Wildland fire ash: Production, composition and eco-hydro-geomorphic effects. *Earth-Science Reviews*, *130*, 103–127. https://doi.org/10.1016/j.earscirev.2013.12.007

Bolyen, E., Rideout, J. R., Dillon, M. R., Bokulich, N. A., Abnet, C. C., Al-Ghalith, G. A., Alexander, H., Alm, E. J., Arumugam, M., Asnicar, F., Bai, Y., Bisanz, J. E., Bittinger, K., Brejnrod, A., Brislawn, C. J., Brown, C. T., Callahan, B. J., Caraballo-Rodríguez, A. M., Chase, J., … Caporaso, J. G. (2019). Reproducible, interactive, scalable and extensible microbiome data science using QIIME 2. *Nature Biotechnology*, *37*(8), 852–857. https://doi.org/10.1038/s41587-019-0209-9

Bruns, T. D., Chung, J. A., Carver, A. A., & Glassman, S. I. (2020). A simple pyrocosm for studying soil microbial response to fire reveals a rapid, massive response by Pyronema species. *PLOS ONE*, *15*(3), e0222691. https://doi.org/10.1371/journal.pone.0222691

Cairney, J. W. G., & Bastias, B. A. (2007). Influences of fire on forest soil fungal communitiesThis article is one of a selection of papers published in the Special Forum on Towards Sustainable Forestry — The Living Soil: Soil Biodiversity and Ecosystem Function. *Canadian Journal of Forest Research*, *37*(2), 207–215. https://doi.org/10.1139/x06-190

Callahan, B. J., McMurdie, P. J., & Holmes, S. P. (2017). Exact sequence variants should replace operational taxonomic units in marker-gene data analysis. *The ISME Journal*, *11*(12), 2639–2643. https://doi.org/10.1038/ismej.2017.119

Caporaso, J. G., Lauber, C. L., Walters, W. A., Berg-Lyons, D., Lozupone, C. A., Turnbaugh, P. J., Fierer, N., & Knight, R. (2011). Global patterns of 16S rRNA diversity at a depth of millions of sequences per sample. *Proceedings of the National Academy of Sciences*, *108*(Supplement_1), 4516–4522. https://doi.org/10.1073/pnas.1000080107

Carini, P., Marsden, P. J., Leff, J. W., Morgan, E. E., Strickland, M. S., & Fierer, N. (2016). Relic DNA is abundant in soil and obscures estimates of soil microbial diversity. *Nature Microbiology*, *2*(3), 1–6. https://doi.org/10.1038/nmicrobiol.2016.242

Certini, G., Moya, D., Lucas-Borja, M. E., & Mastrolonardo, G. (2021). The impact of fire on soil-dwelling biota: A review. *Forest Ecology and Management*, *488*, 118989. https://doi.org/10.1016/j.foreco.2021.118989

Cheeke, T. E., Phillips, R. P., Brzostek, E. R., Rosling, A., Bever, J. D., & Fransson, P. (2017). Dominant mycorrhizal association of trees alters carbon and nutrient cycling by selecting for microbial groups with distinct enzyme function. *New Phytologist*, *214*(1), 432–442. https://doi.org/10.1111/nph.14343

Clements, F. E. (1916). *Plant Succession: An Analysis of the Development of Vegetation*. Carnegie Institution of Washington.

Collins, S. L. (1990). Patterns of Community Structure During Succession in Tallgrass Prairie. *Bulletin of the Torrey Botanical Club*, *117*(4), 397–408. https://doi.org/10.2307/2996837

Collins, S. L., Micheli, F., & Hartt, L. (2000). A method to determine rates and patterns of variability in ecological communities. *Oikos*, *91*(2), 285–293. https://doi.org/10.1034/j.1600-0706.2000.910209.x

Connell, J. H., & Slatyer, R. O. (1977). Mechanisms of Succession in Natural Communities and Their Role in Community Stability and Organization. *The American Naturalist*, *111*(982), 1119–1144.

Cowan, A. D., Smith, J. E., & Fitzgerald, S. A. (2016). Recovering lost ground: Effects of soil burn intensity on nutrients and ectomycorrhiza communities of ponderosa pine seedlings. *Forest Ecology and Management*, *378*, 160–172. https://doi.org/10.1016/j.foreco.2016.07.030

Crow, J. F. (1992). An advantage of sexual reproduction in a rapidly changing environment. *The Journal of Heredity*, *83*(3), 169–173. https://doi.org/10.1093/oxfordjournals.jhered.a111187

Dalling, J. W. (2008). Pioneer Species. In B. Fath (Ed.), *Encyclopedia of Ecology (Second Edition)* (pp. 181–184). Elsevier. https://doi.org/10.1016/B978-0-444-63768-0.00534-5

Day, N. J., Cumming, S. G., Dunfield, K. E., Johnstone, J. F., Mack, M. C., Reid, K. A., Turetsky, M. R., Walker, X. J., & Baltzer, J. L. (2020). Identifying Functional Impacts of Heat-Resistant Fungi on Boreal Forest Recovery After Wildfire. *Frontiers in Forests and Global Change*, *3*. https://doi.org/10.3389/ffgc.2020.00068

Derroire, G., Balvanera, P., Castellanos-Castro, C., Decocq, G., Kennard, D. K., Lebrija-Trejos, E., Leiva, J. A., Odén, P.-C., Powers, J. S., Rico-Gray, V., Tigabu, M., & Healey, J. R. (2016). Resilience of tropical dry forests – a meta-analysis of changes in species diversity and composition during secondary succession. *Oikos*, *125*(10), 1386–1397. https://doi.org/10.1111/oik.03229

Dettman, J. R., Harbinski, F. M., & Taylor, J. W. (2001). Ascospore Morphology Is a Poor Predictor of the Phylogenetic Relationships of Neurospora and Gelasinospora. *Fungal Genetics and Biology*, *34*(1), 49–61. https://doi.org/10.1006/fgbi.2001.1289

Dix, N. J., & Webster, J. (1995). *Fungal Ecology.* Chapman & Hall.

Donato, D. C., Campbell, J. L., & Franklin, J. F. (2012). Multiple successional pathways and precocity in forest development: Can some forests be born complex? *Journal of Vegetation Science*, *23*(3), 576–584. https://doi.org/10.1111/j.1654-1103.2011.01362.x

Dong, K., Tripathi, B., Moroenyane, I., Kim, W., Li, N., Chu, H., & Adams, J. (2016). Soil fungal community development in a high Arctic glacier foreland follows a directional replacement model, with a mid-successional diversity maximum. *Scientific Reports*, *6*(1), Article 1. https://doi.org/10.1038/srep26360

Dooley, S. R., & Treseder, K. K. (2012). The effect of fire on microbial biomass: A meta-analysis of field studies. *Biogeochemistry*, *109*(1/3), 49–61.

Dove, N. C., & Hart, S. C. (2017). Fire Reduces Fungal Species Richness and In Situ Mycorrhizal Colonization: A Meta-Analysis. *Fire Ecology*, *13*(2), Article 2. https://doi.org/10.4996/fireecology.130237746

Dove, N. C., Klingeman, D. M., Carrell, A. A., Cregger, M. A., & Schadt, C. W. (2021). Fire alters plant microbiome assembly patterns: Integrating the plant and soil microbial response to disturbance. *New Phytologist*, *230*(6), 2433–2446. https://doi.org/10.1111/nph.17248

Dunn, P. H., Wells, W. G. I., Dickey, J., & Wohlgemuth, M. (1982). *Role of Fungi in Postfire Stabilization of Chaparral Ash Beds* (PSW-58, pp. 378–381) [Gen. Tech. Rep]. Pacific Southwest Forest and Range Experiment Station, Forest Service, U.S.U.S. Department of Agriculture.

Eisenhauer, N., Schulz, W., Scheu, S., & Jousset, A. (2013). Niche dimensionality links biodiversity and invasibility of microbial communities. *Functional Ecology*, *27*(1), 282–288. https://doi.org/10.1111/j.1365-2435.2012.02060.x

Emerson, M. R. (1948). Chemical Activation of Ascospore Germination in Neurospora crassa1. *Journal of Bacteriology*, *55*(3), 327–330.

Enright, D. J., Frangioso, K. M., Isobe, K., Rizzo, D. M., & Glassman, S. I. (2022). Mega-fire in Redwood Tanoak Forest Reduces Bacterial and Fungal Richness and Selects for Pyrophilous Taxa that are Phylogenetically Conserved. *Molecular Ecology*. https://doi.org/10.1111/mec.16399

Espinosa-de-los-Monteros, J., Martinez, A., & Valle, F. (2001). Metabolic profiles and aprE expression in anaerobic cultures of Bacillus subtilis using nitrate as terminal electron acceptor. *Applied Microbiology and Biotechnology*, *57*(3), 379–384. https://doi.org/10.1007/s002530100749

Evans, S. E., & Wallenstein, M. D. (2012). Soil microbial community response to drying and rewetting stress: Does historical precipitation regime matter? *Biogeochemistry*, *109*(1/3), 101–116.

Feng, S., & Fu, Q. (2013). Expansion of global drylands under a warming climate. *Atmospheric Chemistry and Physics*, *13*(19), 10081–10094. https://doi.org/10.5194/acp-13-10081-2013

Fernandez, C. W., Nguyen, N. H., Stefanski, A., Han, Y., Hobbie, S. E., Montgomery, R. A., Reich, P. B., & Kennedy, P. G. (2017). Ectomycorrhizal fungal response to warming is linked to poor host performance at the boreal-temperate ecotone. *Global Change Biology*, *23*(4), 1598–1609. https://doi.org/10.1111/gcb.13510

Ferrenberg, S., O'Neill, S. P., Knelman, J. E., Todd, B., Duggan, S., Bradley, D., Robinson, T., Schmidt, S. K., Townsend, A. R., Williams, M. W., Cleveland, C. C., Melbourne, B. A., Jiang, L., & Nemergut, D. R. (2013). Changes in assembly processes in soil bacterial communities following a wildfire disturbance. *The ISME Journal*, *7*(6), 1102–1111. https://doi.org/10.1038/ismej.2013.11

Fierer, N., Jackson, J. A., Vilgalys, R., & Jackson, R. B. (2005). Assessment of Soil Microbial Community Structure by Use of Taxon-Specific Quantitative PCR Assays. *Applied and Environmental Microbiology*, *71*(7), 4117–4120. https://doi.org/10.1128/AEM.71.7.4117-4120.2005

Fischer, M. S., Stark, F. G., Berry, T. D., Zeba, N., Whitman, T., & Traxler, M. F. (2021). Pyrolyzed Substrates Induce Aromatic Compound Metabolism in the Post-fire Fungus, Pyronema domesticum. *Frontiers in Microbiology*, *12*, 729289. https://doi.org/10.3389/fmicb.2021.729289

Fox, S., Sikes, B. A., Brown, S. P., Cripps, C. L., Glassman, S. I., Hughes, K., Semenova-Nelsen, T., & Jumpponen, A. (2022). Fire as a driver of fungal diversity—A synthesis of current knowledge. *Mycologia*, *0*(0), 1–27. https://doi.org/10.1080/00275514.2021.2024422

Fukami, T. (2015). Historical Contingency in Community Assembly: Integrating Niches, Species Pools, and Priority Effects. *Annual Review of Ecology Evolution and Systematics*, *46*, 1–23. https://doi.org/10.1146/annurev-ecolsys-110411-160340

Gao, C., Courty, P.-E., Varoquaux, N., Cole, B., Montoya, L., Xu, L., Purdom, E., Vogel, J., Hutmacher, R. B., Dahlberg, J. A., Coleman-Derr, D., Lemaux, P. G., & Taylor, J. W. (2022). Successional adaptive strategies revealed by correlating arbuscular mycorrhizal fungal abundance with host plant gene expression. *Molecular Ecology*, *n/a*(n/a). https://doi.org/10.1111/mec.16343

Gao, C., Montoya, L., Xu, L., Madera, M., Hollingsworth, J., Purdom, E., Singan, V., Vogel, J., Hutmacher, R. B., Dahlberg, J. A., Coleman-Derr, D., Lemaux, P. G., & Taylor, J. W. (2020). Fungal community assembly in drought-stressed sorghum shows stochasticity, selection, and universal ecological dynamics. *Nature Communications*, *11*(1), 34. https://doi.org/10.1038/s41467-019-13913-9

Gassibe, P. V., Fabero, R. F., Hernández-Rodríguez, M., Oria-de-Rueda, J. A., & Martín-Pinto, P. (2011). Fungal community succession following wildfire in a Mediterranean vegetation type dominated by Pinus pinaster in Northwest Spain. *Forest Ecology and Management*, *262*(4), 655–662. https://doi.org/10.1016/j.foreco.2011.04.036

Glassman, S. I., Levine, C. R., DiRocco, A. M., Battles, J. J., & Bruns, T. D. (2016). Ectomycorrhizal fungal spore bank recovery after a severe forest fire: Some like it hot. *The ISME Journal*, *10*(5), 1228–1239. https://doi.org/10.1038/ismej.2015.182

Glassman, S. I., Randolph, J. W., Saroa, S. S., Capocchi, J. K., Walters, K. E., Pulido-Chavez, M. F., & Larios, L. (2021). *Prescribed versus wildfire impacts on exotic plants and soil microbes in California grasslands* (p. 2021.09.22.461426). https://doi.org/10.1101/2021.09.22.461426

Glassman, S. I., Weihe, C., Li, J., Albright, M. B. N., Looby, C. I., Martiny, A. C., Treseder, K. K., Allison, S. D., & Martiny, J. B. H. (2018). Decomposition responses to climate depend on microbial community composition. *Proceedings of the National Academy of Sciences*, *115*(47), 11994–11999. https://doi.org/10.1073/pnas.1811269115

Gottlieb, D. (1950). The physiology of spore germination in fungi. *The Botanical Review*, *16*(5), 229–257. https://doi.org/10.1007/BF02873609

Grady, E. N., MacDonald, J., Liu, L., Richman, A., & Yuan, Z.-C. (2016). Current knowledge and perspectives of Paenibacillus: A review. *Microbial Cell Factories*, *15*(1), 203. https://doi.org/10.1186/s12934-016-0603-7

Gray, L., & Kernaghan, G. (2020). Fungal Succession During the Decomposition of Ectomycorrhizal Fine Roots. *Microbial Ecology*, *79*(2), 271–284. https://doi.org/10.1007/s00248-019-01418-3

Grime, J. P. (1977). Evidence for the Existence of Three Primary Strategies in Plants and Its Relevance to Ecological and Evolutionary Theory. *The American Naturalist*, *111*(982), 1169–1194.

Guhr, A., & Kircher, S. (2020). Drought-Induced Stress Priming in Two Distinct Filamentous Saprotrophic Fungi. *Microbial Ecology*, *80*(1), 27–33. https://doi.org/10.1007/s00248-019-01481-w

Hallett, L. M., Jones, S. K., MacDonald, A. A. M., Jones, M. B., Flynn, D. F. B., Ripplinger, J., Slaughter, P., Gries, C., & Collins, S. L. (2016). codyn: An r package of community dynamics metrics. *Methods in Ecology and Evolution*, *7*(10), 1146–1151. https://doi.org/10.1111/2041-210X.12569

Hanes, T. L. (1971). *Succession after Fire in the Chaparral of Southern California*. *41*(1), 27–52. https://doi.org/doi:10.2307/1942434

Hart, S. C., DeLuca, T. H., Newman, G. S., MacKenzie, M. D., & Boyle, S. I. (2005). Post-fire vegetative dynamics as drivers of microbial community structure and function in forest soils. *Forest Ecology and Management*, *220*(1–3), 166–184. https://doi.org/10.1016/j.foreco.2005.08.012

Hernández-Rodríguez, M., Oria-de-Rueda, J. A., & Martín-Pinto, P. (2013). Post-fire fungal succession in a Mediterranean ecosystem dominated by Cistus ladanifer L. *Forest Ecology and Management*, *289*, 48–57. https://doi.org/10.1016/j.foreco.2012.10.009

Homyak, P. M., Sickman, J. O., Miller, A. E., Melack, J. M., Meixner, T., & Schimel, J. P. (2014). Assessing Nitrogen-Saturation in a Seasonally Dry Chaparral Watershed: Limitations of Traditional Indicators of N-Saturation. *Ecosystems*, *17*(7), 1286–1305. https://doi.org/10.1007/s10021-014-9792-2

Iffis, B., St-Arnaud, M., & Hijri, M. (2014). Bacteria associated with arbuscular mycorrhizal fungi within roots of plants growing in a soil highly contaminated with aliphatic and aromatic petroleum hydrocarbons. *FEMS Microbiology Letters*, *358*(1), 44–54. https://doi.org/10.1111/1574-6968.12533

Illumina. (2011). *Quality Scores for Next-Generation Sequencing*. 2.

Jain, T. B., Gould, W. A., Graham, R. T., Pilliod, D. S., Lentile, L. B., & González, G. (2008). A Soil Burn Severity Index for Understanding Soil-fire Relations in Tropical Forests. *AMBIO: A Journal of the Human Environment*, *37*(7), 563–568. https://doi.org/10.1579/0044-7447-37.7.563

James, S. (1984). Lignotubers and Burls: Their Structure, Function and Ecological Significance in Mediterranean Ecosystems. *Botanical Review*, *50*(3), 225–266.

Kalayu, G. (2019). Phosphate Solubilizing Microorganisms: Promising Approach as Biofertilizers. *International Journal of Agronomy*, *2019*, 1–7. https://doi.org/10.1155/2019/4917256

Kaur, N., Seuylemezian, A., Patil, P. P., Patil, P., Krishnamurti, S., Varelas, J., Smith, D. J., Mayilraj, S., & Vaishampayan, P. (2018). Paenibacillus xerothermodurans sp. Nov., an extremely dry heat resistant spore forming bacterium isolated from the soil of Cape Canaveral, Florida. *International Journal of Systematic and Evolutionary Microbiology*, *68*(10), 3190–3196. https://doi.org/10.1099/ijsem.0.002967

Keeley, J. E., Fotheringham, C. J., & Baer-Keeley, M. (2005). Determinants of Postfire Recovery and Succession in Mediterranean-Climate Shrublands of California. *Ecological Applications*, *15*(5), 1515–1534. https://doi.org/10.1890/04-1005

Keeley, J. E., & Zedler, P. H. (2009). Large, high-intensity fire events in Southern California shrublands: Debunking the fine-grain age patch model. In *Ecological Applications* (Vol. 19, Issue 1, p. 26). https://doi.org/10.1890/08-0281.1

Kennedy, P. G., Peay, K. G., & Bruns, T. D. (2009). Root tip competition among ectomycorrhizal fungi: Are priority effects a rule or an exception? *Ecology*, *90*(8), 2098–2107. https://doi.org/10.1890/08-1291.1

Kindt, R., & Coe, R. (2005). *Tree diversity analysis. A manual and software for common statistical methods for ecological and biodiversity studies*. World Agroforestry Centre (ICRAF).

Kinzig, A. P., & Pacala, S. (2013). 9. Successional Biodiversity and Ecosystem Functioning. In *The Functional Consequences of Biodiversity: Empirical Progress and Theoretical Extensions (MPB-33)* (pp. 175–212). Princeton University Press. https://doi.org/10.1515/9781400847303.175

Koide, R. T., Fernandez, C., & Malcolm, G. (2014). Determining place and process: Functional traits of ectomycorrhizal fungi that affect both community structure and ecosystem function. *New Phytologist*, *201*(2), 433–439. https://doi.org/10.1111/nph.12538

Kozich, J. J., Westcott, S. L., Baxter, N. T., Highlander, S. K., & Schloss, P. D. (2013). Development of a Dual-Index Sequencing Strategy and Curation Pipeline for Analyzing Amplicon Sequence Data on the MiSeq Illumina Sequencing Platform. *Applied and Environmental Microbiology*, *79*(17), 5112–5120. https://doi.org/10.1128/AEM.01043-13

Krappmann, S., & Braus, G. H. (2005). Nitrogen metabolism of *Aspergillus* and its role in pathogenicity. *Medical Mycology*, *43*(s1), 31–40. https://doi.org/10.1080/13693780400024271

Lauber, C. L., Zhou, N., Gordon, J. I., Knight, R., & Fierer, N. (2010). Effect of storage conditions on the assessment of bacterial community structure in soil and human-associated samples. *FEMS Microbiology Letters*, *307*(1), 80–86. https://doi.org/10.1111/j.1574-6968.2010.01965.x

Legg, A. (1992). Fire-site agarics. *Mycologist*, *6*(3), 145–149. https://doi.org/10.1016/S0269-915X(09)80604-6

Lehman, C. L., & Tilman, D. (2000). Biodiversity, Stability, and Productivity in Competitive Communities. *The American Naturalist*, *156*(5), 534–552. https://doi.org/10.1086/303402

Leizeaga, A., Meisner, A., Rousk, J., & Bååth, E. (2022). Repeated drying and rewetting cycles accelerate bacterial growth recovery after rewetting. *Biology and Fertility of Soils*. https://doi.org/10.1007/s00374-022-01623-2

Lekberg, Y., Vasar, M., Bullington, L. S., Sepp, S.-K., Antunes, P. M., Bunn, R., Larkin, B. G., & Öpik, M. (2018). More bang for the buck? Can arbuscular mycorrhizal fungal communities be characterized adequately alongside other fungi using general fungal primers? *New Phytologist*, *220*(4), 971–976. https://doi.org/10.1111/nph.15035

Li, X., Rui, J., Mao, Y., Yannarell, A., & Mackie, R. (2014). Dynamics of the bacterial community structure in the rhizosphere of a maize cultivar. *Soil Biology and Biochemistry*, *68*, 392–401. https://doi.org/10.1016/j.soilbio.2013.10.017

Liu, C. M., Kachur, S., Dwan, M. G., Abraham, A. G., Aziz, M., Hsueh, P.-R., Huang, Y.-T., Busch, J. D., Lamit, L. J., Gehring, C. A., Keim, P., & Price, L. B. (2012). FungiQuant: A broad-coverage fungal quantitative real-time PCR assay. *BMC Microbiology*, *12*(1), 255. https://doi.org/10.1186/1471-2180-12-255

Livne-Luzon, S., Shemesh, H., Osem, Y., Carmel, Y., Migael, H., Avidan, Y., Tsafrir, A., Glassman, S. I., Bruns, T. D., & Ovadia, O. (2021). High resilience of the mycorrhizal community to prescribed seasonal burnings in eastern Mediterranean woodlands. *Mycorrhiza*, *31*(2), 203–216. https://doi.org/10.1007/s00572-020-01010-5

Lofgren, L. A., Uehling, J. K., Branco, S., Bruns, T. D., Martin, F., & Kennedy, P. G. (2019). Genome-based estimates of fungal rDNA copy number variation across phylogenetic scales and ecological lifestyles. *Molecular Ecology*, *28*(4), 721–730. https://doi.org/10.1111/mec.14995

Loreau, M., & de Mazancourt, C. (2008). Species Synchrony and Its Drivers: Neutral and Nonneutral Community Dynamics in Fluctuating Environments. *The American Naturalist*, *172*(2), E48–E66. https://doi.org/10.1086/589746

Lucas-Borja, M. E., Miralles, I., Ortega, R., Plaza-Álvarez, P. A., Gonzalez-Romero, J., Sagra, J., Soriano-Rodríguez, M., Certini, G., Moya, D., & Heras, J. (2019). Immediate fire-induced changes in soil microbial community composition in an outdoor experimental controlled system. *Science of The Total Environment*, *696*, 134033. https://doi.org/10.1016/j.scitotenv.2019.134033

Mandic-Mulec, I., Stefanic, P., & van Elsas, J. D. (2015). Ecology of Bacillaceae. *Microbiology Spectrum*, *3*(2), 3.2.16. https://doi.org/10.1128/microbiolspec.TBS-0017-2013

Martin, M. (2011). *Cutadapt removes adapter sequences from high-throughput sequencing reads*. https://journal.embnet.org/index.php/embnetjournal/article/view/200/458

Mayer, M., Rewald, B., Matthews, B., Sandén, H., Rosinger, C., Katzensteiner, K., Gorfer, M., Berger, H., Tallian, C., Berger, T. W., & Godbold, D. L. (2021). Soil fertility relates to fungal-mediated decomposition and organic matter turnover in a temperate mountain forest. *New Phytologist*, *231*(2), 777–790. https://doi.org/10.1111/nph.17421

McGee, P. A., Markovina, A.-L., Jeong, G. C. E., & Cooper, E. D. (2006). Trichocomaceae in bark survive high temperatures and fire: Trichocomaceae in bark survive high temperatures and fire. *FEMS Microbiology Ecology*, *56*(3), 365–371. https://doi.org/10.1111/j.1574-6941.2006.00079.x

McMullan-Fisher, S. J. M., Tom W. May, Richard M. Robinson, Tina L. Bell, Teresa Lebel, Pam Catcheside, & Alan York. (2011). *Fungi and fire in Australian ecosystems: A review of current knowledge, management implications and future directions*. *59*, 70–90.

McMurdie, P. J., & Holmes, S. (2013). phyloseq: An R Package for Reproducible Interactive Analysis and Graphics of Microbiome Census Data. *PLOS ONE*, *8*(4), e61217. https://doi.org/10.1371/journal.pone.0061217

Monciardini, P., Cavaletti, L., Schumann, P., Rohde, M., & Donadio, S. (2003). Conexibacter woesei gen. Nov., sp. Nov., a novel representative of a deep evolutionary line of descent within the class Actinobacteria. *International Journal of Systematic and Evolutionary Microbiology*, *53*(2), 569–576. https://doi.org/10.1099/ijs.0.02400-0

Moore, E. J. (1962). The Ontogeny of the Sclerotia of Pyronema Domesticum. *Mycologia*, *54*(3), 312–316. https://doi.org/10.1080/00275514.1962.12025004

Neary, D. G., Klopatek, C. C., DeBano, L. F., & Ffolliott, P. F. (1999). Fire effects on belowground sustainability: A review and synthesis. *Forest Ecology and Management*, *122*(1–2), 51–71. https://doi.org/10.1016/S0378-1127(99)00032-8

Nelson, A. R., Narrowe, A. B., Rhoades, C. C., Fegel, T. S., Daly, R. A., Roth, H. K., Chu, R. K., Amundson, K. K., Young, R. B., Steindorff, A. S., Mondo, S. J., Grigoriev, I. V., Salamov, A., Borch, T., & Wilkins, M. J. (2022). Wildfire-dependent changes in soil microbiome diversity and function. *Nature Microbiology*, *7*(9), 1–12. https://doi.org/10.1038/s41564-022-01203-y

Nguyen, H. D., Nickerson, N. L., & Seifert, K. A. (2013). Basidioascus and Geminibasidium: A new lineage of heat-resistant and xerotolerant basidiomycetes. *Mycologia*, *105*(5), 1231–1250. https://doi.org/10.3852/12-351

Nguyen, N. H., Song, Z., Bates, S. T., Branco, S., Tedersoo, L., Menke, J., Schilling, J. S., & Kennedy, P. G. (2016). FUNGuild: An open annotation tool for parsing fungal community datasets by ecological guild. *Fungal Ecology*, *20*, 241–248. https://doi.org/10.1016/j.funeco.2015.06.006

Ofek, M., Hadar, Y., & Minz, D. (2012). Ecology of Root Colonizing Massilia (Oxalobacteraceae). *PLOS ONE*, *7*(7), e40117. https://doi.org/10.1371/journal.pone.0040117

Oksanen, J., Blanchet, G. F., Friendly, M., Kindt, R., Legendre, P., McGlinn, D., Minchin, P. R., O'Hara, R. B., Simpson, G. L., Solymos, P., Stevens, M. H. H., Szoecs, E., & Wagner, H. (2018). *Vegan:Community Ecology Package-Version 2.5.2. Ordination Methods, Diversity Analysis, and Other Functions for Community and Vegetation Ecologist*.

Osborne, B. B., Bestelmeyer, B. T., Currier, C. M., Homyak, P. M., Throop, H. L., Young, K., & Reed, S. C. (2022). The consequences of climate change for dryland biogeochemistry. *New Phytologist*, *236*(1), 15–20. https://doi.org/10.1111/nph.18312

Owen, S. M., Patterson, A. M., Gehring, C. A., Sieg, C. H., Baggett, L. S., & Fulé, P. Z. (2019). Large, high-severity burn patches limit fungal recovery 13 years after wildfire in a ponderosa pine forest. *Soil Biology and Biochemistry*, *139*, 107616. https://doi.org/10.1016/j.soilbio.2019.107616

Pacala, S. W., Canham, C. D., Saponara, J., Silander, J. A., Kobe, R. K., & Ribbens, E. (1996). Forest Models Defined by Field Measurements: Estimation, Error Analysis and Dynamics. *Ecological Monographs*, *66*(1), 1–43. https://doi.org/10.2307/2963479

Pandolfi, J. M. (2008). Succession. In S. E. Jørgensen & B. D. Fath (Eds.), *Encyclopedia of Ecology* (pp. 3416–3424). Academic Press. https://doi.org/10.1016/B978-008045405-4.00547-4

Paredes-Sabja, D., Setlow, P., & Sarker, M. R. (2011). Germination of spores of Bacillales and Clostridiales species: Mechanisms and proteins involved. *Trends in Microbiology*, *19*(2), 85–94. https://doi.org/10.1016/j.tim.2010.10.004

Parson, A., Robichaud, P. R., Lewis, S. A., Napper, C., & Clark, J. T. (2010). *Field guide for mapping post-fire soil burn severity* (RMRS-GTR-243). U.S. Department of Agriculture, Forest Service, Rocky Mountain Research Station. https://doi.org/10.2737

Pavlovska, M., Prekrasna, I., Parnikoza, I., & Dykyi, E. (2021). Soil Sample Preservation Strategy Affects the Microbial Community Structure. *Microbes and Environments*, *36*(1), ME20134. https://doi.org/10.1264/jsme2.ME20134

Pena, R., Offermann, C., Simon, J., Naumann, P. S., Geßler, A., Holst, J., Dannenmann, M., Mayer, H., Kögel-Knabner, I., Rennenberg, H., & Polle, A. (2010). Girdling Affects Ectomycorrhizal Fungal (EMF) Diversity and Reveals Functional Differences in EMF Community Composition in a Beech Forest. *Applied and Environmental Microbiology*, *76*(6), 1831–1841. https://doi.org/10.1128/AEM.01703-09

Pérez-Valera, E., Verdú, M., Navarro-Cano, J. A., & Goberna, M. (2018). Resilience to fire of phylogenetic diversity across biological domains. *Molecular Ecology*, *27*(13), 2896–2908. https://doi.org/10.1111/mec.14729

Pérez-Valera, E., Verdú, M., Navarro-Cano, J. A., & Goberna, M. (2020). Soil microbiome drives the recovery of ecosystem functions after fire. *Soil Biology and Biochemistry*, *149*, 107948. https://doi.org/10.1016/j.soilbio.2020.107948

Petersen, P. M. (1970). Danish fireplace fungi-an ecological investigation on fungi on burns. *Dansk Botanisk Arkiv*, *27*(3), 1–97.

Phillips, L. (2021). *General Field Plot Sampling Protocol for DNA-based analyses (2018-2020)*. Protocols.Io. https://www.protocols.io/view/general-field-plot-sampling-protocol-for-dna-based-btd2ni8e

Pingree, M. R. A., & Kobziar, L. N. (2019). The myth of the biological threshold: A review of biological responses to soil heating associated with wildland fire. *Forest Ecology and Management*, *432*, 1022–1029. https://doi.org/10.1016/j.foreco.2018.10.032

Placella, S. A., Brodie, E. L., & Firestone, M. K. (2012). Rainfall-induced carbon dioxide pulses result from sequential resuscitation of phylogenetically clustered microbial groups. *Proceedings of the National Academy of Sciences*, *109*(27), 10931–10936. https://doi.org/10.1073/pnas.1204306109

Platt, W. J., & Connell, J. H. (2003). Natural Disturbances and Directional Replacement of Species. *Ecological Monographs*, *73*(4), 507–522.

Pourreza, M., Hosseini, S. M., Safari Sinegani, A. A., Matinizadeh, M., & Dick, W. A. (2014). Soil microbial activity in response to fire severity in Zagros oak (Quercus brantii Lindl.) forests, Iran, after one year. *Geoderma*, *213*, 95–102. https://doi.org/10.1016/j.geoderma.2013.07.024

Pressler, Y., Moore, J. C., & Cotrufo, M. F. (2019). Belowground community responses to fire: Meta-analysis reveals contrasting responses of soil microorganisms and mesofauna. *Oikos*, *128*(3), 309–327. https://doi.org/10.1111/oik.05738

Pulido-Chavez, M. F., Alvarado, E. C., DeLuca, T. H., Edmonds, R. L., & Glassman, S. I. (2021). High-severity wildfire reduces richness and alters composition of ectomycorrhizal fungi in low-severity adapted ponderosa pine forests. *Forest Ecology and Management*, *485*, 118923. https://doi.org/10.1016/j.foreco.2021.118923

Qin, Q., & Liu, Y. (2021). Changes in microbial communities at different soil depths through the first rainy season following severe wildfire in North China artificial Pinus tabulaeformis forest. *Journal of Environmental Management*, *280*, 111865. https://doi.org/10.1016/j.jenvman.2020.111865

R Core Team. (2021). *R: A language and environment for statistical computing. R Foundation for Statistical Computing.* https://www.R-project.org/.

Reazin, C., Morris, S., Smith, J. E., Cowan, A. D., & Jumpponen, A. (2016). Fires of differing intensities rapidly select distinct soil fungal communities in a Northwest US ponderosa pine forest ecosystem. *Forest Ecology and Management*, *377*, 118–127. https://doi.org/10.1016/j.foreco.2016.07.002

Reilly, M. J., & Spies, T. A. (2016). Disturbance, tree mortality, and implications for contemporary regional forest change in the Pacific Northwest. *Forest Ecology and Management*, *374*, 102–110. https://doi.org/10.1016/j.foreco.2016.05.002

Ren, C., Chen, J., Lu, X., Doughty, R., Zhao, F., Zhong, Z., Han, X., Yang, G., Feng, Y., & Ren, G. (2018). Responses of soil total microbial biomass and community compositions to rainfall reductions. *Soil Biology and Biochemistry*, *116*, 4–10. https://doi.org/10.1016/j.soilbio.2017.09.028

Rhodes, J. C. (2006). *Aspergillus fumigatus*: Growth and virulence. *Medical Mycology*, *44*(s1), 77–81. https://doi.org/10.1080/13693780600779419

Rice, S. K. (1993). Vegetation establishment in post-fire Adenostoma chaparral in relation to fine-scale pattern in fire intensity and soil nutrients. *Journal of Vegetation Science*, *4*(1), 115–124. https://doi.org/10.2307/3235739

Riley, K. L., & Loehman, R. A. (2016). Mid-21st-century climate changes increase predicted fire occurrence and fire season length, Northern Rocky Mountains, United States. *Ecosphere*, *7*(11), e01543. https://doi.org/10.1002/ecs2.1543

Ross, G. J. S., & Preece, D. A. (1985). The Negative Binomial Distribution. *Journal of the Royal Statistical Society. Series D (The Statistician)*, *34*(3), 323–335. JSTOR. https://doi.org/10.2307/2987659

Rundel, P. W. (2018). California Chaparral and Its Global Significance. In E. C. Underwood, H. D. Safford, N. A. Molinari, & J. E. Keeley (Eds.), *Valuing Chaparral* (pp. 1–27). Springer International Publishing. https://doi.org/10.1007/978-3-319-68303-4_1

Sáenz de Miera, L. E., Pinto, R., Gutierrez-Gonzalez, J. J., Calvo, L., & Ansola, G. (2020). Wildfire effects on diversity and composition in soil bacterial communities. *Science of The Total Environment*, *726*, 138636. https://doi.org/10.1016/j.scitotenv.2020.138636

Schimel, J. P. (2018). Life in Dry Soils: Effects of Drought on Soil Microbial Communities and Processes. *Annual Review of Ecology, Evolution, and Systematics*, *49*(1), 409–432. https://doi.org/10.1146/annurev-ecolsys-110617-062614

Schoch, C. L., Seifert, K. A., Huhndorf, S., Robert, V., Spouge, J. L., Levesque, C. A., Chen, W., Fungal Barcoding Consortium, Fungal Barcoding Consortium Author List, Bolchacova, E., Voigt, K., Crous, P. W., Miller, A. N., Wingfield, M. J., Aime, M. C., An, K.-D., Bai, F.-Y., Barreto, R. W., Begerow, D., … Schindel, D. (2012). Nuclear ribosomal internal transcribed spacer (ITS) region as a universal DNA barcode marker for *Fungi*. *Proceedings of the National Academy of Sciences*, *109*(16), 6241–6246. https://doi.org/10.1073/pnas.1117018109

Seaver, F. J. (1909). Studies in Pyrophilous Fungi: I. The Occurrence and Cultivation of Pyronema. *Mycologia*, *1*, 131–193.

Selbmann, L., Egidi, E., Isola, D., Onofri, S., Zucconi, L., de Hoog, G. S., Chinaglia, S., Testa, L., Tosi, S., Balestrazzi, A., Lantieri, A., Compagno, R., Tigini, V., & Varese, G. C. (2013). Biodiversity, evolution and adaptation of fungi in extreme environments. *Plant Biosystems - An International Journal Dealing with All Aspects of Plant Biology*, *147*(1), 237–246. https://doi.org/10.1080/11263504.2012.753134

Semenova-Nelsen, T. A., Platt, W. J., Patterson, T. R., Huffman, J., & Sikes, B. A. (2019). Frequent fire reorganizes fungal communities and slows decomposition across a heterogeneous pine savanna landscape. *New Phytologist*, *224*(2), 916–927. https://doi.org/10.1111/nph.16096

Shugart, H. H. (2013). Encyclopedia of Biodiversity. In *Succession, Phenomenon Of* (2nd Edition, pp. 63–70). Academic Press.

Sirois, S. H., & Buckley, D. H. (2019). Factors governing extracellular DNA degradation dynamics in soil. *Environmental Microbiology Reports*, *11*(2), 173–184. https://doi.org/10.1111/1758-2229.12725

Slepecky, R. A., & Hemphill, H. E. (2006). The Genus Bacillus—Nonmedical. In M. Dworkin, S. Falkow, E. Rosenberg, K.-H. Schleifer, & E. Stackebrandt (Eds.), *The Prokaryotes: Volume 4: Bacteria: Firmicutes, Cyanobacteria* (pp. 530–562). Springer US. https://doi.org/10.1007/0-387-30744-3_16

Smith, C. J., & Osborn, A. M. (2009). Advantages and limitations of quantitative PCR (Q-PCR)-based approaches in microbial ecology. *FEMS Microbiology Ecology*, *67*(1), 6–20. https://doi.org/10.1111/j.1574-6941.2008.00629.x

Song, Z., Vail, A., Sadowsky, M. J., & Schilling, J. S. (2014). Quantitative PCR for measuring biomass of decomposer fungi in planta. *Fungal Ecology*, *7*, 39–46. https://doi.org/10.1016/j.funeco.2013.12.004

Steindorff, A. S., Carver, A., Calhoun, S., Stillman, K., Liu, H., Lipzen, A., He, G., Yan, M., Pangilinan, J., LaButti, K., Ng, V., Bruns, T. D., & Grigoriev, I. V. (2021). Comparative genomics of pyrophilous fungi reveals a link between fire events and developmental genes. *Environmental Microbiology*, *23*(1), 99–109. https://doi.org/10.1111/1462-2920.15273

Suzuki, A. (2017). Various Aspects of Ammonia Fungi. In T. Satyanarayana, S. K. Deshmukh, & B. N. Johri (Eds.), *Developments in Fungal Biology and Applied Mycology* (pp. 39–58). Springer. https://doi.org/10.1007/978-981-10-4768-8_4

Tatti, E., McKew, B. A., Whitby, C., & Smith, C. J. (2016). Simultaneous DNA-RNA Extraction from Coastal Sediments and Quantification of 16S rRNA Genes and Transcripts by Real-time PCR. *Journal of Visualized Experiments : JoVE*, *112*, 54067. https://doi.org/10.3791/54067

Taylor, D. L., Walters, W. A., Lennon, N. J., Bochicchio, J., Krohn, A., Caporaso, J. G., & Pennanen, T. (2016). Accurate Estimation of Fungal Diversity and Abundance through Improved Lineage-Specific Primers Optimized for Illumina Amplicon Sequencing. *Applied and Environmental Microbiology*, *82*(24), 7217–7226. https://doi.org/10.1128/AEM.02576-16

Tellenbach, C., Grünig, C. R., & Sieber, T. N. (2010). Suitability of Quantitative Real-Time PCR To Estimate the Biomass of Fungal Root Endophytes. *Applied and Environmental Microbiology*, *76*(17), 5764–5772. https://doi.org/10.1128/AEM.00907-10

Tilman, D. (1990). Constraints and Tradeoffs: Toward a Predictive Theory of Competition and Succession. *Oikos*, *58*(1), 3–15. https://doi.org/10.2307/3565355

Tilman, D. (1999). The Ecological Consequences of Changes in Biodiversity: A Search for General Principles. *Ecology*, *80*(5), 1455–1474. https://doi.org/10.1890/0012-9658(1999)080[1455:TECOCI]2.0.CO;2

Tilman, D., Isbell, F., & Cowles, J. M. (2014). Biodiversity and Ecosystem Functioning. *Annual Review of Ecology, Evolution, and Systematics*, *45*(1), 471–493. https://doi.org/10.1146/annurev-ecolsys-120213-091917

Toljander, J. F., Artursson, V., Paul, L. R., Jansson, J. K., & Finlay, R. D. (2005). Attachment of di¡erent soil bacteria to arbuscular mycorrhizal fungal extraradical hyphae is determined by hyphal vitalityand fungal species. *FEMS Microbiol Lett*, 7.

Torti, A., Lever, M. A., & Jørgensen, B. B. (2015). Origin, dynamics, and implications of extracellular DNA pools in marine sediments. *Marine Genomics*, *24*, 185–196. https://doi.org/10.1016/j.margen.2015.08.007

Turnbull, L. A., Levine, J. M., Loreau, M., & Hector, A. (2013). Coexistence, niches and biodiversity effects on ecosystem functioning. *Ecology Letters*, *16*, 116–127. https://doi.org/10.1111/ele.12056

Valencia, E., de Bello, F., Galland, T., Adler, P. B., Lepš, J., E-Vojtkó, A., van Klink, R., Carmona, C. P., Danihelka, J., Dengler, J., Eldridge, D. J., Estiarte, M., García-González, R., Garnier, E., Gómez-García, D., Harrison, S. P., Herben, T., Ibáñez, R., Jentsch, A., … Götzenberger, L. (2020). Synchrony matters more than species richness in plant community stability at a global scale. *Proceedings of the National Academy of Sciences*, *117*(39), 24345–24351. https://doi.org/10.1073/pnas.1920405117

Venables, W. N., & Ripley, B. D. (2002). *Modern Applied Statistics with S* (Fourth edition). Springer. https://www.stats.ox.ac.uk/pub/MASS4/.

Warcup, J. H., & Baker, K. F. (1963). Occurrence of Dormant Ascospores in Soil. *Nature*, *197*(4874), 1317–1318. https://doi.org/10.1038/1971317a0

Whitman, T., Whitman, E., Woolet, J., Flannigan, M. D., Thompson, D. K., & Parisien, M.-A. (2019). Soil bacterial and fungal response to wildfires in the Canadian boreal forest across a burn severity gradient. *Soil Biology and Biochemistry*, *138*, 107571. https://doi.org/10.1016/j.soilbio.2019.107571

Whitman, T., Woolet, J., Sikora, M., Johnson, D. B., & Whitman, E. (2022). Resilience in soil bacterial communities of the boreal forest from one to five years after wildfire across a severity gradient. *Soil Biology and Biochemistry*, *172*, 108755. https://doi.org/10.1016/j.soilbio.2022.108755

Wickham, H. (2016). *ggplot2: Elegant Graphics for Data Analysis.* Springer-Verlag New York. https://ggplot2.tidyverse.org

Willis, A., Bunge, J., & Whitman, T. (2017). Improved detection of changes in species richness in high diversity microbial communities. *Journal of the Royal Statistical Society. Series C (Applied Statistics)*, *66*(5), 963–977.

Woolet, J., & Whitman, T. (2020). Pyrogenic organic matter effects on soil bacterial community composition. *Soil Biology and Biochemistry*, *141*, 107678. https://doi.org/10.1016/j.soilbio.2019.107678

Xiang, X., Gibbons, S. M., Yang, J., Kong, J., Sun, R., & Chu, H. (2015). Arbuscular mycorrhizal fungal communities show low resistance and high resilience to wildfire disturbance. *Plant and Soil*, *397*(1–2), 347–356. https://doi.org/10.1007/s11104-015-2633-z

Xiang, X., Shi, Y., Yang, J., Kong, J., Lin, X., Zhang, H., Zeng, J., & Chu, H. (2014). Rapid recovery of soil bacterial communities after wildfire in a Chinese boreal forest. *Scientific Reports*, *4*(1), Article 1. https://doi.org/10.1038/srep03829

Yachi, S., & Loreau, M. (1999). Biodiversity and ecosystem productivity in a fluctuating environment: The insurance hypothesis. *Proceedings of the National Academy of Sciences*, *96*(4), 1463–1468. https://doi.org/10.1073/pnas.96.4.1463

Yang, T., Tedersoo, L., Lin, X., Fitzpatrick, M. C., Jia, Y., Liu, X., Ni, Y., Shi, Y., Lu, P., Zhu, J., & Chu, H. (2020). Distinct fungal successional trajectories following wildfire between soil horizons in a cold-temperate forest. *New Phytologist*, *227*(2), 572–587. https://doi.org/10.1111/nph.16531

Yang, Zhu, K., Loik, M. E., & Sun, W. (2021). Differential responses of soil bacteria and fungi to altered precipitation in a meadow steppe. *Geoderma*, *384*, 114812. https://doi.org/10.1016/j.geoderma.2020.114812

Yilmaz, P., Parfrey, L. W., Yarza, P., Gerken, J., Pruesse, E., Quast, C., Schweer, T., Peplies, J., Ludwig, W., & Glöckner, F. O. (2014). The SILVA and "All-species Living Tree Project (LTP)" taxonomic frameworks. *Nucleic Acids Research*, *42*(D1), D643–D648. https://doi.org/10.1093/nar/gkt1209

Zhang, H., Qi, W., & Liu, K. (2018). Functional traits associated with plant colonizing and competitive ability influence species abundance during secondary succession: Evidence from subalpine meadows of the Qinghai–Tibetan Plateau. *Ecology and Evolution*, *8*(13), 6529–6536. https://doi.org/10.1002/ece3.4110

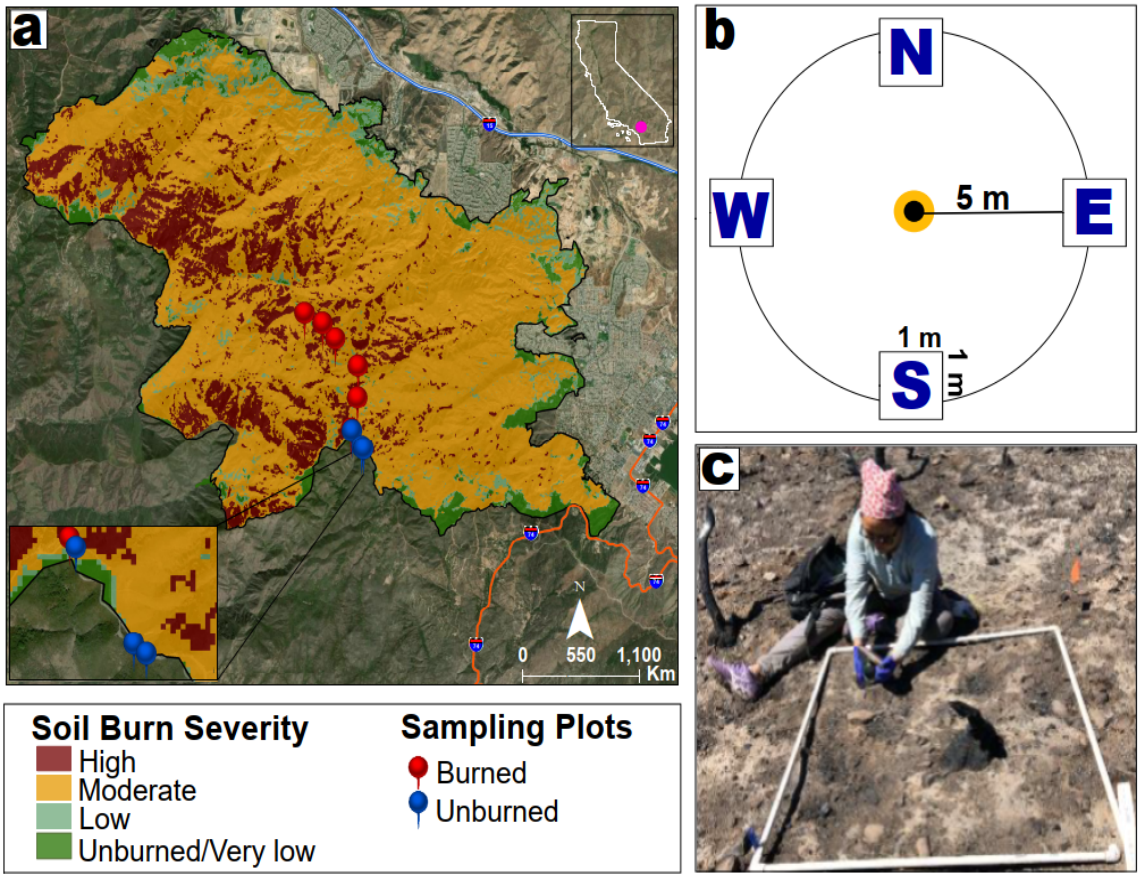

Figure 2.1. A) Location of the study area and plots (6 burned; 3 unburned) within the Holy Fire burn scar in the Cleveland National Forest in southern California. Soil burn severity is based on the USDA BAER classifications made at seven days within fire containment. B) Plot experimental design, each with four 1m^2 subplots placed 5m from the center in each cardinal direction. C) Collection of the top 10 cm of soil beneath the ash with a releasable bulb planter within the 1 m^2 subplots at 17 days post-fire.

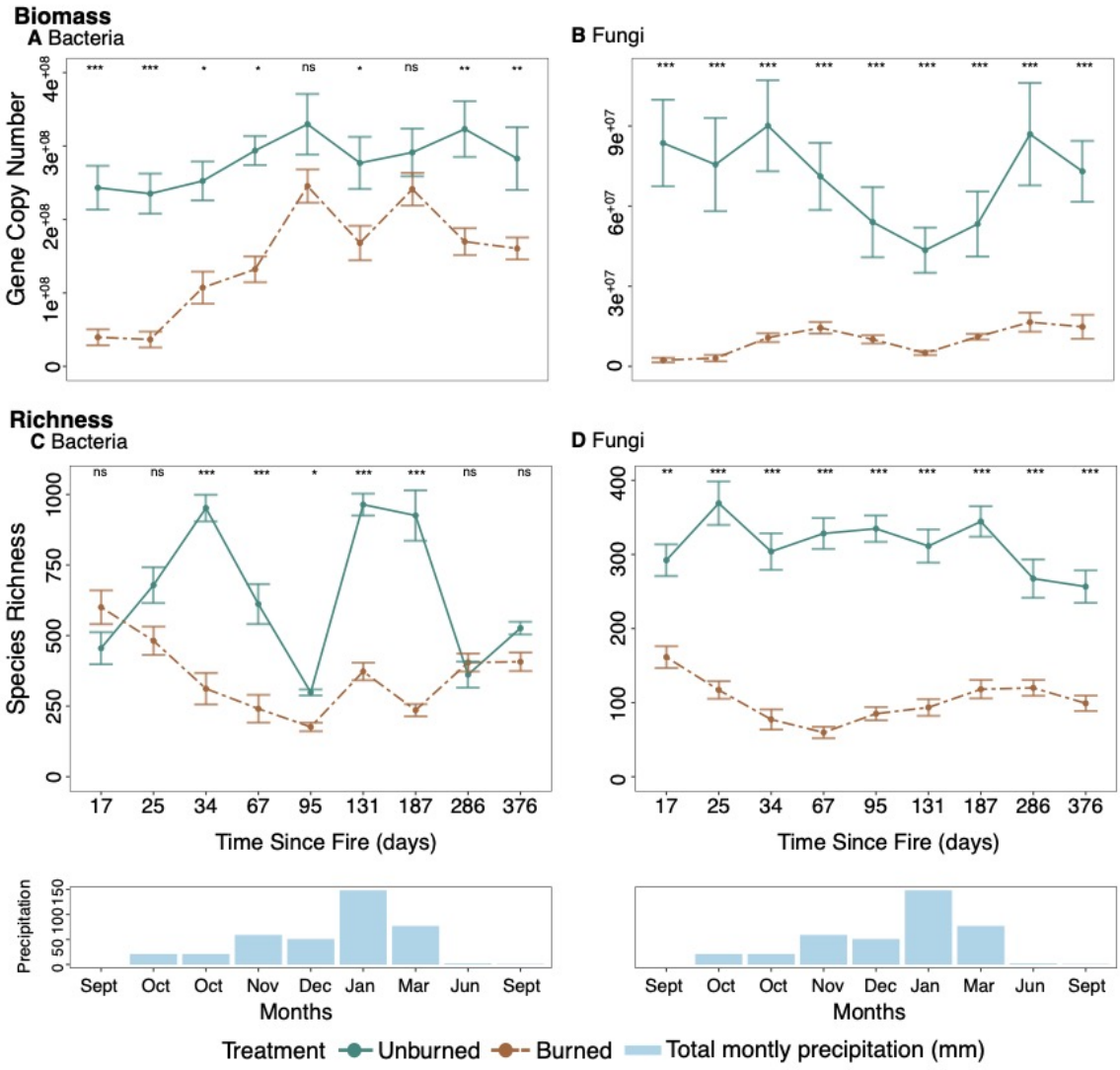

Figure 2.2. Change between burned (brown) and unburned communities (blue-green) for A) bacterial and B) fungal estimated biomass per gram of soil and C) bacterial and D) fungal species richness at each of the nine timepoints in the first post-fire year. Points represent the mean biomass (A, B) and richness (C, D), and bars represent the standard error of the mean for burned versus unburned plots at each timepoint. Note that gene copy number and species richness are displayed on a daily scale, whereas precipitation is on a monthly scale representing total precipitation for the month in which each soil sample was collected. Note, we sampled twice in Oct. The significance of burned versus unburned plots per timepoint is denoted with an asterisk and is based on a negative binomial regression.

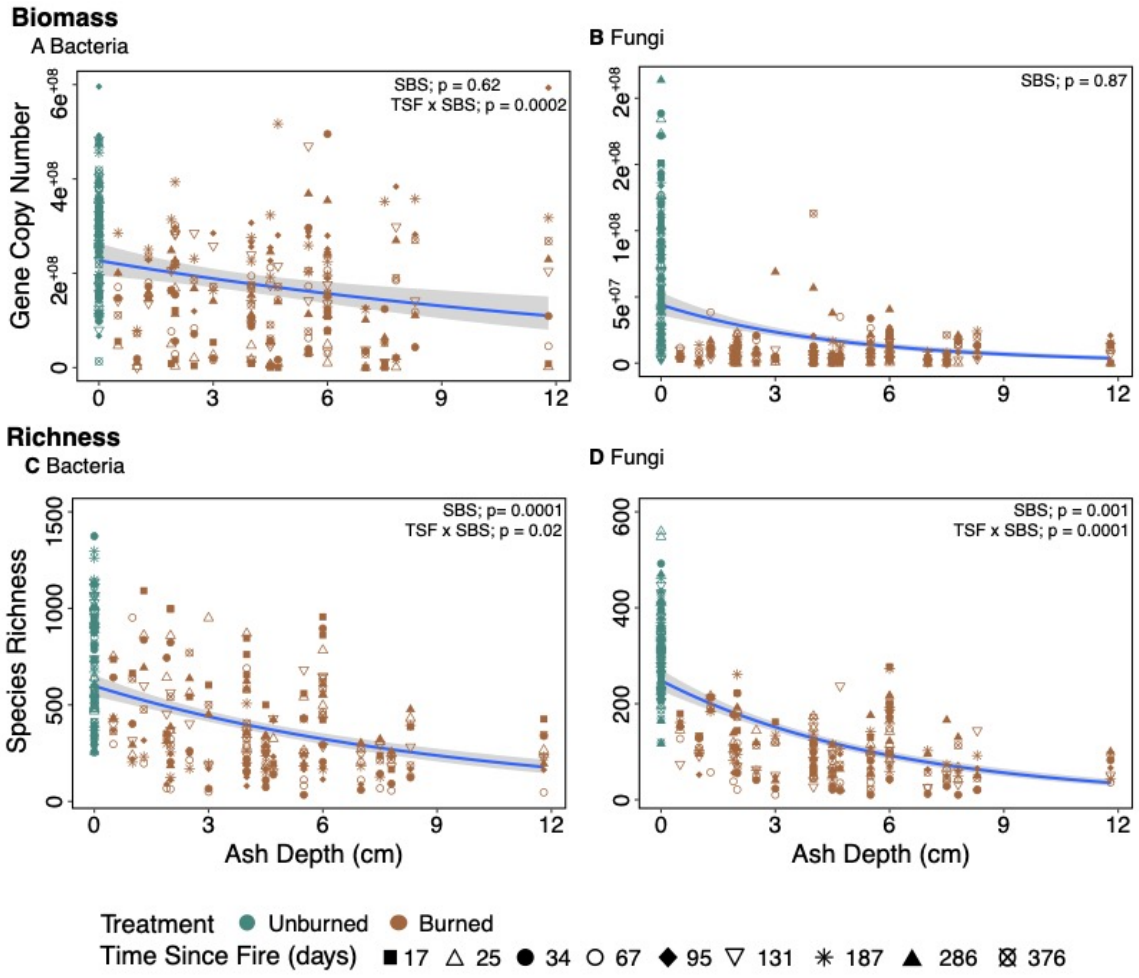

Figure 2.3. Change in estimated biomass and richness with soil burn severity measured as ash depth at 17 days post-fire for A) bacterial and B) fungal biomass per gram of soil and C) bacterial and D) fungal richness. The significance of biomass and species richness against soil burn severity (SBS) and its interaction with time since (TSF) is based on a negative binomial regression (Table S4). The blue line represents the model's prediction, and the gray represents the standard error.

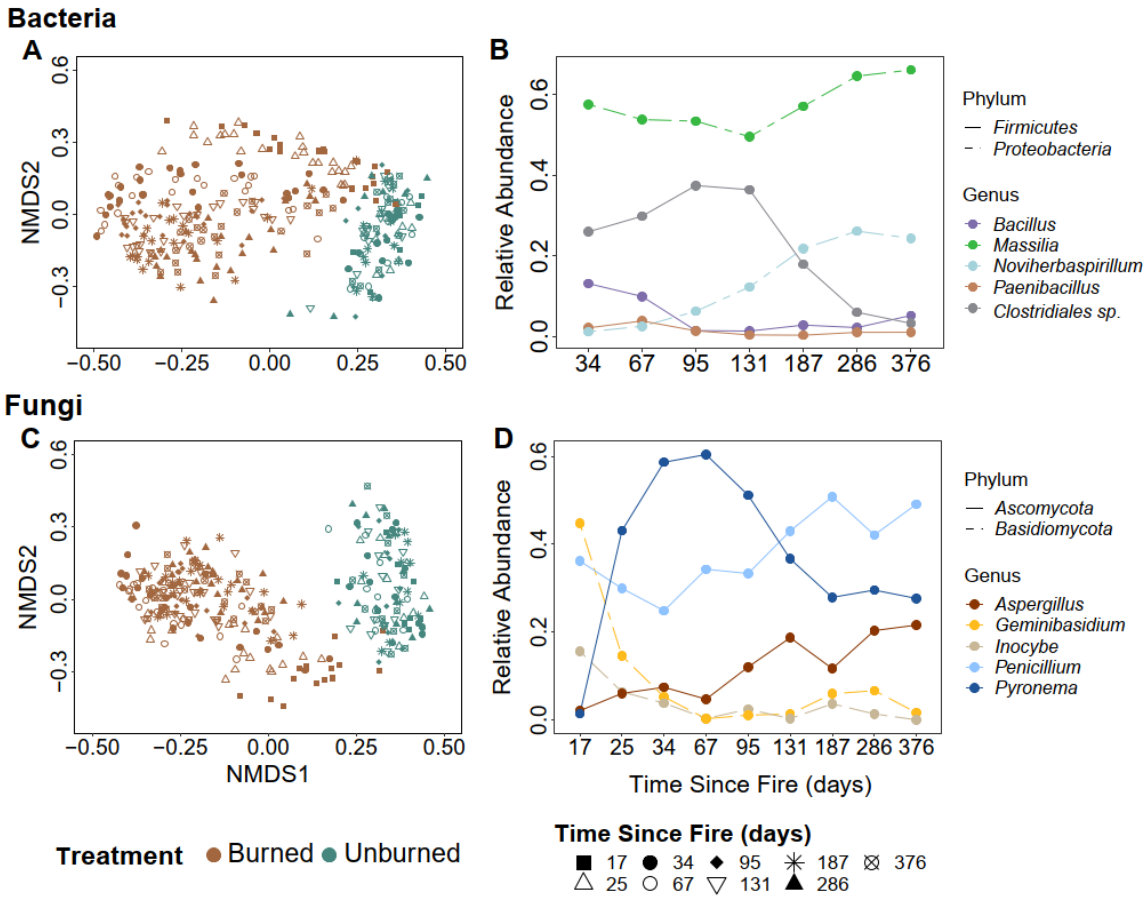

Figure 2.4. NMDS plot of A) bacterial and C) fungal community composition with colors denoting treatment and shape indicating time since fire. The NMDS is based on 3-dimensions and has a stress value of 0.11 for bacteria and 0.12 for fungi. Change in relative sequence abundance of the five most abundant B) bacterial and D) fungal genera in the burned plots over time. Note that the dominance of the top 5 bacterial genera began 34 days post-fire since there was no clear dominance on days 17 and 25 due to the lag in post-fire bacterial declines.

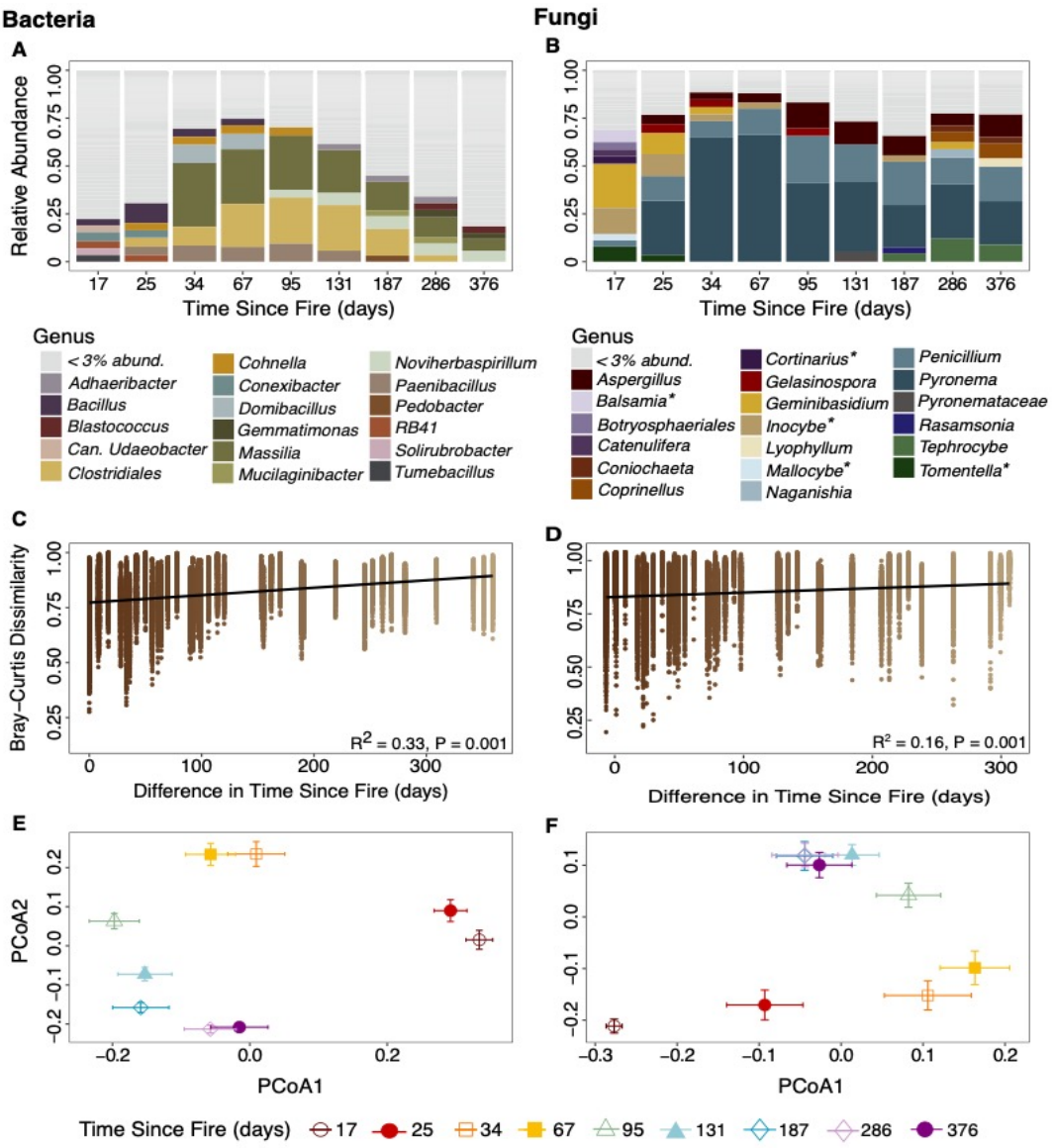

Figure 2.5. Relative sequence abundance of A) bacterial and B) fungal genera (ectomycorrhizal fungi denoted with an asterisk) in burned plots at all 9 timepoints. Mantel correlation between Bray-Curtis dissimilarity and Euclidean temporal distances in C) bacterial and D) fungal community composition in burned plots. Principal components analysis (PcoA) of the mean and standard error Bray-Curtis community dissimilarity at each timepoint for the burned E) bacterial and F) fungal communities. Note that timepoints farther apart with non-overlapping standard error bars indicate a community turnover, whereas overlapping standard error bars represent a lack of compositional turnover. Note that 17 days represents the base level. Thus, the first turnover was initiated at 25 days. Gray bars represent multiple genera of bacteria (A) and fungi (B) that have relative sequence abundance under 3% at each timepoint per treatment. Note that 47% of the bacterial and 20% of the fungal sequences comprise genera <3% relative abundance.

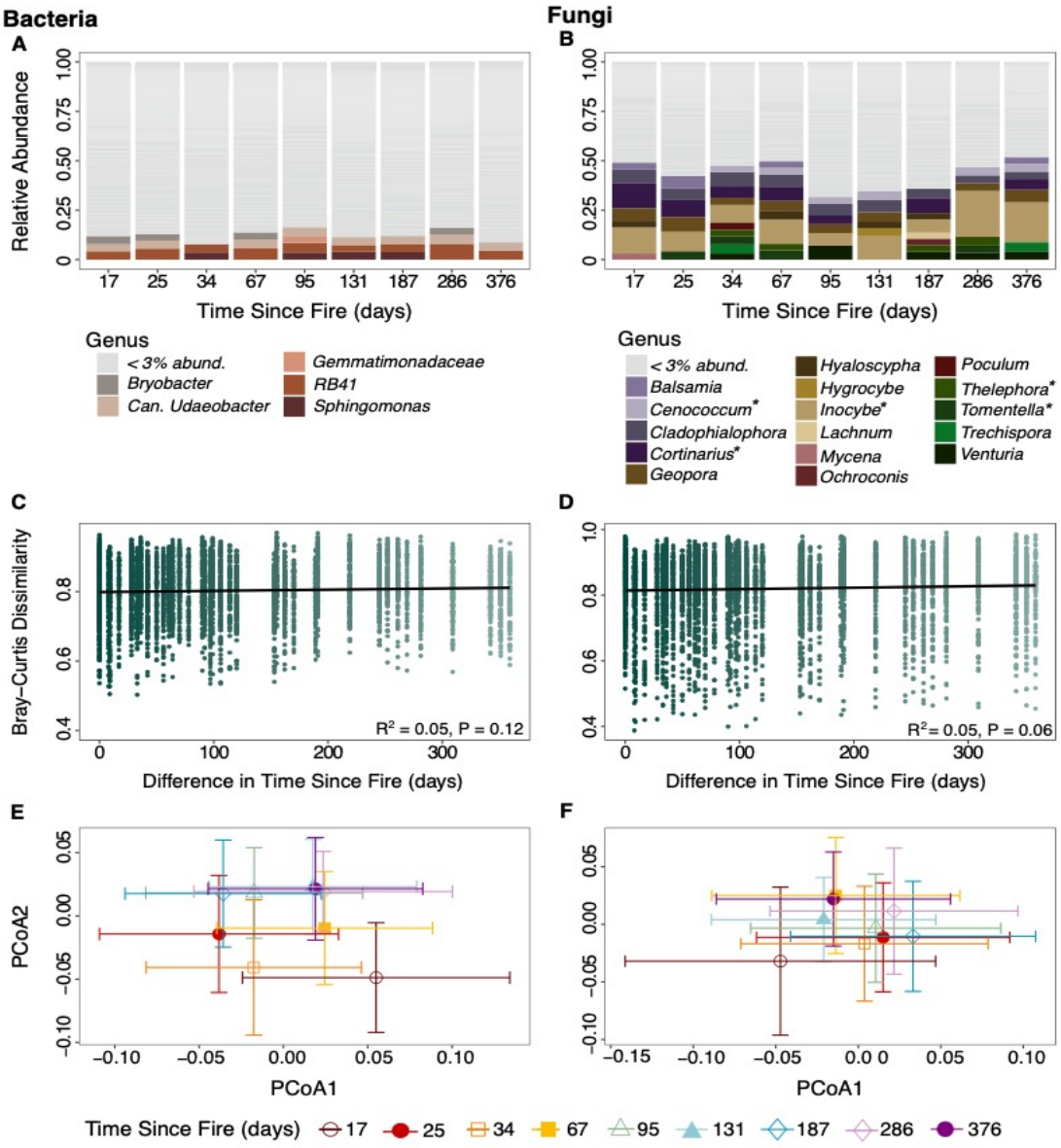

Figure 2.6. Relative sequence abundance of A) bacterial and B) fungal genera (ectomycorrhizal fungi denoted with an asterisk) in unburned plots at all 9-time points. Mantel correlation between Bray-Curtis dissimilarity and Euclidean temporal distances in C) bacterial and D) fungal community composition in unburned plots displaying no significant succession. Principal components analysis (PcoA) of the mean and standard error Bray-Curtis community dissimilarity at each time point for E) bacteria and F) fungi in the unburned plots. In unburned plots, overlapping standard error bars indicate no community turnover across time. Gray bars represent multiple genera of bacteria (A) and fungi (B) that have relative sequence abundance under 3% at each timepoint per treatment. Note the lack of dominance as denoted by the fact that 79% of the bacterial and 51% of the fungal sequences comprise genera <3% relative abundance.

Table 2.1. Pyrophilous bacterial and fungal taxa hypothesized position within Grime's C-S-R succession theory (per traits at the genera level, based on current literature).

Kingdom	Phylum	Genus	Grimmes Traits (CSR)	Trait description	Citation
Bacteria	Firmicute (Bacillota)	*Bacillus*	Survival	Aerobic, Heterotrophic, Antibiotic-producing, thermotolerant; endospore; reduces nitrogen; solubilizes phosphate	Grady et al., 2016; Kaur et al., 2018; Mandic-Mulec et al., 2015; J. et al., 2001; Kalayu, 2019; Slepecky and Hemphill in the Prokaryotes; Espinosa-de-los-Monteros et al., 2001
Bacteria	Firmicute (Bacillota)	*Clostridiales*	Survival, Fast growth	Thermotolerant; endospore; trigger sporulation in response to stress, reduces nitrogen	Grady et al., 2016; Kaur et al., 2018; Mandic-Mulec et al., 2015; Paredes-Sabja et al., 2011; Kalayu, 2019
Bacteria	Firmicute (Bacillota)	*Paenibacillus*	Survival	Aerobic, Heterotrophic, antibiotic producing (Bacteriocins), thermotolerant; endospore; fixes nitrogen	Grady et al., 2016; Kaur et al., 2018; Mandic-Mulec et al., 2015; Monciardini et al., 2003; Slepecky & Hemphill, 2006
Bacteria	Actinobacteria (Actinomycetota)	*Conexibacter*	Competition	Aerobic, Heterotrophic, Antibiotic-producing, reduces nitrogen	Espinosa-de-los-Monteros et al., 2001; Kalayu, 2019
Bacteria	Proteobacteria (Pseudomonadot)	*Massilia*	Fast Growth; Competition	Aerobic, fast reproduction, diverse ecology, exploit resources	Li et al., 2014;Toljander et al., 2005
Bacteria	Proteobacteria (Pseudomonadot)	*Novihersparillium*	Fast Growth; Competition	Fast reproduction, exploit resources; likely PyOM degrader	Baldani et al., 2014; Grady et al., 2016; Woolet & Whitman, 2020
Fungi	Basidiomycota	*Geminibasidium*	Survival	73hermos- and xero-tolerant yeast	Alexopoulous & Mims, 1952
Fungi	Ascomycota	*Pyronema*	Survival Fast Growth	thermotolerant sclerotia; likely PyOM degrader, filamentous,	Moore, 1962; Fisher et al., 2022
Fungi	Ascomycota	*Gelasinospora heterospora*	Survival	Requires heat or chemical treatment for germination, pigmented mycelia	Alexopoulous & Mims, 1952
Fungi	Ascomycota	*Penicillium*	Fast Growth	copious asexual conidia, fast growth, filamentous	Dix & Webster, 1995; McGee et al., 2006;Crow, 1992
Fungi	Ascomycota	*Aspergillus*	Fast Growth	copious asexual conidia, fast growth, filamentous	Dix & Webster, 1995; McGee et al., 2006;Crow, 1992
Fungi	Basidiomycota	*Coprinellus*	Competition	Likely PyOM degrader, filamentous	Steindorff et al., 2021
Fungi	Basidiomycota	*Tephrocybe anthrocophila*	Competition	Affinity for ammonium or nitrogen, filamentous	Suzuki, 2017; Legg, 1992

Chapter III

Microbial-Mediated Pyrogenic Organic Matter and Nitrogen Cycling genes increase over time after a Chaparral wildfire

3.1 Abstract

Wildfires alter soil chemistry and microbial communities, opening niche space for pyrophilous or "fire-loving" microbes to initiate secondary succession. However, wildfires also increase soil nitrogen and transform woody vegetation into difficult-to-decompose pyrogenic organic matter (PyOM), a potential carbon source for pyrophilous microbes. Whether pyrophilous microbes can degrade these post-fire resources has significant implications for global carbon and nitrogen cycling, including carbon sequestration and greenhouse gas emissions. To determine temporal patterns in the functional potential for PyOM degradation and nitrogen cycling, we performed shotgun metagenomics on 30 burned and unburned soils collected at 17, 25, 34, 131, and 376 days after a Southern California chaparral wildfire. In contrast to unburned plots, where relative abundances of genes associated with PyOM degradation and nitrogen cycling

remained stable over time, complementary profiles in burned plots revealed immediate decreases in the relative abundances of PyOM and N genes, followed by dramatic increases over the first post-fire year (167% for PyOM, 117% for N). Genes encoding the degradation pathways for two PyOM degradation intermediates, catechol and protocatechuate, revealed that the easier-to-degrade ortho-cleavage pathways dominated all time points in the burned plots, while genes encoding nitrogen retention pathways (assimilatory and dissimilatory NO_3^- reduction) dominated nitrogen cycling pathways for the entire year. Finally, the dominant pyrophilous bacterial taxa *Massilia* and *Noviherbaspirillium* encoded different PyOM and N processing pathways, suggesting that traits enabling adaptation to wildfires, like post-fire resource acquisition, drive microbial secondary succession.

3.2 Introduction

Soil microbial communities support fundamental post-fire soil processes such as nitrogen (N) immobilization and, thus, storage (Turner *et al.*, 2007) and carbon (C) cycling via decomposition and thus C loss as CO_2 (Liu *et al.*, 2023) or sequestration (Raza *et al.*, 2023). However, understanding the complex functional dynamics of the post-fire soil microbiome remains challenging. With shifting fire regimes resulting in increased fire frequency and severity (Riley & Loehman, 2016), understanding the early functional dynamics of post-fire soil microbial communities is necessary to understand

how species drive secondary successional dynamics and alter important ecosystem functions such as those that affect C sequestration and greenhouse gas emissions.

Wildfires often cause reductions in microbial richness, shifting community composition and allowing pyrophilous or "fire-loving" microbes such as fungal Ascomycetes (Fox *et al.*, 2022; Pulido-Chavez *et al.*, 2023) and bacterial Firmicutes and Actinobacteria (Whitman *et al.*, 2019; Enright *et al.*, 2022; Pulido-Chavez *et al.*, 2023) to initiate secondary succession. However, post-fire secondary succession can trigger a change in resource use that can affect microbial successional dynamics, including successional directionality and community metabolism (Luo *et al.*, 2020). We previously hypothesized that the succession of post-fire microbes is such that initial thermotolerant microbes are succeeded by fast-growing pyrophilous taxa, which are supplemented, later in time, by fungal Basidiomycetes in the genera *Coprinellus, Lyophyllum, Pholiota,* and *Tephrocybe* and bacterial *Noviherbaspirillium* (Pulido-Chavez et al., 2023). These later arrivals might be better suited for the post-fire environment, possibly due their ability to use post-fire resources such as PyOM and N (Fox *et al.*, 2022; Pulido-Chavez *et al.*, 2023). This implies that early post-fire taxa might perform metabolic functions that prime the system for colonization by higher fungal and bacterial taxa, potentially resulting in a new microbial equilibrium. However, whether these simultaneous functional changes are occurring and subsequently affecting microbial successional dynamics is unknown.

Fires alter the C cycle primarily through the combustion of vegetation (Nave *et al.*, 2011) and the abundant formation of Pyrogenic Organic Matter (PyOM), an aromatic

chemically complex C source that is difficult to degrade and thus has a long residence time (Knicker, 2011; Bird *et al.*, 2015). The aromaticity of PyOM requires microbes to encode the genes to cleave the aromatic rings and thus metabolize and attain C (Haddock, 2010). Current evidence from metagenome-assembled genomes (MAGs) shows that *Pyronema domesticum* has a high genomic potential for PyOM degradation (Dove *et al.*, 2022), and lab studies prove that *P. domesticum* indeed can utilize PyOM as its sole C source (Fischer *et al.*, 2021). Moreover, the bacteria *Massilia* and *Noviherbaspirillium* are considered putative PyOM degraders (Perez-Pantoja *et al.*, 2012), suggesting that other pyrophilous microbes might have the genomic potential to use the abundant C sources available after high-severity chaparral wildfires. However, wildfires can also increase the abundance of short-chain alkanes (González-Pérez *et al.*, 2004; Kuhn *et al.*, 2010; Thomas *et al.*, 2012; Badía *et al.*, 2014), such as propane, which are easier to degrade C sources preferentially selected by microbes for consumption (Moucawi *et al.*, 1981; Abbasian *et al.*, 2015; Thomas *et al.*, 2021). However, whether early post-fire microbes have the functional potential to degrade PyOM over alkanes or whether C source selection changes with succession is currently unknown.

In addition to altering the C cycle, fires alter the N cycle through losses via volatilization, reduction of urea hydrolysis (Goberna *et al.*, 2012), and a short-term enrichment of bioavailable N (Neary *et al.*, 1999; Johnson & Curtis, 2001; Dannenmann *et al.*, 2018). However, indirect wildfire effects, such as removal of the vegetation, can increase soil temperature and decrease soil moisture (Neary *et al.*, 1999; Ayiti & Babalola, 2022), resulting in increased aerobic conditions that reduce nitrification (Neary

et al., 1999; Ayiti & Babalola, 2022), but can increase denitrification rates (Stephens & Homyak, 2023). Microbial immobilization can decrease denitrification and thus NO_2 emissions (Chen *et al.*, 2021; Hoang *et al.*, 2022). Conversely, microbial denitrification and urea hydrolysis can increase N_2O emissions (Thomson *et al.*, 2012; Singh *et al.*, 2013; Yoon *et al.*, 2019; Chen *et al.*, 2021; Hoang *et al.*, 2022). Consequently, understanding how post-fire microbes treat this bioavailable N has strong implications for post-fire greenhouse gas emissions. Research in Spanish shrublands showed increases in the relative abundance of genes associated with N incorporation into the ecosytem three years post-fire (Cobo-Díaz *et al.*, 2015). Similarly, in forested ecosystems, the genomic potential for nitrification increased, and denitrification decreased during the first post-fire decade (Dove & Hart, 2017). Thus, although there is evidence that the enrichment of pyrophilous microbes can be associated with concurrent increases in the relative abundances of genes to process increased post-fire bioavailable N, temporal changes in these dynamics following fire are unknown.

We previously showed that microbial successional dynamics began with thermotolerant taxa (Firmicutes and fungal genera *Pyronema* and *Geminibasidium*) that were replaced by fast colonizers (i.e., fungal *Penicillium* and *Aspergillus* and bacterial *Massilia*) followed by taxa with putative N and PyOM degradation capabilities such as *Massilia, Novihersbaspirillum* and fungal Basidiomycetes *Tephrocybe* and *Coprinellus* (Pulido-Chavez *et al.*, 2023). Moreover, we observed five bacterial and six fungal compositional turnover events during post-fire year one (Pulido-Chavez *et al.*, 2023) that suggest underlying community metabolic changes might be driving secondary

succession. Thus, we used a high-resolution temporal sampling of soil microbiomes after a chaparral wildfire and performed a gene-centric metagenomic analysis to determine how dynamic changes in pyrophilous communities relate to post-fire microbial functions and successional dynamics. We selected 5 time points (17, 25, 34, 131, and 376 days post-fire) corresponding to observed microbial compositional turnover events to identify how wildfires affect the diversity and relative abundance of genes driving PyOM degradation and N cycling over time. We tested the hypotheses that the genes encoding potential for H1) degradation of wildfire-induced C sources like PyOM and alkane and H2) processing of abundant bioavailable N will increase over time in burned plots corresponding to microbial community successional dynamics and the increased relative abundance of pyrophilous taxa with the putative abilities to use high post-fire abundances of PyOM and N.

3.3 Methods

3.3.1 Sampling

In 2018, the Holy Fire burned 94 km^2 of Chaparral shrublands in the Cleveland National Forest in Southern California. Seventeen days post-fire, we established nine plots (6 burned and 3 unburned), selecting for similarity in pre-fire vegetation, elevation, and aspect. Each plot contained four 1 m^2 subplots in each cardinal direction for temporal soil sampling of the top 10 cm of mineral soil beneath the ash or the duff (Fig. B.1.1). Soil samples were collected at nine time points within the first year post-fire (i.e.,

17, 25, 34, 67, 95, 131, 187, 286, and 376 days). DNA was extracted from 0.25g of 2 mm sieved soil with Qiagen DNeasy PowerSoil kits, then samples were sequenced with Illumina MiSeq to identify 16S and ITS2 amplicons (Pulido-Chavez *et al.*, 2023).

3.3.2 Metagenomic sequencing

We used the 16S and ITS2 microbiome analysis to select 5 time points (17, 25, 34, 131, and 376 days post-fire) with the most extreme microbial compositional turnover events for metagenomic analyses (Pulido-Chavez *et al.*, 2023). From each of the five timepoints, we selected 3 burned and 3 unburned subplots for a total of 30 metagenomes (15 burned and 15 unburned). Samples were chosen by selecting the DNA samples with the following criteria, 2.5 ng/µl and 230/260 above 1.8, from unburned plot 8 (Fig. B.1.1a) and from two closely situated burned plots with the most similar microbial richness and biomass (plots 2 and 3; Fig. B.1.1a). Metagenomic library preparation and sequencing were performed at the Department of Energy Joint Genome Institute (JGI) in Berkeley, California for 17 samples and at the University of California, Irvine (UCI) Genomics High-Throughput Facility for 13 samples. Libraries were prepared from the frozen DNA extractions using the Kapa Biosystems library preparation kit at JGI and the Illumina Nextera Flex library preparation kit at UCI and were sequenced on the Illumina NovaSeq 6000 platform on an S4 flow cell (151 bp paired-end reads and a depth of 25 Gb/sample). See supplementary data 1 for additional information regarding metagenomic sequencing.

3.3.3 Metagenomics binning

Sequence adapters were removed from the raw reads using BBduk-v38.89 (sourceforge.net/projects/bbmap/) with the following parameters *(*ktrim=r, k=23, mink=11, hdist=*1*). Raw reads were trimmed with Sickle – v1.33, and the quality of trimmed reads was assessed with FastQC – v0.11.2 (Andrews, 2010). Trimmed reads were assembled into contiguous sequences (contigs) with the de novo de Bruijn assembler MEGAHIT – v1.2.9 (Li *et al.*, 2014) with the following parameters (min kmer of 27, max of 127, and increment of 10). Per-contig coverage per sample was calculated using CoverM contig version v0.6.0 (Woodcroft, 2007) with the trimmed mean method to retain only mappings >95% identity and minimum alignment of 75% (Parks *et al.*, 2015). Assembled contigs (>2,500 bp) were binned using MetaBAT2 v2.12.1 with default parameters (Kang *et al.*, 2015) to assemble bacterial metagenome-assembled genomes (MAGs). MAG quality was estimated using checkM v1.1.2 (Parks *et al.*, 2015), and taxonomy was assigned using GTDB-Tk v2.1.1 (Chaumeil *et al.*, 2019) and dereplicated using dRep v3.0.0 (Olm *et al.*, 2017) to remove low-quality MAGs (<50% completion and >10% contamination). See supplementary data 1 for additional information regarding metagenomic assemblies and MAGs.

3.3.4 Contig annotation

To assess the degradation of aromatic hydrocarbons, such as PyOM, we focused our PyOM contig annotation on catechol and protocatechuate, two intermediate aerobic degradation pathways (Fuchs *et al.*, 2011) and short-chain alkane C. To improve

retention and annotation of the samples in a comprehensive manner, all assembled contigs were annotated using three different databases. First, contigs were annotated using HMMER (Eddy, 2011), with hidden Markov models (HMMs) against Kofamscan HMMs (Aramaki *et al.*, 2020) to identify specific genes related to aromatic compound degradation (i.e., catechol and protocatechuate and inorganic N cycling) according to previously established methods (Nelson *et al.*, 2022). Furthermore, we used the Calgary approach to AnnoTating HYDrocarbon (CANT-HYD) degradation genes, which uses HMMs for annotating marker genes involved in aerobic and anaerobic hydrocarbon degradation pathways (Khot *et al.*, 2022). Lastly, we employed the Distilled and Refined Annotation of Metabolism, DRAM (Shaffer *et al.*, 2020) to profile our contigs through multiple databases (i.e., KEGG (Kanehisa & Goto, 2000), UniRef90 (Suzek *et al.*, 2007), MEROPS (Rawlings *et al.*, 2014), and Mmseqs2 (Steinegger & Söding, 2017) with the best hits (based on a bit score of 60) reported for each database. The contig dataset was normalized by calculating the contig length corrected trimmed mean (geTMM) of M values (Smid *et al.*, 2018) using EdgeR (Robinson *et al.*, 2010), normalizing by library depth and gene length as has been previously used for metagenomics data (Capo *et al.*, 2021; Leleiwi *et al.*, 2023; Santos-Medellin *et al.*, 2023). The results from all three annotations were concatenated into one large file, and genes related to aromatic hydrocarbons (PyOM), alkane degradation, N, and urea cycling were selected for all downstream analyses. In the case where contigs contained duplicated annotations, the annotations were manually curated, and the best functional annotation was determined by selecting the annotation with the lowest e-value.

We used results from a DESeq analysis (see details below) to identify genes of interest, then used NCBI BLAST (Bethesda, 2008) to link the MAG catalog to these dominant genes. We filtered the BLAST matches to include only hits with 100% identity and a bit score of at least 100. Therefore, we identified the specific taxa that encoded key genes, including those related to PyOM and N cycling pathways. For a comprehensive computational map illustrating the bioinformatic procedures employed, please refer to the supplementary figure B.1.2.

3.3.5 Statistical analysis

All statistical analyses were performed, and figures were made in R version 4.2.3 (RCoreTeam, 2023; Team, 2023). First, we determine how fire, time, and their interaction impacted the overall composition of genes for PyOM or N cycling with Permutational Multivariate Analysis of Variance (PERMANOVA;(Anderson, 2017) as implemented in the adonis2 function of the vegan package (Oksanen *et al.*, 2022) with 9999 permutations with plot as random effect. Results were visualized using nonmetric multidimensional scaling (NMDS). Ordinations were based on Bray–Curtis distance matrixes using the ordinate function in the phyloseq package (McMurdie & Holmes, 2013). Since alkanes increase post-fire and are preferentially selected by microbes as a C source, we separated alkanes from the PyOM genes for all downstream analyses, allowing us to determine if this preferential uptake also occurs in post-fire systems. Moreover, since urease is vital to hydrolyze urea into ammonia (NH_3^+) (Fernández-García *et al.*, 2020), an essential process that makes N readily available for plant uptake,

we further separated the urea pathway from the N cycling processes, allowing us to determine the effect of fire on these important ureases and thus helping us understand if the post-fire microbes possess ureases which can help us better understand post-fire ecosystem restoration and N cycling.

Second, to determine if microbial functional changes mirrored the rapid compositional changes we previously observed at 17, 25, 34, 131, and 376 days post-fire (Pulido-Chavez *et al.*, 2023), we calculated the homogeneity of variance for burned and unburned communities independently. Furthermore, we used permutest with 9999 permutations and plot as random effect to determine which time points differed for burned and unburned pathways. We used principal coordinates analysis (PCoA) to visualize the differences in the homogeneity of variance of each functional pathway with the vegan package (Oksanen *et al.*, 2022) using Bray-Curtis dissimilarities.

Third, we independently performed generalized negative binomial regression on burned and unburned plots for each pathway to test how the number of PyOM, alkane, N, and urea cycling genes changed over time. The nestedness level was tested using null model and Akaike criteria. Burned PyOM, alkaline, and urea models retained plot, and unburned models retained subplot as random effect. Burned N models required plot, subplot, and time, and unburned N models required time and subplot as random effects. For all models, time was scaled and centered. To visualize how the microbial functional potential changes over time; we visualized the sum geTMM of each PyOM, alkane, N, and urea pathway over time using the phyloseq version 1.42.0 (McMurdie & Holmes, 2013) for each time point in burned and unburned communities independently.

Lastly, to identify the PyOM, alkane, N, and urea genes that were differentially overrepresented in the burned versus the unburned plots at each sampling time point, we employed DESeq2 v1.38.3 (Love *et al.*, 2014). Five separate models in DESeq2 were defined, one per timepoint, to assess the response of functional gene potential and independently identify the difference in response to fire over time for each pathway. Results are based on the DESeq Wald test (adjusted p-value < 0.05 and absolute log2 fold-change >0). The total count of differentially abundant genes was visualized as a bar plot for each independent pathway over time. Moreover, we used the differentially abundant genes at each time point in the burned communities (p_{adj}<0.05) to create a metabolic map for PyOM and N degradation pathways. Furthermore, to link the most abundant genes to their taxonomy, we first selected the genes of interest (most abundant genes based on DESeq results at each time point, log2fold change >0 and p < 0.05) and linked them to their respective taxonomy using our MAG created database (Bethesda, 2008). Taxonomy and functional annotation of the selected group of genes were plotted using ggplot2 (Wickham, 2016). All statistical scripts (R scripts) are publicly available on GitHub: https://github.com/pulidofabs/Chaparral-Metagenomes.

3.4 Results

A total of 2,034 contigs were binned to assemble MAGs, resulting in 455 medium- and high-quality MAGs. Identified taxa represented across all MAGs belonged to the phyla Acidobacteriota, Proteobacteria, and Verrucomicrobiota, with a few

pyrophilous bacteria in the genera *Massilia* and *Noviherbaspirillium* (Supplementary Data 1C). Additional contig information, MAG quality and taxonomy information, and contig taxonomy information for the dominant selected genes are available in Supplementary Data 1C. Metagenomes and MAGs are deposited at NCBI.

3.4.1 Wildfire altered the profile of functional genes for PyOM and N

Fire significantly impacted the profile of functional genes implicated in N and PyOM cycling, leading to significant changes over time (Fig. 3.1; Table B.1.1). Wildfire was the strongest driver of differences in functional potential, explaining 15% of the variation for PyOM ($p = 0.001$; Fig. 3,1a; Table B.1.1) and urea (Fig. 3.1d) and 16% for alkanes ($p = 0.001$; Fig. 3.1b; Table B.1.1) and the remaining N cycling genes (Fig. 3.1c; Table B.1.1). Time had smaller but significant impacts on the functional profiles of these genes, explaining 5% of the variance in PyOM, N, and urea cycling genes and 6% for alkane genes (Table B.1.1). A significant fire-by-time interaction explained 5% of the variation for PyOM and urea and 6% for N, but it had no significant impact on alkanes (Table B.1.1).

While there was no change in the turnover or community-level alterations of the profile of functional genes in the unburned plots (Fig.3.2; betadisper $p>0.05$), the burned plots experienced multiple functional profile turnover periods (Fig.3.2; Table B.1.2). Overall, genes associated with urea processing displayed greater turnover than those associated with the degradation of PyOM, alkanes, and N (Fig.3.2h). Functional genes associated with urea cycling experienced functional turnover at 25, 34, and 131 days

post-fire (Fig.3.2h), while PyOM cycling (Fig.3.2b) and N cycling genes (Fig.3.2f) both experienced two turnover events at days 34 and 131. Finally, genes encoding the functional potential for processing alkanes displayed turnover events at days 25 and 131 post-fire (Fig.3.2d).

3.4.2 Time differentially affected PyOM degradation pathways

While the geTMM normalized gene values associated with PyOM or alkane processing were not affected by wildfire (Table B.1.3, B.1.4), a significant and positive treatment-by-time interaction was observed for PyOM and alkane cycling pathways ($p<0.0001$; Table B.1.3, B.1.4), increasing geTMM values over time compared to 17 days post-fire (Fig 3.3; $p<0.004$; Table B.1.4). This increase is attributed to the increasing number of PyOM genes (Fig. B.1.4), which correlates with the increase microbial diversity and abundance over time (Fig. B.1.4). Moreover, time differentially affected the different steps of PyOM and alkane cycling pathways (Fig. 3.3b, d; Fig. B.1.5; Table B.1.5). Specifically, we detected temporal increases in geTMM values associated with catechol and protocatechuate cycling (Fig. 3.3b, Fig. B.1.5; Table B.1.5). However, the β-ketoadipate (Fig. 3.3b; Fig. B.1.5; Table B.1.5) and all alkane cycling pathways (i.e., methane, alkane, and propane) remained unchanged over time (Fig. 3.3d; Fig. B.1.5; Table B.1.6).

3.4.3 Time differentially affected N degradation pathways

Similarly, wildfire did not directly affect the geTMM values for N or urea cycling

(Table B.1.3), but a treatment-by-time interaction for N and urea increased geTMM values over time when compared to 17 days post-fire, more so for urea (Fig. 3.4c, d) than N ($p<0.02$; Fig. 3.4a, b; Table B.1.3; B.1.4). This increase in geTMM values could be due to increases in diversity and relative abundance over time (Fig. B.1.6). Moreover, time differentially affected the different steps of the N and urea cycling pathways (Fig 3.4; Fig. B.1.7; Table B.1.7, B.1.8). For N cycling, geTMM values for NO_3^- assimilation (assimilatory and dissimilatory) and nitrification significantly increased with time when compared to 17 days post-fire ($p<0.04$; Fig. 3.4b; Fig. B.1.7, Table B.1.7), but time did not affect denitrification or urea cycling geTMM values (Fig. 3.4b,d; Fig. B.1.7, Table B.1.7). However, unburned denitrification geTMM values were significantly and negatively affected by time ($p=0.004$; Fig. 3.4a, Fig. B.1.7, Table B.1.7). For urea, both urea and ornithine geTMM values significantly increased over time ($p<0.004$; Fig 3.4d, Table B.1.8).

3.4.4 Wildfire selects for ortho-cleavage aromatic degradation pathways

Wildfire resulted in a higher number of PyOM degradation genes being significantly differentially abundant within the burned communities as compared to the unburned communities (692 vs 258; $p_{adj} <0.05$; Fig. 3.5,3.8). The functional potential for PyOM degradation genes also differed across the burned plots over time ($p_{adj} <0.05$; Fig. 3.5a, 3.7). Overall, the ortho-cleavage pathway for the protocatechuate and catechol pathways and the β-ketoadipate pathway were differentially abundant in the burned plots throughout the year (17-131d; $p_{adj} <0.05$; Fig. 3.5a, 3.7). In contrast, the meta-cleavage

pathways for catechol and protocatechuate were only differentially abundant in the early post-fire timepoints (p_{adj} <0.05; Fig. 3.5a, 3.7) and at 131d post-fire for catechol meta-cleavage (p_{adj} <0.05; Fig. 3.5a, 3.7). Interestingly, genes associated with aromatic hydrocarbon degradation, related to lignin degradation, were differentially abundant in the unburned communities at 17 and 25 days post-fire (Fig. 3.5a). However, it is noteworthy that the specific genes differed between the burned and unburned communities.

Alkane degradation pathways exhibited differential abundance in genes related to converting acetate to methane (17d-376d; p_{adj} <0.05; Fig. 3.5b), with other degradation steps, such as propane 2-monooxygenase, alkane hydroxylase, and alkane monooxygenase being only overrepresented at 17d post-fire (p_{adj} <0.05; Fig. 3.5b).

3.4.5 Wildfire increased genes for N retention

Wildfires resulted in more differentially abundant N cycling genes within the burned communities than the unburned communities (143 vs 55; p_{adj} <0.05; Fig. 3.5c, 3.8). Overall, at all-time points, the genes encoding N retention pathways, such as assimilatory NO_3^- (*nasABC; NRT, narK, nrtP*, and *nirA*) and dissimilatory NO_2^- (*nirBD, narBlVHY, and nxrB*) reductase and NO_3^- assimilation (*narG, narZ, nrxA*) pathways were differentially abundant in the burned microbial communities (p_{adj}<0.05; Fig. 3.5c, 3.8). In contrast, all urea degradation pathways were significantly abundant in the burned plots at 25, 34, and 131 days post-fire, except at 67 days post-fire, where only the conversion of argininosuccinate to arginine was significantly abundant (p_{adj}<0.05; Fig. 3.5d, 3.8).

3.4.6 Genomic potential of dominant taxa differed in burned and unburned communities

The genomic potential for catechol and protocatechuate ortho-cleavage and β-ketoadipate degradation in the burned plots were abundant in MAGS representing the phyla Proteobacteria, Actinobacteria, and Acidobacteriota (Fig. 3.6, gene *fad;* Supplementary file 1c). Pathway genes for Catechol ortho-cleavage (*CatABC)* and β-ketoadipate (*pcaDLJ, fadA)* degradation were differentially encoded by MAG number CNF2NT9_metabat.6, representing the pyrophilous Proteobacteria *Massilia* (Fig. 3.6), the most dominant bacterial taxa in the post-fire community (Fig S4). The protocatechuate ortho-cleavage pathways, genes *pcaBCH*, were encoded by MAGs representing the Burkholderiales-SG8-41 Solirubrobacteraceae (MAG CNF6NT3_metabat.4) and the dominant pyrophilous *Noviherbaspirillium* (Fig. 3.6, S4; MAGs CNF3ST6_metabat.25). Additionally, genes related to the catechol meta-cleavage pathway (dmpBC, xylEG) were encoded by the MAGs affiliated with the bacterial families Xanthobacteraceae-PALSA-894 (MAG CNF2NT1_metabat.6) and Chthoniobacterales-AV80 (Cat3, MAG CNF6NT3_metabat.11; Fig. 3.6). Furthermore, protocatechuate meta-cleavage degradation genes (*ligClK, galC*) were differentially abundant in MAGs representing the dominant *Noviherbaspirillium* (MAG CNF3ST6_metabat.25) and Xanthobacteraceae-PALSA-894 (MAG CNF2ET2_metabat.2 and CNF2NT1_metabat.6; Fig. 3.6). Although catechol, protocatechuate, and β-ketoadipate genomic potential were differentially abundant at 17 and 25 days post-fire in the unburned plots, the genes and the genera differed and were driven by the MAGs

representing *Bradyrhizobium* (MAG CNF8ET1_metabat.62) and Acidimicrobiales-*AC-14* (MAG CNF8NT3_metabat.96; *pcaD, fadAl; praC, xylH, pracH, ligABC*; Fig. 3.6).

The genes encoding NO_3^- retention pathways, both assimilatory NO_3^- reductase (*nasABC, nirA*) and dissimilatory NO_3^- reductase (*nirBD*), were differentially abundant in the MAGs for the family Actinobacteriota *Arthrobacter* (*NasABC*; MAG CNF3ET9_metabat.15), Micromonosporaceae (*NasABC*; *NirBD*; MAG CNF3ET9_metabat.92) and *Pseudonocardia* (*NirBD*; MAG CNF2NT3_metabat.37; Fig. 3.6). *Massilia* (MAG CNF2NT9_metabat.6) also encoded genes for dissimilatory NO_3^- retention pathways reductase (*nirD*) and NO_3^- retention pathways (MAG CNF2NT9_metabat.6*; NRT, narK, nrtP, nasA*; Fig. 3.6). Furthermore, genes associated with NO_3^- retention pathways assimilation (*NRT, narK, nrtP, nasA*) were differentially abundant within the Actinobacteria, specifically in genera *Arthrobacter* (MAG CNF3ET9_metabat.15) and Micromonosporaceae (MAG CNF3ET9_metabat.92; Fig. 3.6). Like PyOM genes, NO_3^- retention pathways assimilation, reduction, and denitrification in the unburned plots at 17 days post-fire were differentially abundant in the non-pyrophilous bacteria *Bradyrhizobium* (MAG CNF8ET1_metabat.62 and CNF8NT2_metabat.40; *NRT, narK, nrtP, nasAC, napA*; Fig. 3.6).

Discussion

We found that high-severity fire dramatically altered the genomic functional potential within the post-fire soil microbiome, concurrent with large changes in microbial

community composition (Pulido-Chavez et al., 2023). Wildfire increased the geTMM value for PyOM degradation genes over time, and our analyses revealed that catechol and protocatechuate ortho-cleavage (i.e., β-ketoadipate) pathways are the primary encoded mechanisms for PyOM degradation. We also found that wildfire increased the geTMM values for N cycling genes over time, selecting for genes encoding the N retention pathways, via conversion of NO_3^- to biomass and NO_2 to NH_3^+, with significant implications for trace and greenhouse gas emissions. Finally, we found that pyrophilous bacterial taxa that dominated our post-fire chaparral communities (i.e., the Burkholderiales *Massilia,* and *Noviherbaspirillium*) (Pulido-Chavez et al., 2023) encoded multiple but differential PyOM degradation pathways, suggesting that traits enabling adaptation to wildfires like post-fire resource acquisition drive microbial succession.

3.5.1 PyOM geTMM values increased over time

We previously observed patterns of microbial secondary succession in chaparral and hypothesized that these changes aligned with the ability of post-fire microbes to utilize post-fire resources (Pulido-Chavez *et al.*, 2023). Here, we found that geTMM values for genes encoding for PyOM degradation increased over time and were differentially abundant in the burned plots. While bacteria initially decreased in biomass and richness post-fire, they did vary in abundance over time, with some increases in richness observed in bacterial communities at 1 year relative to 17 days post-fire (Pulido-Chavez *et al.*, 2023). Thus, it is plausible that the augmented total number of differentially abundant genes and elevated getTMM values observed in our study over

time, are associated with the emergence of additional species possessing genomic capabilities for PyOM degradation in burned plots.

We previously hypothesized that the succession of post-fire microbes is such that thermotolerant microbes dominate first, followed by fast-colonizers, which are then replaced by microbes capable of capitalizing on post-fire resources, such as PyOM and N (Pulido-Chavez *et al.*, 2023). Our metagenomic data support those inferences from microbiome data and indicate that MAGs representing pyrophilous bacteria (i.e., Proteobacteria *Noviherbaspirillum* and *Massilia)* that dominate during the first-post-fire year encode multiple genes for PyOM and N degradation. Indeed, PyOM treatment (Chen *et al.*, 2021; Cheng *et al.*, 2022; Zeba *et al.*, 2023) and incubation studies (Song *et al.*, 2017; Woolet & Whitman, 2020) have shown that *Noviherbaspirillium* and *Massilia* increase in relative abundance in response to PyOM addition, suggesting that these taxa are readily degrading PyOM as a C source. *Massilia* encoded genes to degrade PyOM via the catechol and β-ketoadipate ortho-cleavage pathway. In contrast, *Noviherbaspirillium* encoded genes for PyOM degradation via the protocatechuate ortho and meta-cleavage pathways, showing that while both taxa might be capable of attaining C via the degradation of PyOM, they do so via different degradation pathways. Previous studies have indicated that microbes utilizing the meta-cleavage pathway tend to experience a growth lag and delayed substrate utilization due to difficulties regulating the upper pathways required to induce degradation of the intermediate PyOM pathways, such as catechol and protocatechuate (Johnson & Beckham, 2015), potentially explain the later appearance of *Noviherbaspirillium* during succession. In contrast, the dominance of

Massilia could be explained by their genomic potential to degrade PyOM via the catechol ortho-cleavage pathway and rapidly accessing C. Although we were unable to detect any fungal-associated contigs for PyOM or N degradation in these data, we have previously found that fungal basidiomycetes *Coprinellus* and *Lyophyllum* increased in abundance in the burned communities 286 days post-fire (Pulido-Chavez *et al.*, 2023). Both fungal basidiomycetes are well-known decomposers (Steindorff et al., 2021) and thus might also encode to better degrade PyOM and coincide with the increase of PyOM cycling genes over time.

Fire selects for microbial taxa that encode genes for alkane degradation. Previous studies have shown that extractable levels of acetate increase post-fire in subsurface soil (Blank *et al.*, 1994). In this study, we demonstrate that bacteria in the early post-fire stages, specifically at 17 and 25 days post-fire, possess the genomic capacity to utilize the abundant post-fire resource, as indicated by the higher abundance of genes such as *ACSS1_2, acs*, and *pta* associated with the alkane degradation, more specifically, with the conversion of acetate-to-methane. This suggests that early post-fire microbes might only be capable of using easier-to-degrade labile C sources and thus readily reproduce and rapidly dominate the ecosystem. However, later in the succession process, the potential depletion of labile C sources leads to microbial community shifts, with microbes capable of using more complex aromatic C sources rapidly dominating the community.

Moreover, while methanogens were not detected in our system, the phylum Proteobacteria and Acidobacteriota contain the *ACSS1_2, acs* genes responsible for the conversion of acetate-to-methane and have been previously been shown to efficiently use

the C produced by methylotrophic bacteria (Morawe *et al.*, 2017). Furthermore, previous studies have shown a cooperative interaction between the bacteria *Bradyrhizobium* (Hanson & Hanson, 1996) and the synergistic interactions involving methanogens, as exemplified by Acidimicrobiales (Koch *et al.*, 2008; Johnson *et al.*, 2009; Morawe *et al.*, 2017). Together, these findings highlight the intricate interactions that may occur post-fire and suggest that metabolic handoffs and cooperative utilization of resources may play crucial roles in shaping post-fire successional and ecosystem dynamics.

3.5.2 Post-fire microbes preferentially retain N and increase nitrification

Coincident with large post-fire increases in bioavailable N (Pulido-Chavez et al., *In prep*), we found that geTMM values for genes encoding nitrification, assimilatory, and dissimilatory N reductase increased over time and were differentially abundant in the burned plots. These results are supported by complementary post-fire studies in coniferous forests (Kurth *et al.*, 2013; Kurth *et al.*, 2014; Dove & Hart, 2017; Dove *et al.*, 2020; Dove *et al.*, 2021; Dove *et al.*, 2022) and chaparral (Hanan *et al.*, 2016) ecosystems indicating enrichment of nitrification in the immediate aftermath of wildfire. In our initial study of post-fire microbiomes, we showed that bacterial taxa in the genera *Massilia* and *Paenibacillus,* previously recognized as being capable of nitrification (Qiao *et al.*, 2020; Wang *et al.*, 2022; Salazar *et al.*, 2023), increased with time and after winter rains (Pulido-Chavez *et al.*, 2023). Moreover, the Actinobacteria genus *Arthrobacter* and family Micromonosporaceae encoded genes for N immobilization, suggesting that the increase in immobilization genes at 131 days could be attributed to heightened

immobilization by *Arthrobacter* and Micromonosporaceae following increased winter rains.

Wildfire's innate ability to promote short-term N losses by stimulating NO_3^- retention pathways production can be detrimental to post-fire ecosystem recovery (Hanan *et al.*, 2016), especially when microbes, the major players in N retention (Knicker, 2007; Hanan *et al.*, 2016), are also affected by the fire. We found that pyrophilous microbes in early post-fire soils (17-25 days post-fire) possess denitrification genes, which could amplify N losses in the form of N_2 or N_2O, powerful greenhouse gases. These results align with a recent review of N emissions in wildfire affected ecosystems (Stephens & Homyak, 2023). However, N loss is transient since post-fire microbes, including those associated with the genera *Arthrobacter, Massilia,* and Micromonosporaceae, can potentially immobilize N by incorporating it into biomass through the assimilatory NO_3^- retention pathways reduction pathway. Moreover, the genera *Massilia, Pseudonocardia,* and family Micromonosporaceae can further convert NO_2^- to NH_3^+ via dissimilatory NO_2^- reductase, making this resource readily available for plant and microbial use. Together, these results show that post-fire microbes possess the genomic potential to retain post-fire ecosystem N. These findings align with prior research indicating the nitrogen-reducing and assimilating capabilities of *Massilia* and *Arthrobacter* (Cacciari *et al.*, 1986; Bailey *et al.*, 2014; Liu *et al.*, 2023), and N retention processes have been observed in various wildfire-affected systems (Xu *et al.*, 2022), including chaparral (Goodridge *et al.*, 2018), and in field studies using biochar or PyOM additions (Bai et al., 2015). Furthermore, metagenomic studies have previously shown enrichment of *nirB/D* genes (N retention

genes) four years post-fire (Dove *et al.*, 2022). These collective results underscore the role that dominant pyrophilous bacteria in fire-adapted chaparral communities may play in the assimilation and retention of N, playing critical roles in mitigating N losses and facilitating ecosystem restoration.

3.5.3 Post-fire chaparral microbes preferentially degrade PyOM via the ortho-cleavage degradation pathway

Microbial taxa enriched in the post-fire soils encoded the ortho-cleavage catechol and protocatechuate pathways for PyOM degradation over the meta-cleavage pathways. However, the bacterial taxa implicated in PyOM degradation only contained functional genes for part of a specific degradation pathway, suggesting that post-fire bacterial communities may thrive via cooperative interactions and metabolic handoffs. Prior studies have shown that the β-ketoadipate pathway (or the ortho pathway) is the most common method for aromatic degradation (Granja-Travez *et al.*, 2020; Weiland *et al.*, 2022) and the preferred route for aromatic degradation for lignin-degrading bacteria (Granja-Travez *et al.*, 2020; Weiland *et al.*, 2022). These results are also supported by data from post-fire coniferous forest soils, which revealed the presence of the ortho-cleavage pathway in over 50% of MAGs recovered from those samples (Nelson *et al.*, 2022) and intriguingly suggests that high-severity fires may always select for ortho-cleavage pathways regardless of the biome.

Furthermore, we found that the genes for the full catechol (*catABC*) and protocatechuate (*pcaHGBCDLJ*) ortho-cleavage degradation pathways were present

across all samples for the entire year. The ortho-cleavage pathways were differentially abundant across multiple taxa in the Proteobacteria including Burkholderiales *SG8-41, Noviherbaspirillum*, *Massilia*, and Xanthobacteraceae *PALSA-894*, Acidobacteriota (Blastocatellia *JADGNW01*, Verrucomicrobiota (Chthoniobacterales *AV80* and Actinobacteriota (*Mycobacterium, Pseudonocardia*, and Solirubrobacteraceae). Previous research indicated that bacteria preferentially utilize the catechol ortho-cleavage pathway while fungi preferentially use the protocatechuate ortho-cleave pathway (Fuchs *et al.*, 2011), suggesting that interspecies competition for the same resource pool may be rampant between pyrophilous bacteria and fungi. Unfortunately, our bioinformatics pipeline did not allow for the recovery of fungal MAGs, thus limiting our insight into the fungal degradation of PyOM.

The catechol and protocatechuate ortho pathways are biochemically conserved with high diversity in the level of gene organization (Parke *et al.*, 2000; Buchan *et al.*, 2004). This indicates the potential for pyrophilous microbes of wildfire-adapted ecosystems, such as chaparral, to exhibit high degree of phylogenetic conservatism, as was previously shown (Enright *et al.*, 2022). Thus, pyrophilous microbes might have evolved mechanism to capitalize on PyOM as a C source, as suggested by the large number of differentially abundant PyOM degradation genes in the burned plots. Indeed, our findings revealed that the Actinomycetales, *Arthrobacter, Pseudonocardia,* Micromonosporaceae, and Mycobacteriale*s CADCTP01* and the Burkholderiales *SG8-41*, *Noviherbaspirillum,* and *Massilia* encoded the PyOM genes that were shown to be differentially abundant in the burned plots. Previous research showed that *Arthrobacter*

(Nelson *et al.*, 2022) and Burkholderiales harbor a high potential for aromatic compound catabolism (Pérez-Pantoja *et al.*, 2012), supporting our results. The ortho pathway provides a growth advantage to microbes (Song *et al.*, 2002) by efficiently converting C to cell mass (Basha *et al.*, 2010; Aghapour *et al.*, 2013) and both pyrophilous *Massilia* and *Noviherbaspirillum* are fast-growing bacteria (Lin *et al.*, 2013; Baldani *et al.*, 2014; Li *et al.*, 2014) that dominated this system (Pulido-Chavez *et al.*, 2023) and contained genes for PyOM degradation. Together, these results suggest that in a post-fire system, where C is bound in difficult-to-degrade PyOM, pyrophilous microbes prefer the easier-to-degrade PyOM pathway (ortho-cleavage pathway), rapidly converting PyOM to biomass and thus dominating and initiating microbial succession, as previously suggested (Pulido-Chavez *et al.*, 2023).

3.6 Conclusions

Our high-resolution gene-centric metagenomic analysis allowed us to detect the rapid enrichment of genomic functional potential for PyOM, inorganic N, alkane, and urea degradation during the first post-fire year, coinciding with the observed dominance of pyrophilous taxa in this post-fire environment. We found that MAGs encoding for pyrophilous *Massilia* and *Noviherbaspirillium* preferentially encode the easier-to-degrade ortho-cleavage catechol and protocatechuate degradation pathways while assimilating N to acquire energy and potentially minimize greenhouse gas emissions. While post-fire microbes can assimilate post-fire resources, they do so by encoding different PyOM and

N degradation pathways, suggesting that metabolic handoffs are common in post-fire communities and traits that evolved for post-fire survival, like resource acquisition, drive microbial secondary successional dynamics. While the capability of post-fire microbes to utilize PyOM and N has been previously hypothesized (Woolet & Whitman, 2020; Pulido-Chavez *et al.*, 2023), and shown for some taxa (Cobo-Díaz *et al.*, 2015; Fischer *et al.*, 2021; Nelson *et al.*, 2022), our research unveils previously unknown functional changes over successional time, filling a critical gap created by previous post-fire sampling efforts. Thus, we provide a deeper understanding about post-fire microbial ecology and provide insight into restoration of important ecosystem functions in fire-affected environments.

3.7 Acknowledgments

We thank UC Riverside the JGI-CSP 507961 award to MFPC and SIG, the BLM JFSP Award #012641-002 and Shipley Skinner Award to MFPC and SIG, the USDA-NIFA Award 2022-67014-36675 to SIG and PMH, and the DOE BER Award DE-SC0023127 to SIG and PMH, and the Mycological Society of America for funding support. We further thank the Cleveland National Forest and the Trabuco Ranger District, including District Ranger Darrel Vance and Emily Fudge, Jeffrey Heys, Lauren Quon, Jacob Rodriguez, and Victoria Stempniewicz, for their help with permitting. We thank the Joint Genome Institute Metagenome Program, including Nicole Shapiro, Natasha Brown, Emiley Eloe-Fadrosh, and Simon Roux, for their help in processing and

submitting our metagenomic samples. Lastly, we thank Judy A. Chung and James Randolph for their help with fieldwork and molecular work and Aral C. Greene, Elizah Stephens, Dylan Enright, and Sameer S. Saroa for fieldwork assistance.

3.8 Competing Interests

The authors declare no competing or conflicts of interest.

3.9 Data Availability Statement

The metagenomic reads and bacterial MAGs have been deposited to the National Center for Biotechnology Information Sequence Read Archive under BioProject X. Amplicon sequence reads for bacterial 16s rRNA and fungal ITS2 have been deposited to the National Center for Biotechnology Information Sequence Read Archive under BioProject PRJNA761539. All statistical R scripts/codes are available on GitHub and include the sample metadata required for analysis https://github.com/pulidofabs/Chaparral-Metagenomes.

3.10 References

Abbasian F, Lockington R, Mallavarapu M, Naidu R. 2015. A Comprehensive Review of Aliphatic Hydrocarbon Biodegradation by Bacteria. *Appl Biochem Biotechnol* **176**(3): 670-699.

Aghapour AA, Moussavi G, Yaghmaeian K. 2013. Biological degradation of catechol in wastewater using the sequencing continuous-inflow reactor (SCR). *Journal of Environmental Health Science and Engineering* **11**: 3.

Anderson MJ 2017. Permutational Multivariate Analysis of Variance (PERMANOVA). *Wiley StatsRef: Statistics Reference Online*: John Wiley & Sons, Ltd, 1-15.

Andrews S 2010. FastQC: A Quality Control Tool for High Throughput Sequence Data [Online].

Aramaki T, Blanc-Mathieu R, Endo H, Ohkubo K, Kanehisa M, Goto S, Ogata H. 2020. KofamKOALA: KEGG Ortholog assignment based on profile HMM and adaptive score threshold. *Bioinformatics* **36**(7): 2251-2252.

Ayiti OE, Babalola OO. 2022. Factors Influencing Soil Nitrification Process and the Effect on Environment and Health. *Frontiers in Sustainable Food Systems* **6**.

Badía D, Martí C, Aguirre AJ, Aznar JM, González-Pérez JA, De la Rosa JM, León J, Ibarra P, Echeverría T. 2014. Wildfire effects on nutrients and organic carbon of a Rendzic Phaeozem in NE Spain: Changes at cm-scale topsoil. *CATENA* **113**: 267-275.

Bailey AC, Kellom M, Poret-Peterson AT, Noonan K, Hartnett HE, Raymond J. 2014. Draft Genome Sequence of Massilia sp. Strain BSC265, Isolated from Biological Soil Crust of Moab, Utah. *Genome Announcements* **2**(6): e01199-01114, 01192/01196/e01199-01114.

Baldani JI, Rouws L, Cruz LM, Olivares FL, Schmid M, Hartmann A 2014. The Family Oxalobacteraceae. In: Rosenberg E, DeLong EF, Lory S, Stackebrandt E, Thompson F eds. *The Prokaryotes*. Berlin, Heidelberg: Springer Berlin Heidelberg, 919-974.

Basha KM, Rajendran A, Thangavelu V. 2010. Recent advances in the Biodegradation of Phenol: A review. **1**: 219-234.

Bethesda. 2008. Building a BLAST database with your (local) sequences:BLAST Command Line Applications User Manual. *National Center for Biotechnology Information*.

Bird MI, Wynn JG, Saiz G, Wurster CM, McBeath A. 2015. The Pyrogenic Carbon Cycle. *Annual Review of Earth and Planetary Sciences* **43**(1): 273-298.

Blank RR, Allen F, Young JA. 1994. Extractable Anions in Soils following Wildfire in a Sagebrush-Grass Community. *Soil Science Society of America Journal* **58**(2): 564-570.

Buchan A, Neidle EL, Moran MA. 2004. Diverse organization of genes of the beta-ketoadipate pathway in members of the marine Roseobacter lineage. *Applied and Environmental Microbiology* **70**(3): 1658-1668.

Cacciari I, Lippi D, Pietrosanti T, Pietrosanti W. 1986. Ammonium assimilation in an Arthrobacter sp. "fluorescens". *Archives of Microbiology* **145**(2): 113-115.

Capo E, Broman E, Bonaglia S, Bravo AG, Bertilsson S, Soerensen AL, Pinhassi J, Lundin D, Buck M, Hall POJ, et al. 2021. Oxygen-deficient water zones in the Baltic Sea promote uncharacterized Hg methylating microorganisms in underlying sediments. *Limnology and Oceanography* **67**(1): 135-146.

Chaumeil P-A, Mussig AJ, Hugenholtz P, Parks DH. 2019. GTDB-Tk: a toolkit to classify genomes with the Genome Taxonomy Database. *Bioinformatics*: btz848.

Chen H, Ma K, Huang Y, Yao Z, Chu C. 2021. Stable Soil Microbial Functional Structure Responding to Biodiversity Loss Based on Metagenomic Evidences. *Frontiers in Microbiology* **12**.

Chen Z, Tu X, Meng H, Chen C, Chen Y, Elrys AS, Cheng Y, Zhang J, Cai Z. 2021. Microbial process-oriented understanding of stimulation of soil N2O emission following the input of organic materials. *Environmental Pollution* **284**: 117176.

Cheng H, Tang G, Wang S, Rinklebe J, Zhu T, Cheng L, Feng S. 2022. Combined remediation effects of biochar and organic fertilizer on immobilization and dissipation of neonicotinoids in soils. *Environ Int* **169**: 107500.

Cobo-Díaz JF, Fernández-González AJ, Villadas PJ, Robles AB, Toro N, Fernández-López M. 2015. Metagenomic Assessment of the Potential Microbial Nitrogen Pathways in the Rhizosphere of a Mediterranean Forest After a Wildfire. *Microbial Ecology* **69**(4): 895-904.

Dannenmann M, Díaz-Pinés E, Kitzler B, Karhu K, Tejedor J, Ambus P, Parra A, Sánchez-Martin L, Resco V, Ramírez DA, et al. 2018. Postfire nitrogen balance of Mediterranean shrublands: Direct combustion losses versus gaseous and leaching losses from the postfire soil mineral nitrogen flush. *Global Change Biology* **24**(10): 4505-4520.

Dove NC, Hart SC. 2017. Fire Reduces Fungal Species Richness and In Situ Mycorrhizal Colonization: A Meta-Analysis. *Fire Ecology* **13**(2): 37-65.

Dove NC, Klingeman DM, Carrell AA, Cregger MA, Schadt CW. 2021. Fire alters plant microbiome assembly patterns: integrating the plant and soil microbial response to disturbance. *New Phytologist* **230**(6): 2433-2446.

Dove NC, Safford HD, Bohlman GN, Estes BL, Hart SC. 2020. High-severity wildfire leads to multi-decadal impacts on soil biogeochemistry in mixed-conifer forests. *Ecol Appl* **30**(4): e02072.

Dove NC, Tas N, Hart SC. 2022. Ecological and genomic responses of soil microbiomes to high-severity wildfire: linking community assembly to functional potential. *ISME J* **16**(7): 1853-1863.

Eddy SR. 2011. Accelerated Profile HMM Searches. *PLOS Computational Biology* **7**(10): e1002195.

Enright DJ, Frangioso KM, Isobe K, Rizzo DM, Glassman SI. 2022. Mega-fire in Redwood Tanoak Forest Reduces Bacterial and Fungal Richness and Selects for Pyrophilous Taxa that are Phylogenetically Conserved. *Molecular Ecology*.

Fernández-García V, Marcos E, Reyes O, Calvo L. 2020. Do Fire Regime Attributes Affect Soil Biochemical Properties in the Same Way under Different Environmental Conditions? *Forests* **11**(3): 274.

Fischer MS, Stark FG, Berry TD, Zeba N, Whitman T, Traxler MF. 2021. Pyrolyzed Substrates Induce Aromatic Compound Metabolism in the Post-fire Fungus, Pyronema domesticum. *Front Microbiol* **12**: 729289.

Fox S, Sikes BA, Brown SP, Cripps CL, Glassman SI, Hughes K, Semenova-Nelsen T, Jumpponen A. 2022. Fire as a driver of fungal diversity — A synthesis of current knowledge. *Mycologia* **114**(2): 1-27.

Fuchs G, Boll M, Heider J. 2011. Microbial degradation of aromatic compounds - from one strategy to four. *Nature Reviews Microbiology* **9**(11): 803-816.

Goberna M, Garcia C, Insam H, Hernandez MT, Verdu M. 2012. Burning fire-prone Mediterranean shrublands: immediate changes in soil microbial community structure and ecosystem functions. *Microb Ecol* **64**(1): 242-255.

González-Pérez JA, González-Vila FJ, Almendros G, Knicker H. 2004. The effect of fire on soil organic matter—a review. *Environment International* **30**(6): 855-870.

Goodridge BM, Hanan EJ, Aguilera R, Wetherley EB, Chen Y-J, D'Antonio CM, Melack JM. 2018. Retention of Nitrogen Following Wildfire in a Chaparral Ecosystem. *Ecosystems* **21**(8): 1608-1622.

Granja-Travez RS, Persinoti GF, Squina FM, Bugg TDH. 2020. Functional genomic analysis of bacterial lignin degraders: diversity in mechanisms of lignin oxidation and metabolism. *Appl Microbiol Biotechnol* **104**(8): 3305-3320.

Haddock JD 2010. Aerobic Degradation of Aromatic Hydrocarbons: Enzyme Structures and Catalytic Mechanisms. *Handbook of Hydrocarbon and Lipid Microbiology*, 1057-1069.

Hanan EJ, Tague C, Schimel JP. 2016. Nitrogen cycling and export in California chaparral: the role of climate in shaping ecosystem responses to fire. *Ecological Monographs* **87**(1): 76-90.

Hanson RS, Hanson TE. 1996. Methanotrophic bacteria. *Microbiological Reviews* **60**(2): 439-471.

Hoang HG, Thuy BTP, Lin C, Vo D-VN, Tran HT, Bahari MB, Le VG, Vu CT. 2022. The nitrogen cycle and mitigation strategies for nitrogen loss during organic waste composting: A review. *Chemosphere* **300**: 134514.

Johnson CW, Beckham GT. 2015. Aromatic catabolic pathway selection for optimal production of pyruvate and lactate from lignin. *Metabolic Engineering* **28**: 240-247.

Johnson DB, Bacelar-Nicolau P, Okibe N, Thomas A, Hallberg KB. 2009. Ferrimicrobium acidiphilum gen. nov., sp. nov. and Ferrithrix thermotolerans gen. nov., sp. nov.: heterotrophic, iron-oxidizing, extremely acidophilic actinobacteria. *International Journal Of Systematic And Evolutionary Microbiology* **59**(5): 1082-1089.

Johnson DW, Curtis PS. 2001. Effects of forest management on soil C and N storage: meta analysis. *Forest Ecology and Management* **140**(2-3): 227-238.

Kanehisa M, Goto S. 2000. KEGG: Kyoto Encyclopedia of Genes and Genomes. *Nucleic Acids Research* **28**(1): 27-30.

Kang DD, Froula J, Egan R, Wang Z. 2015. MetaBAT, an efficient tool for accurately reconstructing single genomes from complex microbial communities. *PeerJ* **3**: e1165.

Khot V, Zorz J, Gittins DA, Chakraborty A, Bell E, Bautista MA, Paquette AJ, Hawley AK, Novotnik B, Hubert CRJ, et al. 2022. CANT-HYD: A Curated Database of Phylogeny-Derived Hidden Markov Models for Annotation of Marker Genes Involved in Hydrocarbon Degradation. *Frontiers in Microbiology* **12**.

Knicker H. 2007. How does fire affect the nature and stability of soil organic nitrogen and carbon? A review. *Biogeochemistry* **85**(1): 91-118.

Knicker H. 2011. Pyrogenic organic matter in soil: Its origin and occurrence, its chemistry and survival in soil environments. *Quaternary International* **243**(2): 251-263.

Koch IH, Gich F, Dunfield PF, Overmann J. 2008. Edaphobacter modestus gen. nov., sp. nov., and Edaphobacter aggregans sp. nov., acidobacteria isolated from alpine and forest soils. *Int J Syst Evol Microbiol* **58**(Pt 5): 1114-1122.

Kuhn TK, Krull ES, Bowater A, Grice K, Gleixner G. 2010. The occurrence of short chain n-alkanes with an even over odd predominance in higher plants and soils. *Organic Geochemistry* **41**(2): 88-95.

Kurth VJ, Fransioli N, Perez FZ, Hart SC, Gehring CA. 2013. Stand-replacing wildfires alter the community structure of wood-inhabiting fungi in southwestern ponderosa pine forests of the USA | Elsevier Enhanced Reader.

Kurth VJ, Hart SC, Ross CS, Kaye JP, Fule PZ. 2014. Stand-replacing wildfires increase nitrification for decades in southwestern ponderosa pine forests. *Oecologia* **175**(1): 395-407.

Leleiwi I, Rodriguez-Ramos J, Shaffer M, Sabag-Daigle A, Kokkinias K, Flynn RM, Daly RA, Kop LFM, Solden LM, Ahmer BMM, et al. 2023. Exposing new taxonomic variation with inflammation - a murine model-specific genome database for gut microbiome researchers. *Microbiome* **11**(1): 114.

Li D, Liu C-M, Luo R, Sadakane K, Lam T-W. 2014. MEGAHIT: An ultra-fast single-node solution for large and complex metagenomics assembly via succinct de Bruijn graph. *arXiv:1409.7208 [q-bio]*.

Li X, Gou X, Long D, Ji Z, Hu L, Xu D, Liu J, Chen S. 2014. Physiological and metabolic analysis of nitrate reduction on poly-gamma-glutamic acid synthesis in Bacillus licheniformis WX-02. *Archives of Microbiology* **196**(11): 791-799.

Lin SY, Hameed A, Arun AB, Liu YC, Hsu YH, Lai WA, Rekha PD, Young CC. 2013. Description of Noviherbaspirillum malthae gen. nov., sp. nov., isolated from an oil-contaminated soil, and proposal to reclassify Herbaspirillum soli, Herbaspirillum aurantiacum, Herbaspirillum canariense and Herbaspirillum psychrotolerans as Noviherbaspirillum soli comb. nov., Noviherbaspirillum aurantiacum comb. nov., Noviherbaspirillum canariense comb. nov. and Noviherbaspirillum psychrotolerans comb. nov. based on polyphasic analysis. *Int J Syst Evol Microbiol* **63**(Pt 11): 4100-4107.

Liu W, Zhang Z, Li J, Wen Y, Liu F, Zhang W, Liu H, Ren C, Han X. 2023. Effects of fire on the soil microbial metabolic quotient: A global meta-analysis. *CATENA* **224**: 106957.

Liu Y, Zhang Y, Huang Y, Niu J, Huang J, Peng X, Peng F. 2023. Spatial and temporal conversion of nitrogen using Arthrobacter sp. 24S4-2, a strain obtained from Antarctica. *Front Microbiol* **14**: 1040201.

Love MI, Huber W, Anders S. 2014. Moderated estimation of fold change and dispersion for RNA-seq data with DESeq2. *Genome Biol* **15**(12): 550.

Luo Y, Huang Y, Xu R-x, Qian B, Zhou J-w, Xia X-l. 2020. Primary and Secondary Succession Mediate the Accumulation of Biogenic Amines during Industrial Semidry Chinese Rice Wine Fermentation. *Applied and Environmental Microbiology* **86**(17): e01177-01120.

McMurdie PJ, Holmes S. 2013. Phyloseq: An R Package for Reproducible Interactive Analysis and Graphics of Microbiome Census Data. . *PLoS One* **8**(4): e61217.

Morawe M, Hoeke H, Wissenbach DK, Lentendu G, Wubet T, Kröber E, Kolb S. 2017. Acidotolerant Bacteria and Fungi as a Sink of Methanol-Derived Carbon in a Deciduous Forest Soil. *Frontiers in Microbiology* **8**.

Moucawi J, Fustec E, Jambu P, Amblfs A, Jacquesy R. 1981. Biooxidation of added and natural hydrocarbons in soils: Effect of iron. *Soil Biology and Biochemistry* **13**(5): 335-342.

Nave L, Vance. E, . CS, Curtis. P. 2011. Fire effects on temperate forest soil C and N storage. *Ecol Appl* **4**: 1189-1201.

Neary DG, Klopatek CC, DeBano LF, Ffolliott PF. 1999. Fire effects on belowground sustainability: a review and synthesis. *Forest Ecology and Management* **122**(1-2): 51-71.

Nelson AR, Narrowe AB, Rhoades CC, Fegel TS, Daly RA, Roth HK, Chu RK, Amundson KK, Young RB, Steindorff AS, et al. 2022. Wildfire-dependent changes in soil microbiome diversity and function. *Nature Microbiology* **7**(9): 1419-1430.

Oksanen J, Simpson G, Blanchet F, Kindt R, Legendre P, Minchin P, O'Hara R, Solymos P, Stevens M, Szoecs P, et al. 2022. vegan: Community Ecology Package.

Olm MR, Brown CT, Brooks B, Banfield JF. 2017. dRep: a tool for fast and accurate genomic comparisons that enables improved genome recovery from metagenomes through de-replication. *The ISME Journal* **11**(12): 2864-2868.

Parke D, D'Argenio DA, Ornston LN. 2000. Bacteria Are Not What They Eat: That Is Why They Are So Diverse. *Journal of Bacteriology* **182**(2): 257-263.

Parks DH, Imelfort M, Skennerton CT, Hugenholtz P, Tyson GW. 2015. CheckM: assessing the quality of microbial genomes recovered from isolates, single cells, and metagenomes. *Genome Research* **25**(7): 1043-1055.

Perez-Pantoja D, Donoso R, Agullo L, Cordova M, Seeger M, Pieper DH, Gonzalez B. 2012. Genomic analysis of the potential for aromatic compounds biodegradation in Burkholderiales. *Environ Microbiol* **14**(5): 1091-1117.

Pérez-Pantoja D, Donoso R, Agulló L, Córdova M, Seeger M, Pieper DH, González B. 2012. Genomic analysis of the potential for aromatic compounds biodegradation in Burkholderiales. *Environmental Microbiology* **14**(5): 1091-1117.

Pulido-Chavez MF, Randolph JWJ, Zalman C, Larios L, Homyak PM, Glassman SI. 2023. Rapid bacterial and fungal successional dynamics in first year after chaparral wildfire. *Molecular Ecology*.

Pulido-Chavez MF, Randolph JWJ, Stephens E, Greene A, Homyak PM, Larios L, Glassman SI. *In Prep.* Microbial-Mediated Pyrogenic Organic Matter and Nitrogen Cycling genes increase over time after a Chaparral wildfire

Qiao Z, Sun R, Wu Y, Hu S, Liu X, Chan J, Mi X. 2020. Characteristics and metabolic pathway of the bacteria for heterotrophic nitrification and aerobic denitrification in aquatic ecosystems. *Environmental Research* **191**: 110069.

Rawlings ND, Waller M, Barrett AJ, Bateman A. 2014. MEROPS : the database of proteolytic enzymes, their substrates and inhibitors. *Nucleic Acids Research* **42**(D1): D503-D509.

Raza T, Qadir MF, Khan KS, Eash NS, Yousuf M, Chatterjee S, Manzoor R, Rehman Su, Oetting JN. 2023. Unrevealing the potential of microbes in decomposition of organic matter and release of carbon in the ecosystem. *Journal of Environmental Management* **344**: 118529.

RCoreTeam 2023. R: A language and environment for statistical computing. R Foundation for Statistical Computing. Vienna, Austria.

Riley KL, Loehman RA. 2016. Mid-21st-century climate changes increase predicted fire occurrence and fire season length, Northern Rocky Mountains, United States. *Ecosphere* **7**(11): e01543.

Robinson MD, McCarthy DJ, Smyth GK. 2010. edgeR: a Bioconductor package for differential expression analysis of digital gene expression data. *Bioinformatics (Oxford, England)* **26**(1): 139-140.

Salazar JM, Calle J, Pereira S, Cordero P, Matovelle C. 2023. Nitrite-Oxidizing Bacterial Strains Isolated from Soils of Andean Ecosystems and Their Potential Use in Nitrogen Reduction. *Sustainability* **15**(12): 9277.

Santos-Medellin C, Blazewicz SJ, Pett-Ridge J, Firestone MK, Emerson JB. 2023. Viral but not bacterial community successional patterns reflect extreme turnover shortly after rewetting dry soils. *Nature Ecology & Evolution* **7**(11): 1809-1822.

Shaffer M, Borton MA, McGivern BB, Zayed AA, Rosa SLL, Solden LM, Liu P, Narrowe AB, Rodríguez-Ramos J, Bolduc B, et al. 2020. DRAM for distilling microbial metabolism to automate the curation of microbiome function. *bioRxiv*: 2020.2006.2029.177501.

Singh J, Kunhikrishnan A, Bolan NS, Saggar S. 2013. Impact of urease inhibitor on ammonia and nitrous oxide emissions from temperate pasture soil cores receiving urea fertilizer and cattle urine. *The Science of the Total Environment* **465**: 56-63.

Smid M, Coebergh van den Braak RRJ, van de Werken HJG, van Riet J, van Galen A, de Weerd V, van der Vlugt-Daane M, Bril SI, Lalmahomed ZS, Kloosterman WP, et al. 2018. Gene length corrected trimmed mean of M-values (GeTMM) processing of RNA-seq data performs similarly in intersample analyses while improving intrasample comparisons. *BMC Bioinformatics* **19**(1): 236.

Song H-K, Song W, Kim M, Tripathi BM, Kim H, Jablonski P, Adams JM. 2017. Bacterial strategies along nutrient and time gradients, revealed by metagenomic analysis of laboratory microcosms. *FEMS Microbiology Ecology* **93**(fix114).

Song J, Sung J, Kim YM, Gerben J Z, Kim E. 2002. Roles of the meta- and the ortho-Cleavage Pathways for the Efficient Utilization of Aromatic Hydrocarbons by Sphingomonas yanoikuyae Bl. *Korean Journal of Microbiology* **38**(4): 245-245.

Steinegger M, Söding J. 2017. MMseqs2 enables sensitive protein sequence searching for the analysis of massive data sets. *Nature Biotechnology* **35**(11): 1026-1028.

Stephens EZ, Homyak PM. 2023. Post-fire soil emissions of nitric oxide (NO) and nitrous oxide (N2O) across global ecosystems: a review. *Biogeochemistry*.

Suzek BE, Huang H, McGarvey P, Mazumder R, Wu CH. 2007. UniRef: comprehensive and non-redundant UniProt reference clusters. *Bioinformatics* **23**(10): 1282-1288.

Team RC 2023. R: A language and environment for statistical computing. R Foundation for Statistical Computing. Vienna, Austria.

Thomas CL, Jansen B, van Loon EE, Wiesenberg GLB. 2021. Transformation of n-alkanes from plant to soil: a review. *SOIL* **7**(2): 785-809.

Thomas T, Gilbert J, Meyer F. 2012. Metagenomics - a guide from sampling to data analysis. *Microbial Informatics and Experimentation* **2**(1): 3.

Thomson AJ, Giannopoulos G, Pretty J, Baggs EM, Richardson DJ. 2012. Biological sources and sinks of nitrous oxide and strategies to mitigate emissions. *Philosophical Transactions of the Royal Society B: Biological Sciences* **367**(1593): 1157-1168.

Turner MG, Smithwick EAH, Metzger KL, Tinker DB, Romme WH. 2007. Inorganic nitrogen availability after severe stand-replacing fire in the Greater Yellowstone ecosystem. *Proceedings of the National Academy of Sciences* **104**(12): 4782–4789.

Wang L, Hao D-C, Fan S, Xie H, Bao X, Jia Z, Wang L. 2022. N2O Emission and Nitrification/Denitrification Bacterial Communities in Upland Black Soil under Combined Effects of Early and Immediate Moisture. *Agriculture* **12**(3): 330.

Weiland F, Kohlstedt M, Wittmann C. 2022. Guiding stars to the field of dreams: Metabolically engineered pathways and microbial platforms for a sustainable lignin-based industry. *Metabolic Engineering* **71**: 13-41.

Whitman T, Whitman E, Woolet J, Flannigan MD, Thompson DK, Parisien M-A. 2019. Soil bacterial and fungal response to wildfires in the Canadian boreal forest across a burn severity gradient. *Soil Biology and Biochemistry* **138**: 107571.

Wickham H. 2016. *ggplot2: Elegant Graphics for Data Analysis*: Springer-Verlag New York.

Woolet J, Whitman T. 2020. Pyrogenic organic matter effects on soil bacterial community composition. *Soil Biology and Biochemistry* **141**: 107678.

Xu W, Elberling B, Ambus PL. 2022. Fire increases soil nitrogen retention and alters nitrogen uptake patterns among dominant shrub species in an Arctic dry heath tundra. *Sci Total Environ* **807**(Pt 3): 150990.

Yoon S, Song B, Phillips RL, Chang J, Song MJ. 2019. Ecological and physiological implications of nitrogen oxide reduction pathways on greenhouse gas emissions in agroecosystems. *FEMS Microbiology Ecology* **95**(6): fiz066.

Zeba N, Berry TD, Fischer MS, Traxler MF, Whitman T. 2023. Soil carbon mineralization and microbial community dynamics in response to PyOM addition: Ecology.

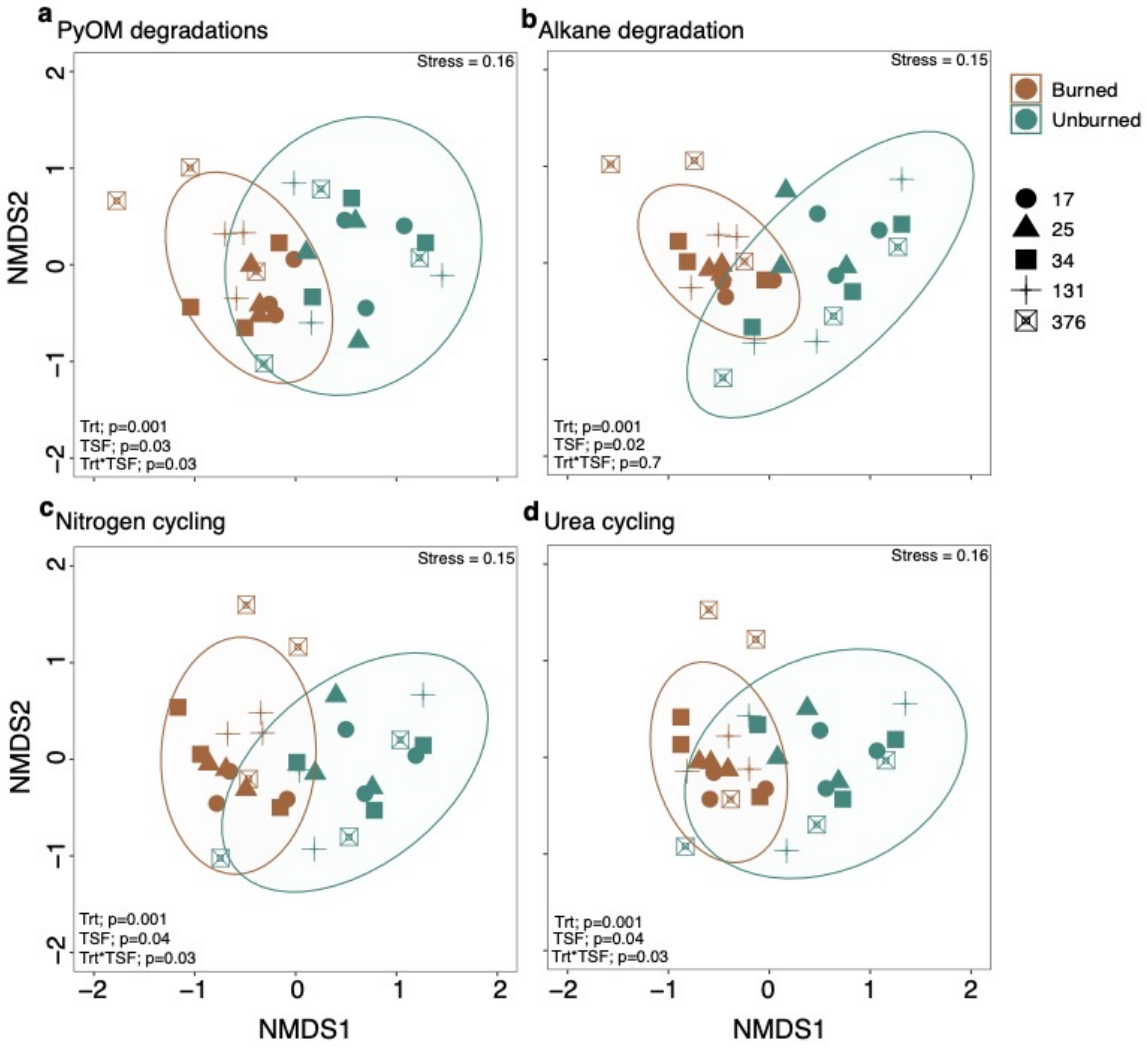

Figure 3.1. Non-metric multidimensional scaling (NMDS) of geTMM normalized a) PyOM b) alkane c) nitrogen and d) urea cycling genes within the microbial communities of burned and unburned soil samples (color) and time since fire (TSF days; shape). Treatment (Trt) and time since fire (TSF) effects based on PERMANOVA ($p < 0.05$). Ellipse represents the 95% confidence level. Genes were annotated using DRAM, CANT-HYD and KEGG) .

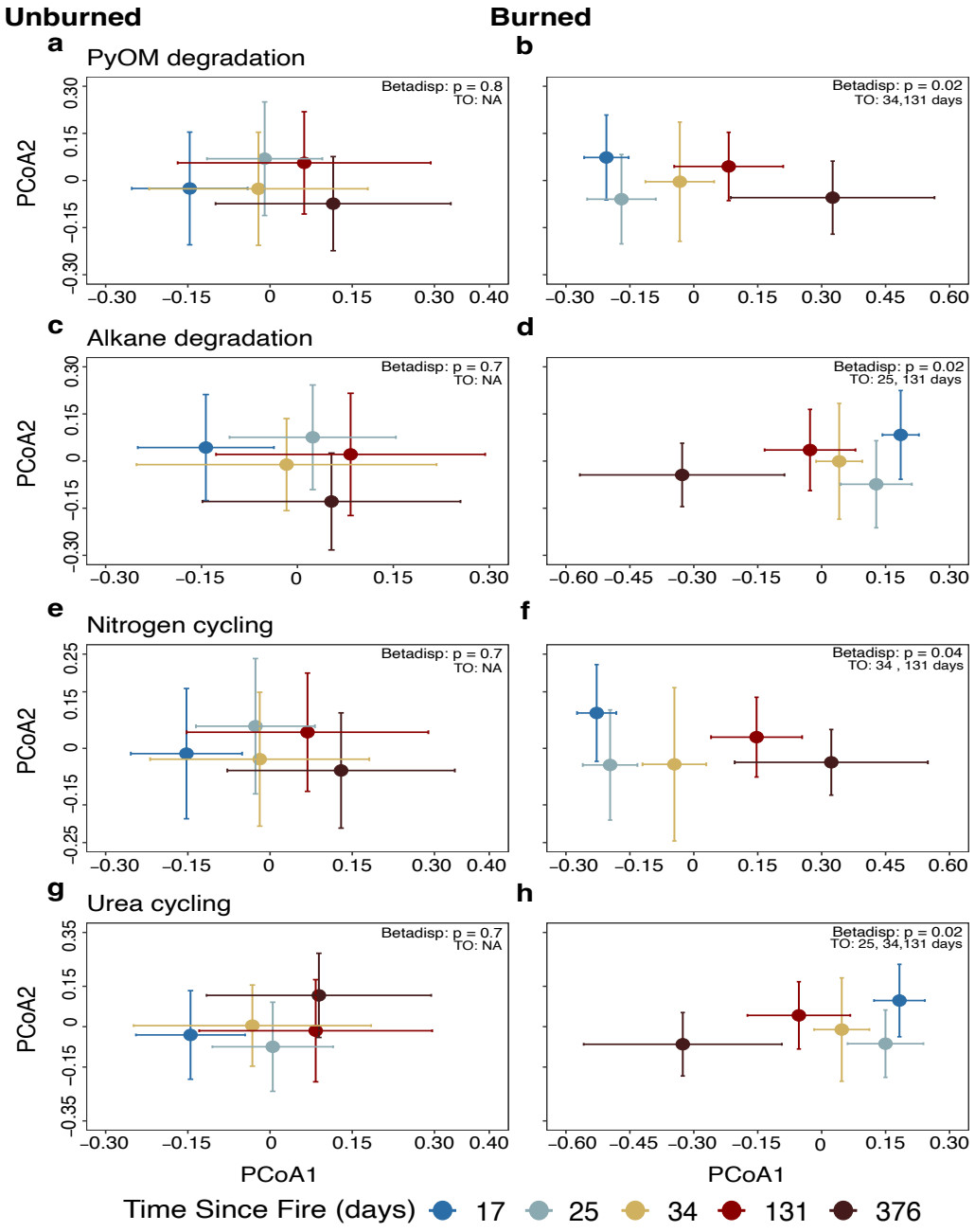

Figure 3.2. Principal component analysis (PCoA) of the mean and standard error Bray-Curtis community dissimilarity at each timepoint (17, 25, 34, 131, 376) for the unburned and burned a,b) PyOM; c,d) Alkane; e,f) Nitrogen and g,h) Urea functional potentials. Note that timepoints further apart with nonoverlapping standard error bars indicate a community turnover, whereas overlapping standard error bars represent a lack of compositional turnover, with 17 days representing the base level (first sampling time point). Thus, the first turnover (TO) was initiated at 25 days.

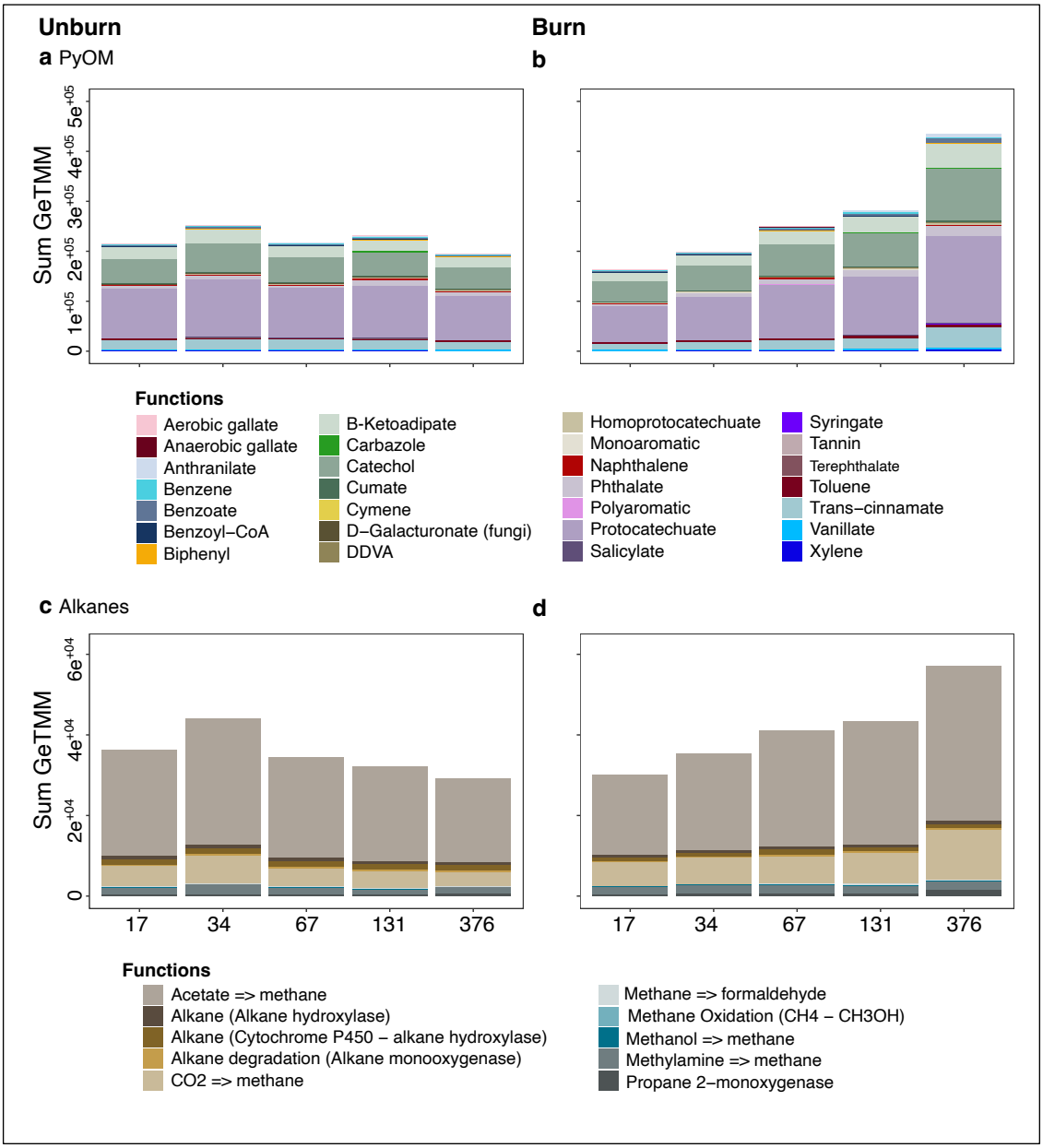

Figure 3.3. Summed geTMM normalized gene abundance over time for a,b) PyOM and c, d) Alkane degradation in the unburned (left panel) and burned (right panel). Colors are based on the general function for each gene.

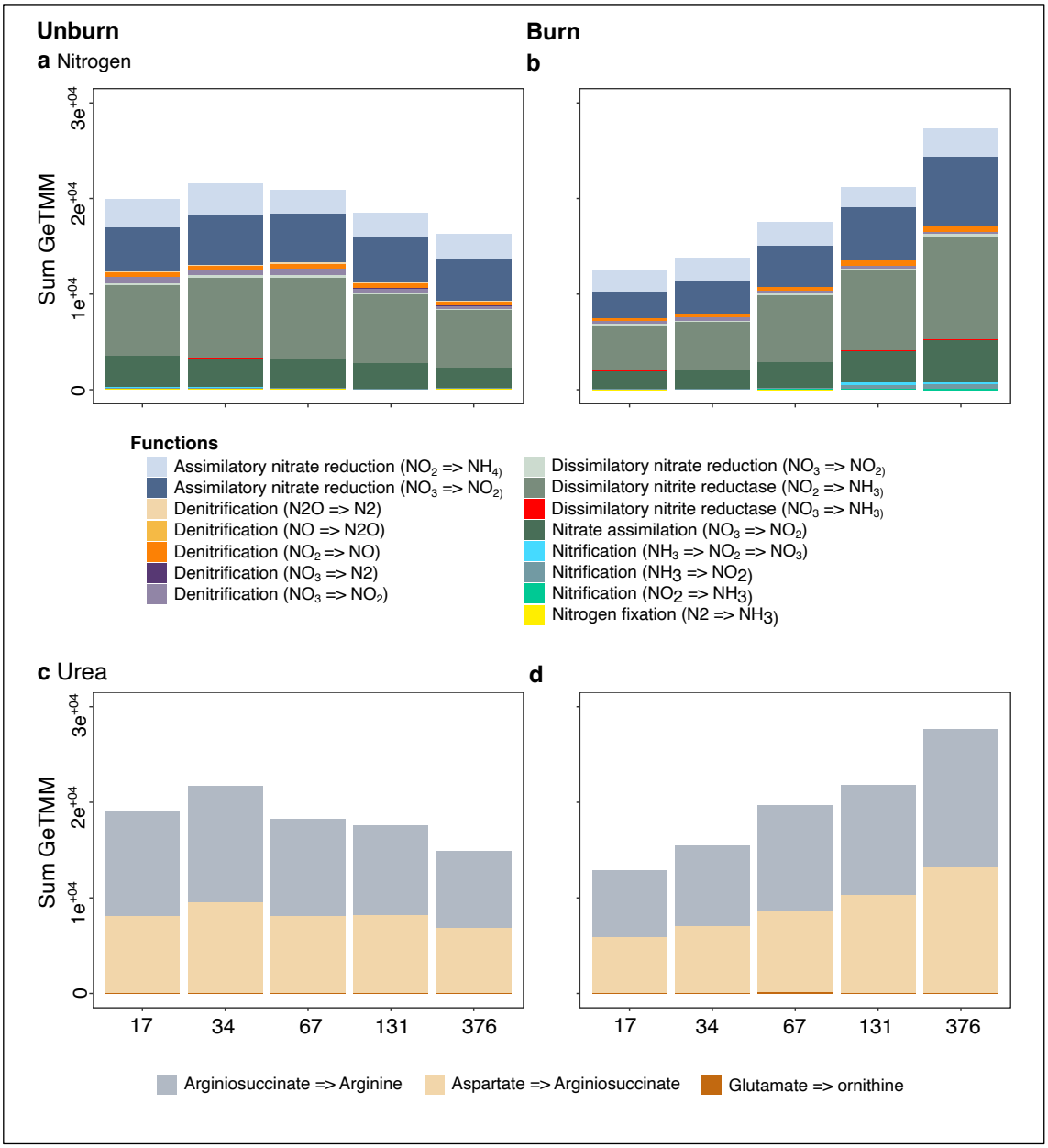

Figure 3.4. Summed geTMM normalized gene abundance over time for a,b) Nitrogen and c, d) Urea cycling genes in the unburned (left panel) and burned (right panel). Colors are based on the general function for each gene.

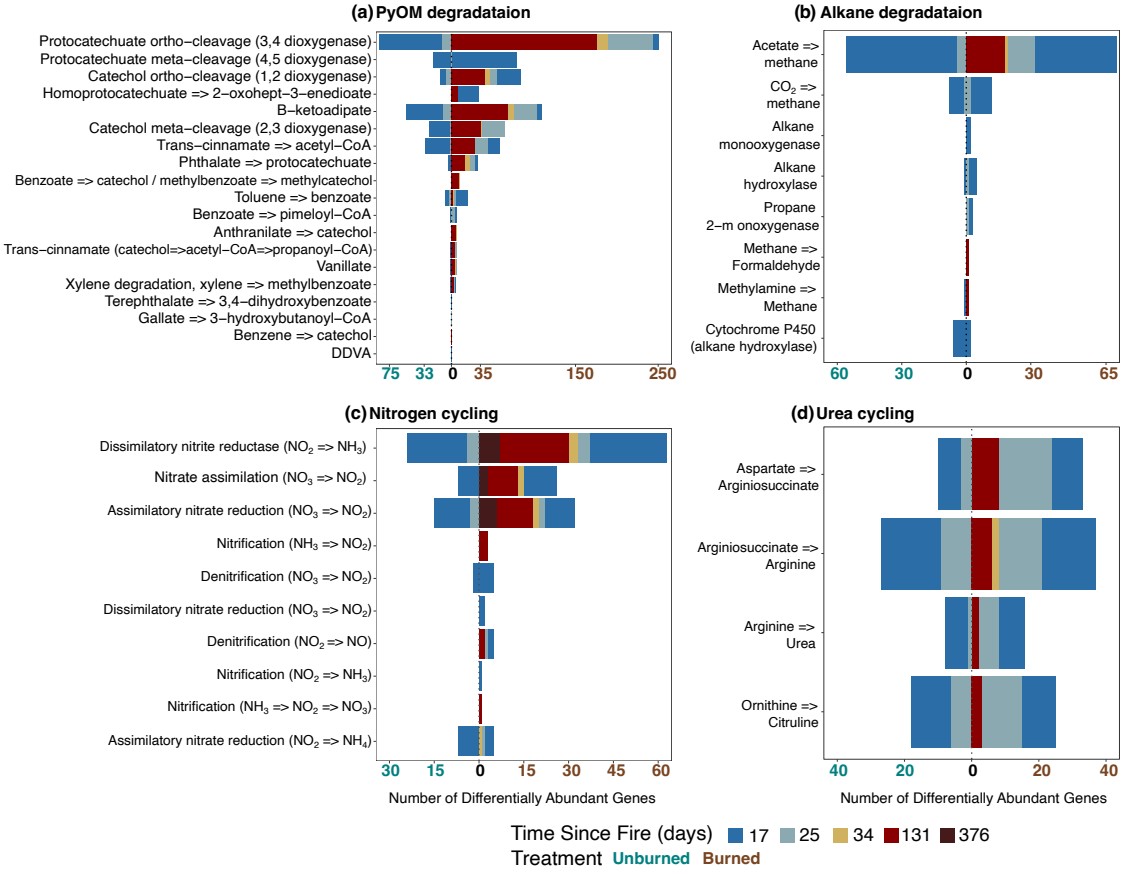

Figure 3.5. Total number of genes that were differentially abundant in the burned plots (brown) versus the unburned plots (blue green; x axis) per each carbon pathway, colored by each sampling time point for a) PyOM, b) Alkane, Nitrogen and d) Urea cycling. Significance based on DESeq2 Wald test (adjusted P value < 0.05 and absolute log2 fold-change >0).

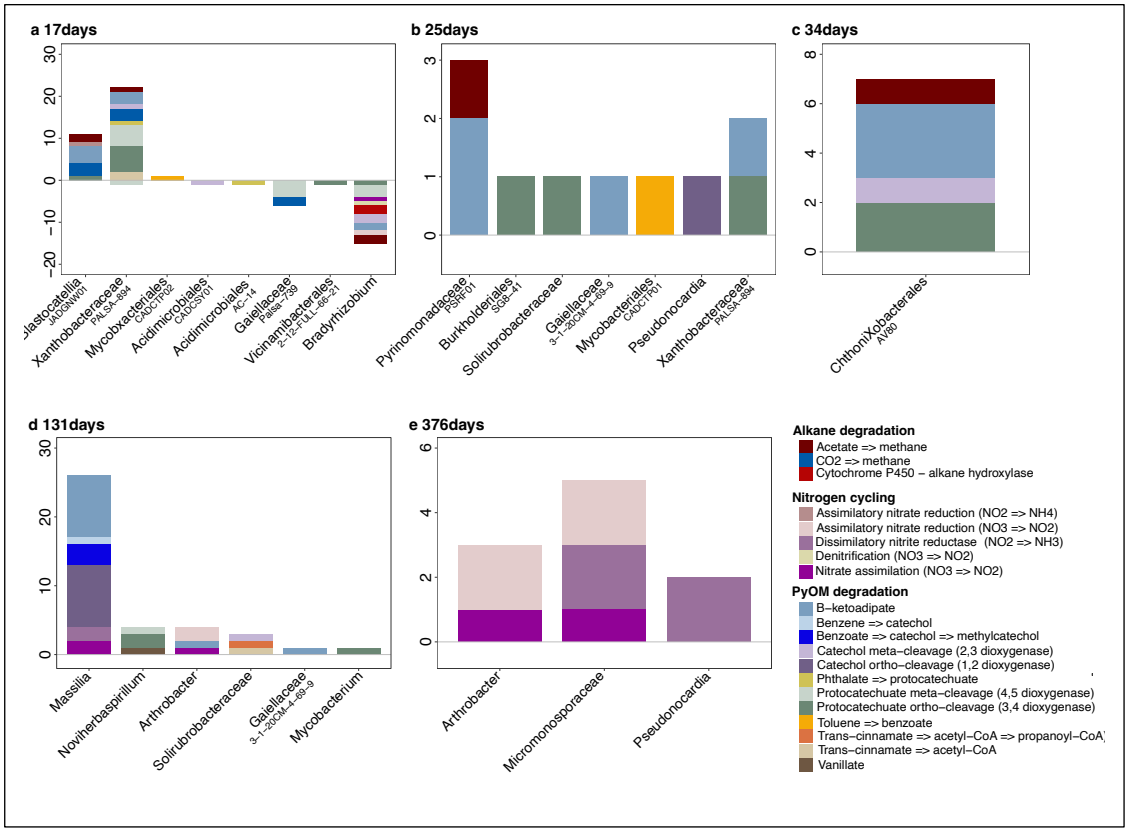

Figure 3.6. Taxonomic annotation for the most dominant, differentially abundant PyOM, nitrogen and urea genes based on DESeq analysis (adjusted P value < 0.05 and absolute log2 fold-change >0). Taxonomy based on blasting contigs against MAGs.

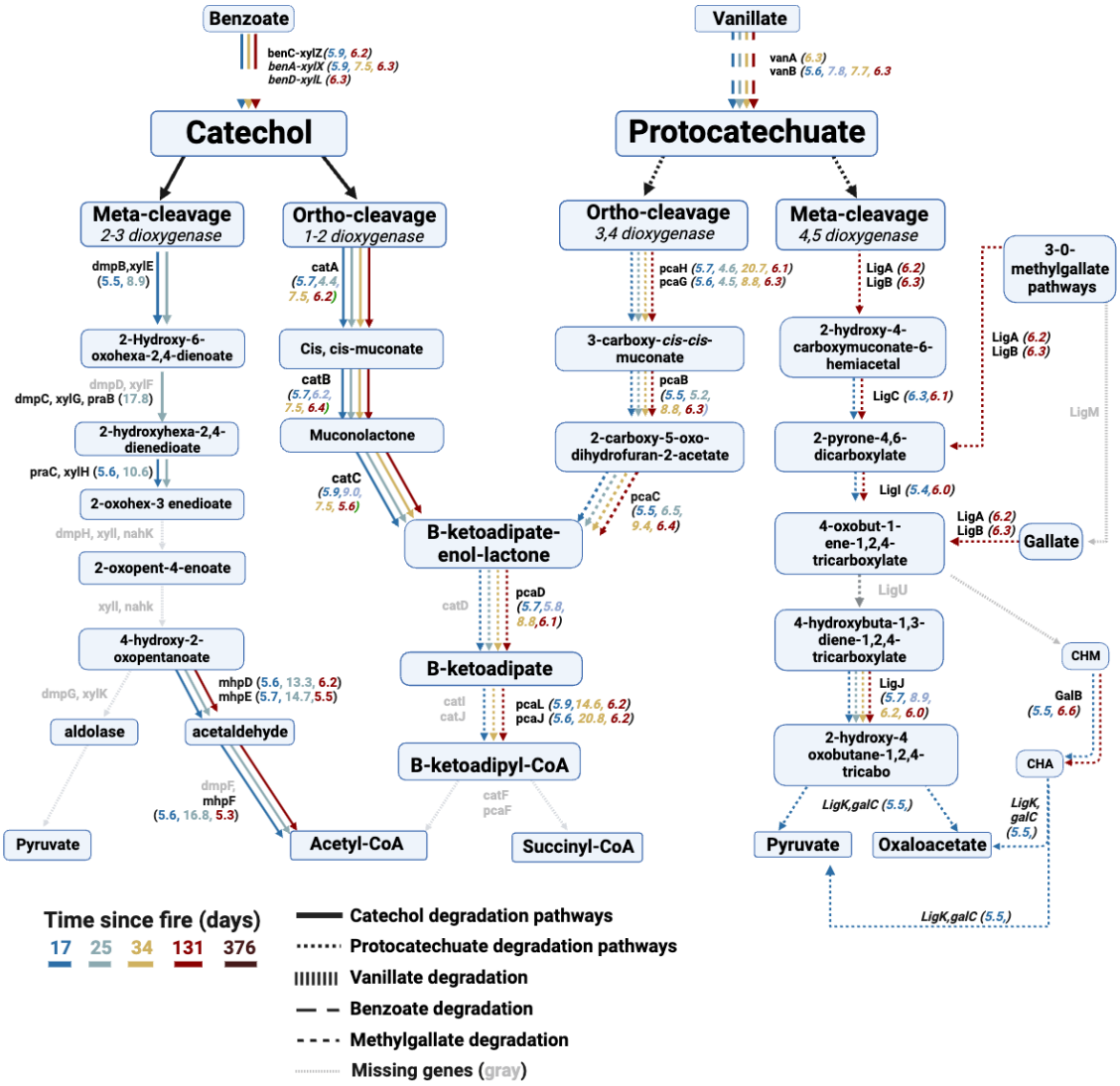

Figure 3.7. The catechol and protocatechuate degradation pathways with arrows indicating genes that were differentially expressed in the burned treatment at each time point (17, 25, 34, 131 and 376 days post-fire; Wald's test in DESeq2; $p<0.05$). Line type represents catechol (solid) and protocatechuate (dashed) cycling pathways and gray solid lines represent pathways that were not expressed during post-fire year one. Numbers in parentheses represent the mean log2fold change (DESeq2) for each represented gene and are colored by the timepoint in which that gene was significantly abundantly represented.

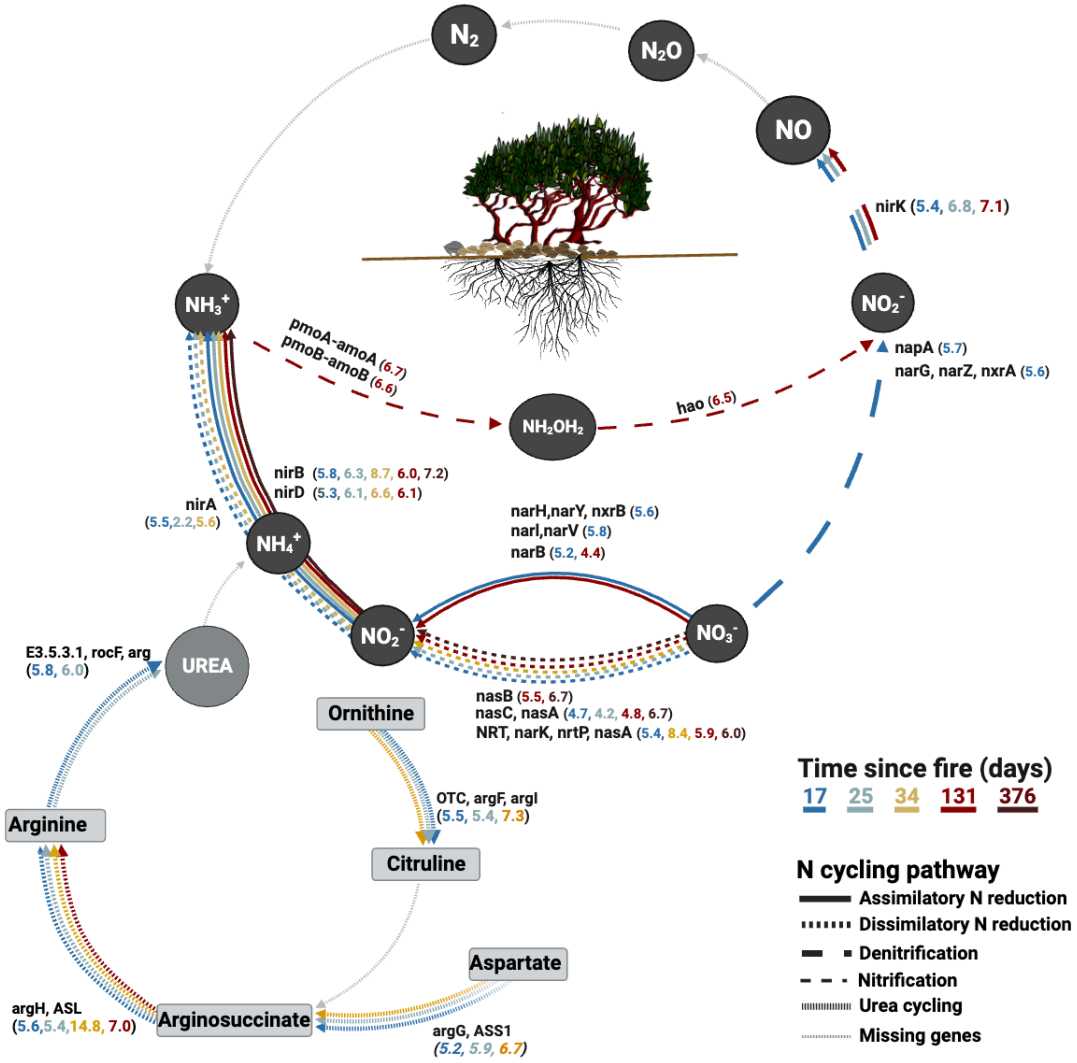

Figure 3.8. The nitrogen cycle with arrows indicating genes that were differentially represented in the burned treatment at each time point (17, 25, 34, 131 and 376 days post-fire; Wald's test in DESeq2; $p<0.05$). Line type represents the different nitrogen cycling pathways, colored by timepoint and gray solid lines represent pathways that were not expressed during post-fire year one. Numbers in parentheses represent the mean log2fold change (DESeq2) for each represented gene and are colored by the timepoint in which that gene was significantly abundantly represented.

Chapter IV

A comprehensive 4.5 year study of microbial resilience and ecosystem recovery after a Chaparral wildfire

4.1 Abstract

High-severity wildfires, common in fire-adapted chaparral ecosystems, substantially impact microbial resilience, affecting community functions and structure and consequently influencing their ability to return to pre-fire conditions. Soil microbes are vital to ecosystem health, driving ecosystem functions such as nutrient cycling and vegetation regeneration. To understand post-fire microbial resilience and factors influencing their recovery, we performed a high-resolution temporal sampling of 17 time points spanning 17 days to 4.5 years post-fire. We estimated impacts on microbial biomass with 16S and 18S qPCR and microbial richness and composition with Illumina MiSeq sequencing of 16S and ITS2 amplicons. Further, we measured vegetation regeneration and key soil variables, including pH, NO_3^-, NH_4^+, moisture content, and

texture, at a subset of the time points. Neither bacterial nor fungal communities recovered to pre-fire conditions. However, bacteria exhibited greater resilience than fungi, recovering in terms of richness within 4.5 years, influenced by factors such as time, vegetation richness, and soil NH_4^+. Fungal richness did not recover, displaying negative correlations with time, burn severity, and proximity to unburned areas, but positive associations with vegetation and soil moisture. Bacterial stability improved with higher richness and reduced dominance, while fungal stability persisted due to the dominance of resilient taxa like *Pyronema, Aspergillus*, and *Penicillium*. These results emphasize the importance of diverse bacterial communities and well-established fungi for ecosystem resilience. Furthermore, our study revealed that both bacterial and fungal species richness had a positive impact on vegetation and a negative effect on soil NH_4^+ concentrations, while NO_3^- levels were specifically correlated with bacterial richness. These findings highlight the complex interconnections between fire and the soil environment while underscoring the vital roles played by microbes in facilitating post-fire ecosystem recovery.

4.2 Introduction

Wildfires are fundamental to ecosystems worldwide (McLauchlan *et al.*, 2020), including chaparral (Pausas *et al.*, 2008; Rundel, 2018). They facilitate the release of nutrients, create open habitats, enhance the diversity of light-loving plants (Pausas & Keeley., 2009), and promote tree regeneration (Certini, 2005). However, the rising

frequency, size, and severity of fires beyond historic levels (Abatzoglou & Williams, 2016; McLauchlan *et al.*, 2020) has raised concerns about the ability of ecosystems to recover (Gill *et al.*, 2022). Severe wildfires can hinder ecosystem recovery by negatively affecting soil microbial communities (DeBano *et al.*, 1998; Pressler *et al.*, 2019; Fox *et al.*, 2022). These microbial communities are crucial for nutrient cycling, litter decomposition, and plant regeneration (van der Heijden *et al.*, 2008; Brundrett, 2009; Bardgett & van der Putten, 2014; Delgado-Baquerizo *et al.*, 2016; Brundrett & Tedersoo, 2018) . Thus, understanding microbial resilience—the ability of ecosystems to recover to pre-disturbance levels while maintaining their fundamental structure and functions (Walker *et al.*, 2004; Allison & Martiny, 2008), is vital to ensuring the long-term health and stability of ecosystems.

Following severe wildfires, rapid microbial mortality creates a niche for a distinct group of pyrophilous or "fire-loving" microbes to dominate the post-fire environment (Fox *et al.*, 2022). These microbes are often phylogenetically conserved within bacterial phyla such as Firmicutes and Actinobacteria and Ascomycete fungal classes such as Eurotiomycetes and Pezizomycetes (Enright *et al.*, 2022). We recently found that chaparral pyrophilous microbes undergo rapid secondary succession and display specific trade-offs in abundance during the first post-fire year (Pulido-Chavez *et al.*, 2023). These patterns mirror vegetation successional dynamics, starting with the initial dominance of surviving thermotolerant microbes, followed by colonization by fast growers, which eventually yield to superior competitors for post-fire resources (Pulido-Chavez *et al.*, 2023). However, plant dynamics indicate that the composition of the surviving vegetation

governs the rate of recovery and succession of the system by facilitating the replacement and establishment of a diverse plant community (Steel *et al.*, 2021). While we previously demonstrated the directional replacement of microbes during the first post-fire year (Pulido-Chavez *et al.*, 2023), it is crucial to understand that resilience plays a pivotal role in facilitating directional succession and, consequently, the ecosystem recovery (Philippot *et al.*, 2021). However, much remains to be understood about the resilience of post-fire microbes, and what factors govern their recovery rate, which limits our ability to predict and manage burned ecosystems.

Wildfires can induce prolonged abiotic pressures on the microbial community by altering the soil environment and plant community (Shade *et al.*, 2012; Jurburg *et al.*, 2017). Wildfires can result in rapid vegetation mortality (Neary *et al.*, 1999; Neary *et al.*, 2005), substantial carbon (C) transformation from woody vegetation to pyrogenic organic matter, PyOM (Certini, 2005), and increases in soil pH, ammonium (NH_4^+) and mineral N (Certini, 2005; Dannenmann *et al.*, 2018). These changes pose threats to microbial resilience, potentially delaying ecosystem recovery. However, pyrophilous fungi like *Pyronema* or bacteria like *Noviherbaspirillium* can capitalize on post-fire resources like PyOM and bioavailable N (Steindorff *et al.*; Woolet & Whitman, 2020; Fischer *et al.*, 2021; Nelson *et al.*, 2022). The ability of post-fire microbes to use post-fire resources may aid in post-fire C and nitrogen (N) cycling, facilitating ecosystem recovery. Indeed, research in shrublands has demonstrated the link between total soil N and the recovery of fungal phylogenetic biodiversity (Pérez-Valera *et al.*, 2020). However, full resilience of ecosystem microbial diversity requires over 20 years (Pérez-

Valera *et al.*, 2018). Recent research has demonstrated rapid changes in microbial communities during the initial phases of secondary succession (Ammitzboll *et al.*, 2022; Pulido-Chavez *et al.*, 2023). Additionally, studies suggest that microbial resilience might be contingent upon the specific ecosystem and severity of the fire (Pinto *et al.*, 2023). Therefore, high-resolution temporal research that captures the early shifts in microbes and the soil environment within ecosystems naturally prone to high severity wildfires, such as chaparral (Barro & Conard, 1991; Rundel, 2018), can provide valuable insights into the mechanisms of microbial resilience and their link to ecosystem recovery.

In the process of ecosystem recovery and succession, factors like diversity, species niche complementarity (coexistence based on resource specialization), and competitive ability tend to increase, leading to enhanced ecosystem stability over time (Odum, 1969; Pickett, 1976). Moreover, vegetation in fire-prone ecosystems can exhibit resistance or resilience to wildfires (Agee, 1993; Steel *et al.*, 2021). In microbial ecology, trends have emerged that suggest that bacteria exhibit greater resistance and resilience to disturbance than fungi due to their faster regeneration times (Dooley & Treseder, 2012; Pressler *et al.*, 2019). For example, bacteria appear resistant to low-severity grassland fires (Semenova-Nelsen *et al.*, 2019; Yang *et al.*, 2020; Glassman *et al.*, 2023). Conversely, high-severity fires result in long-lasting reductions in both bacterial and fungal populations, with recovery taking 5-10 years for bacteria (Xiang *et al.*, 2014; Whitman *et al.*, 2022) and over 20 years for fungi (Kipfer *et al.*, 2011; Pérez-Valera *et al.*, 2018; Pressler *et al.*, 2019). While fire severity affects the rates of bacterial and fungal resilience, fires are incredibly heterogeneous, and many factors, such as distance

to the unburned forest edge, precipitation, and soil properties, likely contribute to rates of microbial resilience.

High-severity wildfires can reset microbial community assembly processes (Ferrenberg *et al.*, 2013), presenting a unique opportunity to investigate the patterns and drivers of microbial resilience. Here, we sampled at high temporal resolution for 17 time points ranging from 17 days to 4.5 years to track changes in vegetation, soil biogeochemical properties, and bacterial and fungal biomass, richness, and composition after a high-severity wildfire in a Southern California chaparral shrubland. These complementary data allowed us to test whether 1) bacterial and fungal biomass, richness, and communities recovered over time, 2) if bacteria were more resilient than fungi, 3) what abiotic and biotic factors predicted microbial resilience, and 4) if microbial richness and composition drove recovery of biogeochemical functions and vegetation over time.

4.3 Methods

4.3.1 Study area, plot design, and soil sampling

In September 2018, the Holy Fire burned 94 km^2 of manzanita (*Arctostaphylos glandulosa*) dominated chaparral shrublands in Southern California's Cleveland National Forest. Seventeen days after fire containment, we established nine plots (6 burned and 3 unburned), each with four 1 m^2 subplots at each cardinal direction (Fig. C.1.1) for repeated soil collection (Pulido-Chavez et al., 2023). Plots were selected for similar pre-fire vegetation, slope, elevation, and aspect. To assess soil burn severity at a scale

relevant to microbial turnover (Bahram et al., 2013), we measured initial ash depth (in cm) at 17 days post-fire, averaging three separate measurements per subplot and used ash depth as a measure of soil burn severity throughout our analysis. Additionally, to assess the potential dispersal of microbes from unburned areas, we determined the nearest distance to unburned areas in each plot (in meters) using ArcGIS by measuring the distance to the center of each plot.

Our study site experiences a Mediterranean-type climate with hot, dry summers and cool, wet winters. During our study, annual average temperatures were 17.2ºC, with total monthly precipitation averaging 36 mm, with most rain falling between November and April. Precipitation information was derived from monthly averages from Sept 2018 to May 2023 and collected from the El Cariso weather station (raws.dri.edu). The soils are mapped in the Cieneba and Friant series and are classified as Typic Xerorthents and Lithic Haploxerolls.

4.3.2 Sample collection

We sampled soil for 17 time points ranging from 17 days to 4.5 years post-fire. We collected soils at the highest resolution during the first post-fire year, resulting in 9 time points corresponding to 17, 25, 36, 67, 95, 131, 187, 286, and 376 days post-fire. For years 2-4, we sampled soils three times a year (winter, spring, and summer/fall) to minimize plot disturbance and to capture the largest seasonal variation. We always collected in August/September after the summer dry season, in January during the peak rainy season, and in May during peak plant productivity. These time points correspond to

16, 20, 23.5, 28, 31.75, 36, 40.35, 44 months post-fire. Sampling time points correspond to nearly 100% vegetation mortality at 17 days (Fig. 4.1a) to recovery of some shrubland vegetation at 5 years post-fire (Fig. 4.1f), but not to the richness or cover of the unburned plots (Fig. 4.1). At each time point, we collected the top 10 cm of mineral soil (A horizons) beneath the ash layer from each burned subplot and below the organic layer in the unburned plots with a ~250 mL releasable bulb planter cleaned with ethanol after each use to prevent cross-contamination, resulting in 36 soil samples (9 plots x 4 subplots) per sampling time point. Soils were placed in individual Whirl-Paks and transported in a cooler to the University of California-Riverside within hours of sampling, stored overnight at 4˚C, and sieved (2mm) in ethanol-cleaned sieves within 24 hours of sampling to minimize microbial community turnover (Phillips, 2021). Gravimetric soil moisture was measured immediately from all samples (weighing 5-10g of soil, drying for 24-48h at 105℃, and reweighing), then a subsample was frozen at -80°C for future DNA extraction, and the rest was air-dried for biogeochemical analysis.

4.3.3 Soil chemistry

We measured gravimetric soil moisture and performed KCL extractions within 24h of collection from fresh soil samples, while all other biogeochemical analyses were performed on air-dried soils. For NH_4^+ and NO_3^-, 3g of fresh soil was mixed for 30 minutes with 30 ml of 2 M KCL solution, filtered with Whatman No. 42 filter paper, and then frozen at -20ºC (Hanan *et al.*, 2016). Frozen KCL extracts were submitted to the Environmental Sciences Research Laboratory (ESRL) at the University of California,

Riverside, for analysis. Extracts were analyzed colorimetrically for NH_4^+ [SEAL method Environmental Protection Agency (EPA)-126-A] and NO_3^- (SEAL method EPA-129-A) using a SEAL AQ-2 discrete analyzer at the Environmental Sciences Research Laboratory at UCR. At 25 days post-fire, we determined soil particle size and textural class (soil texture) by the hydrometer method (Carter & Gregorich, 2008). Bulk density was measured using standard methods (Carter & Gregorich, 2008). Soil pH was determined using an Orion pH meter (ThermoFisher Scientific) on a 1:2 solution of air-dried soil in nanopure water. Soil pH was measured for 15 timepoints except at 34 and 95 days, resulting in 540 samples, and soil NO_3^- and NH_4^+ for 14 timepoints (no data for 34, 67, 95 days, and 44 months post-fire), resulting in 468 samples (9 plots x 4 subplots x 13 time points).

4.3.4 Vegetation field measurements

To measure vegetation regeneration over time, at 17 days post-fire, we measured vegetation composition and cover from the same subplot from which microbial samples were collected. However, since soil removal can affect vegetation recovery, in June 2019 (276 days post-fire), new 1 m^2 vegetation subplots were placed 1 m from the center of the microbial subplots for vegetation measurements (Fig. C.1.1b). Throughout the study, we sampled vegetation six times during spring peak productivity in May/June, corresponding to 17, 286, 376 days and 20, 23.5, 32, and 44 months post-fire. Within each plot, we visually estimated two levels of data following previously used methods (Glassman *et al.*, 2023). We measured the total vegetation cover, such that the composition adds up to

100%, and species composition, which can vary per plot but will add up to at least the total vegetation cover. To ensure precision in our estimates, all estimates above 15% or below 95% were rounded to the nearest divisible by 5 (i.e., 30 not 32). Species names and origin classification followed the Jepson Flora (2022)

4.3.5 DNA extraction, amplification, and sequencing

DNA extractions for all 17-time points were performed over 4.5 years. The first nine time points were extracted in the summer of 2019. Due to a freezer failure, soils from T10, T11, and T12 were thawed before DNA extraction. However, we found that this had a limited effect on microbial richness and composition (Pulido-Chavez et al., in prep). For T1-16, we extracted DNA from 0.25g of soil using ethanol-cleaned spatulas and Qiagen DNeasy PowerSoil Kits, following the manufacturer's protocol with the slight modification of extending centrifugation time to 1.5 min after adding C3. For T17, DNA was extracted with Qiagen PowerSoil Pro kits due to the discontinuation of the Qiagen PowerSoil kits. To improve soil DNA recovery, we modified the Qiagen PowerSoil Pro protocol by adding 100ul of Qiagen ATL tissue lysis buffer buffer to the 0.25g of soil with the 700ul of Qiagen solution CD1 and incubating the samples overnight at 4□C for 16-20hrs. The extracted DNA was stored at -20°C. We amplified extracted DNA using the primer pair ITS4-fun and 5.8S to target the ITS2 region for fungi (Taylor *et al.*, 2016) and the primer pair 515F-806R to amplify the V4 region of the 16S rRNA for bacteria (Caporaso *et al.*, 2011) using the Dual-Index Sequencing Strategy (DIP) (Kozich et al., 2013) as previously published (Pulido-Chavez *et al.*, 2023). In total, the 612 samples (9

plots x 4 subplots x 17 time points), along with negative DNA extractions, PCR controls, as well as mock communities, with 16S and ITS2 pools combined at a 2:3 ratio, were sequenced across seven Illumina MiSeq 2x300bp libraries at UCR Institute for Integrative Genome Biology.

4.3.6 Bacterial and fungal biomass

Since biomass quantification methods for fungi are correlated (Cheeke *et al.*, 2017), we used quantitative (q) PCR to estimate bacterial and fungal gene copy numbers as a proxy for biomass using the Eub338/Eub518 primers for bacteria (Fierer *et al.*, 2005) and FungiQuant-F/FungiQuant-R primers for fungi (Liu *et al.*, 2012). Standard curves were generated using a 10-fold serial dilution of the standards *Saccharomyces cerevisiae* or the 16S region of the bacteria *Escherichia coli* as previously established (Averill & Hawkes, 2016). Quantitative PCR reactions were performed in triplicate of 10ul reactions. Each containing 1 µL undiluted DNA, 1 µL of 0.05M Tris-HCl ph8.3, 1 µL of 2.5mM $MgCl_2$ (New England BioLabs (NEB); Ipswich, MA), 0.5 µL of 0.5mg/ml BSA, 0.5 µL of 0.25mM dNTP (NEB), 0.4 µL of both primers at 0.4µM, 0.5 µL of 20X Evagreen Dye (VWR International; Radnor, PA), 0.1 µL of Taq DNA polymerase (NEB) and 4.6 µL ultra-pure water. The qPCR conditions can be found in (Pulido-Chavez et al., 2023). We employed the CFX384 Touch Real-Time PCR Detection System. Gene copy numbers were generated using the equation 10^ (Cq-b)/m), where Cq is the quantification cycle, calculated as the average per sample in relation to the known/calculated copies in the Cq/threshold cycles. The y-intercept (b) and the slope (m) values were generated with

CFX Maestro software. Values with an $R^2 > 0.994$ were considered acceptable. Gene copy numbers were normalized per gram of dry soil (Tatti *et al.*, 2016).

4.3.7 Bioinformatics

Illumina data was processed with Qiime2 version 2023.2 (Bolyen *et al.*, 2018). The demultiplexed fastQ files from the seven Illumina sequencing runs were individually processed, per library using cutadapt (Martin, 2011) to remove the primers, ran through DADA2 version 2023.2 with the defaults parameters filtering out chimeric sequences, eliminating low-quality regions and generating Amplicon Sequence Variants (ASVs) (Callahan *et al.*, 2017). Bacterial reads were trimmed the forward read to 170 bp and reverse read was truncated to 163 bp and fungi 209 bp and 201 bp, respectively, resulting in an average of 63% of forward and reverse sequences merged for bacteria and 61% merged for fungi. The seven DADA2 outputs were consolidated into one library, singletons sequences were removed, and taxonomy was assigned using the Qiime2 Naïve Bayes Blast+ classifier. We used SILVA version 138.1 for bacterial (Yilmaz *et al.*, 2014) and UNITE version 9.0 for fungal (Abarenkov *et al.*, 2020) taxonomic assignment. We removed bacterial sequences assigned to mitochondria and chloroplasts and fungal sequences not assigned to Kingdom Fungi. Moreover, fungal ASV tables were exported and parsed through FUNGuild (Nguyen, 2018) to assign functional ecological guilds, including only highly probable confidence rankings for ectomycorrhizal fungi. Sequences were submitted to the National Center for Biotechnology Information Sequence Read

Archive under BioProject accession number PRJNA761539 (T1-T9) and SUB13901547 (final submission pending).

4.3.8 Statistical analysis

To evaluate species richness and community resilience in burned and unburned communities, we computed several quantitative stability metrics, including species resistance (Shade *et al.*, 2012), resilience (Shade *et al.*, 2012; Yang *et al.*, 2023), recovery rate, percent recovery to unburned levels (Cole *et al.*, 2014; Jones *et al.*, 2018; Marchand *et al.*, 2021), community stability and community compositional trajectory or the pattern of succession followed by post-fire microbes (i.e., stochastic or directional replacement) (Collins *et al.*, 2000).

First, we calculated species resistance, following the approach outlined by (Orwin & Wardle, 2004; Shade *et al.*, 2012) for bacterial and fungal communities individually. Second, to quantitatively assess resilience, we computed species resilience for each sampling year as the difference in richness between unburned and burned bacterial and fungal communities (independently), tracking changes over time from 17 days to 4.5 years post-fire, as per established methods (Yang *et al.*, 2023). The resilience and resistance index are bound by ±1, where R of 1=full recovery (maximal resilience/resistance); $0 < R < 1$ indicates the slow rate of recovery/resistance, and R of 0 indicates no recovery over time. We then used linear regressions to test how bacterial and fungal resilience changed over time and whether resilience differed between bacterial and fungal communities.

Third, to understand the recovery rate (Cole *et al.*, 2014; Jones *et al.*, 2018; Marchand *et al.*, 2021) and percent recovery to unburned levels for each year (Jones *et al.*, 2018), we applied Equation (1) adapted from (Yang *et al.*, 2023). Bacterial and fungal richness was considered recovered when the richness in the burned communities equaled the initial richness in the unburned communities (as recorded at 17 days post-fire), resulting in a percent recovery value of 0, indicating no difference between sites. Like resilience, we used linear regressions to test how bacterial and fungal recovery rates and percent recovery changed over time and whether the percent recovery and recovery rate differed between bacterial and fungal communities.

a

$$RR = \frac{\left(\left(\frac{\left(F_{End(burn)} - F_{Initial(burn)}\right)}{\left(F_{unburn(mean)} - F_{initial(burn)}\right)}\right) * 100\right)}{Recovery\ Time\ (T)}$$

b

$$PR = ln\left(\frac{F_{End(burn)}}{F_{unburn(mean)}}\right) * 100$$

Lastly, to determine whether microbial successional trajectories are following directional or stochastic patterns of succession, we performed a linear regression analysis, as recommended by Collins et al. (2000) for bacterial and fungal species richness and community composition, independently, using the codyn package (Hallett *et al.*, 2016). Directional change in succession occurs when the regression line is significant, positive, and exhibits a linear pattern. Conversely, a non-significant regression, or a slope that is not significantly different from zero, indicates stochastic variation. Additionally, a negative slope indicates species richness or composition converges toward an earlier time

point (Collins *et al.*, 2000; Hallett *et al.*, 2016). For species richness, the richness was regressed against time. For community composition, we calculated the differences in community composition over increasing time intervals in codyn (Hallett *et al.*, 2016) using Euclidean distance and regressed distance against time lags in ggplot2 (Wickham, 2016). Moreover, we plotted the community successional trajectories using the Bray-Curtis dissimilarity centroids for each time point per burned and unburned communities using Principle Coordinates Analysis (PCoA).

To assess environmental drivers of bacterial and fungal biomass and richness, we conducted separate generalized negative binomial regression analyses for bacterial and fungal richness for burned and unburned samples. Because complete environmental data was unavailable for all sampled time points, our analysis was divided into two separate regression analyses. Regression 1 tested the effects of time, ash depth, distance to the unburned area, average wind speed, and percent soil moisture, clay, and pH and their first-order interactions for 15 time points, excluding 34 and 95 days post-fire. Regression 2 examined the effects of all the variables included in regression 1, in addition to NO_3^-, NH_4^+ , vegetation richness, and vegetation Shannon diversity for six time points (17, 286, 376 days, and 20, 23.5, and 32 months). For both richness and biomass models, for bacteria and fungi independently, we tested the level of nestedness by running null models with different nestedness levels, and the best fit was determined via Akaike Information Criterion (AICc) in the MuMIN package version 1.47.5 (Barton, 2023). In regression 1, we incorporated subplot and time as random effects for burned and unburned richness models. Model 2 for richness involved plot, subplot, and time as

random effects. When considering burned biomass in Model 1, we included plot, subplot, and time as random effects and only plot and time for unburned plots. Additionally, for biomass regression 2, subplot and time were the selected random effects for both burned and unburned models. Marginal and conditional R^2 values were calculated using the r.squaredGLMM function in the MuMIn Package v 1.47.5 (Barton, 2020). All variables were scaled.

To assess the long-term impact of wildfire and time since fire on community composition, we calculated the square-root transformed median using Bray-Curtis dissimilarity per 100 iterations between burned and unburned communities. We then use permutational multivariate analysis of variance (PERMANOVA) (Anderson, 2017) in the vegan package to test how treatment, time, and their interaction influence community composition. Results were visualized using nonmetric multidimensional scaling (NMDS) ordinations.

Given the high turnover rates of post-fire microbes (Pulido-Chavez *et al.*, 2023) and the nonlinear nature of their responses (Glassman *et al.*, 2017), we employed generalized dissimilarity modeling (GDM) (Ferrier *et al.*, 2007) to examine the environmental drivers of bacterial and fungal community composition. Like the richness models, we conducted two separate GDM analyses based on the data partitioning described earlier for species richness. We applied GDMs to bacterial and fungal temporal Bray-Curtis diversity community composition and environmental dissimilarity matrices, following the method by (Ferrier *et al.*, 2007) using the gdm package version 1.5.0-9.1 (Fitzpatrick *et al.*, 2022). All environmental variables were scaled for proper comparison,

and correlated variables were excluded from all analyses. Significance was tested via backward model selection with 999 permutations (Fitzpatrick *et al.*, 2022). All models were fit independently for bacteria and fungi. Results of only the significant variables driving community composition were plotted in ggplot2.

Lastly, to assess the influence of soil microbial communities on the recovery of biogeochemical functions and vegetation over time, we independently conducted Mantel tests on Bray-Curtis dissimilarities of vegetation and bacterial and fungal communities. To test the relationship of bacterial and fungal species richness on vegetation Shannon diversity and soil NO_3^- and NH_4^+, we performed linear mixed effect models (lmer) using the lme4 package in R. All linear regression models (lmer) used subplot as nested effects. Additionally, since ectomycorrhizal fungi are associated with over 80% of plants (van der Heijden *et al.*, 2008), which should increase over succession (Liu *et al.*, 2022), we also used lmer models to see their impact on ecosystem recovery, including vegetation Shannon diversity NO_3^- and NH_4^+ .

4.4 Results

4.4.1 Wildfire had long-term impact on soil parameters and vegetation

Wildfires had long-term significant increases in soil NH_4^+ (Fig. C.1.2a), NO_3^- (Fig. C.1.2b), pH (Fig. C.1.2c), and decreases in soil moisture (Fig. C.1.2d). At 4 years post-fire, NH_4^+ levels were 88% higher, NO_3^- levels were 406% higher, and soil pH was 9% higher in the burned plots than the unburned plots (Fig. C.1.2). In contrast, vegetation

richness decreased post-fire, while Shannon diversity increased after the fire (Fig. C.1.3). Vegetation richness reached its peak at 20 months, being 78% higher than in the unburned plots, and then gradually decreased over time, recovering to unburned levels by 44 months post-fire (Fig. C.1.3a). However, vegetation diversity (Hdiv) rapidly increased post-fire and fluctuated over time, peaking at 23.5 months post-fire, being 96% higher in the burned than unburned plots (Fig. C.1.3b). However, 4.5 years was insufficient time for vegetation Hdiv to recover, remaining 36% higher in the burned plots than the unburned plots (Fig. C.1.3b). While vegetation Hdiv was higher in the burned plots, vegetation community composition differed. The unburned community was dominated by *Arctostaphylos glandulosa* and *Adenostoma fasciculatum*. In contrast, the burn community was more diverse and was dominated by *Eriodictyon parryi*, *Adenostoma fasciculatum*, *Phacelia brachyloba*, *Acmispon glaber, Calystegia macrostegia, Ceanothus oliganthus* and *Crocanthemum scoparium*.

4.4.2 Drivers of bacterial and fungal resilience

Bacterial richness was more resistant and resilient to wildfire than fungal richness (Table C.2.1; 4.2). The high resilience of bacterial biomass and richness was driven by soil pH, distanced to unburned edge, and an interaction between soil burn severity and soil pH for biomass and soil burn severity and its interaction with time for richness (Table C.2.3). When vegetation and soil N concentrations were included in the regression analysis, these variables significantly impacted bacterial biomass and richness (Table C.2.4). While time and NH_4^+ negatively impacted bacterial biomass ($p<0.0001$),

vegetation richness led to positive impacts (p=0.02; Table C.2.4). There was also a notable interaction between time and NH_4^+ and time and soil pH, such that bacterial biomass increased over time as soil pH and NH_4^+ declined (Table C.2.4; Fig. C.1.2a,c). For bacterial richness, both ash depth and a time and NH_4^+ interaction negatively affected richness, whereas the direct effects of NH_4^+ and vegetation richness increased in bacterial richness over time (Table C.2.4).

During the four-year successional study, changes in fungal biomass were driven by a wide array of soil abiotic and site variables (Table C.2.3). Fungal biomass was significantly and positively affected by time and ash depth and interactions between time and ash depth and ash depth and soil moisture. In contrast, fungal biomass was negatively impacted by soil pH, soil moisture, distance to unburned edge, and an interaction between ash depth and soil pH (Table C.2.3). In contrast, changes in fungal richness were positively influenced by soil moisture and an interaction between time and ash depth but negatively impacted by the direct effect of ash depth (Table C.2.3).

Like bacteria, including vegetation metrics and soil N affected fungal biomass and richness (Table C.2.4). Fungal biomass was negatively influenced by the direct effects of time and NH_4^+ and an interaction between time and vegetation richness but was positively influenced by the direct effects of vegetation richness, time and soil pH, and interactions between time and NH_4^+ (Table C.2.4). Fungal richness, which did not recover over time, remained consistently and negatively affected by the direct effects of ash depth, time, vegetation Shannon diversity, and an interaction between time and ash depth (Table C.2.4).

4.4.3 Time and species richness increased bacterial and fungal community stability

Community stability significantly differed between bacterial and fungal communities ($p<0.0001$; Table C.2.5). Burned and unburned bacterial (Fig. 4.2e) and fungal (Fig. 4.2f) community stability was strongly linked to species richness ($p<0.0001$; Table C.2.5), with communities becoming more stable as richness increased (Fig. C.1.4). However, time had a differential impact on bacterial and fungal community stability (Table C.2.7). Unburned bacterial communities remained stable over time ($p<0.02$; Table C.2.6), whereas both burned bacterial (Fig. C.1.a) and fungal communities (Fig. C.1.4b) increased in stability over time (Fig. C.1.4; Table C.2.7). In contrast, unburned fungal communities fluctuated in stability over time (Fig. C.1.4b; Table C.2.6). In addition, time and richness interacted and positively impacted burned bacterial community stability (Fig. 4.2e) but did not affect fungal stability (Fig. 4.2f; Fig. C.1.4; Table C.2.7), showing that the recovery of bacterial richness over time corresponded with increased bacterial community stability.

4.4.4 Burned communities experience post-fire directional change

Wildfires and time since fire had significant direct effects on bacterial ($p<0.0001$; Fig. 4.3a) and fungal community composition ($p<0.0001$; Fig. 4.3b; Table C.2.8). Moreover, we observed an interaction effect of wildfire and time on bacterial and fungal community composition ($p = 0.0001$; Fig. 4.3; Table C.2.8), such that community composition became more similar over time, more for bacteria (Fig. C.1.5) than fungi (Fig. C.1.6), highlighting the resilience of the bacterial communities (Fig. C.1.5), which

appear to be recovering over time, in contrast to the fungal community (Fig. 4.3a,b; Fig. C.1.6).

Trajectory analysis of the PCoA centroids of bacterial (Fig. 4.3c) and fungal communities (Fig. 4.3d) further revealed that wildfire affected their successional trajectories (Fig. 4.3c,d). In contrast to the non-directional stochastic changes observed in unburned bacterial and fungal communities over time (Fig. 4.3c,d; Fig. C.1.7), burned bacterial and fungal communities displayed clear directional succession, diverging away from the unburned communities as succession progressed (Fig. 4.3c, d). Independent time lag analysis of bacterial (slope = 0.01; R^2 =0.01; Fig. 4.3e) and fungal community composition (slop=0.01; R^2=0.02; Fig. 4.3f) further indicates a stochastic change in unburned microbial communities (Fig. 4.3h,g). In contrast, time lag analysis confirmed that burned bacteria (slope = 0.27; R^2=0.15; Fig. 4,3e) and fungal communities (slope = 4.2; R^2 =0.24; Fig. 4.3f) are undergoing slow directional change over time (Fig. 4.3e,f).

4.4.5 Dynamics of bacterial and fungal dominance during succession

Directional changes in bacterial and fungal communities were primally driven by trade-offs in the dominant bacteria (Fig. 4.4a, 4.5a) and fungi (Fig. 4.4c, 4.5b). Notably, both bacterial and fungal communities exhibited higher levels of resilience at the phyla level (Fig. C.1.8) as opposed to the genus levels (Fig. 4.4). Overall, the unburned bacterial (Fig. 4.4b) and fungal (Fig. 4.4d) communities lacked dominance, except for the fungal Basidiomycete and ectomycorrhizal genus *Inocybe* (Fig. 4.4d; Table C.2.9). In contrast, the burned bacterial community displayed large dominance during the first post-

fire year by the Proteobacteria *Massilia,* the Firmicute *Paenibacillus* and the Actinomycete *Conexibacter* (Fig. 4.4a, 4.5a; Table C.2.9). However, dominance diminished over time as more genera increased in relative abundance (>3% relative abundance), leading to a more rich and diverse microbial community from years 2-4.5 (Fig. 4.4a; Table C.2.9) and thus aiding in community resilience. Indeed, *Massilia,* which accounted for an average of 34% of the bacterial community during the first year, decreased to 4% after 16 months and traded off in abundance with the Actinobacteriota *Blastococcus,* which made up, on average 32% of the burned community (95d-44m; Fig. 4.4a, 4.5a; Table C.2.9), leading to an increase in community stability (Fig. 4.5c; Table C.2.9). Moreover, after year one, bacterial communities were equally dominated by taxa in the genera *Bacillus* which on average made up 4% of the community (from year 1-44m post-fire), *Segetibacter* (10%), and *Sphingomonas* (5%*;* Table C.2.9).

In contrast, fungal communities quickly became dominated by the Ascomycetes *Aspergillus,* which on average comprised 7% of the abundance in year one, *Pyronema* (32%), and *Penicillium* (14%; Fig. 4.4c; Table C.2.9). Despite the increased abundance of several genera over time, from year 2-4.5 years, including *Coniochaeta* on average making up 7%, *Coniothyrium* (5%), *Alternaria* (4%), and *Plicaria* (4%), the genera *Pyronema* (11%), *Penicillium* (12%), and *Aspergillus* (6.5%) continued to sustain high levels of dominance throughout succession (Fig. 4.4c, 4.5b; Table C.2.9). Moreover, by the end of year one, and throughout succession, there was a noticeable trade-off in abundance between Ascomycetes and Basidiomycetes (Fig. C.1.8c; Table C.2.9). The Basidiomycetes *Coprinellus* increased from 5% at 286 days to 7% at 44 months postfire.

Additionally, *Naganishia* increased from 4% at 286 days to 5% at 44 months, while *Tephrocybe* increased from 4% at 187 days to *7%* 32 months post-fire (Fig. 4.4c, 4.5b; Table C.2.9). Interestingly, the decline in the abundance of *Pyronema* and the increase in the abundance of *Coprinellus* increased community stability (Fig. 4.5c; Table C.2.9).

The analysis of fungal guild changes over time revealed a significant increase in saprotrophs during the first year, rising from 0.2% to 2% by the end of the year and remaining stable at 2% through 4.5 years (Fig. C.1.9). Additionally, in the burned plots, ectomycorrhizal fungi decreased from 1% at 17 days to .01% at 376 days post-fire but slowly increased over time, making 0.5% of the overall guild community at 44 months post-fire (Fig. C.1.9).

4.4.6 Drivers of bacterial and fungal richness and community composition

Overall, the generalized dissimilarity model (GDM) explained 35% of the variance for burned bacterial and fungal communities, which was increased to 42% for bacteria and 48% for fungi when vegetation and N concentrations were included in the model (Table C.2.10). In all cases, time was the most significant driver of community composition for bacteria (Fig. 4.6a) and fungi (Fig. 4.6b), with time having exponential impacts on community composition at first and eventually plateauing with predictor distance. Geographic distance played a larger but still minor role in shaping fungal community composition (Fig. 4.6c) than bacterial community composition (Table C.2.10; Fig. 4.6a) and soil burn severity also affected fungal community but also plateaued at higher predictor distance (Fig. 4.6c). Interestingly, when we included vegetation and N

metrics in the model, soil burn severity was no longer a driver of fungal community composition (Fig. C.1.10). However, it emerged as a significant driver of bacterial community composition (coefficient = 5; Fig. C.1.10; Table C.2.10), exhibiting a plateauing effect with increased predictor distance. The unburned GDM models explained less variance for both the bacterial (21% variance) and fungal communities (32%) but were increased to 39% for both bacteria and fungi when vegetation and soil N concentrations were included (Fig. C.1.10; Table C.2.11). Unburned bacterial community composition was influenced by percent clay, soil moisture, time, and geographic distance (Fig. C.1.10b; Table C.2.11). Similarly, the unburned fungal community was driven by geographic distance and percent soil clay, geographic distance, and vegetation richness (Fig. C.1.10d; Table C.2.11).

4.4.7 Recovery of soil biogeochemistry and vegetation is linked to microbial species richness

While neither total bacterial nor fungal community composition was correlated to chaparral vegetation in burned or unburned sites ($p>0.05$; Fig. C.1.11), the richness of burned bacterial and fungal communities had a significant impact on vegetation richness (Fig. C.1.12a,b; $p<0.05$) and vegetation Shannon diversity (Fig. 4.7g,h; $p<0.05$). Soil NH_4^+ levels were significantly influenced by the richness of burned bacterial (Fig. 4.7a) and fungal species (Fig. 4.7b; $p<0.05$). Additionally, NO_3^- levels were significantly correlated with bacterial species richness (Fig. 4.7d; $p<0.05$) but not fungal richness (Fig. 4.7e; $p<0.05$). Analysis of the ectomycorrhizal fungi further showed that in the burned

communities, increased in ectomycorrhizal species richness was significantly correlated to increased NH_4^+ ($p=0.02$; Fig. 4.7c) and decreases in NO_3^- ($p=0.01$; Fig. 4.7f). Although we observed a trend of increased vegetation Shannon diversity with increased ectomycorrhizal richness, the results were not statistically significant ($p=0.08$; Fig. 4.7i).

4.5 Discussion

Our study highlights the high resilience of bacteria richness in post-fire ecosystems, recovering to unburned levels within 4.5 years following a high-severity chaparral wildfire. In contrast, fungal biomass, richness, and composition did not recover over time, highlighting their sensitivity to secondary wildfire effects on the environment. Even 4.5 years post-fire, microbial richness continued to be influenced by soil burn severity and time, with vegetation and N playing noteworthy though less significant roles. Additionally, time emerged as the most important factor shaping the composition of both burned bacterial and fungal communities. Lastly, we found that a NH_4^+ and vegetation diversity were significantly correlated with bacterial, fungal, and ectomycorrhizal fungal richness. In contrast, NO_3^- was associated with bacterial and ectomycorrhizal richness, emphasizing the pivotal role of these microbes in post-fire ecosystem recovery.

4.5.1 Contrasting recovery in bacterial and fungal richness

We found that bacteria richness and biomass were more resistant and resilient to wildfire than fungi, corroborating previous studies (Pressler *et al.*, 2019). Although it has

been suggested that bacterial richness would take ~10 years to recover (Xiang *et al.*, 2014; Whitman *et al.*, 2019) and that under the pressures of high-severity wildfires, bacterial communities would experience lower resilience due to increased mortality (Barreiro & Díaz-Raviña, 2021; Pinto *et al.*, 2023), we found that in high-severity burned chaparral, bacterial richness recovered to unburned level in 4.5 years. Given that the impact of high-severity wildfires on microbial resilience is system-specific (Pinto *et al.*, 2023), and considering the historical 30-year burn interval of Southern California chaparral shrublands (Keeley, 1981), along with the rapid regeneration of the fire-adapted chaparral vegetation (Lamont *et al.*, 2011), it is possible that the microbial communities are evolutionarily adapted to this specific fire regime. Consequently, they might have inherent traits that allow for rapid post-fire recovery.

In contrast, we found that neither fungal richness, biomass, nor bacterial or fungal community composition recovered to unburned levels, corroborating previous studies that suggest that it takes fungi over 15-20 years for species richness to recover (Kipfer *et al.*, 2011; Pérez-Valera *et al.*, 2018; Pressler *et al.*, 2019). Interestingly, although we expected fungal richness to increase over time, we found that fungal richness decreased with time since fire. Previous research on post-fire fungi (Greenwood *et al.*, 2023), as well as ectomycorrhizal (Pulido-Chavez *et al.*, 2021; Caiafa *et al.*, 2023; Greenwood *et al.*, 2023), and saprobic fungi in pine forests (Cutler *et al.*, 2017) also reported declining richness over time. The dominance of ectomycorrhizal fungi in the unburned community compared to the predominantly saprotrophic nature of the burned fungal community, coupled with the decline in ectomycorrhizal fungi over time, suggests

that the reduction in overall fungal richness is attributed to the decrease in ectomycorrhizal fungi. Moreover, studies in Chinese temperate forests suggest fungi exhibit higher vegetation specificity than bacteria (Chen *et al.*, 2022). The near-monodominance of manzanita or chamise in chaparral ecosystems, coupled with the absence of understory vegetation, suggest potential host-specificity among post-fire chaparral fungi. Consequently, fungal recovery may remain low until dominant vegetation begins to exclude understory plant species.

Furthermore, chaparral communities are characterized as water-limited environments (Solek & Resh, 2018). Drought mesocosm experiments show that, unlike bacteria, fungal richness decreases over time (Jaeger *et al.*, 2023). In our study, we found that changes in fungal richness were associated with percent soil moisture, indicating that the decline in fungal richness over the 4.5 years of the study is not solely a direct consequence of wildfire. Instead, fungal declines are exacerbated by the persistent moisture deficiency in chaparral ecosystems which are exacerbated by the indirect effects of wildfire, such as increased soil temperature and decreased soil moisture (Hart *et al.*, 2005).

4.5.2 Richness and dominance: differential drivers of burned bacterial and fungal stability

The diversity-stability hypothesis suggests that increased species richness enhances community stability over time (Lehman & Tilman, 2000; Loreau & de Mazancourt, 2013). In our study of burned chaparral, we found that bacterial and fungal

communities follow this traditional hypothesis as both time and species richness positively impacted bacterial and fungal community stability. These findings align with previous research, including short-term bacterial microcosms (Eisenhauer *et al.*, 2012), long-term 120,000-year chronosequence studies (Jangid *et al.*, 2013) and a global study spanning 18 countries and 6 continents (Liu *et al.*, 2012). Thus, bacterial communities are more stable as the different bacterial species host various functions and life strategies, allowing them to respond rapidly to environmental changes while maintaining a stable community (Tilman, 1999; Tilman *et al.*, 2006).

While bacterial richness increased over time and fungi decreased, the overall fungal community displayed a high dominance of key genera throughout the study period. In burned chaparral, we observed that early dominating genera, *Aspergillus, Penicillium,* and *Pyronema,* equalize in dominance over time, as *Geopora, Naganishia, Coprinus,* and *Plicaria* increased in dominance towards the end of the first year and lasted through years 2-4.5 post-fire. In contrast, burned bacterial communities lost dominance over time. These results suggest that for fungi, the continued dominance of a few resilient genera is more critical for increasing community stability than richness. These findings align with previous plant studies, which indicate that community stability is better explained by the dominant species (Grime, 1998; Smith & Knapp, 2003; Wayne Polley *et al.*, 2007). Our results emphasize the applicability of the vegetation community assembly mechanism to soil microbial communities. However, they also show the critical differences in dynamics between bacterial and fungal communities, which are essential for interpreting the recovery, maintenance, and restoration of burned ecosystems.

4.5.3 Directional replacement of species drives bacterial and fungal successional dynamics

While neither the bacterial nor fungal community composition recovered to unburned levels, our findings revealed that both microbial communities are undergoing directional changes, with the bacterial community displaying stronger directional trends than the fungal community. These results contrast with earlier studies that proposed bacterial communities, and to a lesser extent, fungal communities, follow more stochastic successional dynamics during secondary succession (Pinto *et al.*, 2023). However, it is important to note that most previous studies have had limited sampling intervals, potentially missing key successional time points (Dove & Hart, 2017; Pressler *et al.*, 2019; Yang *et al.*, 2020), which our study successfully captured. While directional replacement, or the sequential replacement of taxa in an orderly and predictable manner (Odum, 1969) in vegetation successional dynamics, is considered rare, research demonstrates that directional replacement can occur when fire-dependent species with rapid growth rates thrive due to the abundant resources released by the fire (Platt, 2003). Moreover, for successful ecosystem recovery, post-fire microbes must exhibit high resilience and adaptability to the changing environmental conditions following the fire, ensuring the process of directional replacement. In our study, we observed certain fire resistant fungal and bacterial species like fungal *Pyronema domesticum* (Bruns et al., 2020), Basidiomycete *Geminibasidium, Ascomycete Aspergillus*, and Bacterial *Neobacillus bataviensis* (a member of the Bacillaceae) thrive in heated soils due to their ability to use post-fire resources. These findings suggest that the conditions necessary for

initiating directional replacement in burned microbial communities exist within burned chaparral ecosystems.

Both bacterial and fungal communities demonstrated trade-offs in the abundance of the dominant genera over time. These abundant trade-offs showed that taxa were being replaced and likely drove ecosystem functions. For example, the bacterial Proteobacteria *Massilia,* which has been identified as a pyrophilous bacteria in many ecosystems, including boreal forests (Whitman *et al.*, 2019) and redwood tanoak forests (Enright *et al.*, 2022), was highly dominant in the first year post-fire but started to decline after the first year as the Actinobacteria *Blastococcus* increased in abundance. We recently showed metagenomic evidence that *Massilia* can degrade both PyOM and bioavailable N, both abundant resources in post-fire systems (Pulido-Chavez et al., I*n Prep*). However, *Blastococcus*, which is slow-growing, demonstrates high adaptive capacity and phenotypic plasticity (Montero-Calasanz *et al.*, 2022), which likely made it more resilient and a stronger competitor in the post-fire altered environment, ultimately enhancing community stability. *Pyronema domesticum,* which is well-known as a pyrophilous fungus (Seaver, 1909; Fox *et al.*, 2022), dominated in the first half of the first year post-fire but began to decline as certain pyrophilous Basidiomycetes like *Tephrocybe* and *Coprinellus* increased. *Pyronema*, which likely survives wildfires through thermotolerant sclerotia (Moore, 1962), like *Massilia*, has the capacity to breakdown PyOM (Fischer *et al.*, 2021). However, we speculate that *Coprinellus*, a Basidiomycete decomposer, is a stronger competitor, which also drove it to correlate with community resilience. These findings highlight the intricate and contrasting responses of bacterial and fungal

communities during post-fire succession, shedding light on the complex dynamics of microbial resilience and community stability.

4.5.4 Drivers of bacterial and fungal species richness

While wildfire-induced mortality is the initial driver of change in soil microbial communities (Pulido-Chavez *et al.*, 2021; Pulido-Chavez *et al.*, 2023), we found that ash depth, a metric of soil burn severity, becomes the most important factor negatively impacting bacterial and fungal species richness. This finding corroborates previous studies showing that high soil burn severity results in larger (Pulido-Chavez *et al.*, 2021; Fox *et al.*, 2022; Caiafa *et al.*, 2023) and long-lasting impact on microbial richness (Pulido-Chavez *et al.*, 2021; Dove *et al.*, 2022) and biomass (Dooley & Treseder, 2012; Pulido-Chavez *et al.*, 2023). However, the indirect effects of soil burn severity on the ecosystem have been shown to decrease over time (Certini *et al.*, 2021), and here we found that a time and ash depth interaction positively impacted microbial richness. The positive effect of time and soil burn severity is better explained by the recovery of the ecosystem, such as the regeneration of the vegetation and changes in the soil environment (Neary *et al.*, 1999; Certini, 2005; Certini *et al.*, 2021), which can create niches for different microbial species to thrive.

When vegetation and N metrics were included in the model, we saw that vegetation richness positively affected bacterial richness, while vegetation Shannon diversity affected fungal richness. Previous studies have shown that bacterial and fungal richness are associated with plant diversity (Liu *et al.*, 2020) and that the post-fire

dynamics of plant communities significantly affect fungal (Hart et al., 2005) and bacterial communities (Liang *et al.*, 2016; Liu *et al.*, 2020). Wildfires lead to an increase in bioavailable N (Dannenmann *et al.*, 2018) and an increase in N-fixing vegetation, such as *Ceanothus* and N-fixing bacteria *Paenibacillus* (Monciardini *et al.*, 2003; Slepecky & Hemphill, 2006) and the Bacillaceae *Neobacillus bataviensis* (Yousuf *et al.,* 2017) corroborating previous studies showing that richness of bacterial taxa is closely related to the plant community (Liang *et al.*, 2016; Liu *et al.*, 2020), including exotic plant species (Glassman *et al.*, 2023). Moreover, both manzanita and chamise form ectomycorrhizal associations (Allen *et al.*, 2005), and the observed increase in vegetation richness and Shannon diversity coincides with the increased abundance of ectomycorrhizal genera (*Geopora cooperi* and *Inocybe*). Moreover, as plant richness and diversity increased over time, soil litter and root deposition also increased, thus potentially activating the soil microbial community and creating niches for specific microbial decomposers (Hooper *et al.*, 2000).

Bacterial richness was further driven by NH_4^+ and a time by NH_4^+ interaction corroborating previous studies in pine forests (Li *et al.*, 2019) and Mediterranean ecosystems (Goberna *et al.*, 2021). In our system, we previously found that the bacteria *Massilia* and *Arthrobacter* have genes for assimilatory NO_3^- reductions and dissimilatory NO_2^- reduction (Pulido-Chavez et al., in prep), allowing them to potentially take advantage of the large amounts of post-fire bioavailable N, thus showing that changes in NH_4^+ availability can significantly affect the microbial community over time. Indeed, in our system, NH_4^+ availability decreased over time, decreasing to levels close to unburn

levels at 16 months post-fire, which mimics the decrease in abundance observed for *Massilia* and the increase in bacterial richness observed in the post-fire sites, thus suggesting that declines in abundance of the dominant taxa and increased richness are indeed associated with soil NH_4^+.

4.5.5 Time: the dominant driver of community composition

Building on our initial analysis of the microbial communities from one year post-fire (Pulido-Chavez *et al.*, 2023), we found after year one, time becomes the dominant drive of bacterial and fungal community composition. Similarly, a study of boreal bryosphere communities found that time was the largest driver of bacterial and fungal community composition (Cutler *et al.*, 2017). It is important to note that time indirectly encompasses gradual changes in various soil geochemical, vegetation, and environmental factors. Thus, the significance of time on the community composition can have underlying mechanisms, as indicated by our findings that soil pH, NH_4^+, NO_3^-, soil moisture, and vegetation richness all changed dynamically over time. We were surprised that vegetation was not a significant driver of bacterial or fungal composition. These unexpected results could stem from our limited vegetation data, as we only collected data for five post-fire time points. This lack of data could have limited our ability to fully capture the dynamics between the soil microbes and vegetation over time. Furthermore, although geographic distance had a small but significant effect on community composition, its impact made us confident that the observed successional patterns and

community changes were not due to site differences, especially as geographic distance quickly plateaued in bacterial and fungal communities.

4.5.6 Bacterial and fungal species richness drive post-fire vegetation and N dynamics

Post-fire vegetation restoration was significantly associated with the recovery of bacterial and fungal richness, corroborating previous studies in grassland (Heinen *et al.*, 2020), chaparral (Teste *et al.*, 2017), and forested ecosystems (Hanif *et al.*, 2019). The observed positive impact of microbes on vegetation diversity might be attributed to feedback dynamics (Semchenko *et al.*, 2022). In this scenario, microbes facilitate nutrient access for resprouting vegetation, and reciprocally, the vegetation induces soil changes that potentially enhance microbial survivorship. Moreover, although previous studies have shown that ectomycorrhizal fungi affect vegetation diversity (Kennedy *et al.*, 2011; Bahram & Netherway, 2022), we found this not to be the case. However, it is important to note that although ectomycorrhizal fungi increased in relative abundance over time in the burned plots, they were still less that 1% of the burned community at the end of our study. Moreover, the burned vegetation community was predominantly comprised of non-ectomycorrhizal herbs, thus potentially explaining the lack of association between the ectomycorrhizal community and Shannon diversity. However, we did find that *Geopora cooperi,* dominated later successional stages of the ectomycorrhizal community, corresponding to the increased growth and dominance of woody plant species, thus we speculate the with increased recovery time, the ectomycorrhizal community and thus fungal dynamics will be more closely linked to the vegetation community.

Moreover, we found that post-fire $NH4^+$ levels were driven by bacterial and fungal richness, more so for bacteria than fungi. Post-fire, the increase in NH_4^+ is complemented by the rise in NH_3^+ oxidizing bacteria, as previously shown (Ball *et al.*, 2010). Furthermore, previous research has shown that post-fire microbes can use N (Espinosa-de-los-Monteros *et al.*, 2001; Krappmann & Braus, 2005; Suzuki, 2009; Nelson *et al.*, 2022) and research in burned oak woodlands in Spain (Cobo-Díaz *et al.*, 2015) and our previous study (Pulido-Chavez et al., *In prep*) demonstrated that post-fire microbes possess genes for incorporating N into biomass, effectively limiting N losses in the system. These findings provide insights into the mechanisms through which bacteria and fungi actively contribute to post-fire N dynamics.

In contrast, we found that NO_3^- levels were significantly influenced by bacteria but not fungi. This observation might be attributed to the declining capacity of fungi to assimilate NO_3^- with increasing soil pH, a significant factor influencing fungal biomass in our system and other disturbed systems (Li *et al.*, 2019). Moreover, a higher proportion of bacteria may possess the capacity to assimilate N than their fungal counterparts. This observation aligns with our previous findings, where we demonstrated the abundance of NO_3^- assimilation and assimilatory NO_3^- reduction genes in *Massilia*, a dominant bacterium, during the early post-fire period when NO_3^- concentrations were elevated. Furthermore, the larger population size of bacteria, both in terms of richness and abundance, implies that post-fire bacteria could be outcompeting fungi for available NO_3^-, potentially leading to increased NO_3^- immobilization (Li *et al.*, 2019). This diversity in

the bacterial community could possibly contribute to the effective retention of N in the ecosystem.

4.6 Conclusion

Our study provides the most comprehensive high temporal resolution study of microbial resilience in burned ecosystems to date. Here, we contrast the resilience patterns and successional dynamics of post-fire bacterial and fungal communities in a high-severity burned chaparral ecosystem. While both bacterial and fungal communities did not recover to unburned conditions, bacterial and fungal richness displayed contrasting resilience patterns. Bacterial richness displayed high resilience, recovering to unburned levels in 4.5 years, potentially due to their diverse functions and life strategies that facilitated a more diverse bacterial community over time, as seen after the first post-fire year. In contrast, fungal richness showed little recovery, decreasing over time, suggesting that fungi are more sensitive to fire direct and indirect wildfire effects on the ecosystem. Our research also revealed a directional pattern in post-fire microbial succession, driven by resilient, fire-adapted species that played an essential role in facilitating colonization and thus playing vital roles in enabling species replacement over time and thus driving successional dynamics. Over time, these species played essential roles in facilitating species turnover shaping microbial and ecosystem successional dynamics, such as vegetation and N dynamics. Together, this research shows the intricate relationship between microbial communities, vegetation, and soil geochemistry,

highlighting their importance in promoting the resilience and recovery of ecosystems following high-severity wildfires.

4.7 **Acknowledgments**

We thank UC Riverside, the BLM JFSP Award #012641-002 and Shipley Skinner Award to MFPC and SIG, the USDA-NIFA Award 2022-67014-36675 to SIG and PMH, and the DOE BER Award DE-SC0023127 to SIG and PMH. We further thank the Cleveland National Forest and the Trabuco Ranger District, including District Ranger Darrel Vance and Emily Fudge, Jeffrey Heys, Lauren Quon, Jacob Rodriguez, and Victoria Stempniewicz for their help with permitting and site selection. We thank Stuart Schwab, Noah Teller, Sameer Saroa, and Meg Kargul for help with vegetation sampling and Aral C. Green, who helped with biogeochemical analysis. Lastly, we thank all members of the Glassman and Homyak Labs at UC-Riverside for their help with fieldwork and molecular work.

4.8 Competing Interests

The authors declare no competing interest.

4.9 Data Availability Statement

Raw sequence reads for bacteria and fungi have been submitted to the National Centre for Biotechnology Information (NCBI) Sequence Read Archive. All statistical codes have been made available on GitHub https://github.com/pulidofabs/Bacterial-Fungal-Resilience-to-Wildfire.

4.10 References

2022. California Jepson Flora Project.

Abarenkov K, Zirk A, Piirmann T, Pöhönen R, Ivanov F, Nilsson RH, Kõljalg U 2020. UNITE QIIME release for Fungi 2: UNITE Community.

Abatzoglou JT, Williams AP. 2016. Impact of anthropogenic climate change on wildfire across western US forests. *Proceedings of the National Academy of Sciences* **113**(42): 11770-11775.

Agee JK. 1993. *Fire Ecology of Pacific Northwest Forests*. Washington DC: Island Press.

Allen MF, Egerton-Warburton L, Treseder K, Cario CH, Lindahl A, Lansing J, Querejeta J, Kårén O, Harney S, Zink T. 2005. Biodiversity of Mycorrhizal Fungi in Southern California. Planning for Biodiversity: Bringing Research and Management Together Proceedings of a Symposium for the South Coast Ecoregion: U.S. Department of Agriculture, Forest Service, Pacific Southwest Research Station.

Allison SD, Martiny JBH. 2008. Resistance, resilience, and redundancy in microbial communities. *Proceedings of the National Academy of Sciences* **105**(Supplement 1): 11512-11519.

Ammitzboll H, Jordan GJ, Baker SC, Freeman J, Bissett A. 2022. Contrasting successional responses of soil bacteria and fungi to post-logging burn severity. *Forest Ecology and Management* **508**: 120059.

Anderson MJ 2017. Permutational Multivariate Analysis of Variance (PERMANOVA). *Wiley StatsRef: Statistics Reference Online*: John Wiley & Sons, Ltd, 1-15.

Averill C, Hawkes CV. 2016. Ectomycorrhizal fungi slow soil carbon cycling. *Ecology Letters* **19**(8): 937-947.

Bahram M, Netherway T. 2022. Fungi as mediators linking organisms and ecosystems. *FEMS Microbiology Reviews* **46**(2): fuab058.

Ball PN, MacKenzie MD, DeLuca TH, Holben WE. 2010. Wildfire and charcoal enhance nitrification and ammonium-oxidizing bacterial abundance in dry montane forest soils. *J Environ Qual* **39**(4): 1243-1253.

Bardgett RD, van der Putten WH. 2014. Belowground biodiversity and ecosystem functioning. *Nature* **515**(7528): 505-511.

Barreiro A, Díaz-Raviña M. 2021. Fire impacts on soil microorganisms: Mass, activity, and diversity. *Current Opinion in Environmental Science & Health* **22**: 100264.

Barro SC, Conard SG. 1991. Fire effects on California chaparral systems: an overview. *Environment International* **17**(2-3): 135-149.

Barton K 2023. MuMIn: Multi-Model Inference.

Bolyen E, Rideout JR, Dillon MR, Bokulich NA, Abnet C, Al-Ghalith GA, Alexander H, Alm EJ, Arumugam M, Asnicar F, et al. 2018. QIIME 2: Reproducible, interactive, scalable, and extensible microbiome data science: PeerJ Inc.

Brundrett MC. 2009. Mycorrhizal associations and other means of nutrition of vascular plants: understanding the global diversity of host plants by resolving conflicting information and developing reliable means of diagnosis. *Plant and Soil* **320**(1): 37-77.

Brundrett MC, Tedersoo L. 2018. Evolutionary history of mycorrhizal symbioses and global host plant diversity. *New Phytologist* **220**(4): 1108-1115.

Caiafa MV, Nelson AR, Borch T, Roth HK, Fegel TS, Rhoades CC, Wilkins MJ, Glassman SI. 2023. Distinct fungal and bacterial responses to fire severity and soil depth across a ten-year wildfire chronosequence in beetle-killed lodgepole pine forests. *Forest Ecology and Management* **544**: 121160.

Callahan BJ, McMurdie PJ, Holmes SP. 2017. Exact sequence variants should replace operational taxonomic units in marker-gene data analysis. *The ISME Journal* **11**(12): 2639-2643.

Caporaso JG, Lauber CL, Walters WA, Berg-Lyons D, Lozupone CA, Turnbaugh PJ, Fierer N, Knight R. 2011. Global patterns of 16S rRNA diversity at a depth of millions of sequences per sample. *Proceedings of the National Academy of Sciences* **108**(Supplement_1): 4516-4522.

Carter MR, Gregorich EG. 2008. *Soil Sampling and Methods of Analysis*. Boca Raton: CRC Press, Taylor & Francis Group.

Certini G. 2005. Effects of fire on properties of forest soils: a review. *Oecologia* **143**(1): 1-10.

Certini G, Moya D, Lucas-Borja ME, Mastrolonardo G. 2021. The impact of fire on soil-dwelling biota: A review. *Forest Ecology and Management* **488**: 118989.

Cheeke TE, Phillips RP, Brzostek ER, Rosling A, Bever JD, Fransson P. 2017. Dominant mycorrhizal association of trees alters carbon and nutrient cycling by selecting for microbial groups with distinct enzyme function. *New Phytologist* **214**(1): 432-442.

Chen Y, Xi J, Xiao M, Wang S, Chen W, Liu F, Shao Y, Yuan Z. 2022. Soil fungal communities show more specificity than bacteria for plant species composition in a temperate forest in China. *BMC Microbiology* **22**(1): 208.

Cobo-Díaz JF, Fernández-González AJ, Villadas PJ, Robles AB, Toro N, Fernández-López M. 2015. Metagenomic Assessment of the Potential Microbial Nitrogen Pathways in the Rhizosphere of a Mediterranean Forest After a Wildfire. *Microbial Ecology* **69**(4): 895-904.

Cole LE, Bhagwat SA, Willis KJ. 2014. Recovery and resilience of tropical forests after disturbance. *Nat Commun* **5**: 3906.

Cole LES, Bhagwat SA, Willis KJ. 2014. Recovery and resilience of tropical forests after disturbance. *Nature Communications* **5**: 3906.

Collins SL, Micheli F, Hartt L. 2000. A Method to Determine Rates and Patterns of Variability in Ecological Communities. *Oikos* **91**(2): 285-293.

Cutler NA, Arróniz-Crespo M, Street LE, Jones DL, Chaput DL, DeLuca TH. 2017. Long-Term Recovery of Microbial Communities in the Boreal Bryosphere Following Fire Disturbance. *Microbial Ecology* **73**(1): 75-90.

Dannenmann M, Díaz-Pinés E, Kitzler B, Karhu K, Tejedor J, Ambus P, Parra A, Sánchez-Martin L, Resco V, Ramírez DA, et al. 2018. Postfire nitrogen balance of Mediterranean shrublands: Direct combustion losses versus gaseous and leaching losses from the postfire soil mineral nitrogen flush. *Global Change Biology* **24**(10): 4505-4520.

DeBano LF, Neary DG, Ffolliott PF. 1998. Fire Effects on Ecosystems.

Delgado-Baquerizo M, Maestre FT, Reich PB, Jeffries TC, Gaitan JJ, Encinar D, Berdugo M, Campbell CD, Singh BK. 2016. Microbial diversity drives multifunctionality in terrestrial ecosystems. *Nature Communications* **7**(1): 10541.

Dooley SR, Treseder KK. 2012. The effect of fire on microbial biomass: a meta-analysis of field studies. *Biogeochemistry* **109**(1/3): 49-61.

Dove NC, Hart SC. 2017. Fire Reduces Fungal Species Richness and In Situ Mycorrhizal Colonization: A Meta-Analysis. *Fire Ecology* **13**(2): 37-65.

Dove NC, Tas N, Hart SC. 2022. Ecological and genomic responses of soil microbiomes to high-severity wildfire: linking community assembly to functional potential. *ISME J* **16**(7): 1853-1863.

Eisenhauer N, Scheu S, Jousset A. 2012. Bacterial Diversity Stabilizes Community Productivity. *PLoS One* **7**(3): e34517.

Enright DJ, Frangioso KM, Isobe K, Rizzo DM, Glassman SI. 2022. Mega-fire in Redwood Tanoak Forest Reduces Bacterial and Fungal Richness and Selects for Pyrophilous Taxa that are Phylogenetically Conserved. *Molecular Ecology*.

Espinosa-de-los-Monteros J, Martinez A, Valle F. 2001. Metabolic profiles and aprE expression in anaerobic cultures of Bacillus subtilis using nitrate as terminal electron acceptor. *Applied Microbiology and Biotechnology* **57**(3): 379-384.

Ferrenberg S, O'Neill SP, Knelman JE, Todd B, Duggan S, Bradley D, Robinson T, Schmidt SK, Townsend AR, Williams MW, et al. 2013. Changes in assembly processes in soil bacterial communities following a wildfire disturbance. *ISME J* **7**(6): 1102-1111.

Ferrier S, Manion G, Elith J, Richardson K. 2007. Using generalized dissimilarity modelling to analyse and predict patterns of beta diversity in regional biodiversity assessment. *Diversity and Distributions* **13**(3): 252-264.

Fierer N, Jackson JA, Vilgalys R, Jackson RB. 2005. Assessment of Soil Microbial Community Structure by Use of Taxon-Specific Quantitative PCR Assays. *Applied and Environmental Microbiology* **71**(7): 4117-4120.

Fischer MS, Stark FG, Berry TD, Zeba N, Whitman T, Traxler MF. 2021. Pyrolyzed Substrates Induce Aromatic Compound Metabolism in the Post-fire Fungus, Pyronema domesticum. *Front Microbiol* **12**: 729289.

Fitzpatrick MC, Mokany K, Manion G, Niieto-Lugilde D, Ferrier S 2022. gdm: Fit a Generalized Dissimilarity Model to Tabular Site-Pair Data.

Fox S, Sikes BA, Brown SP, Cripps CL, Glassman SI, Hughes K, Semenova-Nelsen T, Jumpponen A. 2022. Fire as a driver of fungal diversity — A synthesis of current knowledge. *Mycologia* **114**(2): 1-27.

Gill NS, Turner. MG, Brown. CD, Glassman. SI, Haire. SL, Hansen. WD, Pansing. ER, Clair. SBS, Tomback. DF. 2022. Limitations to Propagule Dispersal Will Constrain Postfire Recovery of Plants and Fungi in Western Coniferous *Forests, BioScience,* **72**(4): 347–364.

Glassman SI, Lubetkin KC, Chung JA, Bruns TD. 2017. The theory of island biogeography applies to ectomycorrhizal fungi in subalpine tree "islands" at a fine scale. *Ecosphere* **8**(2): e01677.

Glassman SI, Randolph JWJ, Saroa SS, Capocchi JK, Walters KE, Pulido-Chavez MF, Larios L. 2023. Prescribed versus wildfire impacts on exotic plants and soil microbes in California grasslands. *Applied Soil Ecology* **185**: 104795.

Goberna M, Donat S, Perez-Valera E, Hallin S, Verdu M. 2021. nir gene-based co-occurrence patterns reveal assembly mechanisms of soil denitrifiers in response to fire. *Environ Microbiol* **23**(1): 239-251.

Greenwood L, Nimmo DG, Egidi E, Price JN, McIntosh R, Frew A. 2023. Fire shapes fungal guild diversity and composition through direct and indirect pathways. *Molecular Ecology* **32**(17): 4921-4939.

Grime JP. 1998. Benefits of plant diversity to ecosystems: immediate, filter and founder effects. *Journal of Ecology* **86**(6): 902-910.

Hallett LM, Jones SK, MacDonald AAM, Jones MB, Flynn DFB, Ripplinger J, Slaughter P, Gries C, Collins SL. 2016. codyn: An r package of community dynamics metrics. *Methods in Ecology and Evolution* **7**(10): 1146-1151.

Hanan EJ, D'Antonio CM, Roberts DA, Schimel JP. 2016. Factors Regulating Nitrogen Retention During the Early Stages of Recovery from Fire in Coastal Chaparral Ecosystems. *Ecosystems* **19**(5): 910-926.

Hanif MA, Guo Z, Moniruzzaman M, He D, Yu Q, Rao X, Liu S, Tan X, Shen W. 2019. Plant Taxonomic Diversity Better Explains Soil Fungal and Bacterial Diversity than Functional Diversity in Restored Forest Ecosystems. *Plants* **8**(11): 479.

Hart SC, DeLuca TH, Newman GS, MacKenzie MD, Boyle SI. 2005. Post-fire vegetative dynamics as drivers of microbial community structure and function in forest soils. *Forest Ecology and Management* **220**(1): 166-184.

Heinen R, Hannula SE, De Long JR, Huberty M, Jongen R, Kielak A, Steinauer K, Zhu F, Bezemer TM. 2020. Plant community composition steers grassland vegetation via soil legacy effects. *Ecology Letters* **23**(6): 973-982.

Hooper DU, Bignell DE, Brown VK, Brussard L, Mark Dangerfield J, Wall DH, Wardle DA, Coleman DC, Giller KE, Lavelle P, et al. 2000. Interactions between Aboveground and Belowground Biodiversity in Terrestrial Ecosystems: Patterns, Mechanisms, and Feedbacks. *BioScience* **50**(12): 1049.

Jaeger ACH, Hartmann M, Six J, Solly EF. 2023. Contrasting sensitivity of soil bacterial and fungal community composition to one year of water limitation in Scots pine mesocosms. *FEMS Microbiology Ecology* **99**(6): fiad051.

Jangid K, Whitman WB, Condron LM, Turner BL, Williams MA. 2013. Soil bacterial community succession during long-term ecosystem development. *Molecular Ecology* **22**(12): 3415-3424.

Jones HP, Jones PC, Barbier EB, Blackburn RC, Rey Benayas JM, Holl KD, McCrackin M, Meli P, Montoya D, Mateos DM. 2018. Restoration and repair of Earth's damaged ecosystems. *Proc Biol Sci* **285**(1873).

Jones HP, Jones PC, Barbier EB, Blackburn RC, Rey Benayas JM, Holl KD, McCrackin M, Meli P, Montoya D, Mateos DM. 2018. Restoration and repair of Earth's damaged ecosystems. *Proceedings of the Royal Society B: Biological Sciences* **285**(1873): 20172577.

Jurburg SD, Nunes I, Stegen JC, Le Roux X, Priemé A, Sørensen SJ, Salles JF. 2017. Autogenic succession and deterministic recovery following disturbance in soil bacterial communities. *Scientific Reports* **7**(1): 45691.

Keeley JE. 1981. Distribution of Lightning- and Man-Caused Wildfires in California. *Symposium on Dynamics and Management of Mediterranean Type Ecosystems*.

Kennedy PG, Higgins LM, Rogers RH, Weber MG. 2011. Colonization-competition tradeoffs as a mechanism driving successional dynamics in ectomycorrhizal fungal communities. *PLoS One* **6**(9): e25126.

Kipfer T, Moser B, Egli S, Wohlgemuth T, Ghazoul J. 2011. Ectomycorrhiza succession patterns in Pinus sylvestris forests after stand-replacing fire in the Central Alps. *Oecologia* **167**(1): 219-228.

Krappmann S, Braus GH. 2005. Nitrogen metabolism of Aspergillus and its role in pathogenicity. *Medical Mycology* **43**(s1): 31-40.

Lamont BB, Enright NJ, He T. 2011. Fitness and evolution of resprouters in relation to fire. *Plant Ecology* **212**(12): 1945-1957.

Lehman CL, Tilman D. 2000. Biodiversity, Stability, and Productivity in Competitive Communities. *The American Naturalist,* **156(5)**: 534–552.

Li W, Niu S, Liu X, Wang J. 2019. Short-term response of the soil bacterial community to differing wildfire severity in Pinus tabulaeformis stands. *Scientific Reports* **9**: 1148.

Li X, He H, Zhang X, Yan X, Six J, Cai Z, Barthel M, Zhang J, Necpalova M, Ma Q, Li Z. 2019. Distinct responses of soil fungal and bacterial nitrate immobilization to land conversion from forest to agriculture. *Soil Biology and Biochemistry* **134**: 81-89.

Liang Y, Pan F, He X, Chen X, Su Y. 2016. Effect of vegetation types on soil arbuscular mycorrhizal fungi and nitrogen-fixing bacterial communities in a karst region. *Environmental Science and Pollution Research* **23**(18): 18482-18491.

Liu CM, Kachur S, Dwan MG, Abraham AG, Aziz M, Hsueh P-R, Huang Y-T, Busch JD, Lamit LJ, Gehring CA, et al. 2012. FungiQuant: A broad-coverage fungal quantitative real-time PCR assay. *BMC Microbiology* **12**(1): 255.

Liu L, Zhu K, Wurzburger N, Zhang J. 2020. Relationships between plant diversity and soil microbial diversity vary across taxonomic groups and spatial scales. *Ecosphere* **11**(1): e02999.

Liu S, García-Palacios P, Tedersoo L, Guirado E, van der Heijden MGA, Wagg C, Chen D, Wang Q, Wang J, Singh BK, Delgado-Baquerizo M. 2022. Phylotype diversity within soil fungal functional groups drives ecosystem stability. *Nature Ecology & Evolution* **6**(7): 900-909.

Loreau M, de Mazancourt C. 2013. Biodiversity and ecosystem stability: a synthesis of underlying mechanisms. *Ecology Letters* **16**(s1): 106-115.

Marchand L, Castagneyrol B, Jiménez JJ, Rey Benayas JM, Benot M-L, Martínez-Ruiz C, Alday JG, Jaunatre R, Dutoit T, Buisson E, et al. 2021. Conceptual and methodological issues in estimating the success of ecological restoration. *Ecological Indicators* **123**.

Martin M. 2011. Cutadapt removes adapter sequences from high-throughput sequencing reads.

McLauchlan KK, Higuera PE, Miesel J, Rogers BM, Schweitzer J, Shuman JK, Tepley AJ, Varner JM, Veblen TT, Adalsteinsson SA, et al. 2020. Fire as a fundamental ecological process: Research advances and frontiers. *Journal of Ecology* **108**(5): 2047-2069.

Monciardini P, Cavaletti L, Schumann P, Rohde M, Donadio S. 2003. Conexibacter woesei gen. nov., sp. nov., a novel representative of a deep evolutionary line of descent within the class Actinobacteria. *Int J Syst Evol Microbiol* **53**(Pt 2): 569-576.

Montero-Calasanz MdC, Yaramis A, Rohde M, Schumann P, Klenk H-P, Meier-Kolthoff JP. 2022. Genotype–phenotype correlations within the Geodermatophilaceae. *Frontiers in Microbiology* **13**.

Moore EJ. 1962. The Ontogeny of the Sclerotia of Pyronema Domesticum. *Mycologia* **54**(3): 312-316.

Neary DG, Klopatek CC, DeBano LF, Ffolliott PF. 1999. Fire effects on belowground sustainability: A review and synthesis. *Forest Ecology and Management* **122**(1-2): 51-71.

Neary DG, Ryan KC, DeBano LF. 2005. Wildland fire in ecosystems: effects of fire on soils and water. Ft. Collins, CO: U.S. Department of Agriculture, Forest Service, Rocky Mountain Research Station.

Nelson AR, Narrowe AB, Rhoades CC, Fegel TS, Daly RA, Roth HK, Chu RK, Amundson KK, Young RB, Steindorff AS, et al. 2022. Wildfire-dependent changes in soil microbiome diversity and function. *Nature Microbiology* **7**(9): 1419-1430.

Nguyen. 2018. Longevity of light- and dark-colored basidiospores from saprotrophic mushroom-forming fungi. *Mycologia* **110**(1): 131-135.

Odum EP. 1969. The Strategy of Ecosystem Development. *Science* **164**(3877): 262-270.

Orwin KH, Wardle DA. 2004. New indices for quantifying the resistance and resilience of soil biota to exogenous disturbances. *Soil Biology and Biochemistry* **36**(11): 1907-1912.

Pausas JG, Keeley. JE. 2009. A Burning Story: The Role of Fire

in the History of Life. *BioScience* **59**(7): 593.

Pausas JG, Llovet J, Rodrigo A, Vallejo R. 2008. Are wildfires a disaster in the Mediterranean basin? - A review. *International Journal of Wildland Fire* **17**(6): 713.

Pérez-Valera E, Verdú M, Navarro-Cano JA, Goberna M. 2018. Resilience to fire of phylogenetic diversity across biological domains. *Molecular Ecology* **27**(13): 2896-2908.

Pérez-Valera E, Verdú M, Navarro-Cano JA, Goberna M. 2020. Soil microbiome drives the recovery of ecosystem functions after fire. *Soil Biology and Biochemistry* **149**: 107948.

Philippot L, Griffiths BS, Langenheder S. 2021. Microbial Community Resilience across Ecosystems and Multiple Disturbances. *Microbiology and Molecular Biology Reviews* **85**(2).

Phillips L. 2021. General Field Plot Sampling Protocol for DNA-based analyses (2018-2020). *protocols.io*.

Pickett STA. 1976. Succession: An Evolutionary Interpretation. *The American Naturalist* **110**(971): 107-119.

Pinto R, Ansola G, Calvo L, Sáenz De Miera LE. 2023. High resilience of soil bacterial communities to large wildfires with an important stochastic component. *Science of The Total Environment* **899**: 165719.

Platt WJC, J.H. 2003. Natural Disturbances and Directional Replacement of Species *Ecological Monographs*(73): 507-522.

Pressler Y, Moore JC, Cotrufo MF. 2019. Belowground community responses to fire: meta-analysis reveals contrasting responses of soil microorganisms and mesofauna. *Oikos* **128**(3): 309-327.

Pulido-Chavez MF, Alvarado EC, DeLuca TH, Edmonds RL, Glassman SI. 2021. High-severity wildfire reduces richness and alters composition of ectomycorrhizal fungi in low-severity adapted ponderosa pine forests. *Forest Ecology and Management* **485**: 118923.

Pulido-Chavez MF, Randolph JWJ, Zalman C, Larios L, Homyak PM, Glassman SI. 2023. Rapid bacterial and fungal successional dynamics in first year after chaparral wildfire. *Molecular Ecology*.

Pulido-Chavez MF, Nelson AR, Wilkins MJ, Glassman SI. 2023. Microbial-Mediated Pyrogenic Organic Matter and Nitrogen Cycling genes increase over time aftera Chaparral wildfire. *In Prep*.

Rundel PW 2018. California Chaparral and Its Global Significance. In: Underwood EC, Safford HD, Molinari NA, Keeley JE eds. *Valuing Chaparral*. Cham: Springer International Publishing, 1-27.

Seaver FJ. 1909. Studies in Pyrophilous Fungi: I. The Occurrence and Cultivation of Pyronema. *Mycologia*(1): 131-193.

Semchenko M, Barry KE, de Vries FT, Mommer L, Moora M, Maciá-Vicente JG. 2022. Deciphering the role of specialist and generalist plant–microbial interactions as drivers of plant–soil feedback. *New Phytologist* **234**(6): 1929-1944.

Semenova-Nelsen TA, Platt WJ, Patterson TR, Huffman J, Sikes BA. 2019. Frequent fire reorganizes fungal communities and slows decomposition across a heterogeneous pine savanna landscape. *New Phytologist* **224**(2): 916-927.

Shade A, Peter H, Allison S, Baho D, Berga M, Buergmann H, Huber D, Langenheder S, Lennon J, Martiny J, et al. 2012. Fundamentals of Microbial Community Resistance and Resilience. *Frontiers in Microbiology* **3**.

Shade A, Peter H, Allison SD, Baho DL, Berga M, Burgmann H, Huber DH, Langenheder S, Lennon JT, Martiny JB, et al. 2012. Fundamentals of microbial community resistance and resilience. *Front Microbiol* **3**: 417.

Slepecky RA, Hemphill HE 2006. The Genus Bacillus—Nonmedical. In: Dworkin M, Falkow S, Rosenberg E, Schleifer K-H, Stackebrandt E eds. *The Prokaryotes: Volume 4: Bacteria: Firmicutes, Cyanobacteria*. New York, NY: Springer US, 530-562.

Smith MD, Knapp AK. 2003. Dominant species maintain ecosystem function with non-random species loss. *Ecology Letters* **6**(6): 509-517.

Solek CW, Resh VH 2018. Water Provision in Chaparral Landscapes: Water Quality and Water Quantity. In: Underwood EC, Safford HD, Molinari NA, Keeley JE eds. *Valuing Chaparral: Ecological, Socio-Economic, and Management Perspectives*. Cham: Springer International Publishing, 207-244.

Steel ZL, Foster D, Coppoletta M, Lydersen JM, Stephens SL, Paudel A, Markwith SH, Merriam K, Collins BM. 2021. Ecological resilience and vegetation transition in the face of two successive large wildfires. *Journal of Ecology* **109**(9): 3340-3355.

Steindorff AS, Seong K, Carver A, Calhoun S, Fischer MS, Stillman K, Liu H, Drula E, Henrissat B, Simpson HJ, et al. Diversity of genomic adaptations to the post-fire environment in Pezizales fungi points to crosstalk between charcoal tolerance and sexual development. *New Phytologist* **n/a**(n/a).

Suzuki A. 2009. Propagation strategy of ammonia fungi. *Mycoscience* **50**(1): 39-51.

Tatti E, McKew BA, Whitby C, Smith CJ. 2016. Simultaneous DNA-RNA Extraction from Coastal Sediments and Quantification of 16S rRNA Genes and Transcripts by Real-time PCR. *Journal of Visualized Experiments : JoVE*(112): 54067.

Taylor DL, Walters WA, Lennon NJ, Bochicchio J, Krohn A, Caporaso JG, Pennanen T. 2016. Accurate Estimation of Fungal Diversity and Abundance through Improved Lineage-Specific Primers Optimized for Illumina Amplicon Sequencing. *Applied and Environmental Microbiology* **82**(24): 7217-7226.

Teste FP, Kardol P, Turner BL, Wardle DA, Zemunik G, Renton M, Laliberté E. 2017. Plant-soil feedback and the maintenance of diversity in Mediterranean-climate shrublands. *Science* **355**(6321): 173-176.

Tilman D. 1999. The Ecological Consequences of Changes in Biodiversity: A Search for General Principles101. *Ecology* **80**(5): 1455-1474.

Tilman D, Reich PB, Knops JMH. 2006. Biodiversity and ecosystem stability in a decade-long grassland experiment. *Nature* **441**(7093): 629-632.

Van der Heijden MGA, Bardgett RD, van Straalen NM. 2008. The unseen majority: soil microbes as drivers of plant diversity and productivity and terrestrial ecosystems. **11**: 296-310.

Walker B, Holling CS, Carpenter S, Kinzig A. 2004. Resilience, Adaptability and Transformability in Social–ecological Systems. *Ecology and Society* **9**(2).

Wayne Polley H, Wilsey BJ, Derner JD. 2007. Dominant species constrain effects of species diversity on temporal variability in biomass production of tallgrass prairie. *Oikos* **116**(12): 2044-2052.

Whitman T, Whitman E, Woolet J, Flannigan MD, Thompson DK, Parisien M-A. 2019. Soil bacterial and fungal response to wildfires in the Canadian boreal forest across a burn severity gradient. *Soil Biology and Biochemistry* **138**: 107571.

Whitman T, Woolet J, Sikora M, Johnson DB, Whitman E. 2022. Resilience in soil bacterial communities of the boreal forest from one to five years after wildfire across a severity gradient. *Soil Biology and Biochemistry* **172**.

Wickham H. 2016. *ggplot2: Elegant Graphics for Data Analysis*: Springer-Verlag New York.

Woolet J, Whitman T. 2020. Pyrogenic organic matter effects on soil bacterial community composition. *Soil Biology and Biochemistry* **141**: 107678.

Xiang X, Shi Y, Yang J, Kong J, Lin X, Zhang H, Zeng J, Chu H. 2014. Rapid recovery of soil bacterial communities after wildfire in a Chinese boreal forest. *Scientific Reports* **4**(1): 3829.

Yang S, Zheng Q, Yang Y, Yuan M, Ma X, Chiariello NR, Docherty KM, Field CB, Gutknecht JLM, Hungate BA, et al. 2020. Fire affects the taxonomic and functional composition of soil microbial communities, with cascading effects on grassland ecosystem functioning. *Global Change Biology* **26**(2): 431-442.

Yang W, Yang J, Fan Y, Guo Q, Jiang N, Babalola OO, Han X, Zhang X. 2023. The two sides of resistance–resilience relationship in both aboveground and belowground communities in the Eurasian steppe. *New Phytologist* **239**(1): 350-363.

Yilmaz P, Parfrey LW, Yarza P, Gerken J, Pruesse E, Quast C, Schweer T, Peplies J, Ludwig W, Glöckner FO. 2014. The SILVA and "All-species Living Tree Project (LTP)" taxonomic frameworks. *Nucleic Acids Research* **42**(D1): D643-D648.

Yousuf J, Thajudeen J, Rahiman M, Krishnankutty S, P. Alikunj A, A. Abdulla MH. 2017. Nitrogen fixing potential of various heterotrophic Bacillus strains from a tropical estuary and adjacent coastal regions. *Journal of Basic Microbiology* **57**(11): 922-932.

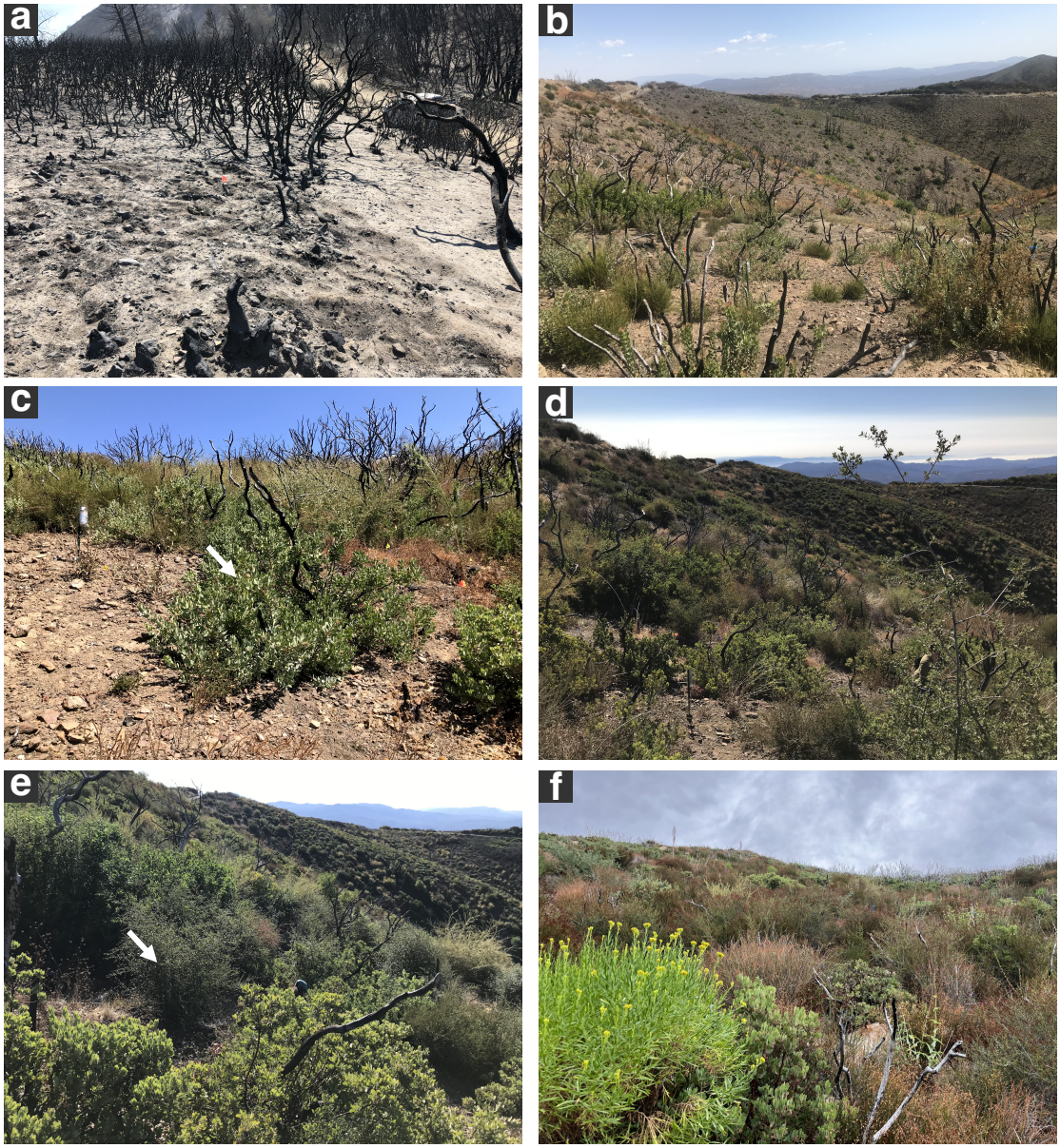

Figure 4.1. Chronosequence photos illustrating the recovery of the Holy Fire in Southern California. Samples were first collected (a) 17 days post-fire (September 2018), with continuous sampling over 5 years. Photos show the burn area at (b) 376 days (1 year, September 2019); (c) two years (September 2020); (d) 3 years (September 2021); (e) 4 years (September 2022); and (f) 5 years post-fire (September 2023). Dominant vegetation in our system, indicated by arrows, includes c) Manzanita (*Arctostaphylos glandulosa*) with some cover of e) chamise (*Adenostoma fasciculatum*).

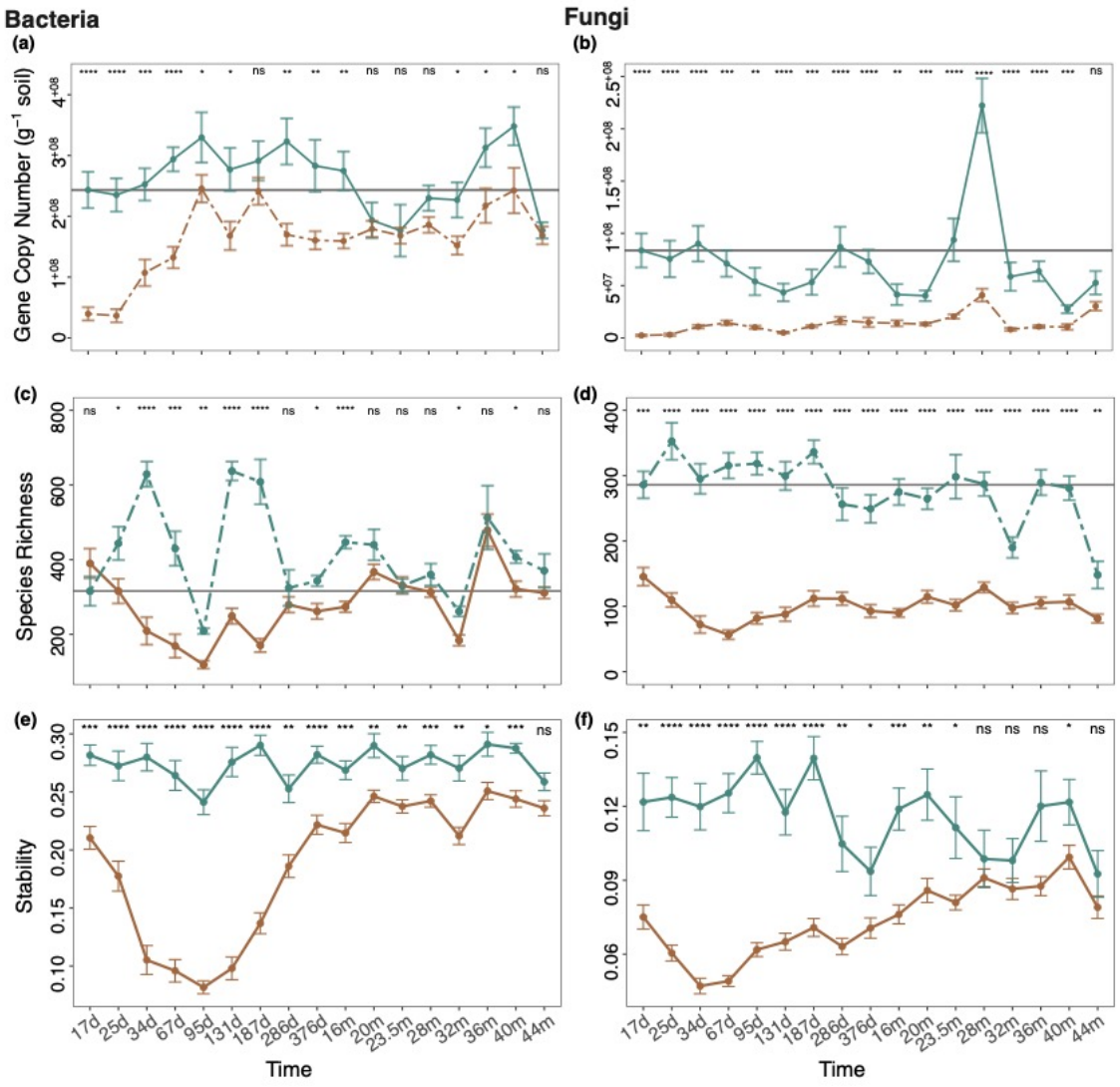

Figure 4.2. Changes in bacterial (a) and fungal (b) biomass, and bacterial (c) and fungal species richness (d) between burned (brown) and unburned (blue-green) plots over time. Time is indicated in days (d) and months (m), spanning from 17 days to 44 months post-fire. The gray horizontal line represents the recovery point (based on biomass and richness at T1 (17 days post-fire). Plots e and f represent the change in community stability over time for both burned and unburned bacterial and fungal communities. The effects of species richness on community stability over time can be found in supplementary figure S4. Significant differences between burned and unburned plots at each timepoint are denoted by asterisks (*** = $p < 0.001$; ** = $p < 0.01$; * = $p < 0.05$) and were determined using a negative binomial regression.

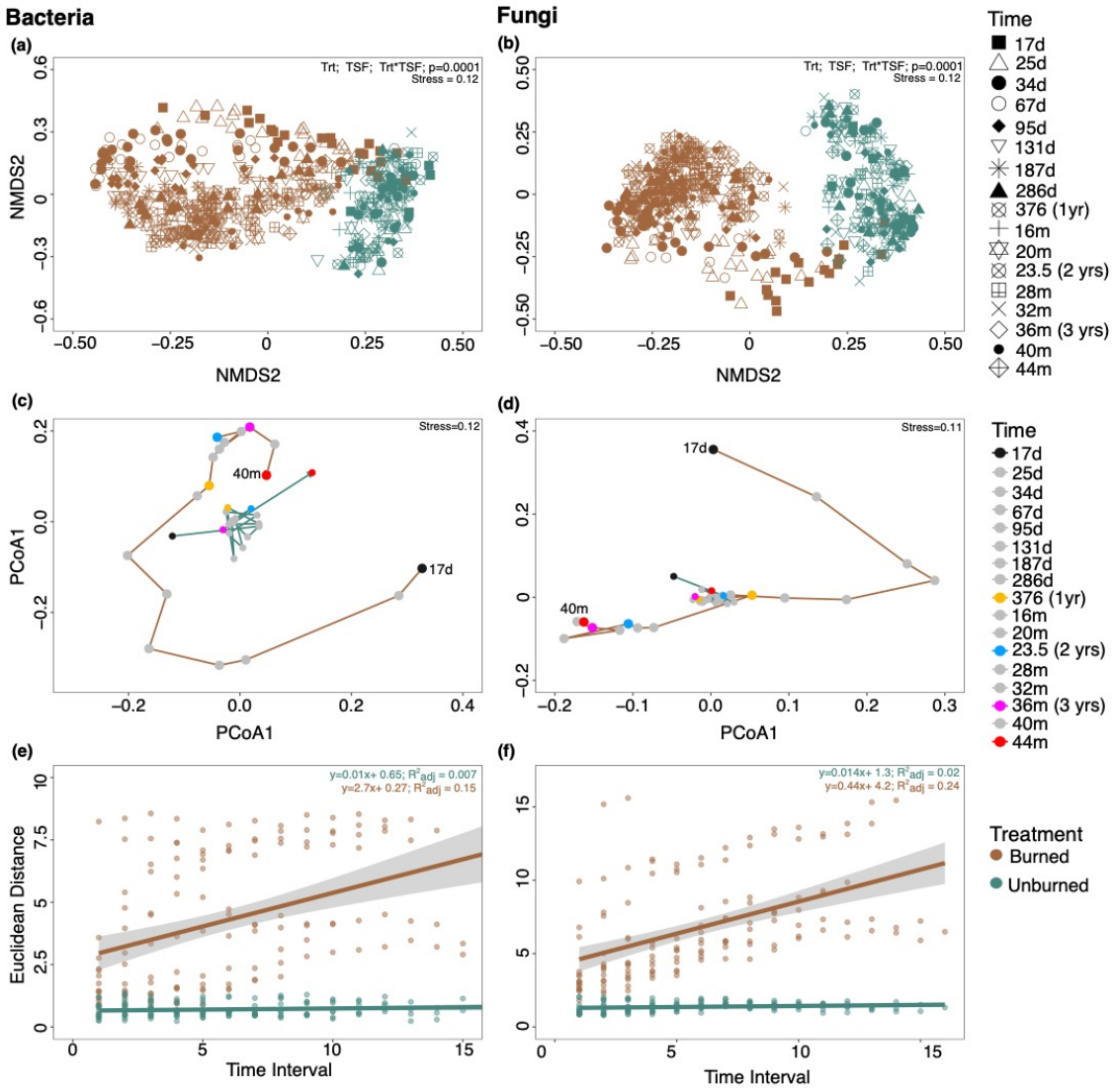

Figure 4.3. Wildfire effects on community composition and successional trajectories. Nonmetric multidimensional scaling (NMDS) plots based on Bray-Curtis dissimilarity and three-dimensions for (a) bacterial and (b) fungal community composition with colors denoting treatment and shape indicating time since fire (d = days and m= months). Trajectory analysis of the Principle Coordinates Analysis (PCoA) centroids of bacterial (c) and fungal communities (d) and confirmation of trajectory analysis based on linear regression of the time lag and Euclidean distance for (e) bacterial and (f) fungal communities. Closer look into the unburned successional dynamics in figure c, d) can be found in supplementary figure S7.

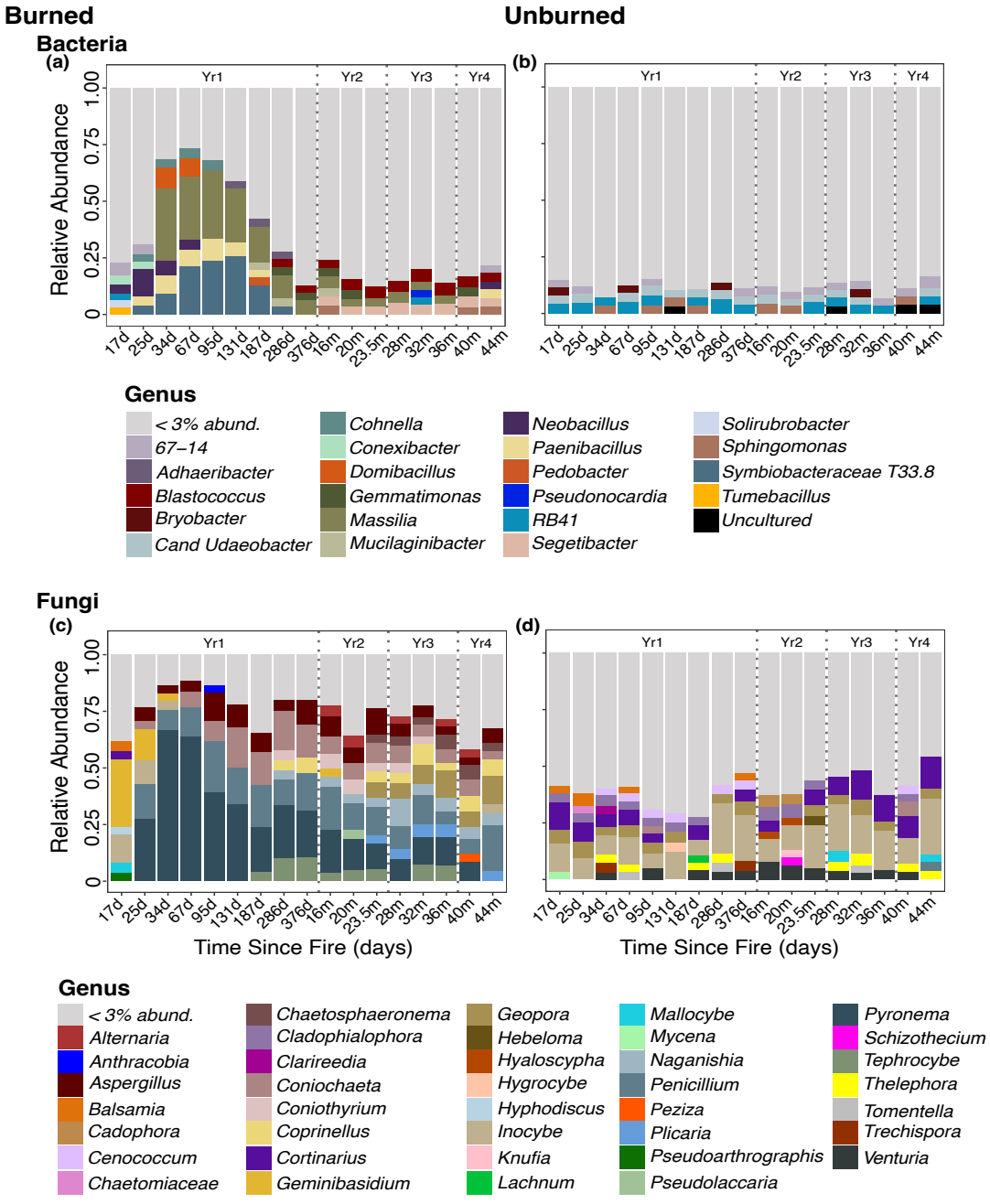

Figure 4.4. Relative sequence abundance of (a) bacterial and (b) fungal genera in burned plots (top panel) and unburned plots (bottom panels) for all seventeen timepoints (44 months). Grey bars represent multiple genera of bacteria (a, c) and fungi (b, d) that have relative sequence abundance under 3% at each timepoint constituting #% of the bacterial and #% of the fungal sequences. Time is indicated in days (d) and months (m), spanning from 17 days to 4.5 years post-fire.

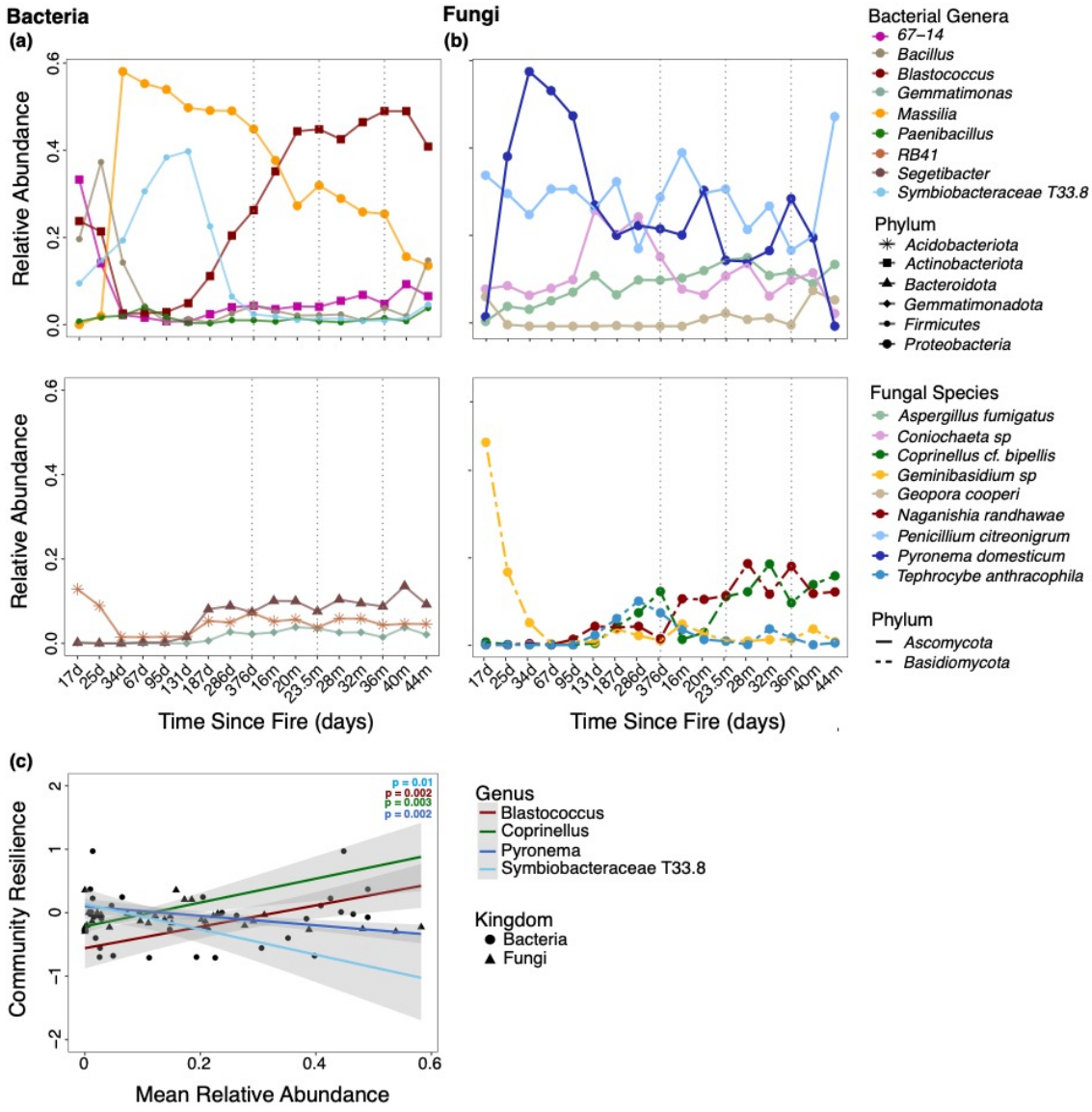

Figure 4.5. Change in relative sequence abundance of the nine most abundant (a) bacterial and (b) fungal genera in the burned plots over time. Time is indicated in days (d) and months (m), spanning from 17 days to 4.5 years post-fire. Plot (c) represents the mean relative abundance of the bacterial and fungal genera that were significant drivers of community stability.

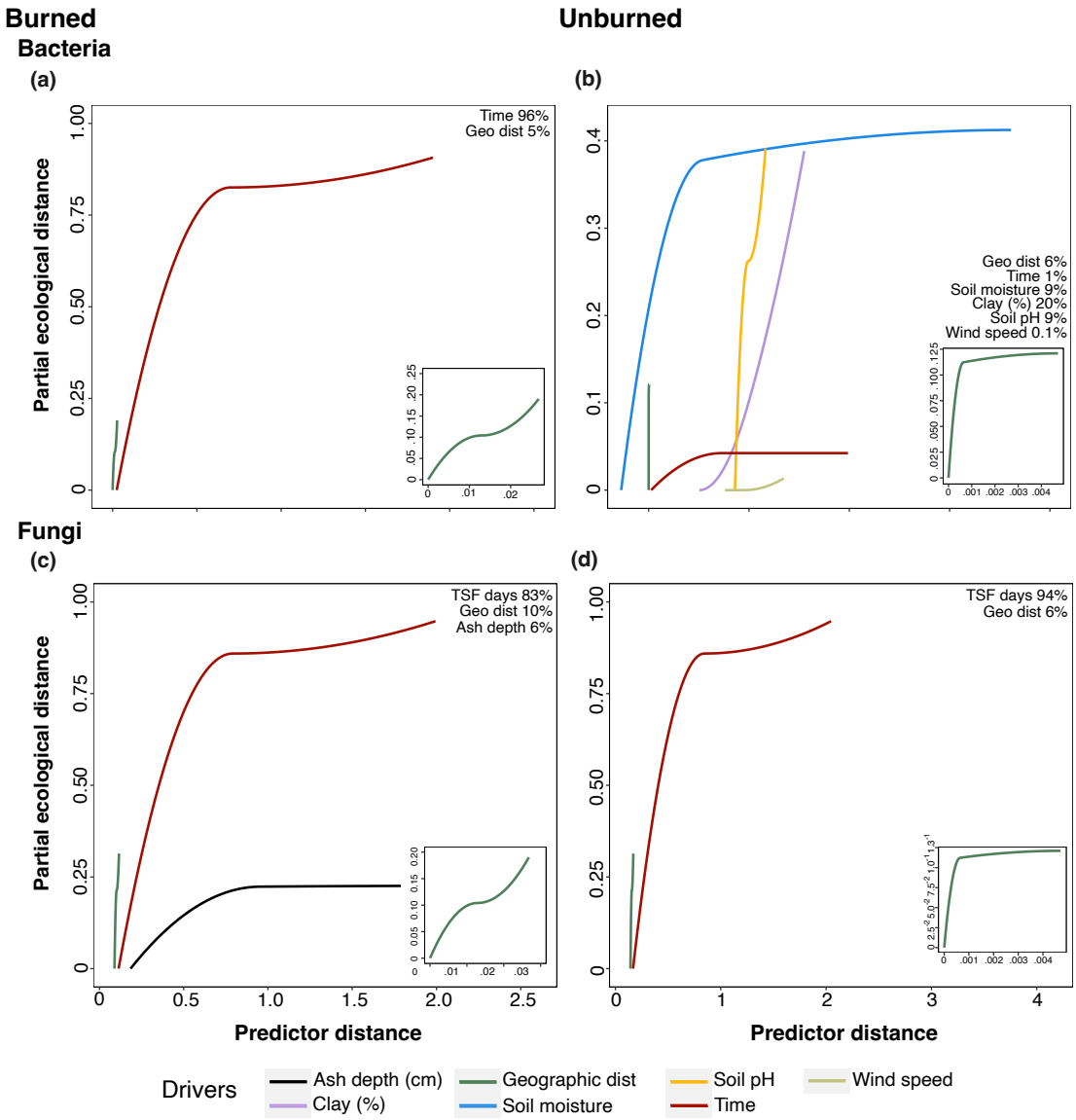

Figure 4.6. Generalized Dissimilarity Models (GDM) of the relationship between a) bacterial and b) fungal observed compositional dissimilarity and predicted community dissimilarity between site pairs. Partial regression fits, for 3 GDM-fitted I-splined for variables significantly associated with c) bacterial and d) fungal beta diversity. Significance based on backward model selection in GDM package, with scaled variables and significance is based on $p<0.05$. Line heights represent the relative contribution of each variable to community composition whereas shape represents how the rate of community turnover varies with the predictor variable between sites. Mod 2 graphs including the vegetation and Nitrogen can be found in supplementary S8.

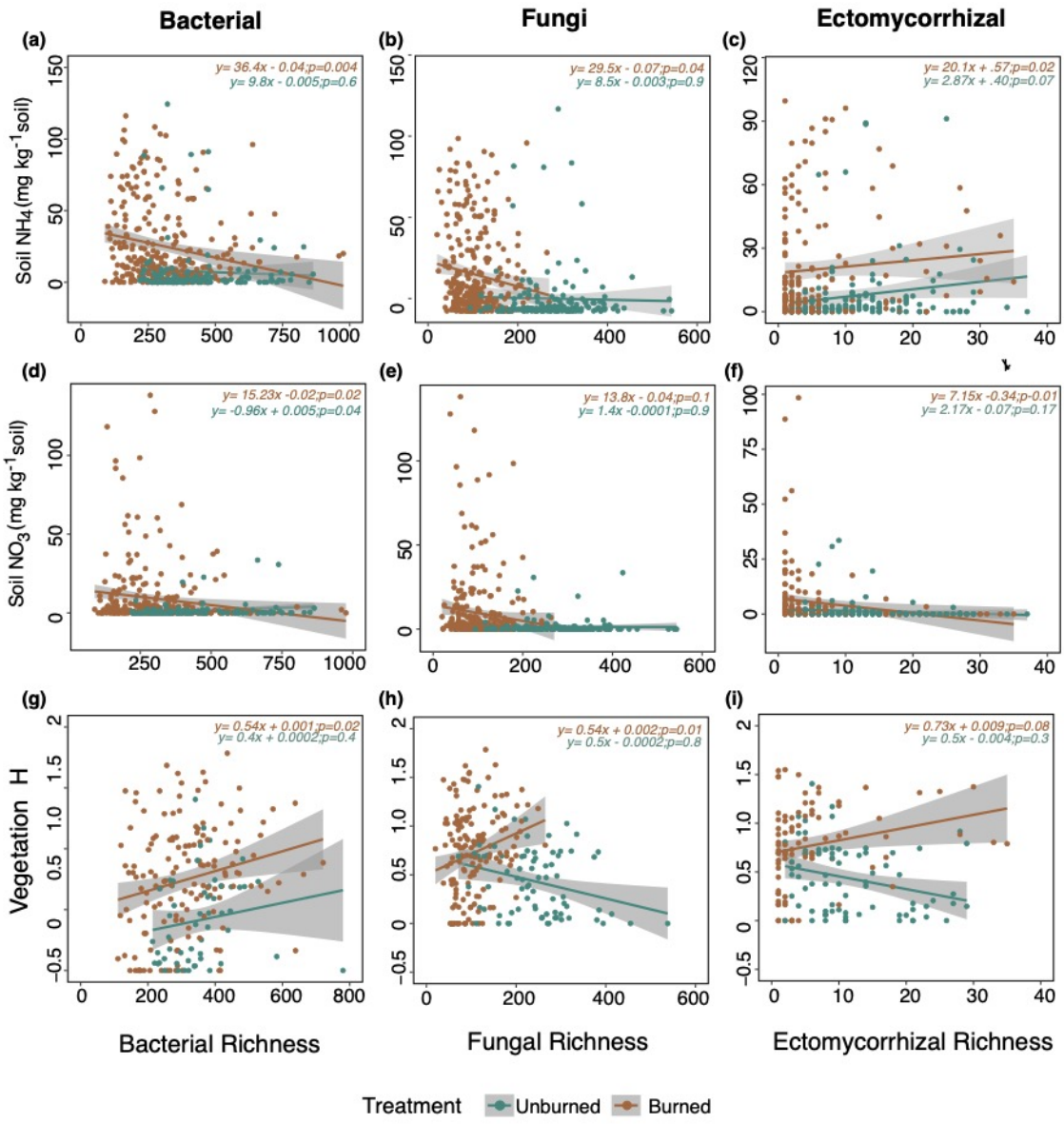

Figure 4.7. Relationship between bacterial, fungal, and ectomycorrhizal species richness and Ammonium (NH4), Nitrate (NO3) and vegetation Shannon diversity (H) in burned (brown) and unburned communities (blue-green). Gray area around the regression line represents the standard error.

Chapter V

General Conclusions

My dissertation research aimed to answer key questions in microbial ecology related to wildfires. It aimed to address critical aspects, such as understanding the direct effects of wildfire and fine-scale succession, determining the links between microbial functions and ecosystem resilience, and identifying the biotic and abiotic drivers of microbial resilience to chaparral wildfires. To do so, I conducted the highest resolution temporal sampling of soil microbial communities post-fire to date, with 17 time points ranging from 17 days to 4.5 years post-fire. My research provides insight into post-fire microbial turnover rates, successional dynamics, microbial functions, and provides important background information for restoration management.

In the first chapter, we identified secondary successional dynamics in bacterial and fungal communities, noting rapid turnover in the burned area. Our observations revealed that these dynamics were driven by dominant bacteria (*Massilia, Paenibacillus,*

and *Noviherbaspirillium*) and fungi (*Geminibasidium, Pyronema, Aspergillus,* and *Penicillium*) that traded-off in abundance over time. We also classified these microbes into putative traits via a literature search and related them to the microbial adaptations of Grime's C-S-R Competition (C), Stress-tolerant (S), and Ruderal (R) (Grime, 1977) such that pyrophilous microbes are either competitive at acquiring post-fire resources, thermotolerant, or fast colonizing (Enright *et al.*, 2022). This classification enabled us to hypothesize that, akin to plants, microbial succession is driven by trade-offs in functional traits. These traits fell in a specific sequence during succession, with thermotolerators dominating first, followed by fast colonizers, and ultimately, competitors capable of capitalizing on post-fire resource acquisition.

In chapter two, we conducted a gene-centric metagenomic analysis of five turnover events observed in the first year to monitor changes in nitrogen (N) cycling and aromatic hydrocarbon degradation genes. Fires transform carbon (C) into pyrogenic organic matter (PyOM), which is difficult to degrade and may lead to C sequestration. This analysis provided valuable insights into the functional changes occurring in pyrophilous microbes over successive stages, crucial for understanding whether the ecosystem will recover or transition to another state. As hypothesized, N and PyOM gene counts increased during succession, reflecting the growing dominance of pyrophilous taxa and the introduction of other species into the system. Moreover, we discovered that dominant pyrophilous bacteria *Massilia* and *Noviherbaspirillium* preferentially select the easier-to-degrade ortho-cleavage catechol and protocatechuate pathways while assimilating N to readily acquire energy, retaining N in the system and minimizing

greenhouse gas emissions. However, the abundant taxa for the different degradation N and PyOM degradation pathways allowed us to hypothesize that pyrophilous microbes readily interact via metabolic handoffs to break down post-fire resources. The observed metabolic strategies, including the efficient utilization of PyOM and N, emphasize the resilience and adaptability of these microbes while providing information on the potential recovery of burned chaparral.

In chapter three, we tested which factors affect bacterial and fungal resilience, or the ability of an ecosystem to recover both functionally and structurally (Allison & Martiny, 2008), stability, and successional dynamics over 4.5 years post-fire. Moreover, we linked microbial resilience to vegetation recovery and several key aspects of soil biogeochemistry. This comprehensive analysis enabled us to present a fine-scale temporal study of the mechanisms driving microbial resilience after a chaparral wildfire, helping lay the foundation for developing comprehensive restoration and management plans. Neither bacterial nor fungal composition recovered to unburned levels during the timespan of the study. However, bacterial richness exhibited higher resistance and resilience than fungi, fully recovering to pre-fire levels within 4.5 years while fungal richness declined in both the burned and unburned plots. The resilience of both groups was intricately connected to vegetation and soil nutrients, underscoring the crucial role of resources in bacterial recovery and fungal maintenance. Moreover, bacterial community stability emerged through increased richness and reduced dominance over time, while the persistent dominance of early pyrophilous fungi *Pyronema, Aspergillus*, and *Penicillium* characterized fungal stability, highlighting the unique trajectories of bacterial and fungal

communities. This distinction underscores the diverse trajectories of bacterial and fungal communities, indicating that niche complementarity enhances bacterial resilience and stability in response to environmental changes. In contrast, fungal stability relies on well-established potential keystone taxa, which is crucial for maintaining ecosystem functions in post-fire systems.

While our study revealed valuable insights into the successional dynamics of post-fire bacteria and fungi, categorizing them within existing theoretical frameworks, further research is essential to fully develop microbial successional dynamics theories. This necessitates expanding our sampling efforts across multiple chaparral ecosystems and other burned environments to validate the identified patterns. Additionally, our metagenomic analysis were limited by our inability to assembled fungal metagenomically assembled genomes (MAGs). The presence of key fungal decomposers (*Coprinus* and *Tephrocybe*) in later successional periods coinciding with increased PyOM and N cycling genes raises questions about the functional dynamics of this community and its effects on fungal resilience. The intriguing possibility of cross-feeding dynamics in the bacterial community, suggested by the diverse array of N and PyOM genes in my metagenomic analysis, underscores the need for comprehensive characterization of the fungal community using metagenomics, encompassing both bacterial and fungal MAGs. This analysis is crucial for determining whether pyrophilous microbes possess the complete enzymatic machinery to degrade PyOM or N independently, or if these genes are distributed across the community, necessitating metabolic handoffs. Investigating these aspects further will elucidate the intricate post-fire microbial interactions. Continued

research in these areas will significantly enhance our understanding of microbial succession and the factors influencing microbial resilience following wildfires. Additionally, this knowledge will inform the development of post-fire management strategies that integrate microbial communities, shaping more effective and ecologically sound approaches to functionally and structurally restore wildfire affected ecosystem.

5.1 References

Allison SD, Martiny JBH. 2008. Resistance, resilience, and redundancy in microbial communities. *Proceedings of the National Academy of Sciences* **105**(Supplement 1): 11512-11519.

Enright DJ, Frangioso KM, Isobe K, Rizzo DM, Glassman SI. 2022. Mega-fire in Redwood Tanoak Forest Reduces Bacterial and Fungal Richness and Selects for Pyrophilous Taxa that are Phylogenetically Conserved. *Molecular Ecology*.

Grime PJ. 1977. Evidence for the Existence of Three Primary Strategies in Plants and Its Relevance to Ecological and Evolutionary Theory. *The American Naturalist* **111**(982): 1169-1194.

Appendix A: Supplemental Information for Chapter II

Rapid Bacterial and Fungal Successional Dynamics in First Year After Chaparral wildfire

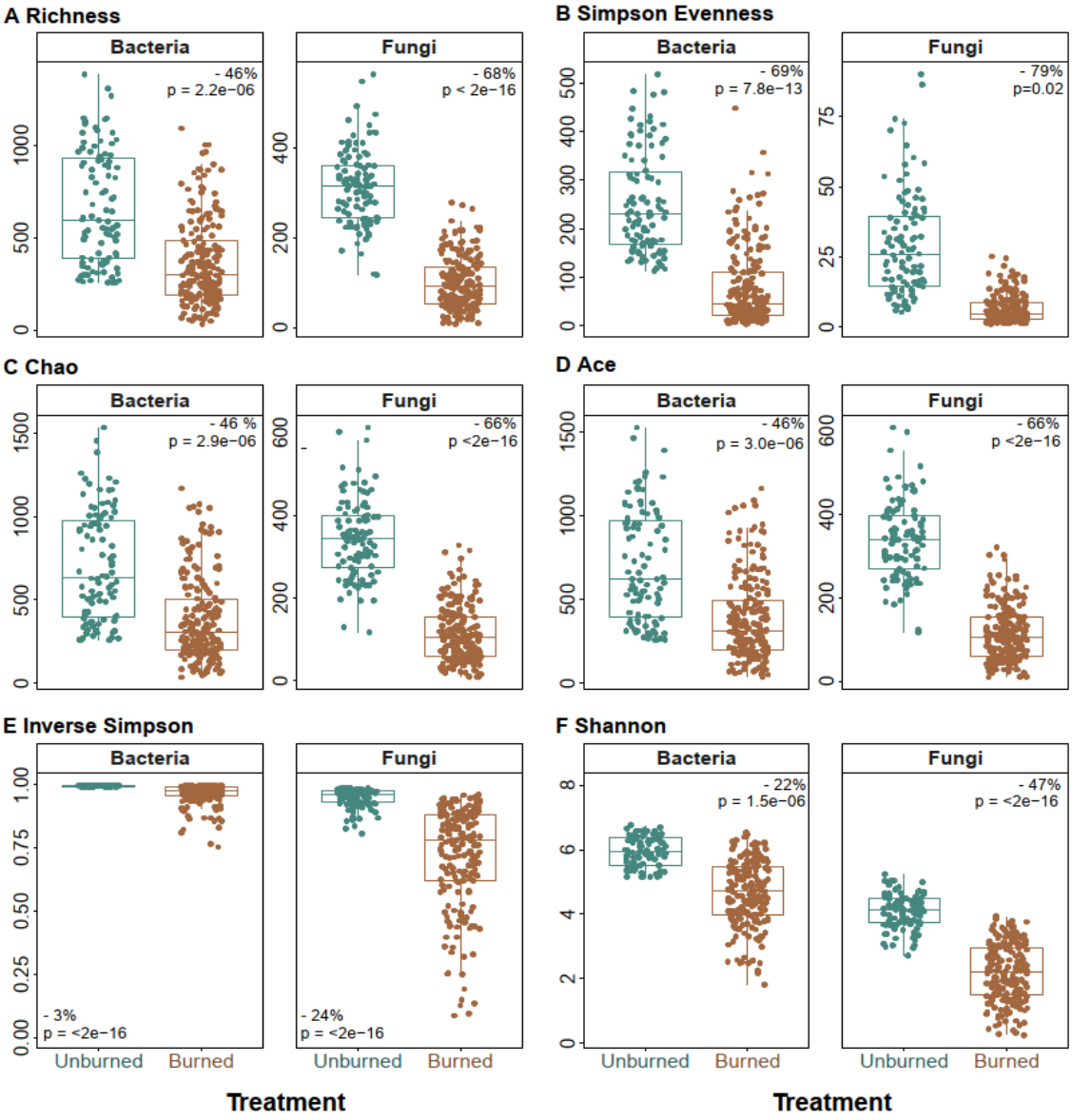

Figure A.1.1. Comparison of alpha diversity metrics for bacteria and fungi between burned (brown) and unburned (blue-green) plots for A) observed species richness (ASVs), B) Simpson, C) Chao1, D) ACE, E) Inverse Simpson (dominance), and E) Shannon. Significance based on negative binomial regression with plots and time since fire as random effects for all alpha metrics except for bacteria inverse Simpson which was based on a generalized mixed effect model. Percent value represents the percent change in alpha diversity from the unburned to burned communities, where the negative value represents a decrease in alpha diversity.

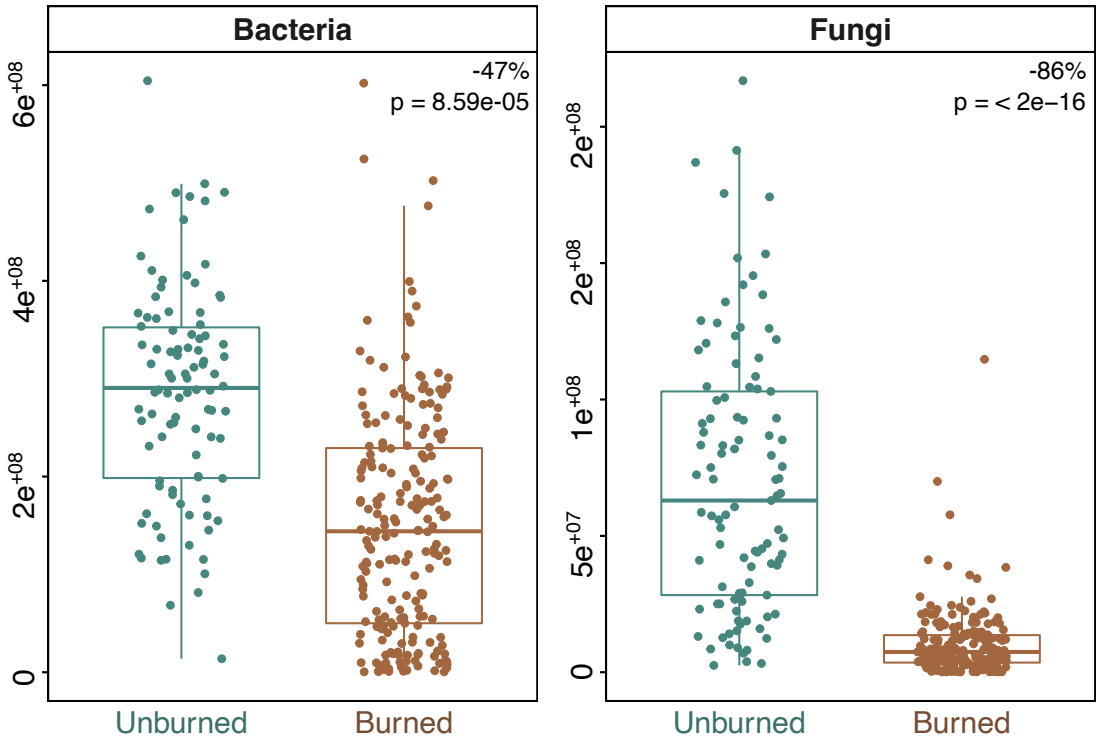

Figure A.1.2. Change in average A) bacterial and B) fungal estimated biomass (per gram of soil) between the burned (brown) and unburned (blue-green) communities across all time points. Boxes represent the 25th and 75th quartiles, and the horizontal line is the median of the data—significance based on negative binomial regressions with plot and time since fire as random effects. Percent value represents the percent change in biomass from the unburned to burned communities, where the negative value represents a decrease in biomass.

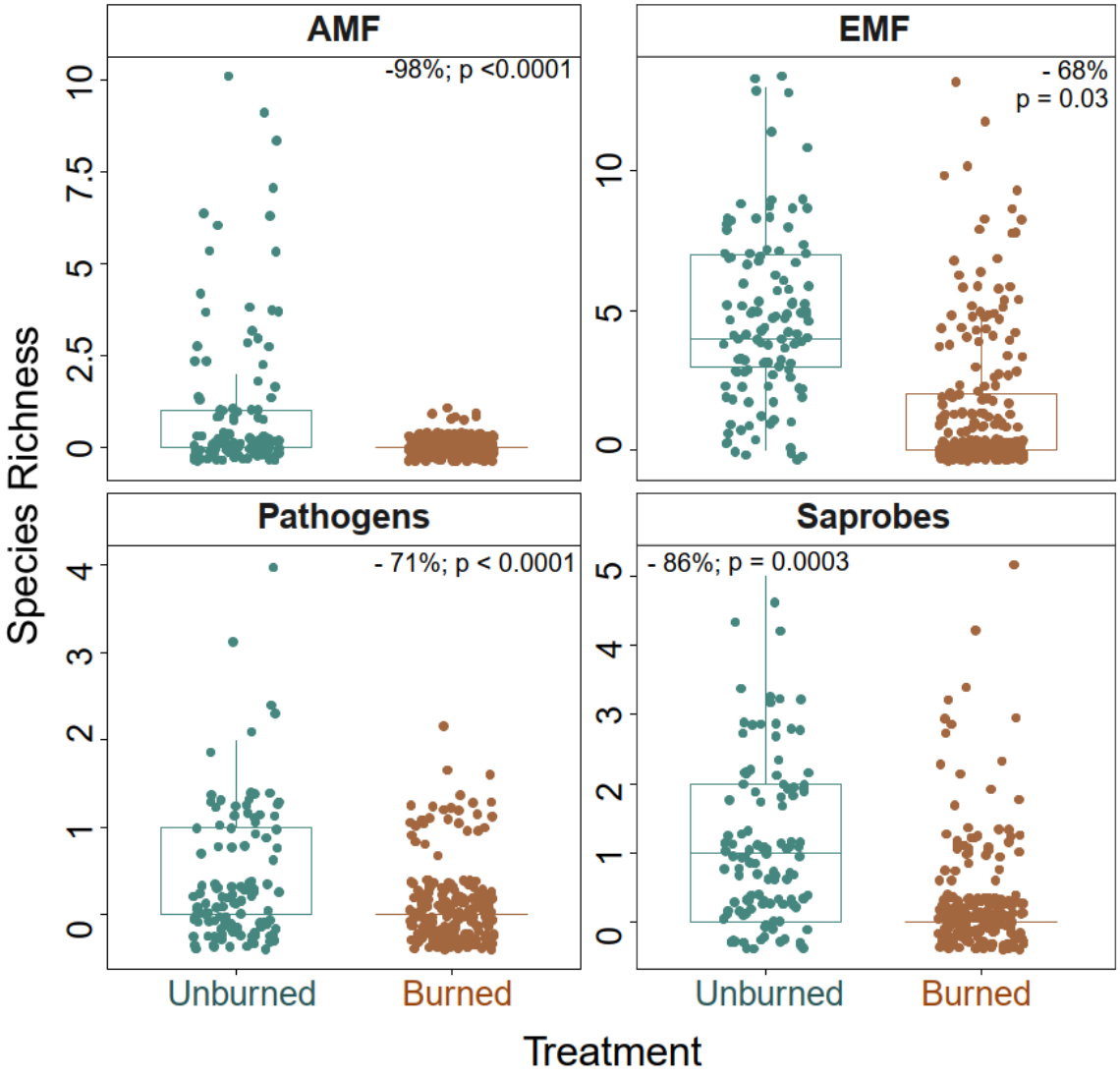

Figure A.1.3. Change in average richness for A) arbuscular mycorrhizal fungi (AMF), B) ectomycorhizal fungi (EMF), C) pathogenic, and D) saprobic fungi between burned (brown) and unburned (blue-green) plots across all time points. Boxes represent the 25th and 75th quartiles, and the horizontal line is the median of the data. Significance based on negative binomial regressions with plot, subplot, and time since fire as random effects. Percent value represents the percent change in species richness from the unburned to burned communities, where the negative value represents a decrease in richness.

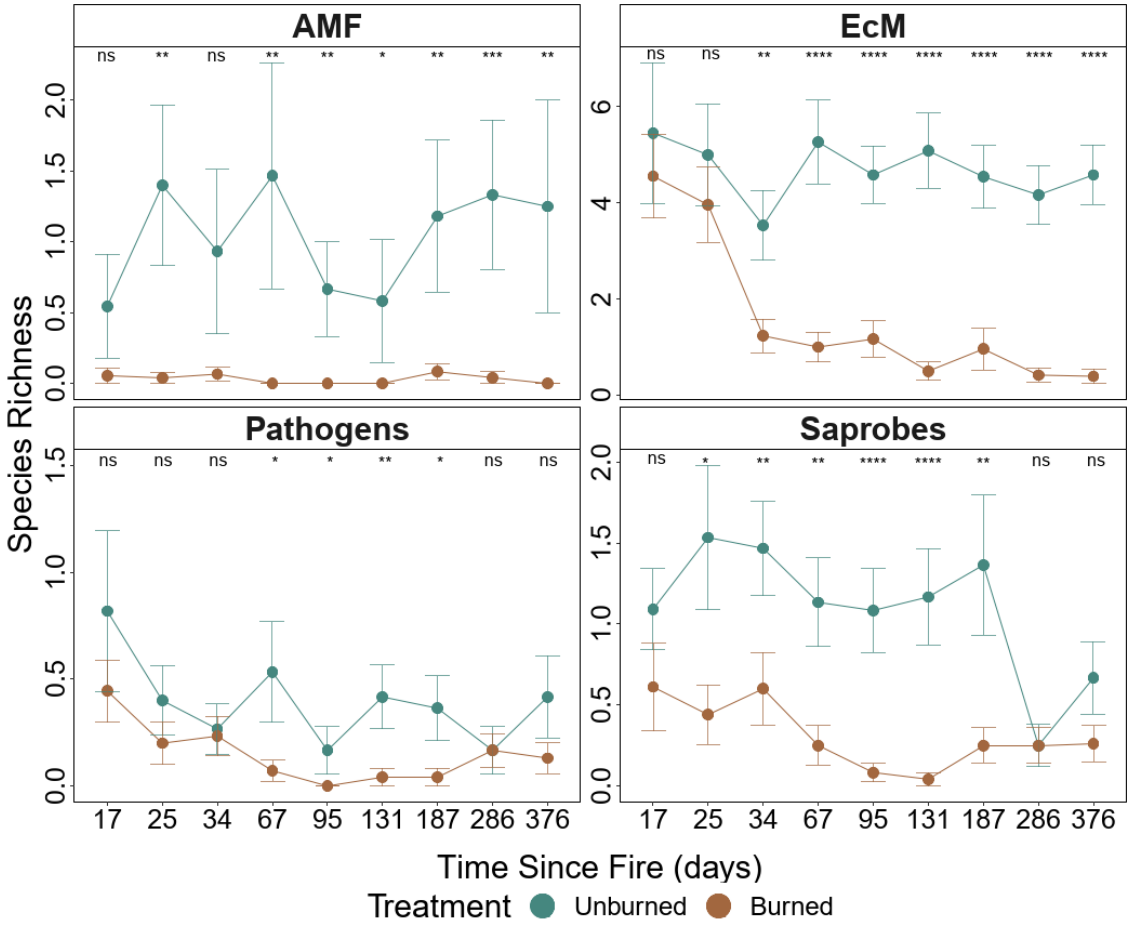

Figure A.1.4. Change of species richness in burned (brown) versus unburned (blue-green) plots at each of the 9-time points for all four fungal guilds (arbuscular mycorrhizal fungi (AMF); ectomycorrhizal fungi (EMF), pathogens, and saprobes). Points represent the mean, and bars represent the standard error of the mean.

.

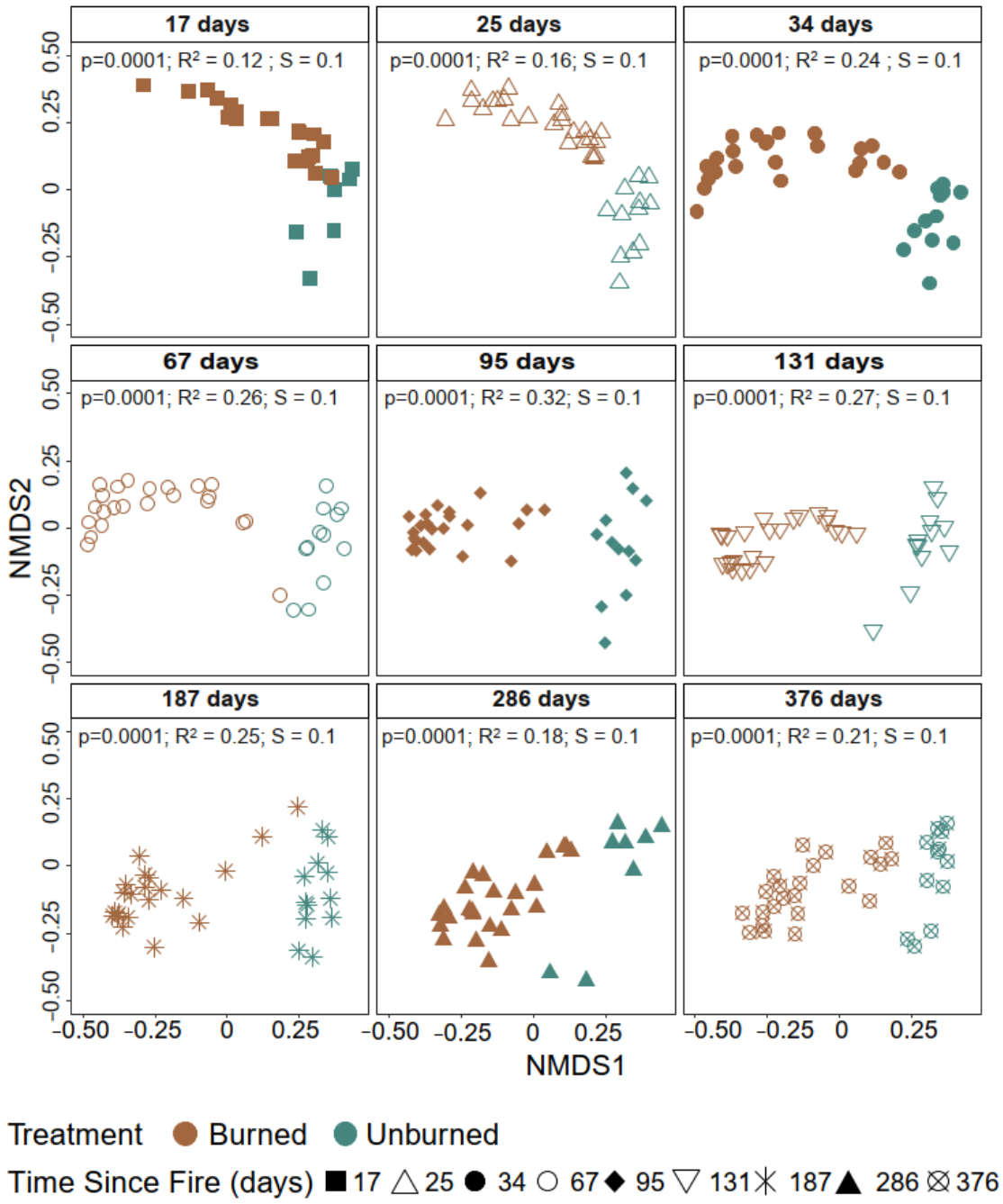

Figure A.1.5. NMDS plots for bacterial community composition in burned (brown) versus unburned (blue-green) plots at each of the 9-time points with R^2, significance, and stress (S) based on ADONIS. NMDS is based on the Bray-Curtis dissimilarity matrix on 3-dimensions

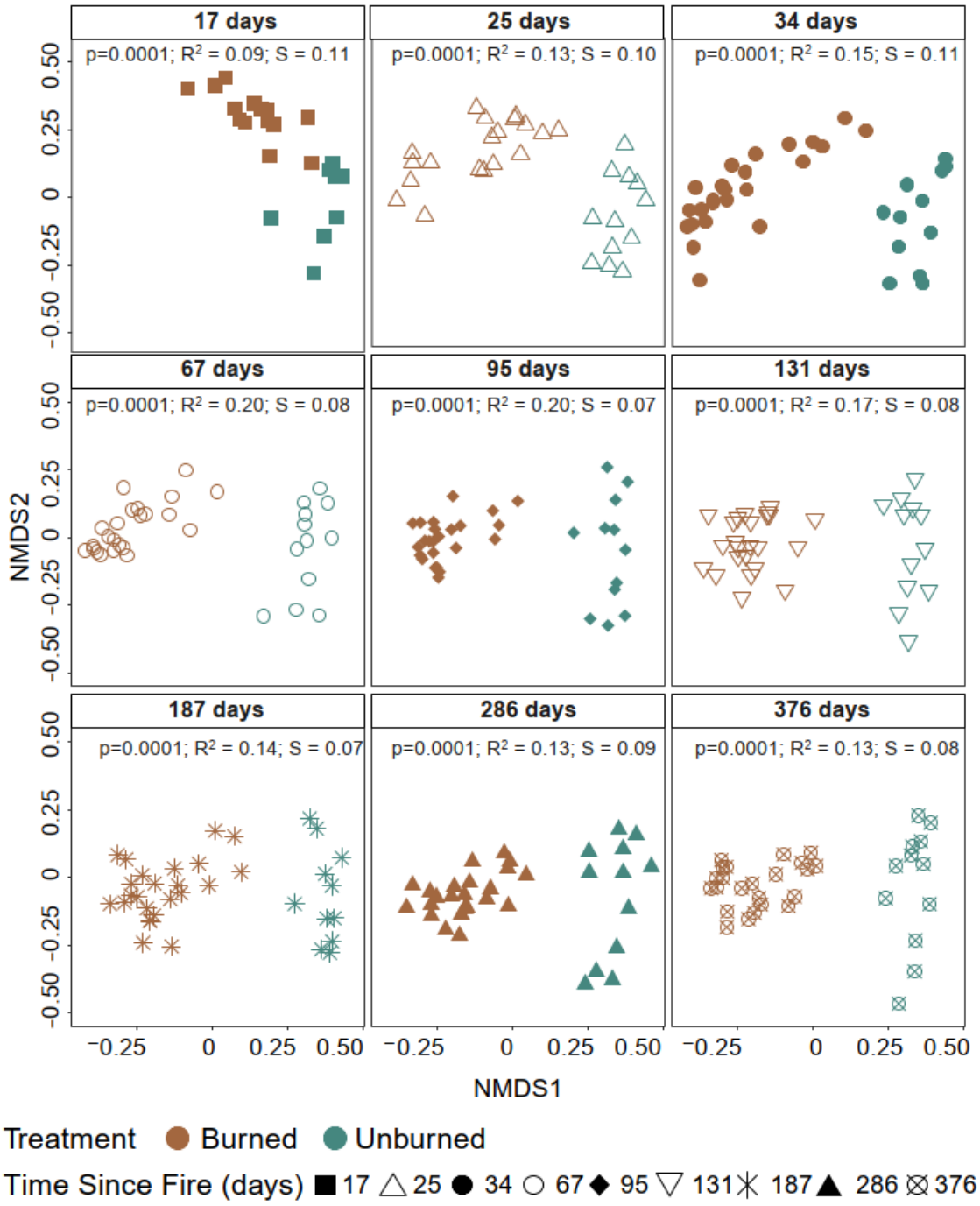

Figure A.1.6. NMDS plots for fungal community composition in burned (brown) versus unburned (blue-green) plots at each of the 9-time points with R^2, significance, and stress (S) based on ADONIS. NMDS is based on the Bray-Curtis dissimilarity matrix on 3-dimensions.

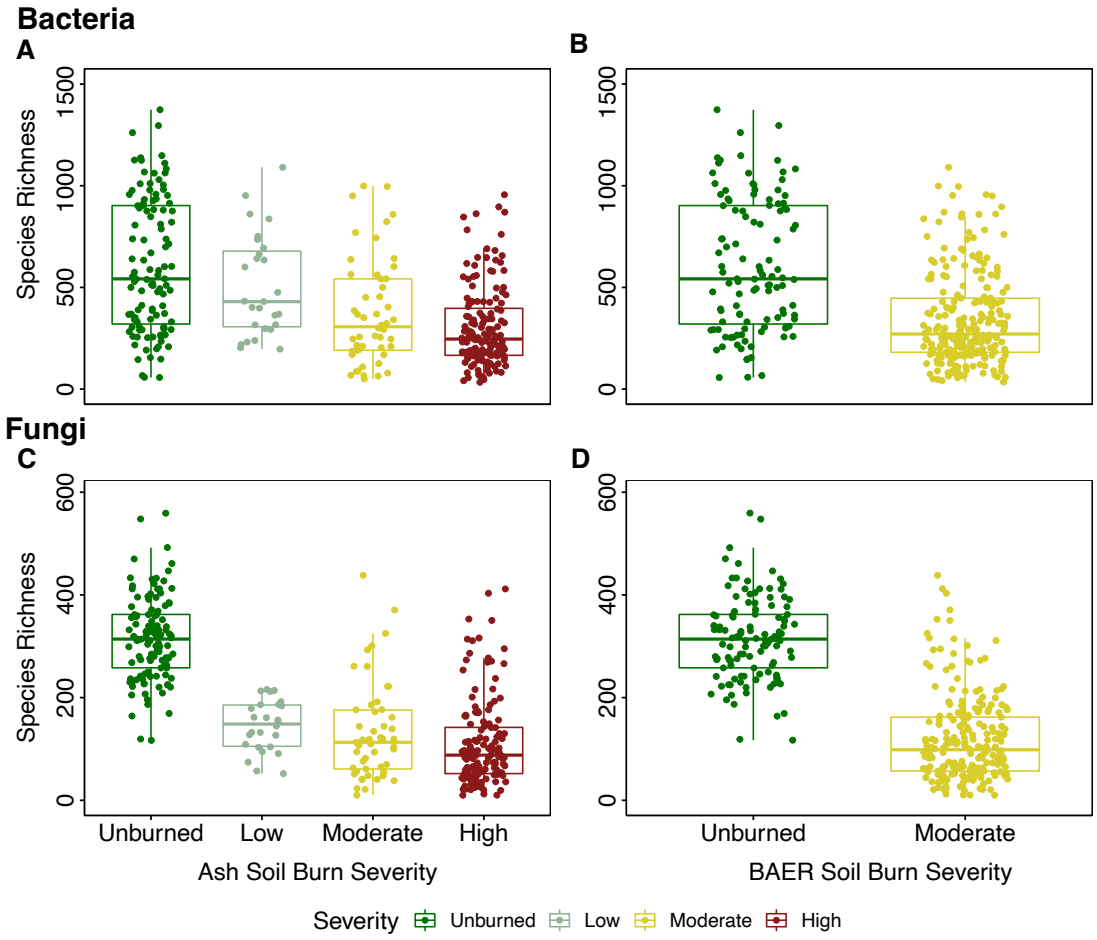

Figure A.1.7. Soil burn severity effect on species richness. Severity categories were based on initial ash depth (cm) following Parson et al., 2010 (unburned = 0 cm; Low = 0.1-1.49 cm; Moderate = 1.5-2.9cm; and High => 3.0cm) and compared to BAER soil burn severity categories.

Table A.2.1. Holy Fire Site-specific characteristics for the nine sampling plots (6 burned, 3 unburned) located within the 2018 Holy Fire.

Site ID	Treatment	Latitude	Longitude	Elevation	Soil pH		Soil Taxonomic Class
					25 days	376 days	
CNF01	Burned	33.6901	-117.463	1228	7.25	6.33	Cieneba series; Loamy, mixed, superactive, nonacid, thermic, shallow Typic Xerorthents (Entisols)
CNF02	Burned	33.69537	-117.471	1260	6.71	6.74	
CNF03	Burned	33.69326	-117.467	1237	6.79	7.1	
CNF04	Burned	33.68456	-117.457	1260	7.11	6.84	Friant series; Loamy, mixed, superactive, thermic Lithic Haploxerolls (Mollisols)
CNF05	Burned	33.67809	-117.457	1195	6.94	7.17	
CNF06	Burned	33.67168	-117.459	1285	6.92	7.48	
CNF07	Unburned	33.67135	-117.459	1283	6.1	6.85	
CNF08	Unburned	33.66813	-117.456	1250	6.12	6.88	
CNF09	Unburned	33.6678	-117.455	1240	6.18	6.18	

Table A.2.2. Total sequences and ASVs per control (positive mock communities and negative DNA extraction and PCR controls) based on Qiime2 data. Note rarefying removed all negative controls. Mock communities were manually removed after verification of taxonomy with Zymo Mock information.

Organism	Sample Type	Seq/Sample	ASVs	ASVs After Rarefaction
Fungi	All	78,202	11,480	7,445
Bacteria	All	31,052	33,078	24,874
Fungi	Mock	2997*	5*	removed
	Neg DNA Extraction	235*	9*	removed
	Neg PCR control	183*	5*	removed
Bacteria	Mock	33533*	10*	removed
	Neg DNA Extraction	1668*	12*	removed
	Neg PCR control	194*	5*	removed

* Denotes: average sequence per sample

Table A.2.3. Descriptive statistics and percent change in estimated biomass (per gram soil) and species richness (observed ASV's) between treatment (unburned (burned)) and time since fire for bacteria and fungi. The mean copy number is based on the 16S rRNA for bacteria and 18S rRNA for fungi.

		Biomass		**Richness**	
	Time since fire (days)	**Mean Copy Num.** (g^{-1} soil)	**% Change**	**Mean ASVs**	**% Change**
Bacteria	17	243,288,300 (39,632,680)	-84	462 (604)	31
	25	235,169,333 (36,530,267)	-84	688 (486)	-29
	34	252,455,133 (107,186,067)	-58	962 (313)	-67
	67	293,834,733 (132,186,480)	-55	621 (250)	-60
	95	329,736,333 (245,489,900)	-26	302 (180)	-41
	131	276,979,018 (167,983,317)	-39	972 (378)	-61
	187	291,303,200 (241,265,883)	-17	933 (244)	-74
	286	323,115,100 (169,881,567)	-47	368 (411)	12
	376	283,013,818 (160,504,850)	-43	533 (411)	-23
Fungi	17	83,624,650 (2,345,940)	-97	292(161)	-45
	25	75,569,867 (3,067,448)	-96	369(117)	-68
	34	90,105,000 (10,755,267)	-88	305(77)	-75
	67	71,132,133 (14,439,620)	-80	328(60)	-82
	95	54,003,967 (10,113,017)	-81	335(85)	-75
	131	43,502,333 (4,985,833)	-89	312(93)	-70
	187	53,313,133 (11,076,350)	-79	344(118)	-66
	286	86,949,156 (16,557,783)	-81	268(119)	-55
	376	73,025,167(14,810,867)	-80	257(99)	-61

Table A.2.4. Model summary results of the effect of treatment (burned vs. unburned), time since fire (TSF in days), precipitation (mm), and soil burn severity measured as ash depth (cm) at day 17 on bacterial and fungal estimated biomass (per gram soil) and richness (observed ASV's). Significance is based on the negative binomial generalized mixed effect models with plot, subplot, and time since fire as the random effect for richness and plot and time since fire as random effect for estimated biomass (gram per soil)—significance at $p<0.05$ (bold).

	Bacteria			**Fungi**		
	Est.	**z value**	**P value**	**Est.**	**z value**	**P value**
Biomass						
(Intercept)	19.45	91.46	**< 2e-16**	18.01	79.91	**< 2e-16**
Treatment (Burned)	-0.82	-3.29	**0.001**	-2.11	-7.62	**2.47E-14**
TSF	0.15	1.17	0.24	-0.02	-0.16	0.87
Precipitation	0.05	0.39	0.70	-0.16	-1.06	0.29
Soil burn severity (ash depth)	-0.01	-0.50	0.62	-0.0004	-0.01	0.99
Treatment (Burned): Precip	0.30	3.02	**0.003**	0.20	1.61	0.11
TSF x Soil burn severity (ash depth)	0.06	3.72	**0.0002**	-	-	-
Treatment (Burned) x TSF	-	-	-	0.44	3.46	**0.001**
Random Effects						
Variance/Std.Dev	$0.08/0.29_{Plot;}$ $0.11/0.33_{TSF}$			$0.08/0.29_{Plot;}$ $0.11/0.33_{TSF}$		
Mar. R^2 / Cond. R^2 (delta)	0.30/0.46			0.47/0.56		
Richness						
(Intercept)		47.27	**<0.0001**	5.8	54.69	**<0.0001**
Treatment (Burned)		-2.56	**0.01**	-0.9	-5.76	**<0.0001**
TSF		-0.84	0.4	0.19	2.13	**0.03**
Precipitation		1.38	0.17	-0.01	-0.36	0.72
Soil burn severity (ash depth)		-3.83	**0.0001**	-0.07	-3.48	**0.001**
TSF x Precipitation		-4.64	**<0.0001**	0.34	3.27	**0.001**
TSF x Soil burn severity (ash depth)		2.38	**0.02**	0.03	3.82	**0.0001**
Random Effects						
Variance/Std.Dev	0.02/0.13Plot 0.02/0.14Subplot 0.08/0.28 TSF			$0.02/0.12_{Plot}$ $0.04/0.20_{Subplot}$ $0.01/0.08_{TSF}$		
Mar R^2 / Cond. R^2 (delta)	0.32/0.57			0.63/0.74		

Table A.2.5. Model summary results of the effect of treatment (burned vs. unburned), time since fire (TSF in days), precipitation (mm), and ash depth (cm) on arbuscular fungi (AMF), ectomycorrhizal fungi (EMF), Saprobes and Pathogens. Significance based on the negative binomial generalized mixed effect models with plot, subplot, and time since fire as random effect—significance at $p<0.05$ (bold).

	AMF			**EMF**		
	Est.	**z value**	**P value**	**Est.**	**z value**	**P value**
(Intercept)	-0.98	-1.71	0.09	1.52	4.57	**<0.0001**
Treatment (Burned)	-4.10	-4.34	**<0.0001**	-1.09	-2.18	**0.03**
TSF	-	-	-	-0.09	-1.25	0.21
Soil burn severity (ash depth)	-	-	-	-0.19	-2.77	**0.01**
Precipitation	-	-	-	0.00	-0.06	0.95
Treatment (Burned) x Precipitation	-	-	-	-0.37	-3.92	**<0.0001**
Treatment (Burned) x TSF	-	-	-	-0.68	-7.04	**<0.0001**
Random Effects						
Variance/Std.Dev	$0.23/0.48_{Plot}$ $0.45/0.67_{Subplot}$ $0.03/0.17_{TSF}$			$6.3e^{-10}/2.5e^{-05}_{Plot}$ $3.06/1.75_{Subplot}$ $0.06/0.25_{TSF}$		
Mar R^2 / Cond. R^2	0.55/0.81			0.20/0.37		
	Saprobes			**Pathogens**		
	Est.	**z value**	**P value**	**Est.**	**z value**	**P value**
(Intercept)	-0.06	-0.35	0.73	-1.28	-4.83	**<0.0001**
Treatment (Burned)	-1.96	-7.37	**<0.0001**	-1.48	-3.63	**0.0003**
TSF	-0.36	-3.07	**0.002**	-	-	-
Precipitation	-	-	-	0.09	0.52	0.60
Treatment (Burned) x Precipitation	-	-	-	-0.88	-2.16	**0.03**
Treatment (Burned) x TSF	0.68	3.42	**0.001**	-	-	-
Random Effects						
Variance/Std.Dev	$1.01e^{-11}/3.2e^{-06}_{Plot}$ $0.18/0.42_{Subplot}$ $0.01/0.08_{TSF}$			$7.2e^{-12}/2.7e^{-06}_{Plot}$ $0.34/0.58_{Subplot}$ $3.9e^{-13}/6.3e^{-07}_{TSF}$		
Mar R^2 / Cond. R^2	0.21/0.25			0.11/0.16		

Table A.2.6. Permutational multivariate analysis of variance (PERMANOVA) of bacterial and fungal community composition and the effects of treatment (burned vs. unburned), time since fire (TSF) in days, Initial ash depth (soil burn severity), and total precipitation (mm) and their respective interactions. Significance $p<0.05$ (bold).

	Variable	Sum of Sqs.	R2	F	P value
Bacteria	Treatment	14.34	0.13	50.47	**0.0001**
	Time since fire	4.33	0.04	15.25	**0.0001**
	Total Precipitation	3.20	0.03	11.26	**0.0001**
	Initial Ash Depth	1.98	0.02	6.97	**0.0001**
	Treatment x Initial Ash Depth	2.27	0.02	8.00	**0.0001**
	Treatment x Total Precipitation	1.53	0.01	5.39	**0.0001**
	Time since fire x Initial Ash Depth	0.52	0.005	1.82	**0.03**
Fungi	Treatment	12.49	0.10	34.52	**0.0001**
	TSF	1.80	0.01	4.98	**0.0001**
	Total Precipitation	1.12	0.01	3.10	**0.0001**
	Initial Ash Depth	2.32	0.02	6.40	**0.0001**
	Treatment x Time Since Fire	1.16	0.01	3.21	**0.0005**
	Treatment x Total Precipitation	0.66	0.01	1.82	**0.02**
	Time since fire x Initial Ash Depth	0.43	0.003	1.17	0.23

Table A.2.7. Measures of successional dynamics for bacterial and fungal communities between treatments (burned vs. unburned) where the unburned values are inside the parenthesis. Turnover rates (proportion of species that differ between time points), appearance (relative species appearance between time points) and disappearance (relative species disappearance between time points), rates of change (rate of directional change in community composition over time), Stability (of total species abundance as a measure of equilibrium) and Synchrony (a measure of whether abundance fluctuations are homo- or heterogeneous over time). Higher values represent a higher rate for each category.

Microbe	TSF days	Turnover Rate	Appearance	Disappearance	Rate of change	Stability	Synchrony
Bacteria	25	0.59 (0.54)	0.25 (0.40)	0.34 (0.14)	0.16 (0.12)	8.35 (5.36)	0.03 (0.22)
	34	0.51 (0.50)	0.15 (0.21)	0.36 (0.29)			
	67	0.45 (0.43)	0.21 (0.27)	0.24 (0.16)			
	95	0.50 (0.56)	0.15 (0.14)	0.35 (0.42)			
	131	0.37 (0.40)	0.19 (0.16)	0.19 (0.24)			
	187	0.50 (0.58)	0.31 (0.21)	0.19 (0.38)			
	286	0.50 (0.64)	0.28 (0.32)	0.22 (0.32)			
	376	0.50 (0.35)	0.26 (0.25)	0.24 (0.10)			
Fungi	25	0.61 (0.50)	0.26 (0.37)	0.34 (0.13)	0.49 (0.08)	6.42 (8.58)	0.04 (0.05)
	34	0.52 (0.43)	0.14 (0.30)	0.38 (0.13)			
	67	0.52 (0.53)	0.28 (0.28)	0.24 (0.25)			
	95	0.42 (0.47)	0.27 (0.25)	0.15 (0.23)			
	131	0.52 (0.57)	0.29 (0.27)	0.23 (0.30)			
	187	0.55 (0.53)	0.40 (0.24)	0.15 (0.29)			
	286	0.53 (0.53)	0.15 (0.24)	0.38 (0.29)			
	376	0.42 (0.58)	0.19 (0.31)	0.23 (0.27)			

Appendix B: Supplemental Information for Chapter III

Microbial-Mediated Pyrogenic Organic Matter and Nitrogen Cycling genes increase over time after a Chaparral wildfire

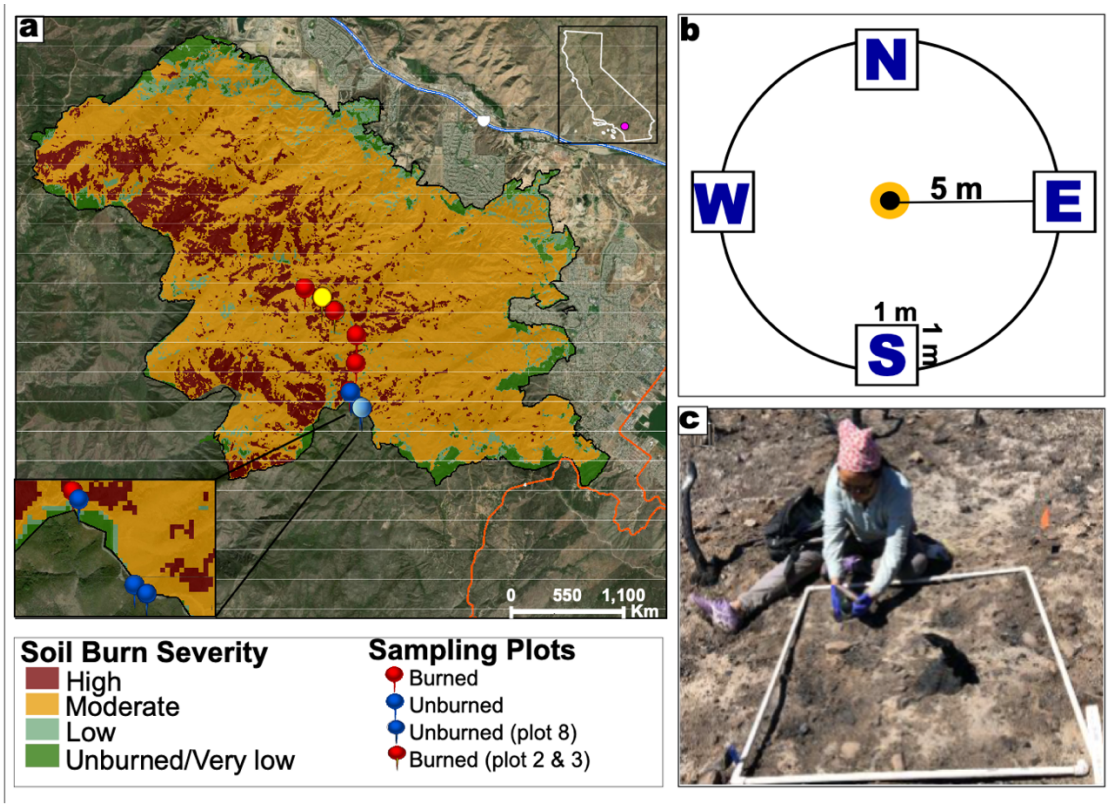

Figure B.1.1. Map of the sampling area a) Burned Area Emergency Response (BAER) map of the soil burn severity within the 2018 Holy Fire, with the b) sampling design for 9 plots (6 burned, 3 unburned) each with 4 subplots 1m2 for soil sampling over time. Samples used for this study were plot 2 (yellow pin) and plot 8 (light blue pin) c) Sampling of the top 10 cm of soil within subplot. Figure adapted from (Pulido-Chavez et al., 2023)

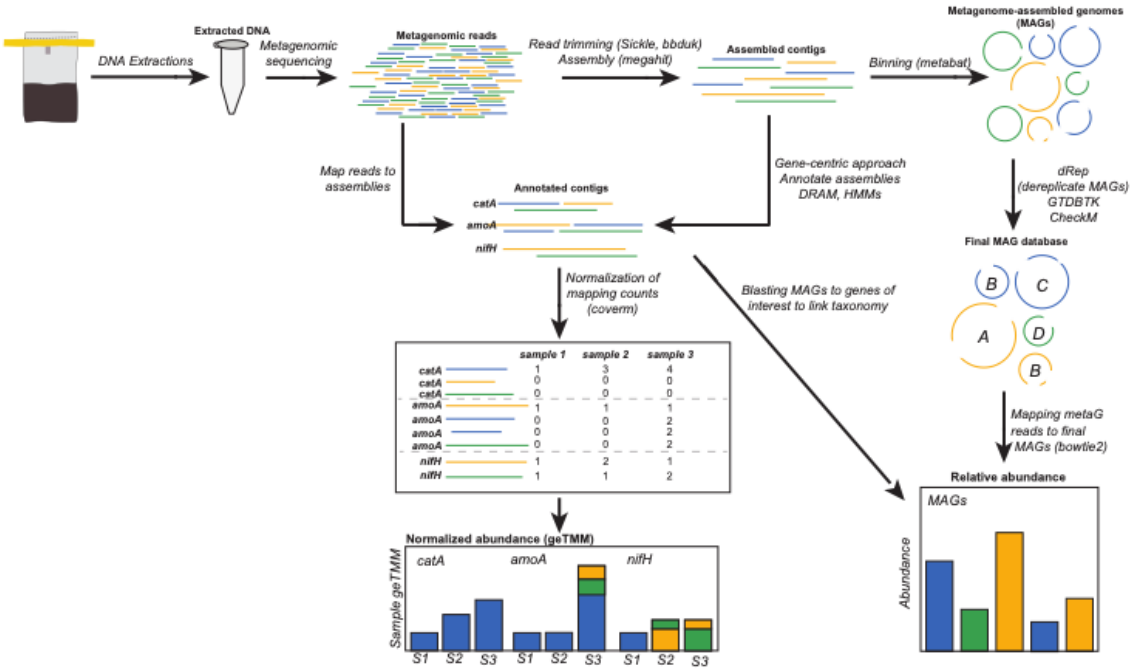

Figure B.1.2. Detailed methodological map for the bioinformatic steps used to analyze Illumina NovaSeq shotgun metagenomic samples.

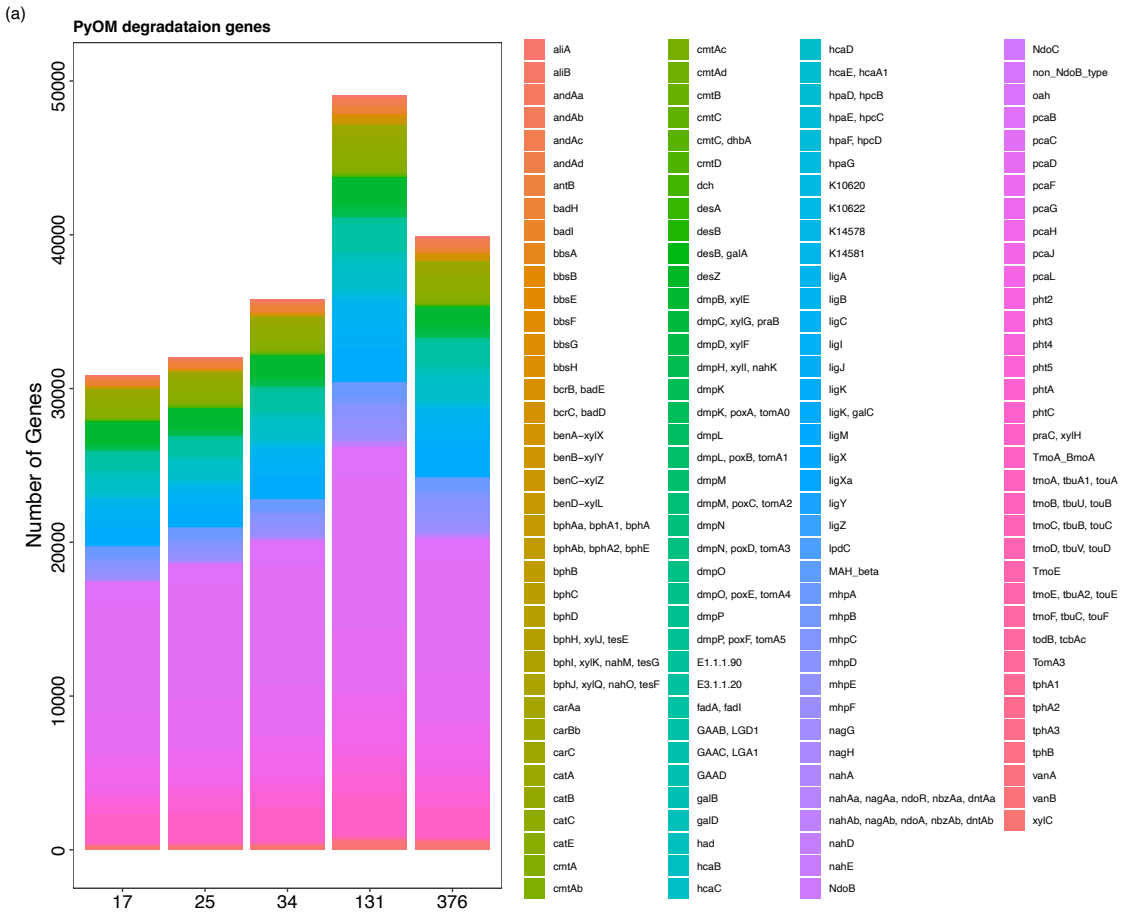

Figure B.1.3. Total number of unique Pyrogenic Organic Matter (PyOM) cycling genes across time (in days) in the burned plots. Depicting increases in genes relate to increases in species richness with potential increases in relative abundance at 131 days post-fire.

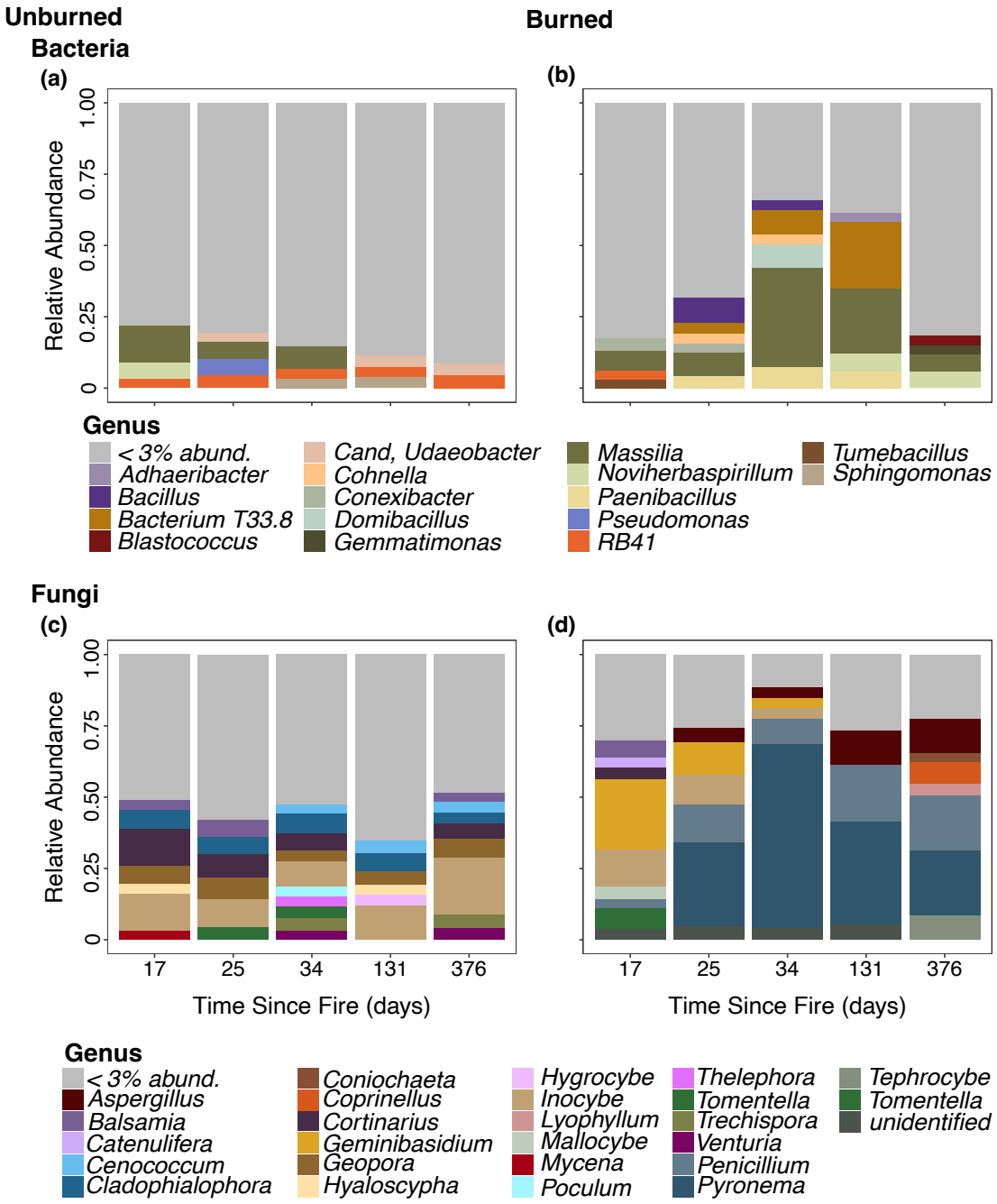

Figure B.1.4. Relative abundance of the bacterial and fungal community over time for timepoints (17,34, 67, 131, and 376d post-fire). Only taxa that make up above 3% of the relative abundance are shown, taxa <3% are represented in gray.

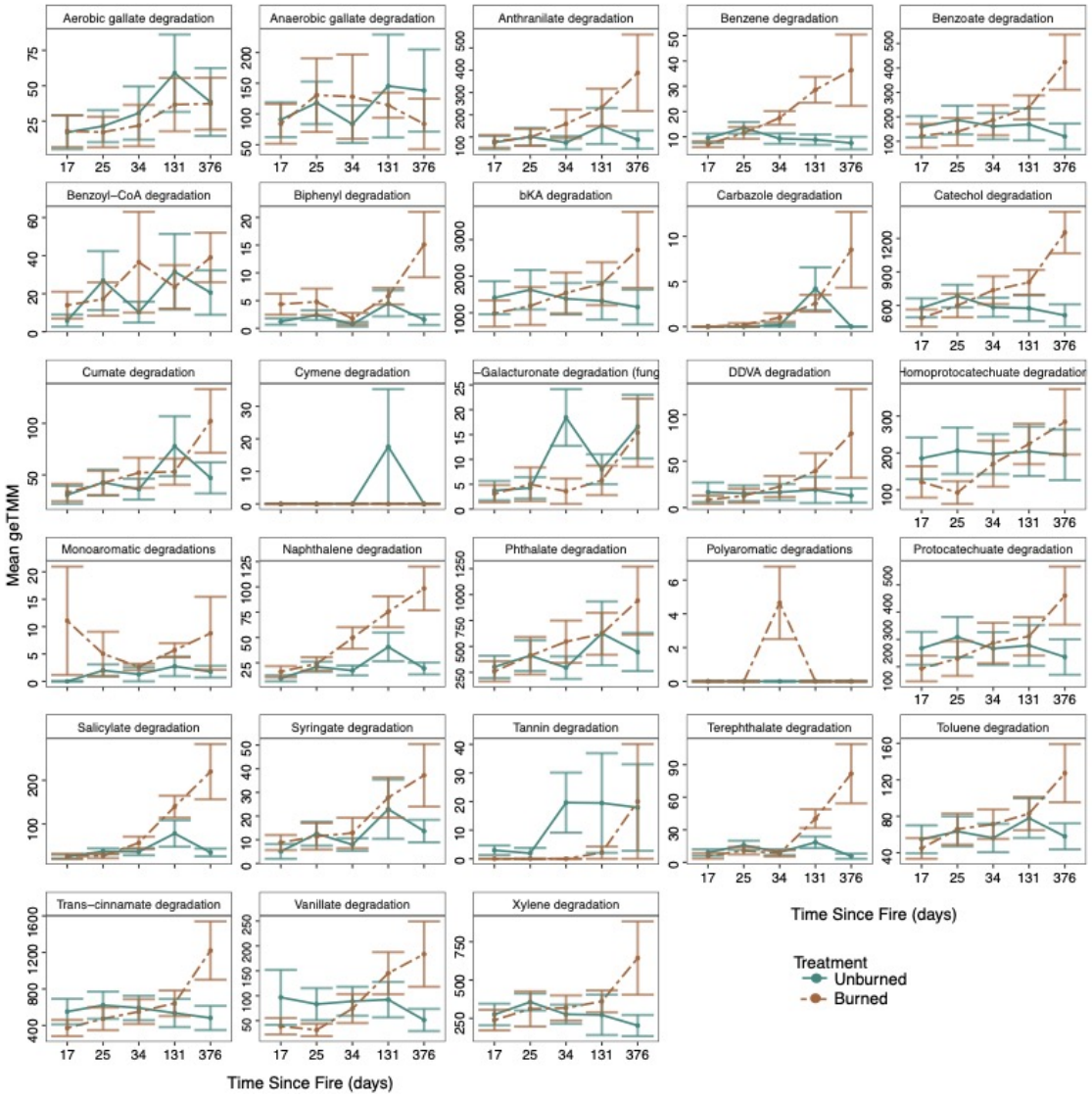

Figure B.1.5. Effect of time (in days) on all Pyrogenic Organic Matter (PyOM) pathways between the burned (brown) and unburned (blue-green). Where mean geTMM are the contigs normalized by contig length corrected trimmed mean (geTMM) and normalized by library depth and gene length.

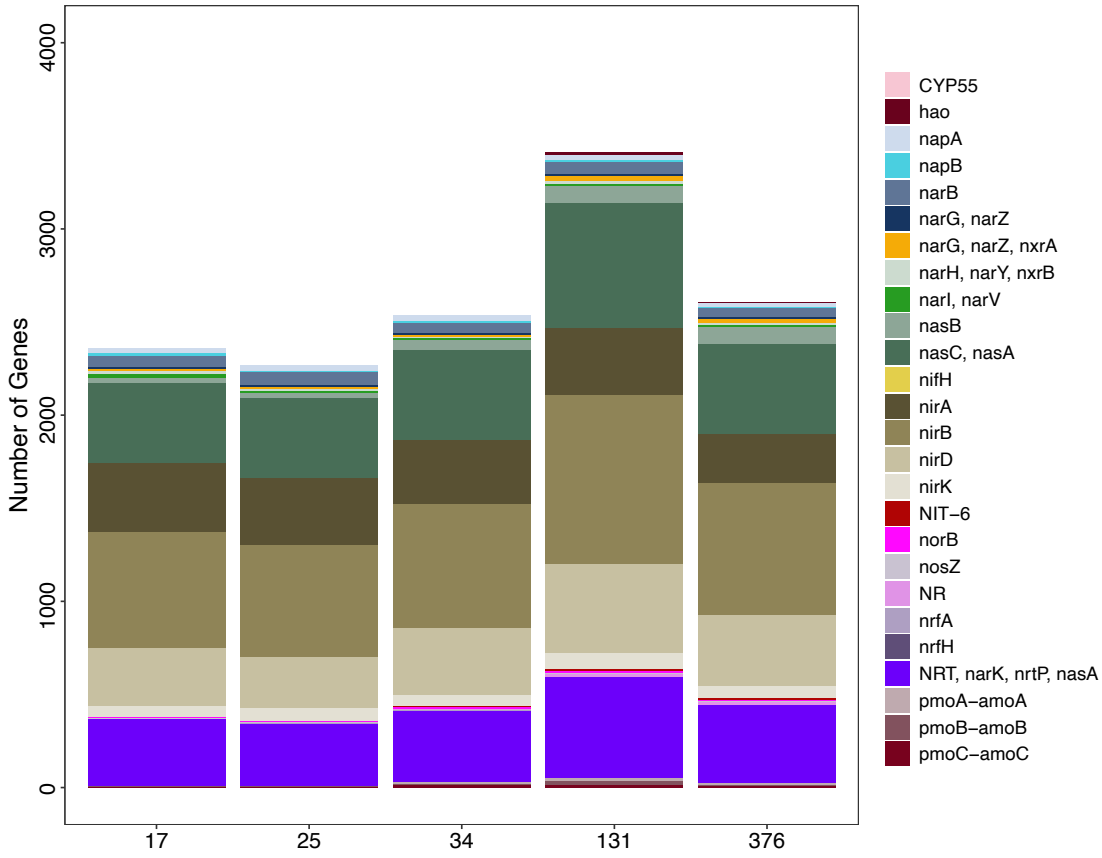

Figure B.1.6. Total number of unique nitrogen cycling genes across time (in days) in the burned plots. Depicting increases in genes relate to increases in species richness with potential increases in relative abundance at 131 days post-fire.

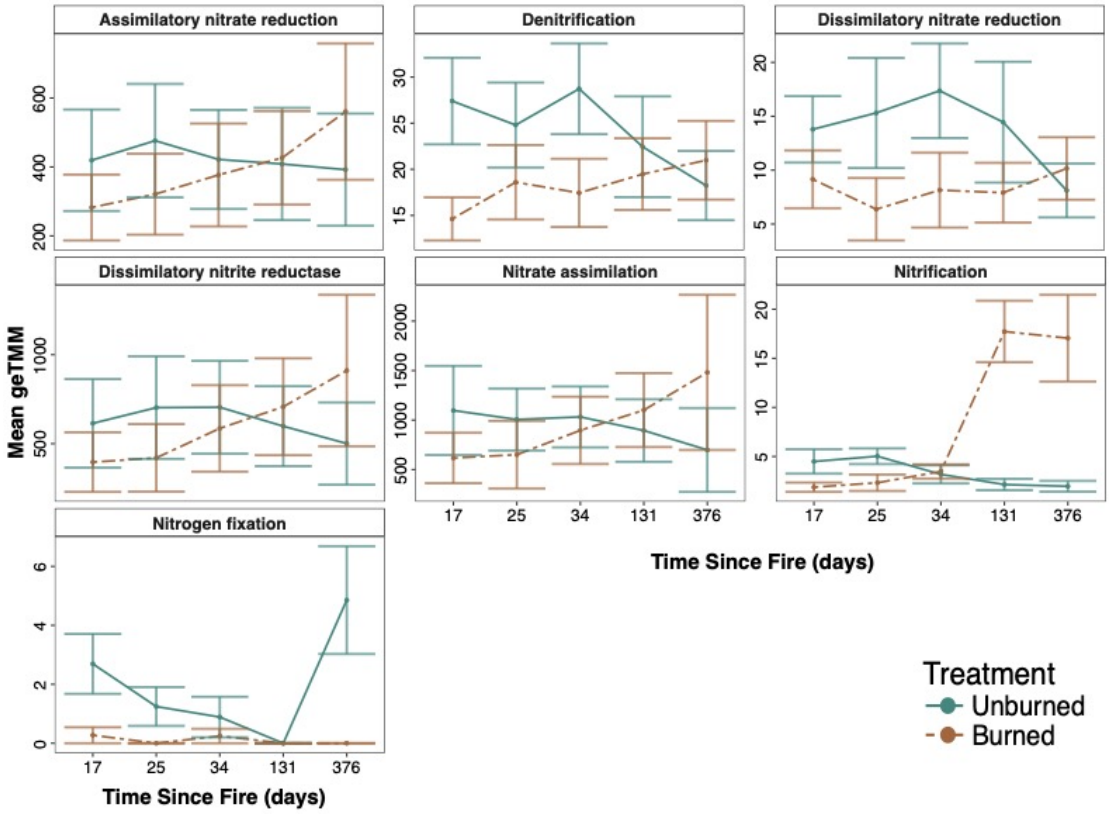

Figure B.1.7. Effect of time (in days) on all Nitrogen cycling pathways between the burned (brown) and unburned (blue-green). Where mean geTMM are the contigs normalized by contig length corrected trimmed mean (geTMM) and normalized by library depth and gene length.

Table B.2.1. Permanova results of the effects of treatment and time since fire (days) on alkane, PyOM, nitrogen and urea gene composition. Significance based on $p<0.05$, and based on Bray-Curtis dissimilarity.

Functional Gene	Variable	Sum of Sqs	R2	F	Pr (>F)
Alkanes	Treatment (burned)	1.47	0.16	5.59	**0.001**
	TSF days	0.51	0.06	1.95	**0.02**
	Treatment x TSF days	0.43	0.05	1.63	0.07
PyOM	Treatment (burned)	1.39	0.15	5.25	**0.001**
	TSF days	0.49	0.05	1.84	**0.03**
	Treatment x TSF days	0.47	0.05	1.76	**0.03**
Nitrogen	Treatment (burned)	1.51	0.16	5.65	**0.001**
	TSF days	0.45	0.05	1.69	**0.04**
	Treatment x TSF days	0.53	0.06	1.97	**0.02**
Urea	Treatment (burned)	1.39	0.15	5.35	**0.001**
	TSF days	0.47	0.05	1.83	**0.02**
	Treatment x TSF days	0.47	0.05	1.81	**0.04**

Table B.2.2. Permutest results for the betadisper analysis for nitrogen, urea, PyOM and Alkane pathways, based on 9999 permutations and "plot" as random effect.

			Sum Sq	Mean Sq	F	Pr(>F)
Nitrogen	Burn	Groups	0.07	0.02	**3.82**	**0.04**
		Residuals	0.04	0.004		
	Unburn	Groups	0.01	0.003	0.52	0.7
		Residuals	0.06	0.01		
Urea	Burn	Groups	0.08	0.02	**4.51**	**0.03**
		Residuals	0.04	0.004		
	Unburn	Groups	0.01	0.003	0.52	0.7
		Residuals	0.06	0.01		
PyOM	Burn	Groups	0.10	0.02	**5.32**	**0.02**
		Residuals	0.05	0.005		
	Unburn	Groups	0.01	0.002	0.39	0.8
		Residuals	0.06	0.01		
Alkane	Burn	Groups	0.08	0.02	**4.65**	**0.02**
		Residuals	0.04	0.004		
	Unburn	Groups	0.01	0.003	0.50	0.7
		Residuals	0.05	0.01		

DF (4), Residuals (10), N permutations (9999) per pathway

Table B.2.3. Generalized negative binomial result for the effects of treatment, time since fire (days) and their interaction on nitrogen. urea, pyrogenic organic matter (PyOM) and alkane cycling genes. Significance based on $p<0.05$, denoted in bold.

Nitrogen				**Urea**		
	Estimate	**Std. Error**	**Pr(>|z|)**	**Estimate**	**Std. Error**	**Pr(>|z|)**
(Intercept)	4.57	0.26	**<2e-16**	7.09	0.26	**<2e-16**
Treatment (Burned)	0.02	0.32	0.96	0.11	0.31	0.71
TSF days	**-0.19**	0.10	0.06	-0.16	0.07	**0.02**
Treatment (Burned) x TSF days	0.37	0.16	**0.02**	0.28	0.01	**<2e-16**
Random Effects						
Tsf/Subplot Margina/Conditional R2	0.014/0.11			0.08/ 0.99		

PyOM				**Alkane**		
	Estimate	**Std.Error**	**Pr(>|z|)**	**Estimate**	**Std.Error**	**Pr(>|z|)**
(Intercept)	5.63	0.29	**< 2e-16**	5.63	0.29	**< 2e-16**
Treatment (Burned)	0.28	0.34	0.41	0.28	0.34	0.41
TSF1	-0.19	0.07	**3.0E-03**	-0.19	0.07	**0.003**
Treatment (Burned) x TSF1	0.38	0.07	**4.2E-08**	0.38	0.07	**4.2E-08**
Random Effects						
Tsf/Subplot Margina/Conditional R2	0.026/0.18			0.013/0.31 0.03/ 0.18		

Table B.2.4. Generalized negative binomial regression for the effects of time since fire (days) nitrogen. urea, cycling genes. Significance based on p<0.05, denoted in bold.

Nitrogen				**Urea**		
	Est	**Std. Error**	**p**	**Est**	**Std. Error**	**p**
(Intercept)	4.64	0.34	**<2e-16**	7.19	0.25	**<2e-16**
Treatment (Burned)	-0.35	0.46	0.45	-0.52	0.31	0.09
TSF25	0.31	0.35	0.37	0.23	0.01	**<2e-16**
TSF34	-0.08	0.33	0.81	-0.18	0.01	**<2e-16**
TSF131	-0.24	0.33	0.46	-0.21	0.01	**<2e-16**
TSF376	-0.42	0.34	0.21	-0.38	0.01	**<2e-16**
Treatment (Burned) : TSF25	-0.16	0.52	0.76	0.39	0.03	**<2e-16**
Treatment (Burned) : TSF34	0.35	0.53	0.51	0.69	0.02	**<2e-16**
Treatment (Burned) : TSF131	0.70	0.48	0.14	0.92	0.02	**<2e-16**
Treatment (Burned) : TSF376	0.99	0.50	**0.05**	1.04	0.02	**<2e-16**
Random Effects						
Plot	0.24					
Marginal/conditional R2 var	0.021/ 0.12					

PyOM				**Alkane**		
	Est	**Std. Error**	**p**	**Est**	**Std. Error**	**p**
(Intercept)	5.76	0.30	**< 2e-16**	5.76	0.30	**< 2e-16**
Treatment (Burned)	-0.28	0.37	0.45	-0.28	0.37	0.45
TSF25	0.29	0.14	**0.03**	0.29	0.14	**0.03**
TSF34	-0.25	0.13	**6.1E-02**	-0.25	0.13	0.06
TSF131	-0.33	0.13	**0.01**	-0.33	0.13	**0.01**
TSF376	-0.50	0.14	**0.0002**	-0.50	0.14	**0.0002**
Treatment (Burned) : TSF25	0.01	0.23	**9.6E-01**	0.01	0.23	0.96
Treatment (Burned) : TSF34	0.73	0.26	**0.004**	0.73	0.26	**0.004**
Treatment (Burned) : TSF131	0.78	0.19	**0.0001**	0.78	0.19	**5.3E-05**
Treatment (Burned) : TSF376	1.25	0.22	**0.000**	1.25	0.22	**2.6E-08**
Random Effects						
Subplot	0.33			TSF/Subplot		
Marginal/conditional R2 var	0.04 / 0.20			0.04/ 0.20		

Table B.2.5. Generalized negative binomial regression for the effects of time (days) on all the different PyOM cycling (C) pathways for burned and unburned plots independently. Significance based on p<0.05, denoted in bold.

	Burn				Unburn			
PyOM pathways		**Est.**	**z value**	**P**	**Est.**	**z value**	**P**	**R2 (B),(Un)**
Catechol Meta	(Int)	6.29	23.54	**< 2e-16**	5.99	18.27	**<2e-16**	(0.04/0.21),
	TSF	0.21	2.92	**0.004**	-0.19	-2.44	**0.01**	(0.025/0.31)
Catechol Ortho	(Int)	6.56	25.14	**< 2e-16**	6.26	25.08	**<2e-16**	(0.1/0.29),
	TSF	0.30	3.23	**0.001**	-0.22	-2.42	**0.0155**	(0.054/0.28)
Aerobic Gallate	(Int)	2.80	8.04	**8.9E-16**	3.40	8.40	**<2e-16**	(0.07/0.9),
	TSF	0.17	5.06	**4.3E-07**	0.24	0.73	0.463	(0.04/0.01)
Anaerobic Gallate	(Int)	4.50	16.93	**<2e-16**	4.49	16.64	**<2e-16**	(0.04/0.3),
	TSF	-0.13	-0.86	0.393	0.06	0.52	0.605	(0.01/0.61)
Benzene	(Int)	2.79	10.74	**< 2e-16**	1.92	5.00	**5.7e-07**	(0.13/0.27),
	TSF	0.39	3.91	**9.3E-05**	-0.29	-2.78	**0.01**	(0.05/0.38)
Benzoate	(Int)	5.12	19.60	**< 2e-16**	4.80	17.00	**<2e-16**	(0.13/0.29),
	TSF	0.38	3.72	**0.0002**	-0.25	-2.36	**0.02**	(0.06/0.3)
BenzoykCoA	(Int)	5.12	19.60	**< 2e-16**	2.92	8.46	**<2e-16**	(0.012/0.01)
	TSF	0.38	3.72	**0.0002**	0.17	0.43	0.668	
Biphenyl	(Int)	1.37	2.83	**0.005**	-0.06	-0.11	0.912	(0.12/0.20),
	TSF	0.53	2.02	**0.04**	-0.11	-0.34	0.734	(0.004/0.31)
bka	(Int)	7.04	25.75	**<2e-16**	6.91	26.30	**<2e-16**	(0.06/0.17)
	TSF	0.30	2.03	**0.04**	-0.18	-1.30	0.193	
Carbazole	(Int)	-0.05	-0.14	0.89	-2.34	-1.23	0.221	(0.6/0.8),
	TSF	1.05	11.60	**<2e-16**	0.06	0.40	0.691	(0.0004/0.96)
Cumate	(Int)	3.78	14.76	**<2e-16**	3.47	9.45	**<2e-16**	(0.06/0.13),
	TSF	0.33	2.47	**0.01**	-0.03	-0.15	0.883	(0.0003,0.19)
Dgalac	(Int)	1.09	2.36	**0.02**	0.77	0.61	0.542	(0.21/0.80),
	TSF	0.46	10.14	**<2e-16**	0.03	0.14	0.891	(1.3e-04/0.82)
DDVA	(Int)	3.22	11.84	**<2e-16**	2.77	7.35	**2.0E-13**	(0.22/0.22),
	TSF	0.70	2.35	**0.02**	-0.08	-0.21	0.837	(2.9e-03/2.9e-03)
PCA Meta	(Int)	5.87	17.62	**< 2e-16**	5.96	17.32	**< 2e-16**	(0.11/0.4),
	TSF	0.36	5.11	**3.3E-07**	-0.18	-2.68	**0.01**	(0.03/0.41)
PCA Ortho	(Int)	7.89	32.00	**<2e-16**	7.75	27.51	**<2e-16**	(0.034/0.22),
	TSF	0.17	1.89	**0.06**	-0.18	-2.06	**0.04**	(0.04/0.33)
Naphthalene	(Int)	3.75	14.96	**< 2e-16**	2.65	7.03	**2.1e-12**	(0.23/0.34),
	TSF	0.56	4.67	**3.0E-06**	-0.02	-0.16	0.871	(3.6e-04/0.3)
Phathalete	(Int)	6.09	32.45	**<2e-16**	5.87	19.32	**<2e-16**	(0.43/0.99),
	TSF	0.28	73.67	**<2e-16**	0.08	0.34	0.736	(0.003/0.07)
Syringate	(Int)	2.40	5.82	**5.8E-09**	1.14	1.09	0.276	(0.2/0.5),
	TSF	0.52	2.92	**0.003**	0.15	0.92	0.356	(0.005/0.92)
Terephthalate	(Int)	2.67	9.00	**<2e-16**	2.40	13.01	**<2e-16**	(0.6/0.94),
	TSF	0.71	31.99	**<2e-16**	-0.25	-1.33	0.182	(0.05/0.05)
Toluene	(Int)	4.10	15.00	**<2e-16**	3.73	10.61	**<2e-16**	(0.04/0.15)
	TSF	0.26	2.30	**0.02**	-0.14	-1.20	0.232	
Trans	(Int)	6.18	22.61	**< 2e-16**	6.07	21.76	**<2e-16**	(0.08/0.20),
	TSF	0.35	3.01	**0.003**	-0.17	-1.36	0.174	(0.02/0.2)
Vanillate	Int)	4.10	13.44	**<2e-16**	4.28	11.68	**<2e-16**	(0.36/0.97),
	TSF	0.41	34.07	**<2e-16**	-0.24	-1.02	0.308	(0.04/0.1)
Xylene	(Int)	5.62	19.60	**< 2e-16**	5.43	24.82	**<2e-16**	(0.13/0.53),
	TSF	0.26	2.62	**0.01**	-0.24	-2.53	**0.01**	(0.13/0.5)

Table B.2.6. Generalized negative binomial regression for the effects of time (days) on all the different Alkane degradation pathways for burned plots. Significance based on $p<0.05$, denoted in bold.

		Burn			Unburn			
Alkane pathways		**Est**	**z value**	**P**	**Estimate**	**z value**	**P**	**R2 (B),(Un)**
Methane	(Int)	5.51	21.43	**<2e-16**	5.37	23.46	**<2e-16**	(0.013/0.07), (0.02/0.07)
	TSF	0.17	1.49	0.136	-0.19	-1.56	0.119	
Alkane	(Int)	5.08	14.81	**<2e-16**	5.15	10.27	**<2e-16**	(0.0001/0.5), (0.01/0.70)
	TSF	-0.01	-0.10	0.919	-0.12	-1.15	0.252	
Propane	(Int)	5.30	19.61	**<2e-16**	4.47	11.76	**<2e-16**	(0.23/0.43), (0.01/0.7)
	TSF	0.37	2.21	**0.0275**	-0.08	-0.59	0.554	

Table B.2.7. Generalized negative binomial regression for the effects of time (days) on all the different Nitrogen cycling pathways for burned and unburned plots independently. Significance based on p<0.05, denoted in bold.

	Burn				Unburn			
		Est	**z value**	**P value**	**Est**	**z value**	**P value**	**R2 (B),(Un)**
Dissimilatory Nitrite	(Int)	6.03	19.04	**<2e-16**	6.15	19.21	< 2e-16	(0.1/0.99), (0.07/ 0.99)
	TSF days	0.20	2.06	**0.0397**	-0.18	-3.15	**0.002**	
Assimilatory Nitrite Reductase	(Int)	-6.55	-4.99	**5.9E-07**	2.52	3.28	**0.001**	(0.04/1), (0.06/0.73)
	TSF days	1.71	8.50	**< 2e-16**	-0.41	-1.34	0.18	
Assimilatory Nitrate Reductase	(Int)	1.29	2.17	**0.03**	6.14	28.19	**<2e-16**	(0.0006/0.42), (0.003/0.04)
	TSF days	-0.03	-0.19	0.85	-0.07	-0.35	0.72	
Dissimilatory Nitrate Reductase	(Int)	5.97	19.49	**<2e-16**	1.99	3.55	**0.0004**	(0.023/0.1), (0.1/0.63)
	TSF days	0.18	0.93	0.35	-0.44	-3.24	**0.001**	
N assimilation	(Int)	6.58	22.12	**<2e-16**	6.60	21.95	**<2e-16**	(0.15/0.59), (0.14/0.62)
	TSF days	0.27	2.11	**0.03**	-0.28	-1.98	0.05	
Nitrite Reductase	(Int)	3.28	10.85	**<2e-16**	3.48	8.71	**<2e-16**	(6.23e-04/0.17), (0.05/0.63)
	TSF days	0.12	1.06	0.29	-0.24	-2.63	**0.01**	
Denitrification	(Int)	2.04	5.66	**1.5E-08**	2.24	5.55	**2.9E-08**	(0.06/0.4)
	TSF days	-0.03	-0.24	0.81	-0.31	-2.85	**0.004**	
Nitrite oxireductase	(Int)	0.41	0.40	0.69	1.14	2.28	**0.02**	(0.013/0.7), (0.15/0.54)
	TSF days	-0.23	-0.98	0.33	-0.57	-3.14	**0.002**	
Nitrification	(Int)	1.24	1.88	0.06	0.57	2.13	**0.03**	(0.26/0.71), (0.02/0.12)
	TSF days	1.11	2.04	**0.04**	-0.20	-0.82	0.41	
Fixation	(Int)	-15.61	-1.68	0.09	-1.17	-1.12	0.27	(0.61/0.99), (0.0006/0.72)
	TSF days	-9.23	-1.15	0.25	0.06	0.08	0.94	

Table B.2.8. Generalized negative binomial regression for the effects of time (days) on all the different urea cycling (C) pathways for burned and unburned plots independently. Significance based on p<0.05, denoted in bold.

	Burned				Unburn			
Urea cycling		Est.	**z value**	**P value**	**Est.**	**z value**	**P value**	**R2 (B),(Un)**
Urea	(Int)		25.30	**<2e-16**		30.65	**<2e-16**	
	TSF		1.04	0.30		-55.53	**<2e-16**	(0.10/0.99)
Ornithine biosynthesis	(Int)		3.16	**0.002**		2.86	**0.004**	(0.14/0.4), (0.02/0.02)
	TSF		-1.55	0.12		0.41	0.68	

Appendix C: Supplemental Information for Chapter IV

A comprehensive 4.5 year study of microbial resilience and ecosystem recovery after a Chaparral wildfire

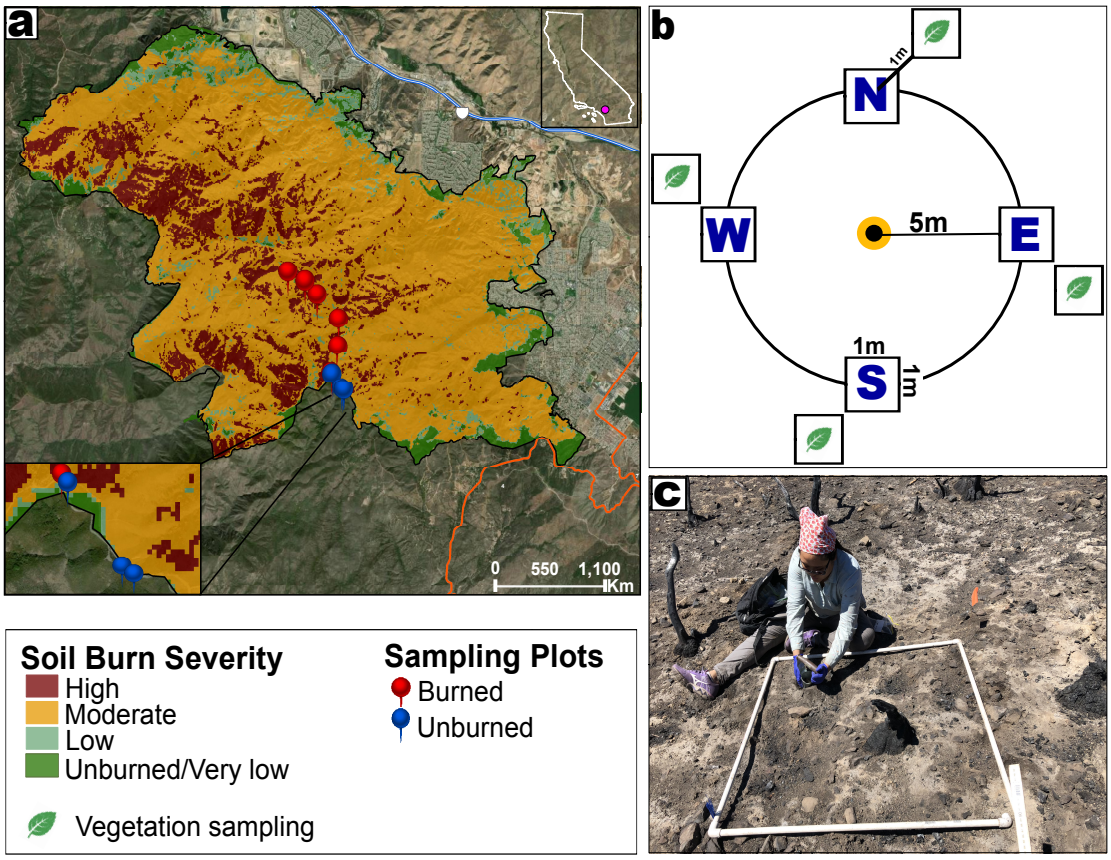

Figure C.1.1. (a) Study area and plots (6 burned; 3 unburned) located within the Holy Fire burn scar in the Cleveland National Forest in southern California. Soil burn severity is classified based on the BAER classifications. (b) Experimental plot design, each featuring four 1 m2 soil sampling subplots placed 5 m from the center in each cardinal direction. Vegetation sampling plots (1 m^2) were positioned 1 m from the center of each soil sampling plot. (c) Soil samples were collected from the top 10 cm of soil beneath the ash (or beneath the organic layer in unburned plots) using a releasable bulb planter, spanning from 17 days to 44 months post-fire. Figure adapted from (Pulido-Chavez et al., 2023).

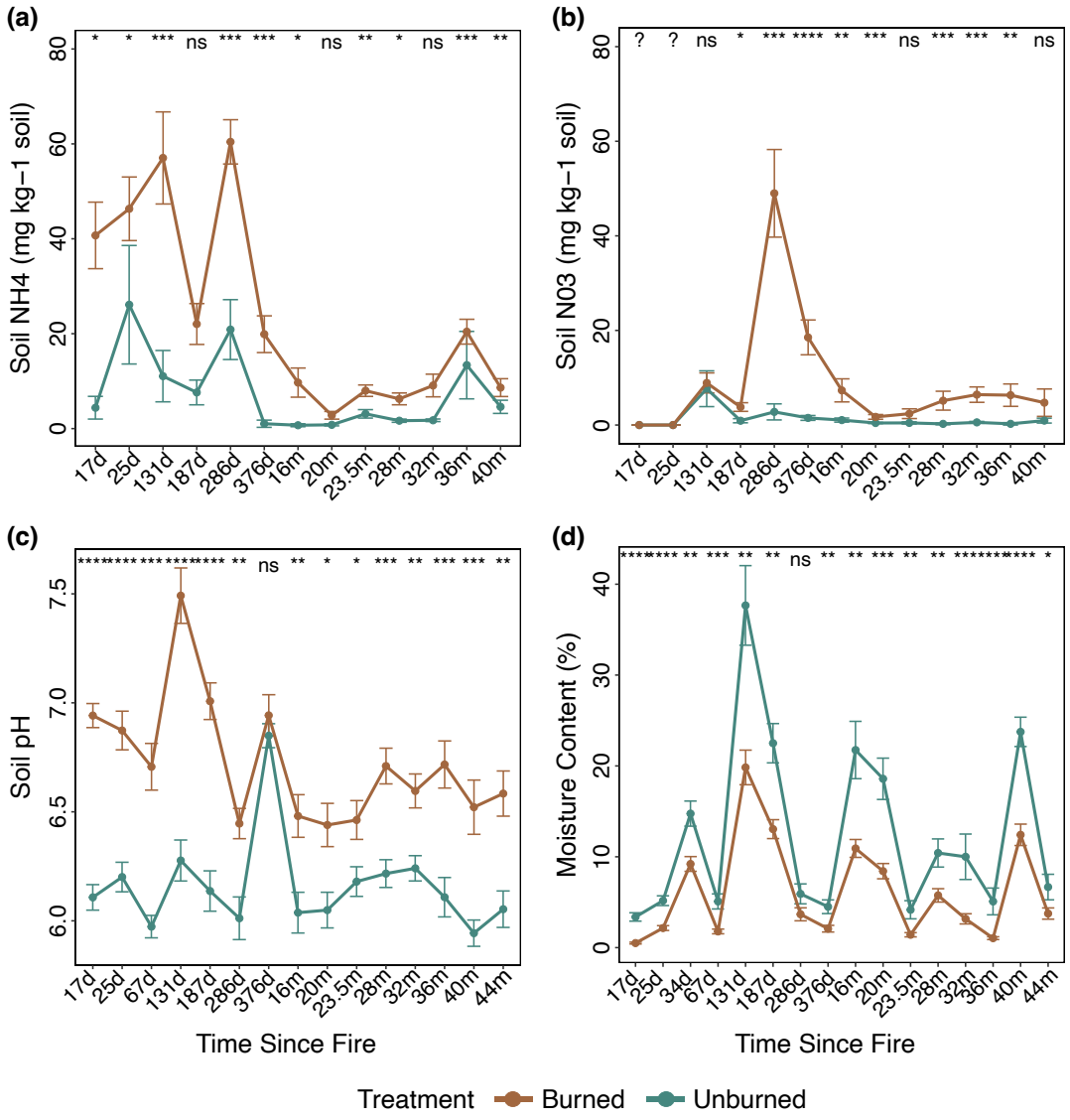

Figure C.1.2. Comparison between burned (brown) and unburned communities (blue-green) for (a) soil NH4, (b) soil NO3, (c) soil pH, and (d) moisture content at each of the sampling timepoints over 4.5 years. Points represent the mean values of soil NH4, soil NO3, soil pH, and moisture content, while bars indicate the standard error of the mean for burned versus unburned plots at each timepoint.

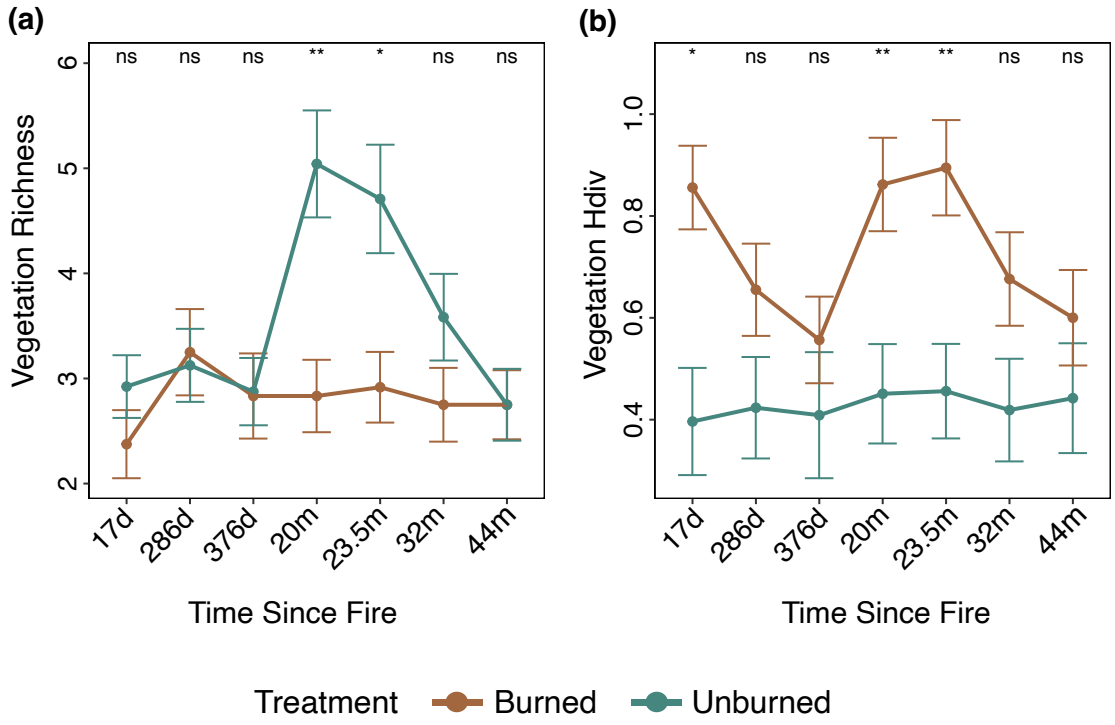

Figure C.1.3. Comparison of vegetation richness (a) and Shannon diversity (b) between burned (brown) and unburned communities (blue-green) at each of the seven timepoints over 4.5 years. Points represent the mean richness and Shannon diversity, while bars indicate the standard error of the mean for burned versus unburned plots at each timepoint..

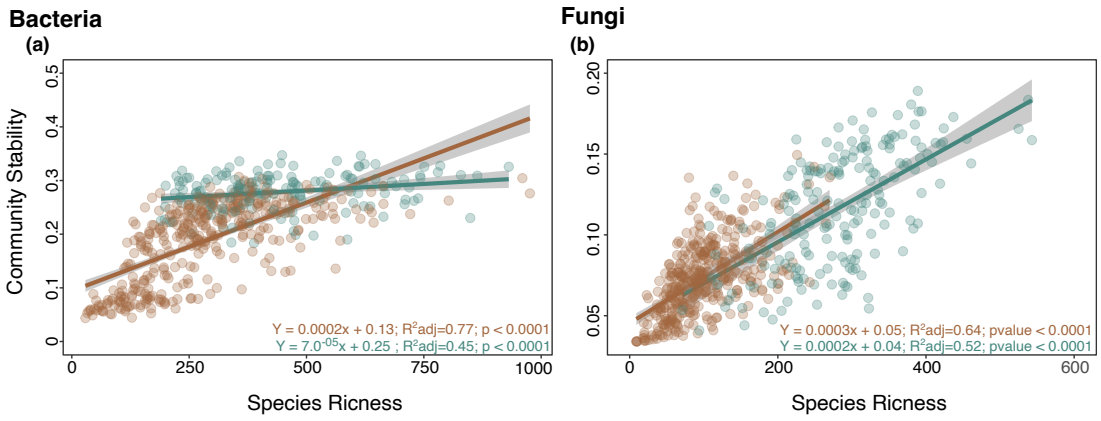

Figure C.1.4. Effect of species richness on (a) bacterial and (b) fungal community stability over time in unburned (blue-green) and burned (brown) plots.

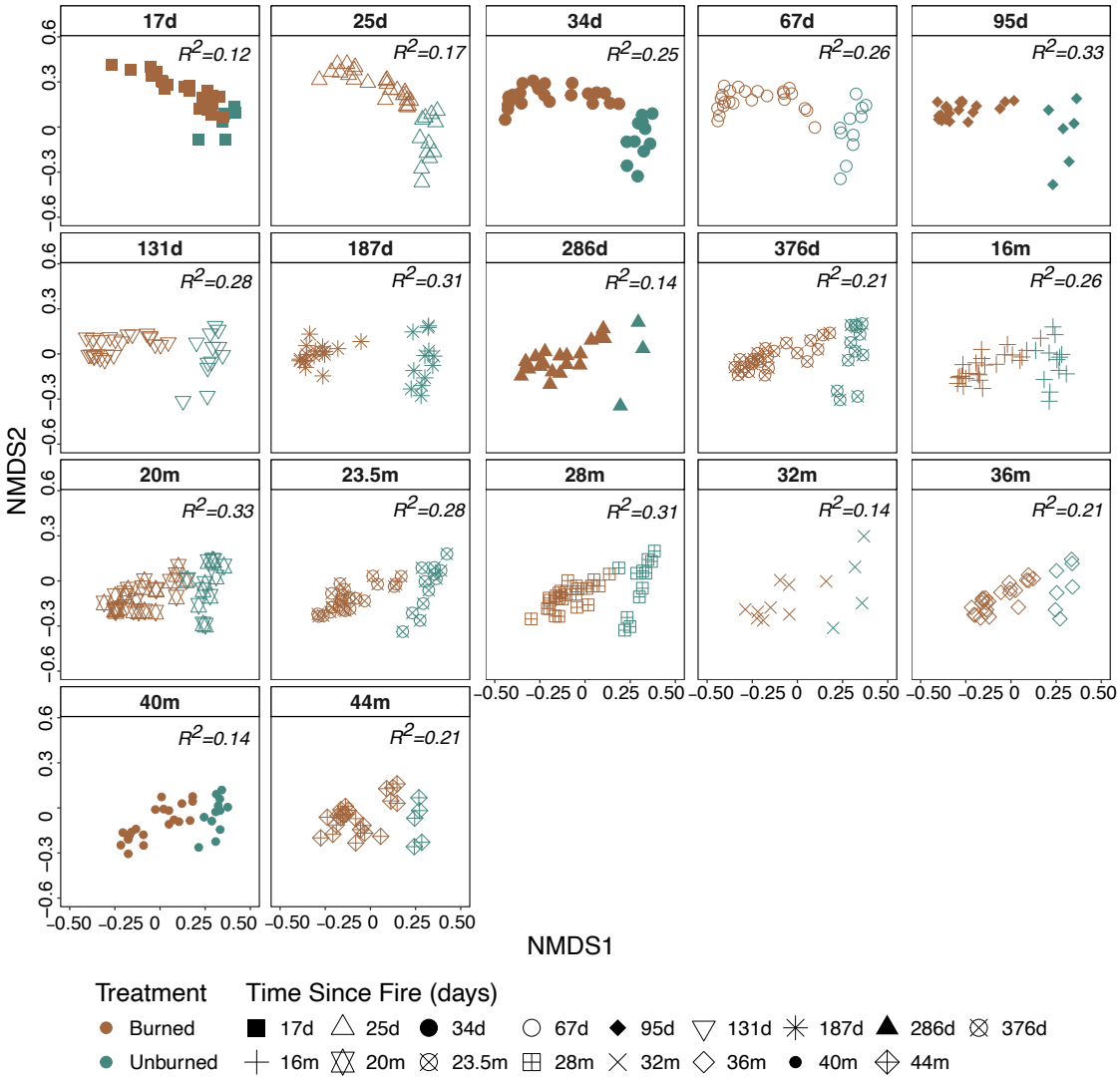

Figure C.1.5. Nonmetric multidimensional scaling (NMDS) plot illustrating bacterial community composition at each sampling time point (d = days, m = months), with treatment indicated by color and time since fire denoted by shape. The NMDS is represented in three dimensions. R2 values are derived from PERMANOVA analysis conducted with 999 iterations.

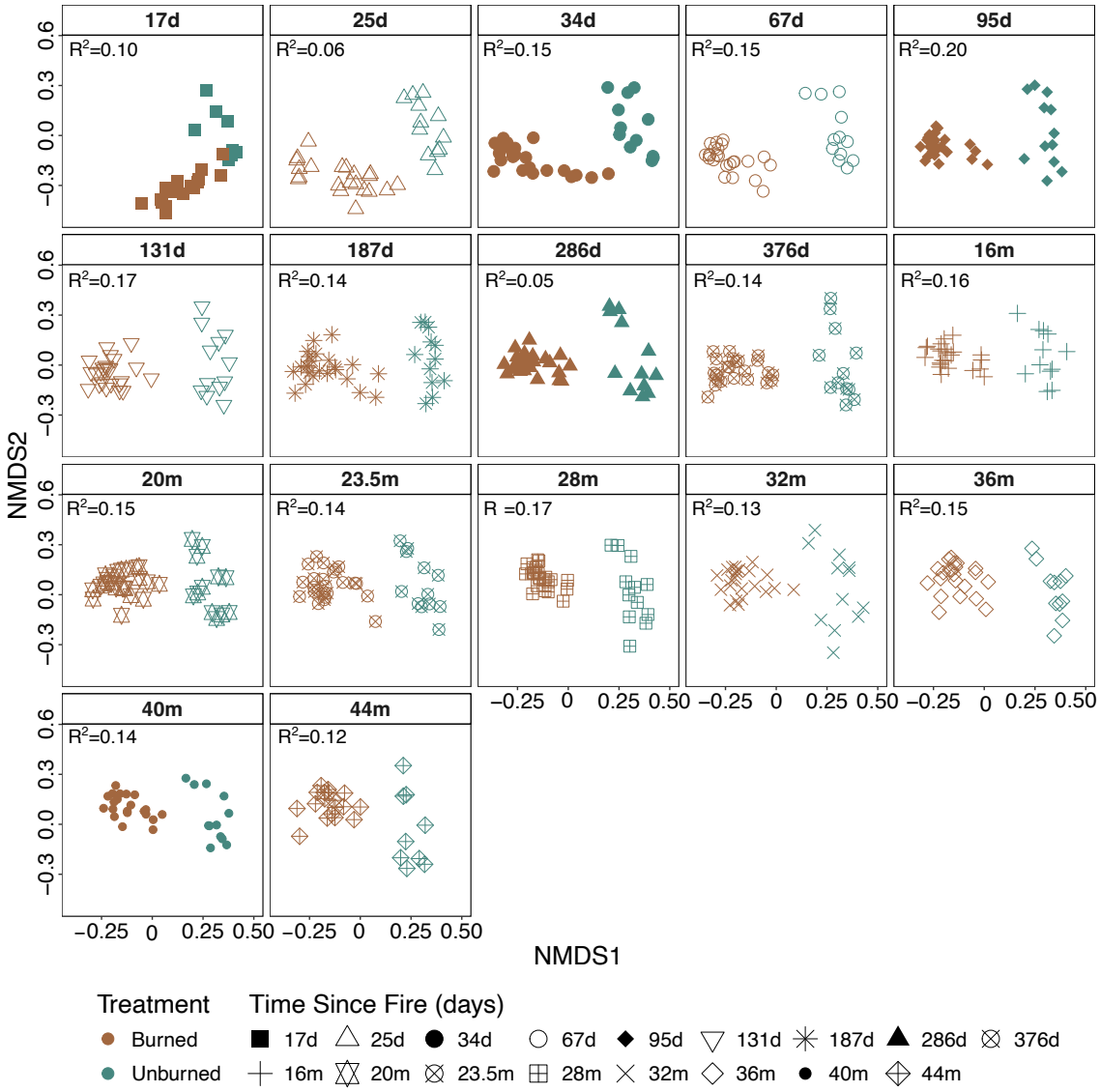

Figure C.1.6. Nonmetric multidimensional scaling (NMDS) plot illustrating fungal community composition at each sampling time point (d = days, m = months), with treatment indicated by color and time since fire denoted by shape. The NMDS is represented in three dimensions. R2 values are derived from PERMANOVA analysis conducted with 999 iterations.

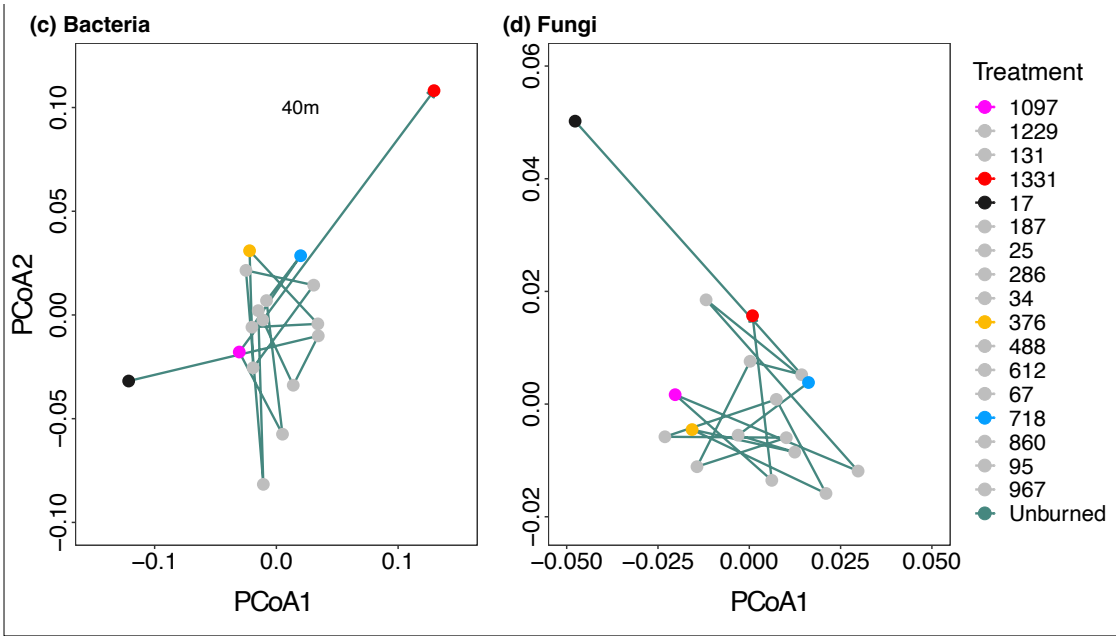

Figure C.1.7. Successional trajectory analysis of Principal Coordinates Analysis (PCoA) centroids for (a) bacterial and (b) fungal communities in unburned plots over the 4.5-year study period. The complete set of figures for both burned and unburned plots can be found in the manuscript (Fig 2).

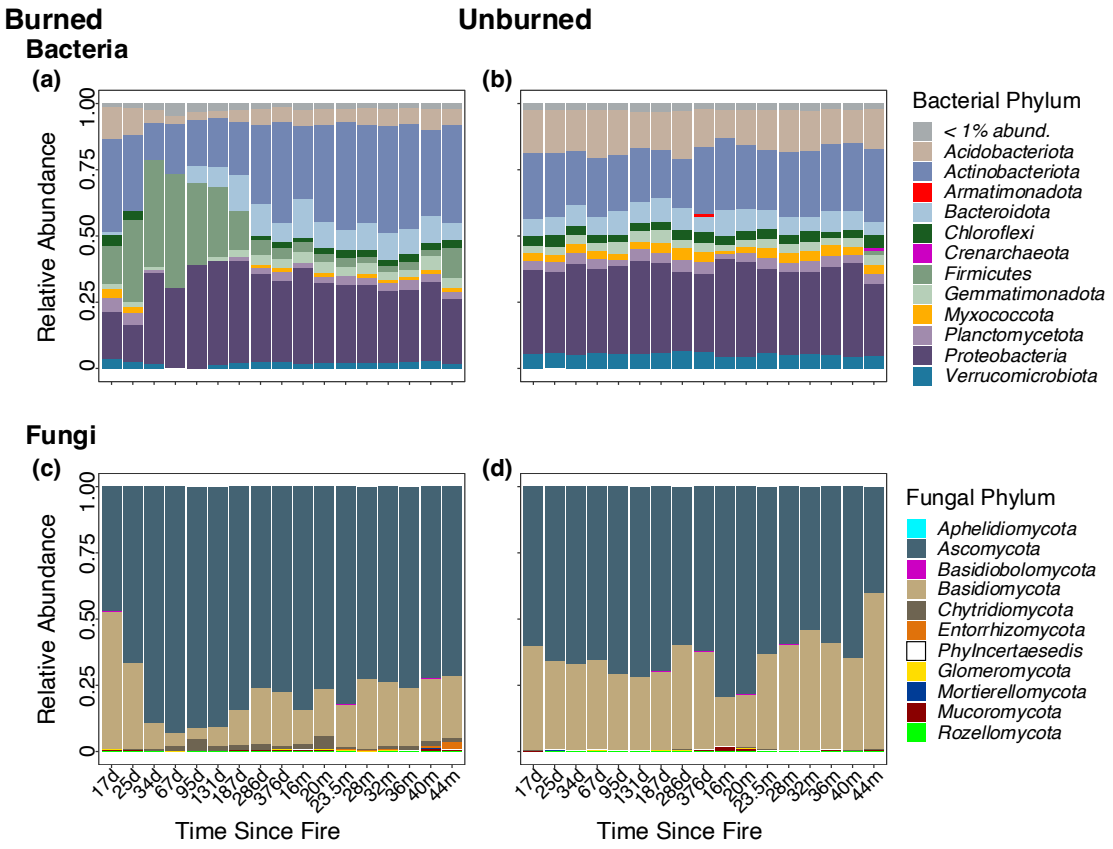

Figure C.1.8. Relative sequence abundance of (a) bacterial and (b) fungal phyla in burned plots (left) and unburned plots (right) across 17 timepoints (ranging from 17 days (d) to 44 months (m)). Grey bars in bacterial burned (a) and unburned (b) plots represent multiple bacterial phyla with relative abundance under 1% at each timepoint per treatment.

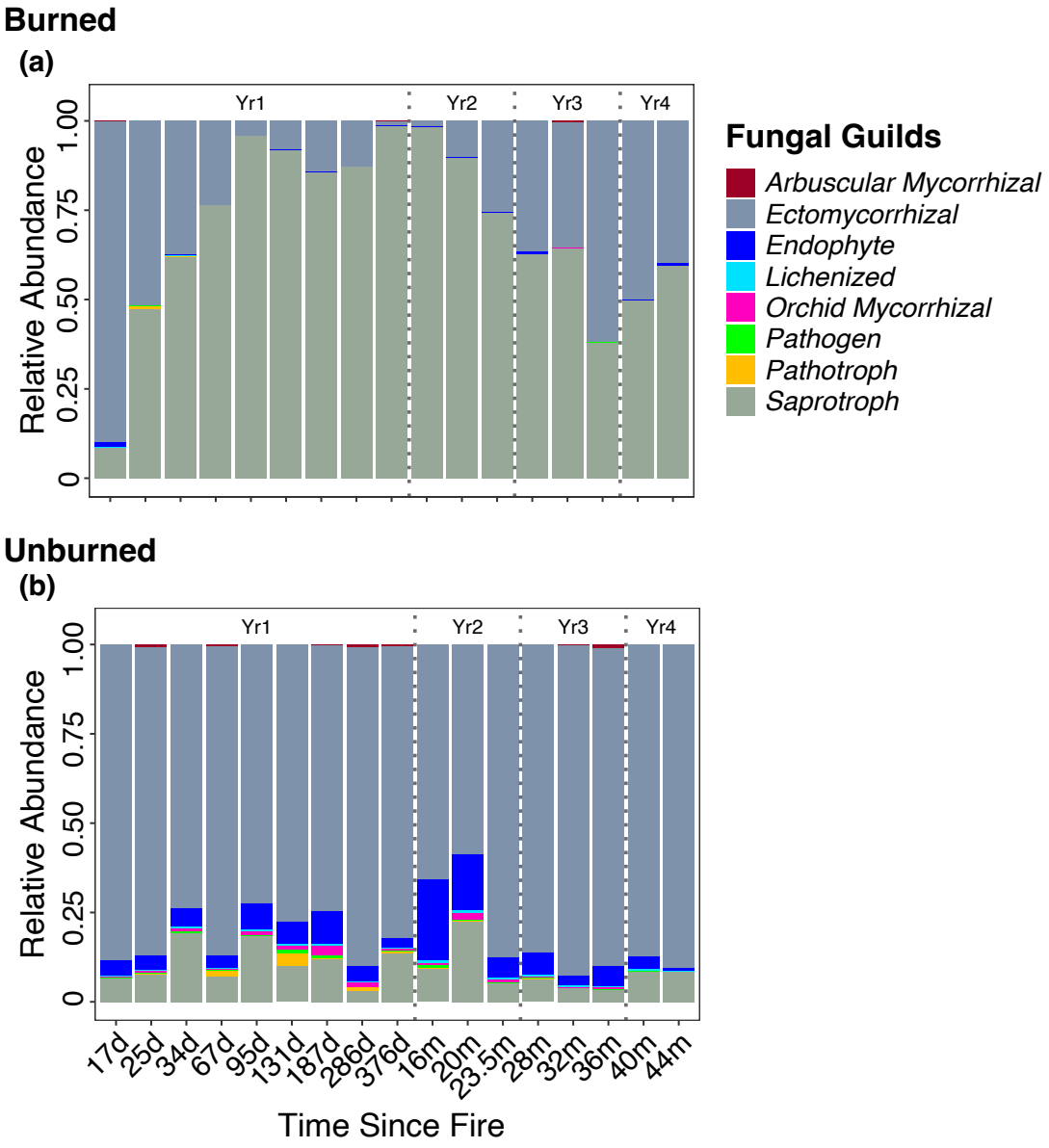

Figure C.1.9. Relative sequence abundance of fungal guilds (highly probable annotations) in burned plots (left) and unburned plots (right) across 17 timepoints (ranging from 17 days (d) to 44 months (m)).

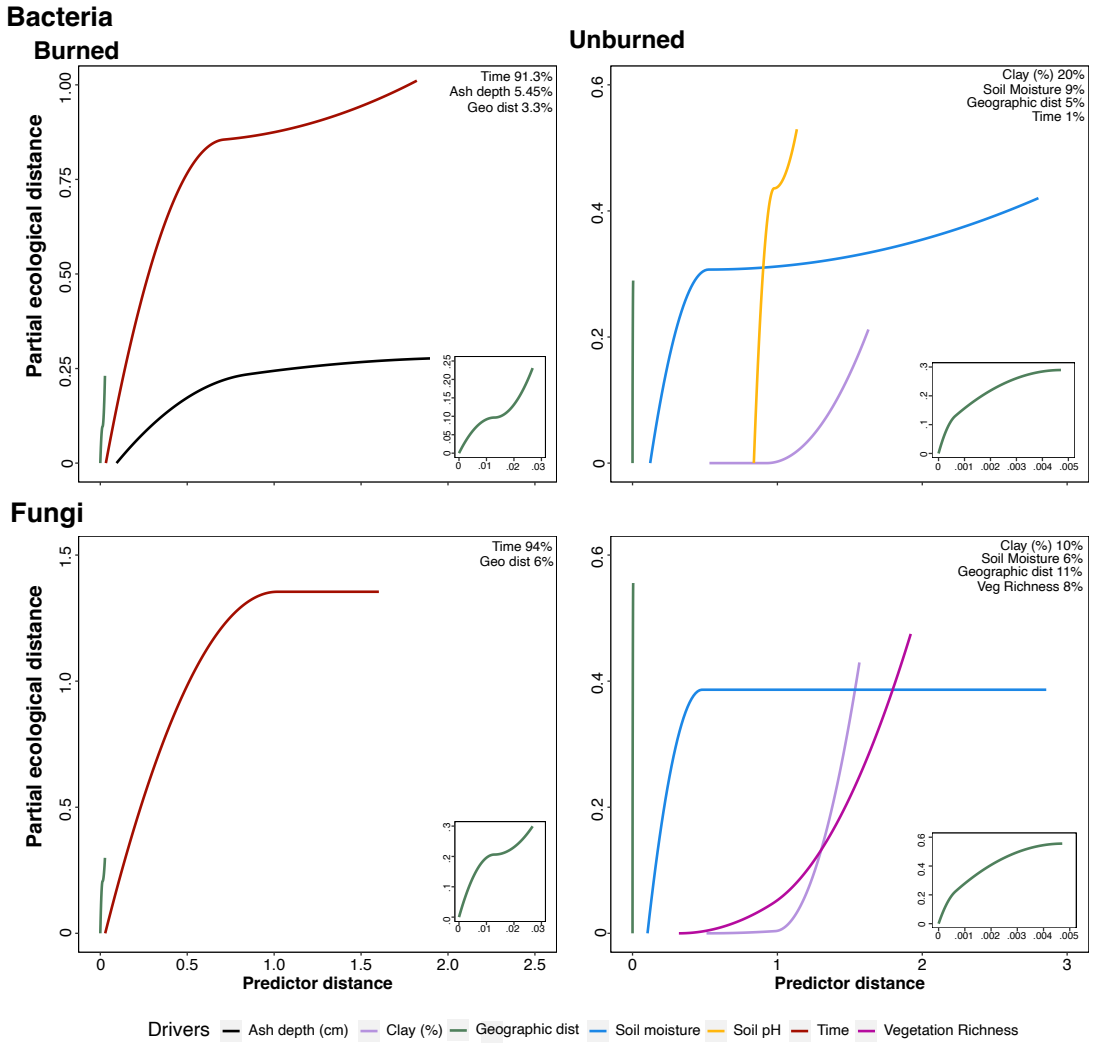

Figure C.1.10. Generalized Dissimilarity Models (GDM) of the relationship between a) bacterial and b) fungal observed compositional dissimilarity and predicted community dissimilarity between site pairs. Partial regression fits, for 3 GDM-fitted I-splined for variables significantly associated with c) bacterial and d) fungal beta diversity. Significance based on backward model selection in GDM package, with scaled variables and significance is based on $p<0.05$. Line heights represent the relative contribution of each variable to community composition whereas shape represents how the rate of community turnover varies with the predictor variable between sites.

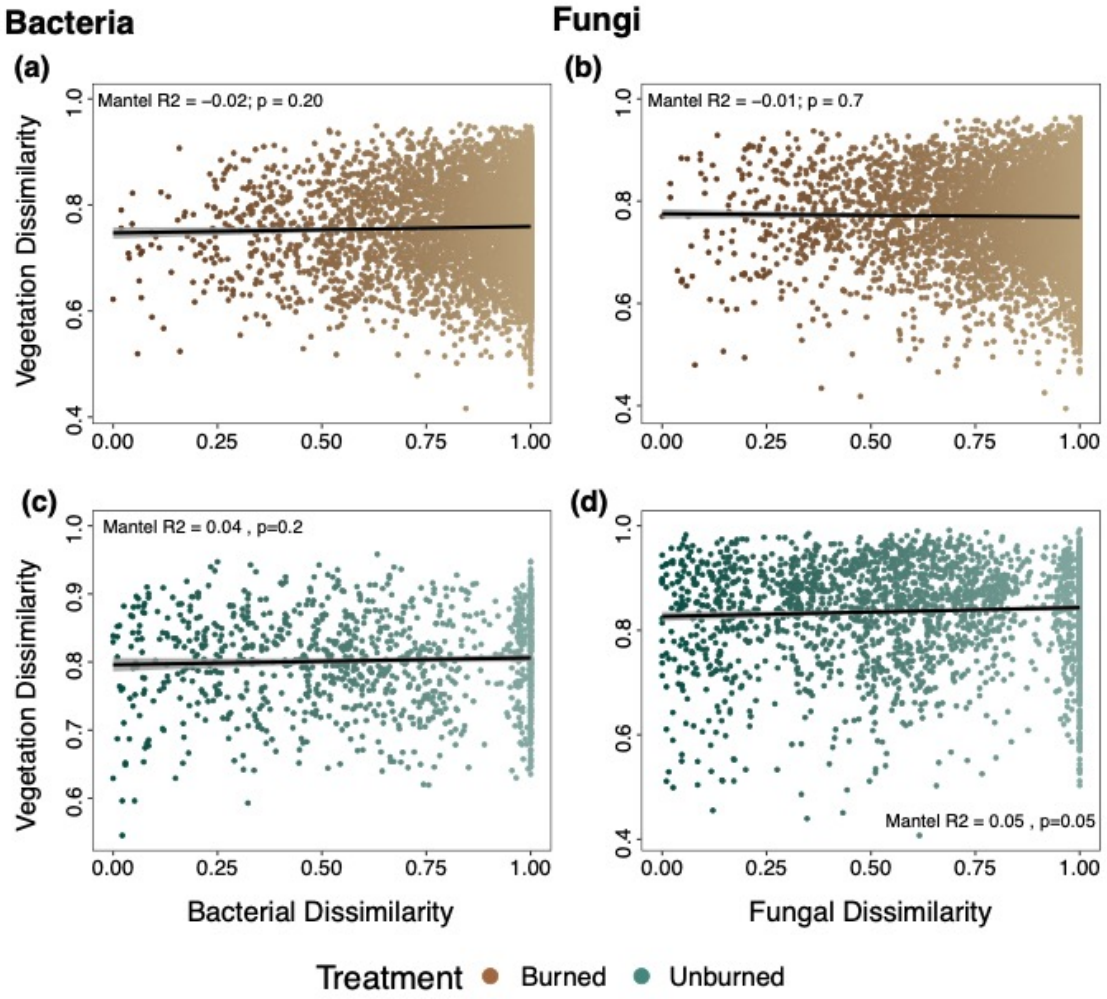

Figure C.1.11. Mantel correlations between total a) bacterial and b) fungal community composition and vegetation community composition. Both vegetation and microbial dissimilarity are based on Bray-Curtis.

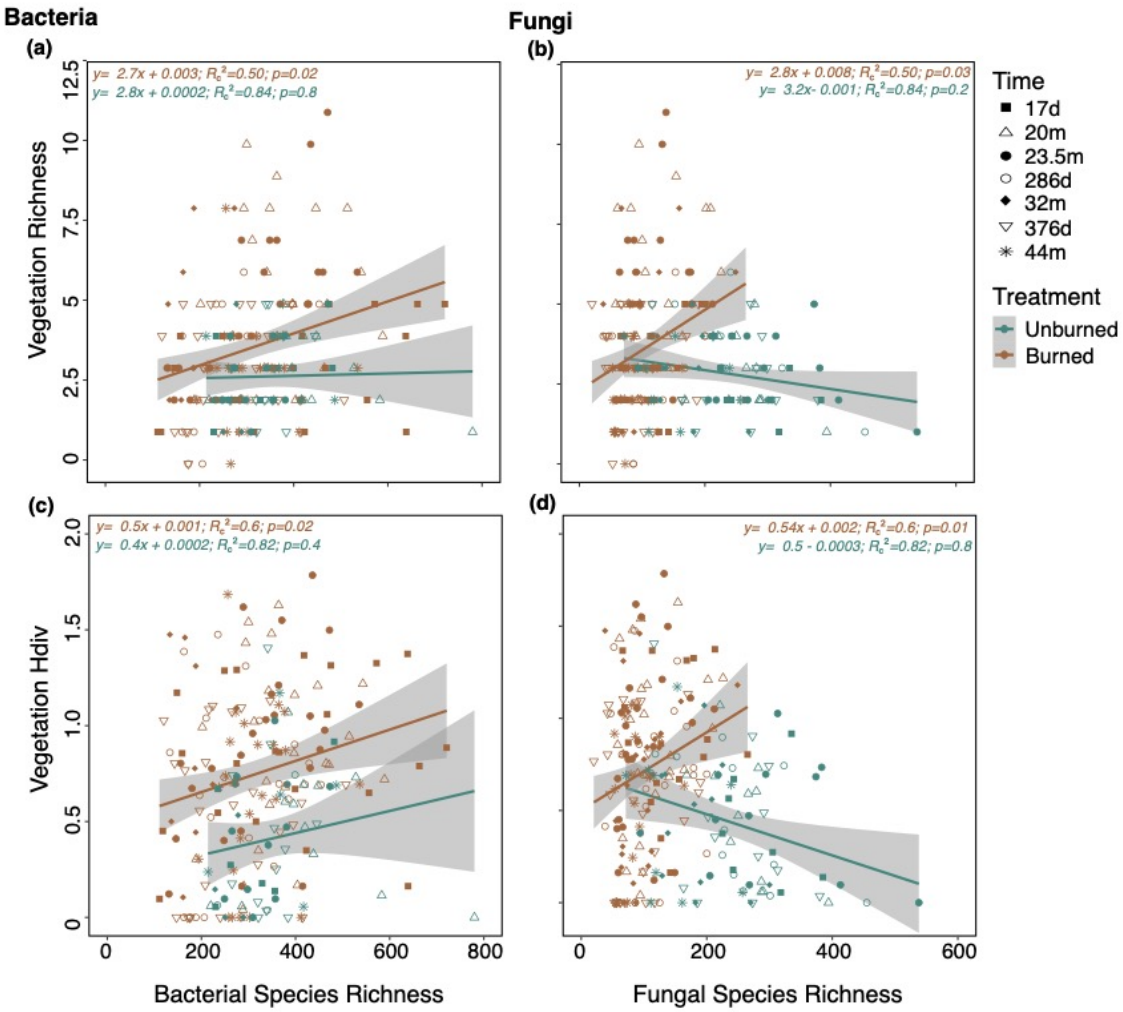

Figure C.1.12. Relationship between bacterial and fungal species richness and (a, b) vegetation richness, and (c, d) vegetation Shannon diversity in burned (brown) and unburned communities (blue-green). Points are shaped according to time in days (d) and months (m), and the gray area around the regression line represents the standard error.

Table C.2.1. Difference in resilience, recovery rate and percent recovery for burned bacterial and fungal communities independently. Significance shown in bold ($p<0.05$).

		Estimate	Std. Error	t value	Pr(>|t|)	Adj R^2
Resilience						
Bacteria	(Intercept)	-0.35	0.14	-2.53	**0.02**	0.24
	TSF days	0.001	0.0002	2.47	**0.03**	
Fungi	(Intercept)	-0.22	0.05	-4.34	**0.001**	0.011
	TSF days	0.0002	7.5E-05	3.23	**0.01**	
Recovery Rate						
Bacteria	(Intercept)	5.27	1.39	3.78	**0.002**	0.13
	TSF days	-0.005	0.002	-2.63	**0.02**	
Fungi	(Intercept)	-1.12	0.33	-3.36	**0.004**	0.27
	TSF days	0.001	0.0005	2.33	**0.03**	
Recovery Percent						
Bacteria	(Intercept)	74.62	9.86	7.57	1.7E-06	0.13
	TSF days	0.03	0.01	1.86	0.08	
Fungi	(Intercept)	-1.12	0.33	-3.36	**0.004**	0.41
	TSF days	0.001	0.0005	2.33	**0.03**	

Table C.2.2. Linear regression comparing the effect of time on bacterial and fungal resilience and recovery percent. Recovery rate was based on Kruskal-Wallis due to non-normality. Significance shown in bold ($p<0.05$).

	Estimate	Std. Error	t value	Pr(>|t|)	Adj R2
Resilience					
(Intercept)	-0.35	0.10	-3.37	**0.002**	0.24
TSF days	0.0005	0.0002	3.29	**0.003**	
Kingdom (Fungi)	0.14	0.15	0.93	0.36	
TSF days x Kingdom (Fungi)	-0.0003	0.0002	-1.24	0.22	
Percent Recovery					
(Intercept)	74.62	7.25	10.30	**2.30E-11**	0.67
TSF days	0.03	0.01	2.53	**0.02**	
Kingdom (Fungi)	-40.56	10.25	-3.96	**0.0004**	
TSF days x Kingdom (Fungi)	-0.03	0.02	-1.68	0.10	

Recovery Rate (Kruskal-Wallis)

	X2	df	p-value
Kingdom (Fungi)	20.989	1	**4.62E-06**

Table C.2.3. Table of multivariate negative binomial regressions from backward model selection and based on stepwise AIC for biomass (top section) and richness (bottom section) for bacterial and fungal communities for Model 1 which contains 15 timepoints (no timepoint 3 and 5, 34 and 67 days post-fire, due to missing soil pH and soil moisture). Drivers include time since fire, ash depth in cm, soil pH, percent soil moisture, distance to unburn locations, and average wind speed (m/s). Significance shown in bold ($p<0.05$). All variables were scaled.

Biomass

		Bacteria			**Fungi**	
Predictors	*Est*	*Statistic*	*p-value*	*Est*	*Statistic*	*p-value*
(Intercept)	16.38	15.22	**<0.001**	17.64	337.4	**<0.001**
Time (days)	0.32	1.39	0.16	0.32	5.77	**<0.001**
Ash depth (cm)	1.9	1.84	0.07	1.01	16.02	**<0.001**
Soil pH	2.57	2.44	**0.02**	-0.95	-14.9	**<0.001**
% Soil Moisture	0.02	0.12	0.90	-0.45	-6.66	**<0.001**
Distance Unburn	-0.56	-7.15	**<0.001**	-0.61	-13.39	**<0.001**
Time x Ash depth	0.26	1.94	0.05	0.37	6.69	**<0.001**
Ash depth x Soil ph	-2.24	-2.2	**0.03**	-1.52	-28.84	**<0.001**
Ash depth x Soil Moisture	0.17	1.47	0.14	0.34	6.22	**<0.001**
Random Effects						
σ^2		0.4			0.6	
$\tau_{00\ Time/Plot/Subplot}$		0.19/ /			0.42/0.01/0.02	
$N_{Time/Plot/Subplot}$		15/6/24			15/6/24	
Observations		349			348	
Marginal R^2 / Condt. R^2		0.312 / 0.533			0.261 / 0.575	

Richness

		Statistic			*Statistic*	
Predictors	*Est*		*p-value*	*Est*		*p-value*
(Intercept)	6.45	18.66	**<0.001**	4.72	30.07	**<0.001**
Time	-0.05	-0.43	0.66	-0.15	-1.35	0.18
Ash depth (cm)	-0.44	-4.28	**<0.001**	-0.4	-3.16	**0.002**
Wind speed	-0.17	-1.88	0.06	-	-	-
Time x Ash depth	0.27	4.37	**<0.001**	0.24	3.78	**<0.001**
% Soil Moisture	-	-	-	0.19	3.48	**<0.001**
Random Effects						
σ^2		0.11			0.11	
$\tau_{00\ Time/Subplot}$		0.05/0.04			0.05/0.07	
$N_{Time/Subplot}$		15/24			15/24	
Observations		330			337	
Marginal R^2 / Condt R^2		0.194 / 0.546			0.119 / 0.575	

Table C.2.4. Table of multivariate negative binomial regressions from backward model selection and based on stepwise AIC for biomass (top section) and richness (bottom section) for bacterial and fungal communities for Model 2 which contains 6 timepoints only, as this were the only timepoint for which we had vegetation and soil nitrogen measurement. Drivers include time since fire, ash depth in cm, soil pH, percent soil moisture, distance to unburn locations, and average wind speed (m/s), vegetation richness and Shannon diversity, and soil nitrate NO3 and ammonia (NH4). Significance shown in bold ($p<0.05$). All variables were scaled.

	Bacteria			**Fungi**		
Biomass						
Predictors	*Est.*	*Statistic*	*p*	*Est.*	*Statistic*	*p*
(Intercept)	27.9	14.25	**<0.001**	30.51	9.18	**<0.001**
Time	-10.18	-5.25	**<0.001**	-12.82	-4.07	**<0.001**
Soil pH	-1.32	-4.75	**<0.001**	-2.12	-4.66	**<0.001**
NH4	-0.86	-6.03	**<0.001**	-1.06	-4.93	**<0.001**
Clay (%)				-0.27	-0.7	0.48
Vegetation Richness	0.31	2.31	**0.02**	2.23	3.11	**0.002**
Veg Hdiv	-	-	-	-1.15	-1.9	0.06
Distance Unburn	-0.62	-5.73	**<0.001**	-0.74	-3.21	**0.001**
Time x Soil pH	1.51	5.31	**<0.001**	1.98	4.42	**<0.001**
Time x NH4	1.57	6.83	**<0.001**	1.5	4.15	**<0.001**
Time x Hdiv	-	-	-	1.23	1.96	0.05
Time x Veg Richness	-	-	-	-1.83	-2.75	**0.01**
Random Effects						
σ^2		0.39			0.58	
$\tau_{00\ TSFdays/\ /Subplot}$		4.591e-12/5.402e-12			0.18/0.08	
$N_{\ TSFdays/\ Subplot}$		6/24			6/24	
Observations		140			139	
Marginal R^2 / Condt R^2		0.605 / NA			0.566 / 0.700	
Richness						
Predictors	*Log-Mean*	*Statistic*	*p*	*Est*	*Statistic*	*p-value*
(Intercept)	5.85	27.56	**<0.001**	4.86	28.00	**<0.001**
Time	-0.13	-0.68	0.50	-0.33	-2.95	**0.003**
Ash depth (cm)	-0.53	-4.48	**<0.001**	-0.35	-2.25	**0.02**
NH4	0.15	2.05	**0.04**	-	-	-
Veg Richness	0.46	2.75	**0.01**	-	-	-
Soil Moisture	-0.02	-0.18	0.86	-	-	-
Time x Ash depth	0.20	1.99	0.05	0.25	2.14	**0.03**
Time x NH4	-0.39	-2.70	**0.01**	-	-	-
Time x Veg Richness	-0.25	-1.92	0.06	-	-	-
Ash Depth x Soil Moisture	0.15	1.84	0.07	-	-	-
Vegetation Hdiv	-	-	-	0.22	2.31	**0.02**
Random Effects						
σ^2		0.07			0.09	
$\tau_{00\ TSFdays/\ Plot/Subplot}$		0.02/0.02/0.01			0.0003/0.02/0.05	
$N_{\ TSFdays/\ Plot/Subplot}$		6/6/24			6/6/24	
Observations		125			136	
Marginal R^2 / Condt R^2		0.311 / 0.583			0.111 / 0.501	

Table C.2.5. Generalized liner regression results testing the difference in community stability between burned and unburned communities (treatment), and kingdoms (bacteria vs. fungi). Significance shown in bold ($p<0.005$).

	Est	T	P-value
(Intercept)	0.27	31.78	
Treatment (Burned)	0.28	34.6	**< 2.2e-16**
Taxa (Fungi)	-9.10E-02	-13.32	**< 2.2e-16**
Treatment (Burned) x Taxa (Fungi)	-0.16	-36.25	**< 2.2e-16**
	4.80E-02	8.85	
Random effects			
TSF days/Plot	5.7e-04/6.1e-05		
Marginal and Conditional R^2	0.68/0.76		

Table C.2.6. Overall effects of time and species richness (observed ASV) and their first order interactions on unburned bacterial and fungal community stability. Significance shown in bold ($p<0.05$).

	Bacteria			**Fungi**		
	Est	***t value***	***P-value***	***Est***	***t value***	***P-value***
Intercept)	0.24	21.68		0.05	3.83	
Time	6.0^{-06}	0.36	**0.02**	-1.5^{-05}	-0.93	0.67
Richness	6.6^{-05}	3.54	**<0.0001**	2.3^{-04}	5.68	**<2e-16**
Time x Richness	1.7^{-08}	0.46	0.65	6.5^{-08}	1.21	0.23
Random effects						
Time/Subplot	$1.28^{-05}/4.2^{-04}$			$1.3^{-05}/4.2^{-04}$		
Marginal/condt R^2	0.11/0.44			0.37/0.54		

Table C.2.7. Overall effects of time and species richness (observed ASV) and their first order interactions on burned bacterial and fungal community stability. Significance shown in bold ($p<0.05$).

	Bacteria			Fungi		
	Est	***t value***	***P-value***	***Est***	***t value***	***P-value***
(Intercept)	0.07	6.27		0.04	13.479	
Time	1.3^{-04}	6.93	**2.9^{-07}**	1.8^{-05}	4.1	**< 2e-16**
Richness	2.6^{-04}	14.2	**< 2.2^{-16}**	2.4^{-04}	11.0	**< 2e-16**
Time x Richness	-1.4^{-07}	-5.11	**3.3^{-07}**	6.9^{-08}	1.895	0.06
Random effects						
Time/Subplot	0.001/0.0001			$0.00002/4.9e^{-06}$		
Marginal and condt R^2	0.62/0.80			0.61/0.65		

Table C.2.8. Permutational multivariate analysis of variance (PERMANOVA) for bacterial and fungal community composition. Based on 9999 permutations. Significance $p<0.05$ (bold).

		Sum of Sqs	R2	Pr(>F)
Bacteria	Treatment	8.56	0.04	**0.0001**
	Time since fire (TSF)	5.91	0.03	**0.0001**
	Treatment x TSF	3.41	0.02	**0.0001**
Fungi	Treatment	8.56	0.04	**0.0001**
	Time since fire (TSF)	5.91	0.03	**0.0001**
	Treatment x TSF	3.41	0.02	**0.0001**

Table C.2.9. Mean and percent change in relative abundance of the most dominant bacterial and fungal genera in the burned plots over time. Time is denoted as days (d) and months (m). Percent changes in relative abundance is based in comparison of relative abundance at each progressive timepoint to 17 days post-fire (base level).

Time	Bacterial Genus	mean	percent	Fungal Genus	mean	percent
17d	Blastococcus	0.014	0%	Pyronema	0.031	0%
25d	Blastococcus	0.016	1506%	Pyronema	0.266	75390%
34d	Blastococcus	0.003	-7824%	Pyronema	0.629	191933%
67d	Blastococcus	0.004	-7012%	Pyronema	0.627	191316%
95d	Blastococcus	0.010	-2673%	Pyronema	0.375	110229%
131d	Blastococcus	0.013	-597%	Pyronema	0.331	96091%
187d	Blastococcus	0.022	6055%	Pyronema	0.191	51214%
286d	Blastococcus	0.038	17321%	Pyronema	0.226	62409%
376d	Blastococcus	0.039	17858%	Pyronema	0.196	53021%
16m	Blastococcus	0.040	19074%	Pyronema	0.186	49572%
20m	Blastococcus	0.052	27266%	Pyronema	0.135	33465%
23.5m	Blastococcus	0.058	31906%	Pyronema	0.111	25557%
28m	Blastococcus	0.054	29060%	Pyronema	0.095	20457%
32m	Blastococcus	0.061	33992%	Pyronema	0.123	29320%
36m	Blastococcus	0.056	30805%	Pyronema	0.125	30058%
40m	Blastococcus	0.052	27618%	Pyronema	0.080	15809%
44m	Blastococcus	0.046	23114%	Pyronema	0.007	-7908%
17d	Bryobacter	0.022	0%	Penicillium	0.029	0%
25d	Bryobacter	0.017	-2283%	Penicillium	0.144	39716%
34d	Bryobacter	0.006	-7228%	Penicillium	0.081	18089%
67d	Bryobacter	0.006	-7236%	Penicillium	0.128	34204%
95d	Bryobacter	0.006	-7088%	Penicillium	0.220	66044%
131d	Bryobacter	0.004	-8012%	Penicillium	0.157	44021%
187d	Bryobacter	0.007	-6901%	Penicillium	0.185	53761%
286d	Bryobacter	0.010	-5534%	Penicillium	0.109	27545%
376d	Bryobacter	0.011	-5004%	Penicillium	0.162	45883%
16m	Bryobacter	0.011	-5008%	Penicillium	0.186	54267%
20m	Bryobacter	0.011	-4808%	Penicillium	0.121	31569%
23.5m	Bryobacter	0.012	-4375%	Penicillium	0.128	34135%
28m	Bryobacter	0.011	-4788%	Penicillium	0.100	24462%
32m	Bryobacter	0.011	-5141%	Penicillium	0.131	35246%
36m	Bryobacter	0.012	-4437%	Penicillium	0.051	7660%
40m	Bryobacter	0.016	-2906%	Penicillium	0.067	13214%
44m	Bryobacter	0.012	-4370%	Penicillium	0.202	59652%
17d	Cohnella	0.018	0%	Aspergillus	0.004	0%
25d	Cohnella	0.035	9234%	Aspergillus	0.057	147665%
34d	Cohnella	0.040	12132%	Aspergillus	0.036	88771%
67d	Cohnella	0.043	14171%	Aspergillus	0.051	131241%
95d	Cohnella	0.046	15669%	Aspergillus	0.126	339822%
131d	Cohnella	0.022	2501%	Aspergillus	0.097	261103%
187d	Cohnella	0.012	-3148%	Aspergillus	0.084	223962%
286d	Cohnella	0.006	-6422%	Aspergillus	0.051	131594%
376d	Cohnella	0.008	-5642%	Aspergillus	0.111	297749%
16m	Cohnella	0.005	-7156%	Aspergillus	0.089	237482%
20m	Cohnella	0.004	-7843%	Aspergillus	0.073	193885%
23.5m	Cohnella	0.005	-7064%	Aspergillus	0.112	302715%
28m	Cohnella	0.005	-7459%	Aspergillus	0.060	156698%
32m	Cohnella	0.004	-7588%	Aspergillus	0.054	139964%
36m	Cohnella	0.004	-7958%	Aspergillus	0.034	84596%
40m	Cohnella	0.003	-8502%	Aspergillus	0.030	74714%
44m	Cohnella	0.026	4356%	Aspergillus	0.066	174466%
17d	Conexibacter	0.040	0%	Alternaria	0.000	0%
25d	Conexibacter	0.031	-2390%	Alternaria	0.012	1272233%
34d	Conexibacter	0.006	-8499%	Alternaria	0.006	589549%
67d	Conexibacter	0.006	-8566%	Alternaria	0.004	377894%
95d	Conexibacter	0.003	-9257%	Alternaria	0.024	2406775%
131d	Conexibacter	0.004	-8988%	Alternaria	0.028	2904030%
187d	Conexibacter	0.004	-8940%	Alternaria	0.022	2222724%
286d	Conexibacter	0.010	-7409%	Alternaria	0.009	941832%
376d	Conexibacter	0.020	-5123%	Alternaria	0.005	551004%
16m	Conexibacter	0.013	-6773%	Alternaria	0.048	4953330%
20m	Conexibacter	0.018	-5604%	Alternaria	0.051	5212007%
23.5m	Conexibacter	0.021	-4682%	Alternaria	0.028	2836811%
28m	Conexibacter	0.017	-5678%	Alternaria	0.034	3519902%
32m	Conexibacter	0.015	-6152%	Alternaria	0.020	2023031%
36m	Conexibacter	0.014	-6472%	Alternaria	0.038	3868868%
40m	Conexibacter	0.016	-5935%	Alternaria	0.037	3780559%
44m	Conexibacter	0.020	-5102%	Alternaria	0.015	1495477%
17d	Domibacillus	0.001	0%	Coniochaeta	0.023	0%
25d	Domibacillus	0.012	171274%	Coniochaeta	0.037	5787%
34d	Domibacillus	0.094	1433318%	Coniochaeta	0.042	7781%
67d	Domibacillus	0.082	1253884%	Coniochaeta	0.074	21403%
95d	Domibacillus	0.019	286111%	Coniochaeta	0.091	28608%
131d	Domibacillus	0.011	162422%	Coniochaeta	0.185	68916%
187d	Domibacillus	0.011	158836%	Coniochaeta	0.144	51391%
286d	Domibacillus	0.006	82501%	Coniochaeta	0.180	66460%
376d	Domibacillus	0.012	167988%	Coniochaeta	0.150	53881%
16m	Domibacillus	0.012	168806%	Coniochaeta	0.076	22516%

20m	Domibacillus	0.008	110746%	Coniochaeta	0.070	19740%
23.5m	Domibacillus	0.012	178759%	Coniochaeta	0.090	28346%
28m	Domibacillus	0.006	85855%	Coniochaeta	0.078	23065%
32m	Domibacillus	0.005	67065%	Coniochaeta	0.053	12468%
36m	Domibacillus	0.006	83418%	Coniochaeta	0.064	17083%
40m	Domibacillus	0.003	31902%	Coniochaeta	0.078	23043%
44m	Domibacillus	0.016	233554%	Coniochaeta	0.037	5834%
17d	Massilia	0.004	0%	Naganishia	0.000	0%
25d	Massilia	0.004	1370%	Naganishia	0.000	-5567%
34d	Massilia	0.320	836905%	Naganishia	0.001	162235%
67d	Massilia	0.280	731450%	Naganishia	0.001	88271%
95d	Massilia	0.312	816534%	Naganishia	0.012	1366308%
131d	Massilia	0.258	672419%	Naganishia	0.019	2183628%
187d	Massilia	0.168	434042%	Naganishia	0.019	2215468%
286d	Massilia	0.111	282816%	Naganishia	0.039	4592972%
376d	Massilia	0.070	176281%	Naganishia	0.016	1855166%
16m	Massilia	0.054	134026%	Naganishia	0.047	5569970%
20m	Massilia	0.039	92400%	Naganishia	0.037	4341369%
23.5m	Massilia	0.037	87346%	Naganishia	0.037	4400137%
28m	Massilia	0.047	113159%	Naganishia	0.124	14619287%
32m	Massilia	0.038	90494%	Naganishia	0.047	5495374%
36m	Massilia	0.034	80307%	Naganishia	0.063	7455776%
40m	Massilia	0.020	43750%	Naganishia	0.053	6179650%
44m	Massilia	0.020	43433%	Naganishia	0.054	6365426%
17d	Paenibacillus	0.026	0%	Geopora	0.020	0%
25d	Paenibacillus	0.039	5176%	Geopora	0.002	-8984%
34d	Paenibacillus	0.084	22459%	Geopora	0.002	-9159%
67d	Paenibacillus	0.077	19813%	Geopora	0.001	-9673%
95d	Paenibacillus	0.096	27472%	Geopora	0.000	-9796%
131d	Paenibacillus	0.062	14031%	Geopora	0.000	-9865%
187d	Paenibacillus	0.034	3335%	Geopora	0.002	-8827%
286d	Paenibacillus	0.012	-5335%	Geopora	0.018	-1152%
376d	Paenibacillus	0.015	-3988%	Geopora	0.001	-9749%
16m	Paenibacillus	0.013	-5102%	Geopora	0.002	-8899%
20m	Paenibacillus	0.009	-6361%	Geopora	0.022	602%
23.5m	Paenibacillus	0.006	-7592%	Geopora	0.074	26456%
28m	Paenibacillus	0.005	-8119%	Geopora	0.069	23751%
32m	Paenibacillus	0.006	-7587%	Geopora	0.082	30321%
36m	Paenibacillus	0.005	-7999%	Geopora	0.124	50940%
40m	Paenibacillus	0.004	-8306%	Geopora	0.070	24222%
44m	Paenibacillus	0.039	5183%	Geopora	0.126	51842%
17d	Segetibacter	0.001	0%	Coprinellus	0.000	0%
25d	Segetibacter	0.001	3608%	Coprinellus	0.000	-8361%
34d	Segetibacter	0.001	-3599%	Coprinellus	0.000	-6214%
67d	Segetibacter	0.001	2894%	Coprinellus	0.000	-8243%
95d	Segetibacter	0.002	12768%	Coprinellus	0.000	-6065%
131d	Segetibacter	0.008	72076%	Coprinellus	0.005	113167%
187d	Segetibacter	0.022	227710%	Coprinellus	0.021	482315%
286d	Segetibacter	0.031	328444%	Coprinellus	0.046	1071720%
376d	Segetibacter	0.018	185169%	Coprinellus	0.069	1593834%
16m	Segetibacter	0.037	397055%	Coprinellus	0.008	175616%
20m	Segetibacter	0.033	351126%	Coprinellus	0.012	275486%
23.5m	Segetibacter	0.033	345614%	Coprinellus	0.048	1109182%
28m	Segetibacter	0.053	567996%	Coprinellus	0.043	984633%
32m	Segetibacter	0.046	494200%	Coprinellus	0.096	2229270%
36m	Segetibacter	0.052	554087%	Coprinellus	0.030	677201%
40m	Segetibacter	0.051	547779%	Coprinellus	0.064	1470545%
44m	Segetibacter	0.040	428778%	Coprinellus	0.073	1679683%
17d	Sphingomonas	0.008	0%			
25d	Sphingomonas	0.005	-3540%			
34d	Sphingomonas	0.008	-946%			
67d	Sphingomonas	0.003	-6202%			
95d	Sphingomonas	0.007	-2105%			
131d	Sphingomonas	0.009	1094%			
187d	Sphingomonas	0.012	4148%			
286d	Sphingomonas	0.012	3800%			
376d	Sphingomonas	0.010	2048%			
16m	Sphingomonas	0.038	35308%			
20m	Sphingomonas	0.016	9254%			
23.5m	Sphingomonas	0.017	10340%			
28m	Sphingomonas	0.019	12299%			
32m	Sphingomonas	0.017	10052%			
36m	Sphingomonas	0.020	14452%			
40m	Sphingomonas	0.030	25808%			
44m	Sphingomonas	0.032	28520%			

Table C.2.10. Burned Generalized Dissimilarity Model (GDM) models for bacterial (left) and fungal (right) community composition. All variables were scaled and significance tested via 999 permutations via backward model selection. Top panels are based on model 1 variables (). Bottom panel are model 2 include the variables in model 1, plus NH4, NO3 and vegetation richness and Shannon diversity.

Mod 1

	Bacteria		**Fungi**	
	Importance	*P-value*	*Importance*	*P-value*
Geographic	4.58	0	10.07	0
Time	95.82	0	82.57	0
Distance Unburn	NA	NA	-	-
Ash depth (cm)	NA	NA	5.80	0
Soil Moisture	NA	NA	NA	NA
Clay (%)	NA	NA	NA	NA
Soil pH	NA	NA	NA	NA
Wind speed	NA	NA	-	-
			-	-
Model deviance	2203.33		2540.47	
Percent deviance explained	34.87		34.77	
Model p-value	0		0	

Mod 2: Vegetation + Nitrogen

	Importance	*P-value*	*Importance*	*P-value*
Geographic	3.31	0	6.315	0
Vegetation Hdiv	NA	NA	NA	NA
Time	91.29	0	93.992	0
Ash depth (cm)	5.45	0	NA	NA
Soil Moisture	NA	NA	NA	NA
Clay (%)	NA	NA	NA	NA
NO3	NA	NA	NA	NA
NH4	NA	NA	NA	NA
Vegetation Richness	NA	NA	NA	NA
Soil pH	NA	NA	NA	NA
Wind speed	NA	NA	-	-
Model deviance	317.154		370.78	
Percent deviance explained	42.683		48.111	
Model p-value	0		0	

All models fitted with permutations 999

Table C.2.11. Unburned Generalized Dissimilarity Model (GDM) models for bacterial (left) and fungal (right) community composition. All variables were scaled and significance tested via 999 permutations via backward model selection. Top panels are based on model 1 variables (). Bottom panel are model 2 include the variables in model 1, plus NH4, NO3 and vegetation richness and Shannon diversity.

Mod 1

	Bacteria		**Fungi**	
	Importance	*P-value*	*Importance*	*P-value*
Geographic	5.135	0	8.374	0
Time	0.904	0	1.257	0
Soil Moisture	8.657	0	NA	NA
Clay (%)	19.789	0	19.429	0
Soil pH	8.854	0	NA	NA
Wind speed	0.073	0	-	-
Model deviance	268.306		615.974	
Percent deviance explained	20.522		32.398	
Model p-value	0		0	

Mod 2: Vegetation + Nitrogen

	Importance	*P-value*	*Importance*	*P-value*
Geographic	8.797	0	11.36	0
Vegetation Hdiv	NA	NA	NA	NA
Soil Moisture	15.891	0	6.17	0
Clay (%)	4.558	0	9.66	0
NH4	NA	NA	-	-
Vegetation Richness	NA	NA	8.297	0
Soil pH	6.96	0	NA	NA
Wind speed	NA	NA	NA	NA
Model deviance	23.122		95.34	
Percent deviance explained	39.004		39.49	
Model p-value	0		0	